

**THE ROLE OF MYOCARDIAL FIBROSIS IN OUTCOME  
FOLLOWING MITRAL VALVE REPAIR IN DEGENERATIVE  
MITRAL REGURGITATION**

**BOYANG LIU**

A thesis submitted to the University of Birmingham for the degree of

**DOCTOR OF PHILOSOPHY**

Institute of Cardiovascular Sciences  
School of Clinical and Experimental Medicine  
College of Medical and Dental Sciences  
University of Birmingham  
March 2020

UNIVERSITY OF  
BIRMINGHAM

**University of Birmingham Research Archive**

**e-theses repository**

This unpublished thesis/dissertation is copyright of the author and/or third parties. The intellectual property rights of the author or third parties in respect of this work are as defined by The Copyright Designs and Patents Act 1988 or as modified by any successor legislation.

Any use made of information contained in this thesis/dissertation must be in accordance with that legislation and must be properly acknowledged. Further distribution or reproduction in any format is prohibited without the permission of the copyright holder.

## ABSTRACT

Primary degenerative mitral regurgitation (MR) is a disease of increasing prevalence. Its optimal management is surgical repair, but surgery timings remain controversial. Current guidelines that suggest ‘watchful-waiting’ have been criticised for promoting rescue surgery after the establishment of symptoms or left ventricular (LV) dysfunction.

Conversely, non-selective early surgical approaches result in unnecessary surgery for some patients.

Myocardial fibrosis has been hypothesised to accumulate in MR, leading to eventual overt LV dysfunction. This thesis examines this hypothesis, assesses the prognostic impact of myocardial fibrosis, and determines its value as a biomarker for optimising the timing of surgery.

In a prospective multicentre study of severe MR patients, I provide definitive histological evidence for the presence of myocardial fibrosis, before the onset of symptoms. Due to its patchy nature, non-invasive quantification of fibrosis on cardiac magnetic resonance (CMR) was a superior marker of preoperative myocardial function and symptom burden.

However, neither histology- nor CMR-derived fibrosis correlated with postoperative outcomes. Despite successful surgery, symptomatic patients continued to possess worse cardiopulmonary exercise (CPET) performance and symptom burden quantified via patient-response questionnaires (PROMs) compared to asymptomatic patients, providing additional support for the benefits of early surgery. Further evaluation of surveillance CPET and PROMs is indicated for patients in whom early surgery is clinically inappropriate.

## **DEDICATION**

*To my wonderful wife, Grace  
and my adventurous daughters, Alicia and Emily.*

## ACKNOWLEDGEMENTS

This research was conducted under the supervision of Dr Richard Steeds (Consultant Cardiologist), Dr Nicola Edwards (Consultant Cardiologist) and Professor Gerard Nash (Professor of Cardiovascular Rheology) at the University Hospital Birmingham and the University of Birmingham.

I am forever indebted to my lead supervisor, Dr Richard Steeds, for his outstanding mentorship and intellectual insights. His ongoing support, friendship and motivational energy have resulted in the success of this research project and reaffirmed my plans for a career in clinical non-invasive cardiology.

I am also extremely grateful for the excellent mentorship and invaluable advice provided by my co-supervisors Dr Nicola Edwards and Professor Gerard Nash.

Thanks must also go to my fellow clinical researchers Dr Shanat Baig, Dr Anna Price, Dr Manvir Hayer and Dr Ravi Vijapurapu, for their camaraderie and involvement with this work. Thank you to Mr James Hodson for providing me with continued statistical advice and patience as I gradually mastered SPSS over the course of this project.

I would like to acknowledge the British Heart Foundation for supporting this research through the award of a Project Grant (PG/14/74/31056), and also all the patients who enthusiastically participated; without them, this project would not have been feasible.

Finally, I would like to thank my wife, Grace. You have been neverendingly supportive and understanding during this research and thesis write up period; none of my achievements would have been possible without your encouragement.

## EXTENT OF PERSONAL CONTRIBUTION

All work presented in this thesis was carried out by myself, with the following notable exceptions. The original research hypothesis and grant funding were obtained by Dr Richard Steeds and Dr Nicola Edwards. Approval from the Research Ethics Committee and the study sponsor was sought by myself. I was responsible for recruiting and consenting all patients at the three surgical sites, for arranging and performing all study visits. I was responsible for the ethics committee amendments and maintained all regulatory documents with assistance from the research nurse team.

Cardiac magnetic resonance studies were acquired by me, with assistance from my clinical research fellow colleagues (Dr Shanat Baig, Dr Anna Price, Dr Manvir Hayer and Dr Ravi Vijapurapu). I performed all cardiopulmonary exercise testing; cardiopulmonary stress echocardiogram was performed Dr Richard Steeds, Dr Nicola Edwards and myself. I analysed all cardiac magnetic resonance studies, including volumetric assessments, T1 mapping and myocardial strain quantifications. Dr Ahmed Dardeer performed additional myocardial strain quantifications in healthy controls, allowing me to assess the inter-observer reproducibility of the cardiac magnetic resonance feature-tracking technique. I analysed all data prior to un-blinding of the study and performed statistical analyses with assistance from the statistician Mr James Hodson.

Intra-operative surgical biopsy specimens were taken by cardiac surgeons Mr Moninder Bhabra, Mr Ramesh Patel, Mr Thomas Barker, Mr Nicolas Nikolaidis and Mr Stephen Billing. I fixed these specimens in formalin and delivered them from the three surgical sites to the histopathology department of University Hospital Birmingham where stained microscopy slides were provided to me for further analyses. Subjective histological

examination of the biopsy sections was carried out by Dr Desley Neil. High magnification digital scanning of histological slides and objective histological fibrosis quantification was performed by me.

I performed blood tests and delivered serum samples for biomarker analyses at the clinical biochemistry and immunology departments of University Hospital Birmingham, University of Birmingham, and Liverpool Clinical Laboratories. The separation of serum from blood as performed by myself and clinical biochemists at the Wellcome Clinical Research Facility.

For the pilot studies presented within the appendix, I recorded and analysed signal-averaged electrocardiograms. Holter electrocardiograms data were analysed by cardiac physiologists at University Hospital Birmingham before I categorised the data into Lown-Wolf grading. 4D flow cardiac magnetic resonance studies were obtained by myself and Dr Victoria Stoll; analyses of 4D flow studies were performed by Dr Victoria Stoll.

My supervisors Dr Richard Steeds, Dr Nicola Edwards and Professor Gerard Nash all provided assistance throughout the study with general advice, guidance and writing of manuscripts.

## TABLE OF CONTENTS

<b>CHAPTER 1 INTRODUCTION.....</b>	<b>1</b>
1.1 Overview.....	1
1.2 Mitral valve anatomy and function in health .....	4
1.2.1 Leaflets .....	4
1.2.2 Annulus.....	4
1.2.3 Chords.....	8
1.2.4 Papillary muscles.....	8
1.3 Classification of primary mitral regurgitation .....	10
1.4 Natural history and diagnosis of mitral regurgitation.....	12
1.4.1 Natural history .....	12
1.4.2 Diagnosis and mechanistic evaluation.....	13
1.4.3 Quantification of mitral regurgitation.....	18
1.5 Management of primary mitral regurgitation .....	29
1.5.1 Mitral valve surgery.....	29
1.5.2 International guidelines .....	30
1.5.3 Controversy in the timing of surgery.....	34
1.6 Myocardial response to primary mitral regurgitation .....	37
1.6.1 The dynamic myocardial matrix.....	37
1.6.2 Insight into ventricular remodelling from animal models.....	39
1.6.3 Clinical models of ventricular response to primary mitral regurgitation .....	40
1.7 Non-invasive monitoring of myocardial fibrosis.....	45
1.7.1 Serum biomarkers of myocardial fibrosis .....	45
1.7.2 Functional markers of myocardial fibrosis.....	46
1.7.3 Direct myocardial fibrosis imaging.....	48
1.7.4 Rationale for CMR-derived ECV as an early marker of ventricular remodelling in MR .....	53
1.8 Summary.....	54
1.9 Aims and hypotheses .....	57
<b>CHAPTER 2 METHODS: ASSESSMENT OF FUNCTIONAL STATUS, BIOCHEMICAL MARKERS AND CARDIOVASCULAR STRUCTURE AND FUNCTION.....</b>	<b>59</b>
2.1 Study design.....	59



2.1.1	Subjects.....	60
2.1.2	Ethics .....	61
2.1.3	Study promotion .....	61
2.2	Current and future strategies for risk stratification.....	65
2.2.1	Symptomatology.....	65
2.2.2	Echocardiography .....	68
2.2.3	Cardiac magnetic resonance .....	71
2.2.4	Cardiopulmonary exercise test .....	86
2.2.5	Exercise stress echocardiography .....	88
2.2.6	Haematology and biochemistry .....	91
2.2.7	Inflammation and fibrosis markers.....	91
2.3	Histology.....	92
2.3.1	Validation of collagen volume fraction quantification techniques.....	96
2.4	Perioperative outcomes and postoperative follow-up.....	100
2.5	Statistical analyses and power calculation.....	101
2.5.1	Power calculation .....	101
2.5.2	General data handling.....	101
2.5.3	Statistical methods.....	102
2.5.4	Regression models .....	102
2.5.5	Assessment of reproducibility .....	103
2.6	Summary.....	103
<b>CHAPTER 3 VALIDATION: NOVEL TECHNIQUES FOR MYOCARDIAL DEFORMATION ANALYSES.....</b>		<b>104</b>
3.1	Introduction.....	104
3.1.1	Deformation imaging.....	104
3.1.2	2D versus 3D feature tracking for the left ventricle .....	105
3.1.3	Right ventricular feature tracking in mitral valve disease.....	106
3.2	Aims and hypotheses .....	107
3.2.1	Hypotheses .....	107
3.2.2	Aims .....	107
3.2.3	Endpoints.....	108
3.3	Methods .....	108
3.3.1	Study population.....	108
3.3.2	CMR acquisition and analyses .....	109

3.3.3	Reproducibility Studies .....	114
3.3.4	Comparison of strain with other measures of systolic function .....	114
3.3.5	Statistical analyses .....	114
3.4	Results.....	115
3.4.1	Demographics, ventricular volumes and ejection fraction .....	115
3.4.2	Left ventricular reproducibility .....	115
3.4.3	Reference values for left ventricular global strain and strain rate.....	122
3.4.4	Factors influencing left ventricular 3D FT-CMR.....	125
3.4.5	Segmental Strain.....	125
3.4.6	Comparison of strain with other measures of systolic function .....	130
3.4.7	Right ventricular reproducibility .....	130
3.4.8	Reference values for RV strain and strain rate .....	134
3.5	Discussion.....	136
3.5.1	Left ventricular feature tracking.....	136
3.5.2	Right ventricular feature tracking.....	139
3.5.3	Limitations.....	140
3.5.4	Summary.....	141

**CHAPTER 4 CHARACTERISATION OF THE PRIMARY DEGENERATIVE MITRAL REGURGITATION DISEASE PROCESS – THE MITRAL FINDER STUDY..... 142**

4.1	Introduction.....	142
4.2	Aims.....	143
4.3	Methods .....	143
4.4	Results.....	144
4.4.1	Recruitment .....	144
4.4.2	Baseline demographics .....	144
4.4.3	Imaging characterisation of primary degenerative MR.....	148
4.4.4	Exercise capacity in primary degenerative MR.....	152
4.4.5	Exercise stress echocardiographic characterisation of primary degenerative MR	154
4.4.6	Sub-cohort analyses of asymptomatic patients.....	157
4.4.7	Longitudinal changes following conservative management .....	160
4.5	Discussion.....	162
4.5.1	Cohort representation .....	162

4.5.2	Comparison of surgical and non-surgical study arms .....	163
4.5.3	Longitudinal changes in ECV with conservative management.....	164
4.5.4	Limitations.....	164
4.5.5	Summary.....	165
<b>CHAPTER 5 HISTOLOGICAL QUANTIFICATION OF FIBROSIS IN PRIMARY MITRAL REGURGITATION.....</b>		<b>166</b>
5.1	Introduction.....	166
5.1.1	Histological characterisation of the myocardium in primary degenerative MR 166	
5.2	Aims and hypotheses .....	168
5.3	Methods .....	168
5.3.1	Histological techniques.....	169
5.3.2	Statistical analyses.....	171
5.4	Results.....	171
5.4.1	Histology of surgical myocardial biopsies .....	173
5.4.2	Impact of Fibrosis on Ventricular Structure and Function .....	178
5.4.3	Clinical Impact of Fibrosis on Symptoms and Exercise Capacity .....	185
5.4.4	Fibrosis and Biomarkers.....	186
5.5	Discussion.....	191
5.5.1	Limitations.....	194
5.5.2	Conclusions .....	195
<b>CHAPTER 6 PREOPERATIVE PREDICTORS OF PERI-OPERATIVE SURGICAL OUTCOMES.....</b>		<b>196</b>
6.1	Introduction.....	196
6.2	Aims and hypotheses .....	197
6.3	Methods .....	198
6.3.1	Statistical analyses.....	199
6.3.2	Missing data.....	200
6.4	Results.....	200
6.4.1	Baseline clinical data .....	200
6.4.2	Operative outcomes .....	204
6.4.3	Risk factor analyses .....	208
6.5	Discussion.....	212
6.6	Limitations .....	214

6.7	Summary .....	215
<b>CHAPTER 7 DETERMINANTS OF MEDIUM TERM POSTOPERATIVE VENTRICULAR REMODELLING AND PATIENT OUTCOMES.....</b>		<b>216</b>
7.1	Introduction.....	216
7.2	Aims and hypotheses .....	217
7.3	Methods .....	217
7.3.1	Statistical analyses.....	218
7.4	Results.....	218
7.4.1	Recruitment and follow-up.....	218
7.4.2	Baseline clinical data .....	220
7.4.3	Surgical outcomes following hospital discharge.....	220
7.4.4	Imaging characterisation following mitral valve surgery.....	222
7.4.5	Symptom burden and exercise capacity following mitral valve surgery.....	225
7.4.6	Postoperative determinants of reverse left ventricular remodelling.....	228
7.4.7	Determinants of a favourable postoperative outcome .....	230
7.5	Discussion.....	234
7.6	Limitations .....	237
7.7	Summary.....	238
<b>CHAPTER 8 CONCLUSIONS – FUTURE DIRECTIONS .....</b>		<b>240</b>
8.1	Summary of thesis findings .....	240
8.2	Future directions .....	244
8.2.1	How do we manage asymptomatic patients not wishing for early surgery? .....	244
8.2.2	Does fibrosis evaluation using imaging have a role in symptomatic severe MR patients, who are later in their disease process? .....	245
8.2.3	Why does late gadolinium enhancement develop in MR and is it of prognostic importance? .....	246
8.3	Conclusion .....	247
<b>REFERENCES .....</b>		<b>248</b>
<b>APPENDIX I: PILOT STUDY ON FIBROSIS AND ARRHYTHMIC RISK.....</b>		<b>268</b>
10.1	Background.....	268
10.1.1	Aims and hypotheses.....	270
10.2	Methods .....	271
10.3	Results .....	275
10.4	Discussion.....	278

<b>APPENDIX II: LIST OF PUBLICATIONS ARISING DIRECTLY FROM THIS WORK.....</b>	<b>280</b>
<b>APPENDIX III: LIST OF ABSTRACTS ARISING DIRECTLY FROM THIS WORK.....</b>	<b>281</b>

## LIST OF FIGURES

<b>Figure 1.1</b> Prevalence of moderate or severe mitral regurgitation in population-based studies, demonstrating a higher prevalence with increasing age. ....	3
<b>Figure 1.2</b> En-face view of the MV demonstrating mitral annulus, scallops and commissures. ....	6
<b>Figure 1.3</b> Schematic representation of the mitral annulus, highlighting its non-planar saddle-shaped nature. ....	7
<b>Figure 1.4</b> Schematic diagram of mitral valve apparatus, illustrating the attachment of chords to papillary muscles. ....	9
<b>Figure 1.5</b> Spectrum of primary degenerative mitral regurgitation. ....	11
<b>Figure 1.6</b> Example of PISA on colour Doppler. ....	23
<b>Figure 1.7</b> Example of continuous wave Doppler of the mitral regurgitation jet. ....	24
<b>Figure 1.8</b> Traditional model of left ventricular remodelling in mitral regurgitation. ....	43
<b>Figure 1.9</b> Apical spherical remodelling in MR. ....	44
<b>Figure 1.10</b> Sub-types of left ventricular myocardial wall strain. ....	47
<b>Figure 1.11</b> Schematic diagram illustrating types of myocardial fibrosis. ....	51
<b>Figure 2.1</b> Study design flowchart. ....	63
<b>Figure 2.2</b> NYHA classification versus cardiopulmonary exercise test performance in patients with aortic stenosis (156). ....	66
<b>Figure 2.3</b> Standard cardiac magnetic resonance imaging protocol. ....	74
<b>Figure 2.4</b> Imaging planes for dedicated mitral valve views in a patient with P2 and P3 scallop prolapse. ....	75
<b>Figure 2.5</b> 3(3)3(3)5 MOLLI scheme for T1 mapping in the heart (133). ....	78
<b>Figure 2.6</b> Illustrative example of ROI and 20:20 offset approaches to T1 quantification in a native MOLLI sequence. ....	83
<b>Figure 2.7</b> Effect of endocardial and epicardial offsets on calculated ECV. ....	84
<b>Figure 2.8</b> Stress echocardiography protocol. ....	90
<b>Figure 2.9</b> User supervised training of CVF quantification using Ilastik. ....	94

<b>Figure 2.10</b> Visual illustration of the data output following the Ilastik based characterisation of EHVG and MT sections into fibrosis and muscle tissue. ....	98
<b>Figure 2.11</b> Scatter plots demonstrating relationship of collagen volume fraction results between automated classification by Ilastik and expert quantification for Masson’s Trichrome (top) and Elastic Van Gieson (bottom). ....	99
<b>Figure 3.1</b> Steps taken for 3D FT-CMR. ....	110
<b>Figure 3.2</b> Contouring for RV strain, with the timing of peak strain interpretation on the strain curve. ....	113
<b>Figure 3.3</b> Bland-Altman plots for intra-observer bias for 3D peak GCS, GRS, and GLS. ....	120
<b>Figure 3.4</b> Bland-Altman plots for inter-observer bias for 3D peak GCS, GRS, and GLS. ....	121
<b>Figure 3.5</b> 16 segment model illustrating peak $GCS \pm SD$ with mean intra-observer absolute bias $\pm SD$ and ICC. ....	127
<b>Figure 3.6</b> 16 segment model illustrating peak $GRS \pm SD$ with mean absolute intra-observer bias $\pm SD$ and ICC. ....	128
<b>Figure 3.7</b> 16 segment model illustrating peak $GLS \pm SD$ with mean absolute intra-observer bias $\pm SD$ and ICC. ....	129
<b>Figure 3.8</b> Correlation of 3D GCS against LVEF. ....	131
<b>Figure 3.9</b> Bland-Altman plot illustrating inter-observer bias for RV $E_{II}$ . ....	133
<b>Figure 4.1</b> Mitral FINDER study patient recruitment summary. ....	146
<b>Figure 4.2</b> Illustrative example of the appearance of myocardial fibrosis on CMR. ....	151
<b>Figure 5.1</b> Manual quantification of myofiber cross sectional area using ZEN. ....	170
<b>Figure 5.2</b> Distribution of A) cardiomyocyte CSA and B) CVF, in controls and MR patients (left), and their relationship with increasing symptoms in MR patients (right). ...	175
<b>Figure 5.3</b> Histological specimens from mitral regurgitation patients and controls. ....	176
<b>Figure 5.4</b> Modified Bland-Altman plot of the consistency of CVF by biopsy site. ....	177
<b>Figure 5.5</b> Impact of myocardial fibrosis in primary degenerative mitral regurgitation. .	182
<b>Figure 5.6</b> Relationship between ECV and histological evidence of interstitial fibrosis on biopsy ( $CVF_{mean}$ ). ....	183

<b>Figure 5.7.</b> Box plot illustrating the distribution of patient symptoms according to NYHA class. ....	184
<b>Figure 7.1</b> Flow diagram summarising patient recruitment and follow-up. ....	219
<b>Figure 7.2</b> Scatter plot demonstrating the relationship between preoperative and magnitude of change in postoperative CMR parameters for A) ECV and B) LVEF. ....	224
<b>Figure 7.3</b> Clustered bar chart showing mean postoperative CMR values based on preoperative symptom status. ....	229



## LIST OF TABLES

<b>Table 1.1</b> Quantitative and qualitative methods of MR quantification via echocardiography (29).....	19
<b>Table 1.2</b> Grading the severity of primary chronic MR by echocardiography (43). .....	25
<b>Table 1.3</b> Classes of recommendations utilised by European and American guidelines....	31
<b>Table 1.4</b> Levels of evidence utilised by European and American guidelines .....	32
<b>Table 1.5</b> Summary of current European (24) and American (20, 25) guidance on the timing of surgery for primary mitral regurgitation.....	33
<b>Table 1.6</b> Spectrum of adaptive processes in ventricular remodelling with primary mitral regurgitation and corresponding imaging observations. Text in bold highlights areas which this thesis investigates. ....	56
<b>Table 2.1</b> Study eligibility criteria (152). ....	64
<b>Table 2.2</b> Baseline echocardiographic parameters collected from clinically indicated studies (163). ....	69
<b>Table 3.1</b> Baseline demographics of 100 healthy subjects. ....	117
<b>Table 3.2</b> Ventricular volumes and function according to age decile.....	118
<b>Table 3.3</b> 2D vs 3D intra- and inter-observer reproducibility for peak strain and strain rates.....	119
<b>Table 3.4</b> Comparison of 2D vs. 3D FT-CMR strains and strain rates.....	123
<b>Table 3.5</b> Reference values for 3D FT-CMR.....	124
<b>Table 3.6</b> .....	126
<b>Table 3.7</b> Reproducibility studies for RV free-wall deformation. ....	132
<b>Table 3.8</b> Reference values for RV strain and strain rate strain. ....	135
<b>Table 4.1</b> Baseline clinical characteristics of surgical versus non-surgical patients. ....	147
<b>Table 4.2</b> Cardiac magnetic resonance characteristics of surgical and non-surgical patients. ....	150
<b>Table 4.3</b> Cardiopulmonary exercise test parameters .....	153
<b>Table 4.4</b> Exercise stress echocardiography parameters at rest and peak exercise. ....	156

<b>Table 4.5</b> Sub-cohort analyses between NYHA class I patients opting for surgical and non-surgical management.....	158
<b>Table 4.6</b> Longitudinal CMR parameters in conservatively managed asymptomatic MR patients (N=12).....	161
<b>Table 5.1</b> Clinical characteristics of conservative and surgical patients. ....	172
<b>Table 5.2</b> Correlation of histological fibrosis against non-invasive preoperative imaging parameters.....	180
<b>Table 5.3</b> Cardiac magnetic resonance parameters according to the sub-type of MR.....	181
<b>Table 5.4</b> Baseline characteristics of surgical patients according to symptom status. ....	187
<b>Table 5.5</b> Linear regression analyses of symptom burden against histology, cardiac imaging and pulmonary pressures. ....	188
<b>Table 5.6</b> Spearman’s correlation between NYHA class, MLHFQ and %PredVO2max.	189
<b>Table 5.7</b> Correlation of serum biomarkers against histological and imaging measures of myocardial fibrosis. ....	190
<b>Table 6.1</b> Comparison of clinical parameters between asymptomatic and symptomatic surgical patients. ....	202
<b>Table 6.2</b> Summary of operative and postoperative parameters in the Mitral FINDER cohort.....	206
<b>Table 6.3</b> Risk factor exploration for primary endpoints.....	209
<b>Table 6.4</b> Summary of sub-cohort analyses for determination of primary endpoints .....	211
<b>Table 7.1</b> Summary of the incidences of adverse events during postoperative follow-up in symptomatic and asymptomatic MR patients.....	221
<b>Table 7.2</b> Comparison of CMR parameters before and after surgery.....	223
<b>Table 7.3</b> Changes in exercise parameters following surgery according to preoperative symptom status (N=89). ....	226
<b>Table 7.4</b> Changes in objective measures of symptom burden following surgery according to preoperative symptom status (N=94). ....	227
<b>Table 7.5</b> Correlations between preoperative parameters and secondary outcomes. ....	232
<b>Table 10.1</b> Lown-Wolf classification of ventricular ectopy .....	274

<b>Table 10.2</b> Relationship between LGE presence and MR subtype.....	276
<b>Table 10.3</b> Electrocardiographic characteristics of surgical and non-surgical cohorts ....	277

## LIST OF ABBREVIATIONS

95% CI	95% confidence interval
AF	atrial fibrillation
AMVL	anterior mitral valve leaflet
AT	anaerobic threshold
BD	Barlow's disease
BMI	body mass index
BSA	body surface area
CMR	cardiac magnetic resonance
CVF	collagen volume fraction
eGFR	estimated glomerular filtration rate
ECM	extracellular matrix
ECV	extracellular volume
$E_{11}$	two-dimensional peak longitudinal strain
FED	fibroelastic deficiency
FT-CMR	feature tracking-cardiac magnetic resonance
GCS	global circumferential strain
GLS	global longitudinal strain
GRS	global radial strain
IQR	interquartile range
LA	left atrium
LGE	late gadolinium enhancement
LV	left ventricle
LVEDd	left ventricular end diastolic dimension
LVEDV	left ventricular end diastolic volume
LVEDVi	left ventricular end diastolic volume indexed for body surface area
LVEF	left ventricular ejection fraction
LVESd	left ventricular end systolic dimension
LVESV	left ventricular end systolic volume

LVESVi	left ventricular end systolic volume indexed for body surface area
LVM	left ventricular mass
LVMi	left ventricular mass indexed for body surface area
MR	mitral regurgitation
MV	mitral valve
MVP	mitral valve prolapse
NTproBNP	N-terminal prohormone of brain natriuretic peptide
PMVL	posterior mitral valve leaflet
RA	right atrium
RV	right ventricle
RVEDV	right ventricular end diastolic volume
RVEDVi	right ventricular end diastolic volume indexed for body surface area
RVEF	right ventricular ejection fraction
RVESV	right ventricular end systolic volume
RVESVi	right ventricular end systolic volume indexed for body surface area
sPAP	systolic pulmonary artery pressure
SD	standard deviation
SV	stroke volume
TOE	transoesophageal echocardiogram
TTE	transthoracic echocardiogram
VCO <sub>2</sub>	carbon dioxide production
VE	minute ventilation
VO <sub>2</sub>	oxygen consumption

# CHAPTER 1

## INTRODUCTION

### 1.1 Overview

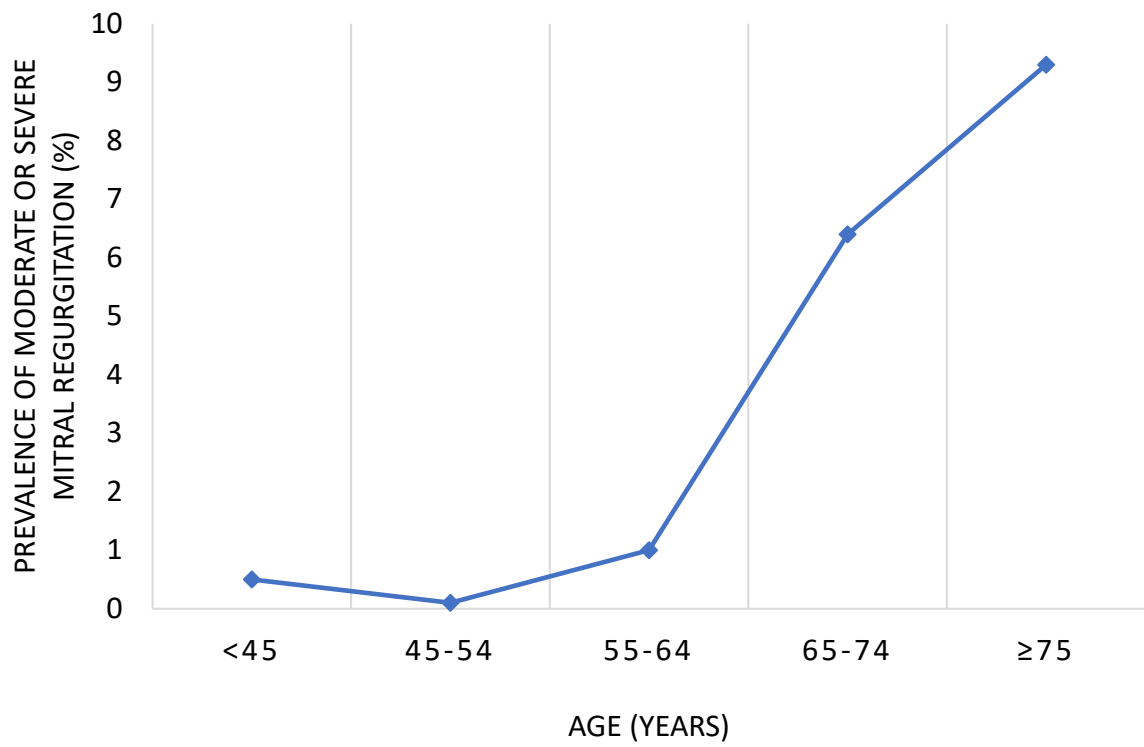
Mitral regurgitation (MR), defined as the systolic retrograde flow of blood from the left ventricle (LV) into the left atrium (LA), is the most common form of valvular disease in the USA, affecting 2.5% of the general population and over 10% of those aged above 75 years (**Figure 1.1**) (1). It is the second most frequent valve disease requiring surgery in Europe (2), and the prevalence of moderate-to-severe MR is expected to double by 2030 due to an ageing population, representing a growing health problem of developed nations (2).

Primary degenerative MR occurs due to an intrinsic abnormality of the valve apparatus and is associated with high morbidity and mortality which directly correlate to the severity of the regurgitation (3). Secondary MR occurs due to a fault with the left ventricle (LV) but the valve apparatus remains intact and is not covered within the scope of this thesis. As there are no known medical therapies which alter disease progression in primary degenerative MR, care is focused on regular clinical surveillance in valve clinics and timely surgical intervention which improves outcome and allows the restoration of normal life expectancy (4, 5).

The challenge arises because the assessment and quantification of regurgitation severity is imperfect, and symptom status and ventricular function are not directly related to increasing regurgitation severity (6).

Instead, it is believed that the progression of MR triggers remodelling of the myocardium, which in turn leads to functional impairment. Finally, for chronic primary MR, its onset is insidious and progression is often slow, meaning that a long period is required for repeat assessment. The work presented within this thesis aims to tackle the challenges we face in the management of chronic primary MR through the characterisation of myocardial remodelling and quantification of sub-clinical changes in patients' symptom burden, for the purposes of identifying novel biomarkers which can optimise the timing of surgery.

**Figure 1.1** Prevalence of moderate or severe mitral regurgitation in population-based studies, demonstrating a higher prevalence with increasing age.



Adapted from Nkomo et al. 2006 (1).



## 1.2 Mitral valve anatomy and function in health

The mitral valve (MV) apparatus is an intricate set of anatomical structures, consisting of anterior and posterior leaflets that take origin from the MV annulus, and are connected via tendinous cords to the ventricle and papillary muscles (7). The functional competence of the MV is determined not only by the structures intrinsic to the MV apparatus but is also reliant upon the normal structure and function of the LA and LV.

### 1.2.1 Leaflets

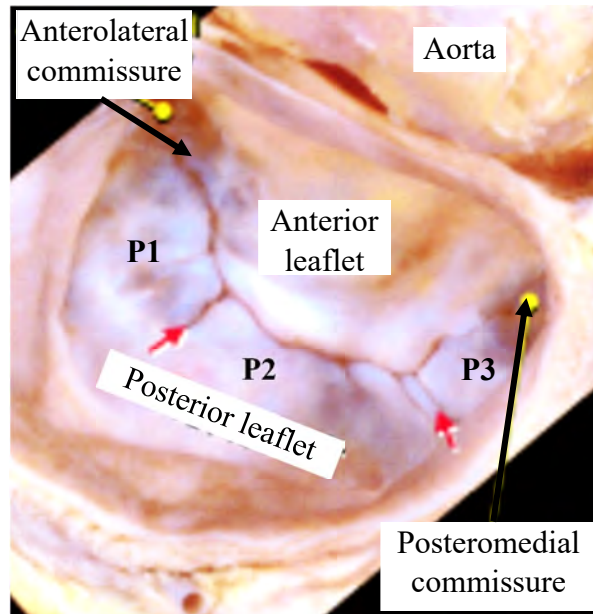
The posterior mitral valve leaflet (PMVL) guards two-thirds of the circumference of the MV orifice and usually has two minor indentations or clefts, which divides the leaflet into 3 scallops (**Figure 1.2**). These scallops are referred to as P1 (anterolateral), P2 (middle) and P3 (posteromedial) according to the Carpentier classification (8). The anterior mitral valve leaflet (AMVL) guards the remaining one-third of the circumference of the MV orifice but has few or no marginal indentations. Despite this, the opposing corresponding area of AMVL is termed A1, A2 and A3 scallops. When the MV is closed, each end of the closure line is referred to as a commissure, termed the anterolateral and posteromedial commissures. Complete coaptation and correct apposition (symmetrical overlap, usually a minimum of 4-5mm) of both leaflets are essential in preventing regurgitation.

### 1.2.2 Annulus

The MV annulus consists of fibrocollagenous elements from which the fibrous core of the leaflets take origin, and it is this variation of elements that define the change in shape of the annulus during the cardiac cycle to ensure optimal efficiency in valvular action (7). The normal annulus is oval in shape with the diameter through the commissures larger

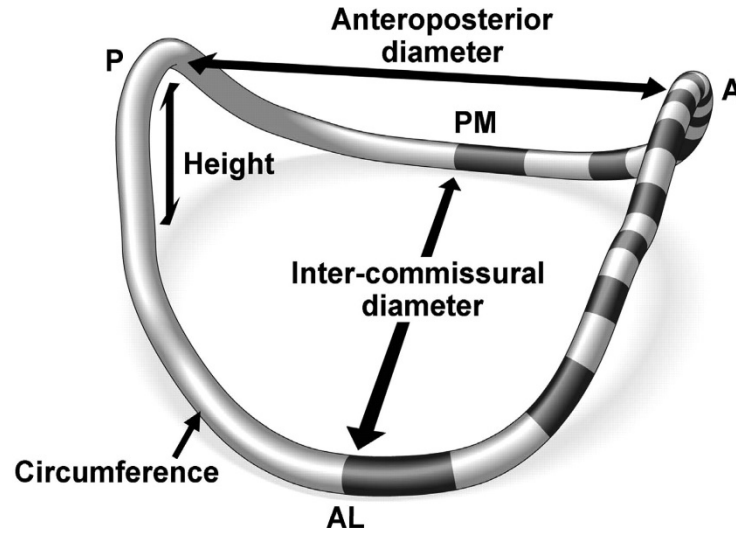
than the anteroposterior diameter (running through A2 / P2 scallops). Furthermore, the annulus is nonplanar with the anterior and posterior aspects raised compared to the intercommissural points to create a saddle shape (**Figure 1.3**) (9). In MR, both annular shape and its deformation pattern during the cardiac cycle may be distorted, contributing to MV incompetence.

**Figure 1.2** En-face view of the MV demonstrating mitral annulus, scallops and commissures.



Red arrows highlight the presence of clefts between the scallops P1-P3 in the PMVL. Reproduced, with permission, from Ho et al. 2002 (10).

**Figure 1.3** Schematic representation of the mitral annulus, highlighting its non-planar saddle-shaped nature.



Reproduced with permission from Grewal et al. 2010 (9).

### 1.2.3 Chords

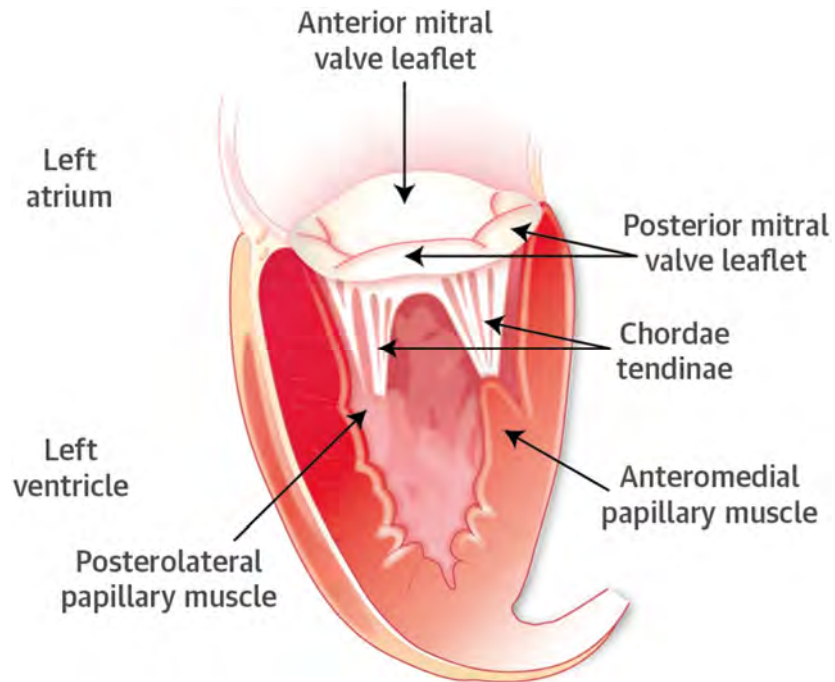
From the leaflets, tendinous chords anchor the leaflets to the LV and papillary muscles (**Figure 1.4**). These chords are classified as either primary, secondary or tertiary depending on their attachment (11). Primary chords connect the free edge of the leaflet to papillary muscles. Secondary chords attach the body of the leaflet to papillary muscles. Tertiary chords are only found in the basal zone of the PMVL and attach directly to the LV wall.

The thinner primary chords maintain leaflet apposition and facilitate valve closure, so that sectioning results in acute MR. Sectioning secondary chords, in contrast, does not produce mitral regurgitation, and it is believed that they play a role in maintaining normal LV size and geometry (12).

### 1.2.4 Papillary muscles

Papillary muscles, located in the anterolateral and posteromedial positions, arise from the apical and middle thirds of the LV (**Figure 1.4**). The anterolateral papillary muscle is usually single but contains a groove in the same direction as the MV commissure and is supplied by the left anterior descending and the diagonal or a marginal branch of the circumflex artery. In contrast, the posteromedial location usually consists of two to three muscles, or a single muscle with two or three heads and is supplied by the right coronary or left circumflex artery depending on dominance (13).

**Figure 1.4** Schematic diagram of mitral valve apparatus, illustrating the attachment of chords to papillary muscles.



Reproduced, with permission, from Asgar et al 2015 (14).

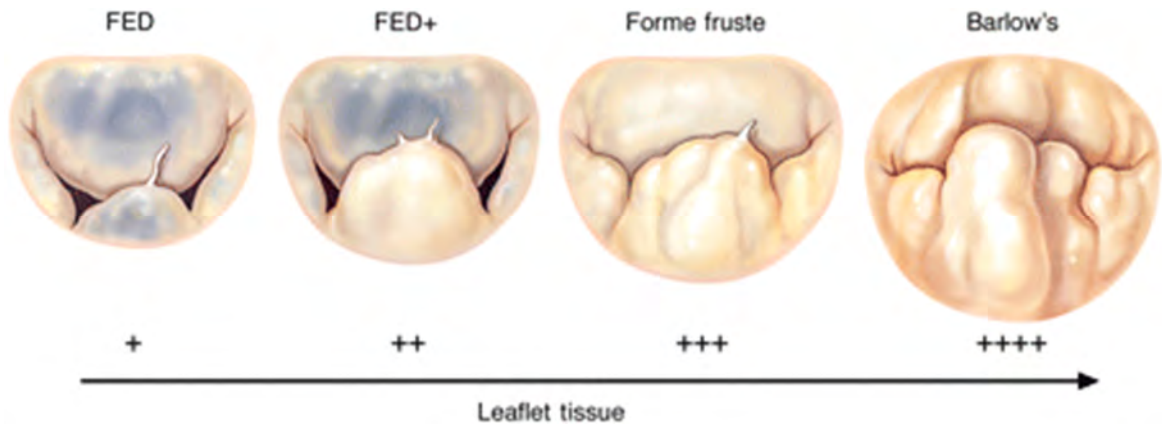
### 1.3 Classification of primary mitral regurgitation

The most common cause of primary MR in the developed world is degeneration of the valve, with less common causes including rheumatic heart disease and infective endocarditis. This thesis will now focus on primary degenerative MR.

Primary degenerative MR represents a spectrum of pathological processes observed in clinical practice (**Figure 1.5**) (15). This ranges from fibroelastic deficiency (FED), which was first described by Carpentier, where chordal rupture results in a simple flail scallop (16), to the multi-segment prolapse of one or both thickened and myxomatous leaflets in Barlow's disease (BD) (17). *Forme fruste* was the descriptive label given to cases where some but not all features of BD were present, highlighting that there is a spectrum of lesions (15).

In addition to the above classification systems, a widely adopted surgical classification of MR was offered by Carpentier (8). The Carpentier classification, based upon leaflet motion, denotes type I MR as those with normal motion (as in cases of annular dilatation or leaflet perforation), type II as cases with increased motion (prolapsing or flail leaflet), and type III as cases with restricted leaflet motion (rheumatic or ischaemic). Primary degenerative MR is therefore classed as Carpentier type II.

**Figure 1.5** Spectrum of primary degenerative mitral regurgitation.



Fibroelastic deficiency (FED) is characterised by thin-leaflets with a single scallop prolapse. Barlow's disease is characterised by myxomatous leaflets with multi-segment prolapse. Reproduced with permission from Adams et al. 2010 (15).



## 1.4 Natural history and diagnosis of mitral regurgitation

### 1.4.1 Natural history

The prevalence of primary mitral valve prolapse (MVP) has been estimated to be 1.7% in the general US population (1). The severity of MR tends to worsen during longitudinal follow-up with one study on 74 patients with at least mild degenerative MR reporting average annual increases in regurgitant volume of 7.4ml or regurgitant fraction of 2.9% (18). However, there is wide individual variation with regression of regurgitant severity and increase in regurgitation volume of >8ml occurring in 11% and 51% respectively. On multivariate analyses, progression of annular dilatation and development of new flail leaflets were independent predictors of worsening MR (18).

The symptoms and signs associated with MR include exertional dyspnoea, orthopnoea, fatigue, peripheral and pulmonary oedema, and palpitations arising from associated atrial arrhythmias (19, 20).

Difficulty in the management of primary MR partly arises due to the occasionally conflicting longitudinal data. On the one hand, it is well established that clinical symptoms may be absent for years despite severe regurgitation (21). Conversely, it is also recognised that the overall morbidity and mortality associated with MR is high and seems to be directly related to the severity of regurgitation (3). In those with severe primary MR, when medically treated, mortality may be as high as 6.3% per annum, increasing to 34% per annum if patients were experiencing any New York Heart Association (NYHA) class III or IV dyspnoea (22). Amongst patients with severe MR and NYHA class I or II symptoms, the rate of heart failure, atrial fibrillation, and death or surgery were 63±8, 30±12, and

90±3% respectively at 10 years (22). In a recent epidemiological study of community patients identified via the Mayo Clinic and Rochester Epidemiology Project over a 10-year period, a diagnosis of primary MR in a community with modern facilities, diagnostic expertise and easy access to cardiac surgery, was still associated with increased mortality rates (relative risk 1.73, 95% confidence interval 1.53 – 1.96, P<0.0001) compared to the general population (23). This level of risk persists even in those patients with few comorbidities and good underlying ventricular function. There are no known medical therapies which can reduce MR progression or the associated risk of mortality, therefore management focuses on accurate diagnosis and periodic evaluation to optimise the timing of surgery (22, 24, 25).

#### 1.4.2 Diagnosis and mechanistic evaluation

MR is usually diagnosed on clinical examination through auscultation (17) or via transthoracic echocardiography (TTE) (20). MR may be discovered incidentally or after the onset of symptoms. However, active screening in the community with echocardiography has revealed a hidden burden of valve disease (26).

TTE is the first-line investigation in the diagnosis of MR, assessment of its severity, and quantification of its effects on chamber sizes, ventricular function, and the pulmonary circulation (24). Furthermore, precise anatomical characterisation of the individual components of the valvular and sub-valvular apparatus is recommended for determining the mechanism and reparability of MR (27). Whilst TTE may be sufficient in some cases, transoesophageal echocardiography (TOE) is generally recommended, particularly in the presence of suboptimal imaging quality (24).

Accurate identification of the underlying mechanism of MR, including the assessment of leaflets, annulus, chordate tendonnae and papillary muscles is essential. Confirmation that the MR is primary rather than secondary will alter whether a valve repair or replacement is more likely. It is widely accepted that the successful repair of a valve is always superior to replacement in primary MR, and indeed, for patients with severe but asymptomatic primary degenerative MR, a high probability of a durable repair is a prerequisite for proceeding with surgery (24). For primary degenerative MR, the repair of a single scallop prolapse is simple, whereas repairing a large floppy valve with bileaflet multi-segmental involvement and higher prolapsing height is technically complex as it may require multiple resections or patch augmentation. Whilst echocardiography remains gold-standard in the assessment of MV structure and can provide an objective means of predicting mitral repair complexity (28), there is growing data on the role of CMR (29). The following section will review the relative role of echocardiography vs CMR.

#### *1.4.2.1 Identification of prolapse and assessment of leaflets*

While two dimensional (2D) TTE is recommended as the first-line examination, three dimensional (3D) TTE provides incremental value in establishing the lesion, leaflet at fault and location of the segments involved compared to 2D TTE, with an accuracy that is equivalent to 2D multiplane transoesophageal echocardiography (TOE) (30). 3D TOE has the greatest overall accuracy as a result of higher specificity in the segmental localisation of defects (92.8%) compared to surgical findings and is particularly effective in the localisation of flail defects (99%). Moreover, 3D TOE has the advantage of producing both static and dynamic measurements of MV anatomy and pathology that can predict

both the complexity of repair and likely outcome at surgery, including prolapse height, prolapse volume, anterior leaflet surface area and leaflet length (28, 30). These measurements can be made with high accuracy and reproducibility on both 2D and 3D echocardiography due to high temporal resolution and improved frame rates with the development of multi-line focussed transmit and receive systems.

In contrast, although there are data that suggest CMR may be as good as 2D TTE and 2D TOE in the detection of billowing, prolapse, and flail leaflets, studies are limited and comparisons with 3D echocardiography are lacking. Moreover, CMR for detection of leaflet abnormalities requires a dedicated set of sequences that requires time and experience (31). Using a set protocol with dedicated valve imaging planes on CMR, one group were able to diagnose the presence of PMVL prolapse with 100% sensitivity and AMVL leaflet prolapse with 78% sensitivity when compared to 2D TTE, but the study did not compare accuracy to surgical findings (32). In another study of 27 patients, CMR correctly identified the presence or absence of a segmental defect in 82% comparing to 2D TTE (33). In 43 patients using surgical findings as the reference standard, results on CMR and 2D TOE were concordant in terms of diagnosing prolapse and identification of the leaflet at fault but data on identification of the scallop at fault was not given (34). Correct identification not only of the leaflet at fault but of the specific scallop is now the expected standard in preoperative assessment of primary MR, and the degree of accuracy in the existing literature for CMR does not match the current capabilities of 3D echocardiography.

#### *1.4.2.2 Annulus*

In MR patients, three-dimensional transoesophageal echocardiography (3D TOE) has highlighted that there are not only alterations in the saddle shape at rest, but also impairment of its dynamic movements during systole (early systolic area contraction and deepening of the saddle-shape), which are required for reducing mechanical stress across the mitral leaflets and maintaining normal valve competence (9, 35). The mechanism of annular distortion is different between primary and secondary MR, and different across different primary MR cases, highlighting the key role 3D echo imaging plays during the preoperative assessment of MR.

Two difficulties have been encountered in establishing an optimal imaging strategy for the MV annulus: firstly, the surgical reference for sizing is performed in a de-aired heart and therefore these measurements do not correspond to 'live' imaging; secondly, 3D TOE has highlighted that the annulus is not fixed but dynamic throughout the cardiac cycle, with change in size (early systolic area contraction) and shape (deepening of the saddle-shape) (9). There are no data on the accuracy of CMR based assessment of MV annular dimensions compared to echocardiography or surgical findings in primary MR.

Measurements of annular dimension on 2D TTE are limited by the use of standard imaging planes that do not necessarily measure the correct annular dimension, meaning that 3D echocardiography is currently gold-standard for annulus imaging (9).

#### *1.4.2.3 Assessment of chordae*

The location and attachment of the primary and secondary chordae is critical to current surgical strategies for MV repair. The location, length and thickness of the mitral chordae

can be measured on 2D echo due to higher spatial resolution and are best visualised on 2D TOE from the transgastric view (36). Although the subvalvular apparatus, including chordae, leaflets and papillary muscle attachments, can be seen routinely on CMR, detailed assessment is much more limited compared with 2D echo which, remains the modality of choice.

#### *1.4.2.4 Assessment of papillary muscles*

Assessment of papillary muscle location, displacement and function (whether ruptured, fibrotic, infarcted or displaced) is important for establishing the mechanism of the MR yet there are no comparative data on the utility of echo and CMR in this regard. Data with echo is more compelling; 2D TTE has demonstrated abnormal superior displacement of PM tips during systole as one mechanism contributing to MV prolapse (37). 3D TOE has demonstrated PM displacement secondary to progressive LV dilatation with resultant leaflet tethering, as well as the relationship between PMs and LV wall which may assist surgical planning of MV repair (38).

There are limited data on the use of CMR to locate, size and track PM displacement; its main advantage over echocardiography lies in its ability for myocardial characterisation. Papillary muscle fibrosis is readily observed in primary MR as late gadolinium enhancement (LGE) on CMR (39). There is growing evidence that this may have important mechanical and electrophysiological implications. Preliminary studies have demonstrated a reduction in papillary muscle contraction in MR patients compared to controls (40), and a higher prevalence of papillary muscle fibrosis has been observed in

MR patients who were victims of sudden cardiac death (41), with increased papillary muscle traction demonstrated to lower the threshold for ventricular arrhythmia (42).

In summary echo remains the current gold standard for anatomic and functional assessment of the MV apparatus in primary MR, enabling precise localisation of the abnormality and determination of aetiology, as well as being key for planning and guiding intervention. There are very limited data on the role of CMR in defining mitral apparatus anatomy with the restricted spatial and temporal resolution remaining key barriers. CMR may have a potential use in the detection of papillary muscle fibrosis, but more data is required on its clinical implications.

### 1.4.3 Quantification of mitral regurgitation

#### *1.4.3.1 Quantification by echocardiography*

The accurate quantification of regurgitation severity is essential for the management of MR. Echocardiography is the first-line imaging modality for establishing the severity of MR. There are multiple qualitative, semi-quantitative and quantitative methods for the quantification of MR via echocardiography. No single methodology is gold standard with each technique featuring a unique set of advantages and limitations (**Table 1.1**). Current guidelines recognise this and recommends a multi-parametric approach to the grading of MR severity (43). This means that the echocardiographer needs to be aware of the different sensitivity, specificity and limitations of each technique, and weigh up the impact of each parameter, for example, giving particular weight to the qualitative appearance of flow convergence throughout systole and semi-quantitative appearance of systolic flow reversal in the pulmonary veins in identifying severe MR.

**Table 1.1** Quantitative and qualitative methods of MR quantification via echocardiography (29).

Method	Advantages	Limitations
<b>Quantitative quantification</b>		
<b>Stroke volumes method (2D/3D)</b> $(R_{Vol} = SV_{MV} - SV_{LVOT})$  <i>Method 1</i> $R_{Vol} = (Area_{MV} \times VTI_{MV}) - (Area_{LVOT} \times VTI_{LVOT})$  <i>Method 2</i> $R_{Vol} = (LVEDV - LVESV) - (Area_{LVOT} \times VTI_{LVOT})$	Quantitative methods which can be used for multiple or eccentric jets	Different $SV_{LVO}$ can be obtained via $(Area_{LVOT} \times VTI_{LVOT})$ or $(LVEDV - LVESV)$  Measurement errors in annular dimension are squared to calculate area, which is multiplied by error in VTI, resulting in poor inter-observer agreement (44)  Optimal LV volumes and LVOT area require 3D echo +/- contrast
<b>Flow convergence method by PISA</b>  $R_{Vol} = EROA \times VTI_{reg}$  Where: $EROA = 2\pi r^2 \times Vr / PeakV_{reg}$	Independent predictive power with outcome (3)  Rapid to perform	PISA inaccurate in presence of eccentric or multiple jets  PISA not applicable when PISA shell is not hemispherical  Multiple measurement errors are compounded  Low expert reproducibility (45)
<b>Qualitative quantification</b>		
<b>PISA</b>	Fast and simple method that assumes a hemispherical convergence of flow towards a circular regurgitant orifice	PISA inaccurate in presence of eccentric or multiple jets  Overestimation when MR not holosystolic



<b>VC width</b>	Easily measured in parasternal LAX view  Good for differentiating mild from severe MR	Limited for multiple jets  Convergence zone needs to be visualised for adequate measurement Overestimation when MR not holosystolic
<b>3D VC area on colour Doppler</b>	Direct measurement on 3D echo  Can measure multiple jets of differing directions	Limited temporal and spatial resolution  Subject to colour Doppler blooming  Overestimation when MR not holosystolic  Cumbersome to analyse
<b>Colour flow jet area</b>	Easy to measure in apical view	Unreliable, dependent on haemodynamic loading conditions
<b>Pulmonary vein flow</b>	Systolic flow reversal in more than one vein is specific for severe MR  Normal pulmonary venous flow suggests absence of severe MR	Mild or moderate MR directed into pulmonary vein can alter flow pattern  Large left atrium may make inaccurate

*Abbreviations: 2D 2 dimension; 3D 3 dimension; EROA effective regurgitant orifice area; LV left ventricle; LVEDV left ventricular end-diastolic volume; LVESV left ventricular end-systolic volume; LVOT left ventricular outflow tract; MV mitral valve; PISA proximal isovelocity surface area;  $R_{vol}$  regurgitant volume; SV stroke volume; VC vena contracta; VTI velocity time integral.*

Colour Doppler can be used to visualise the Doppler shift occurring as a result of the mitral valve regurgitation jet (43). The width of the jet at its narrowest, termed the vena contracta (VC), occurs when the regurgitant jet crosses the mitral valve. VC is a good indicator of MR severity because it correlates with the cross-sectional area of the orifice via which the regurgitation occurs. Additionally, as ventricular blood accelerates towards the atrium during ventricular systole, a hemispherical shaped proximal flow convergence zone is created where the velocity of blood exceeds the aliasing velocity (also termed the Nyquist limit, defined as half of the sampling rate of the echo probe). The radius of this hemisphere where blood velocity equals the Nyquist limit, can be used to calculate the proximal isovelocity surface area (PISA). This allows the derivation of regurgitant volume using the equation:

$$\text{Mitral regurgitant volume } (Q) = \text{PISA} \times \text{Nyquist limit}$$

Additionally, by utilising the conservation of mass principle, we can also derive the effective regurgitant orifice area (EROA) across the MV using the equation:

$$\text{EROA} = Q \div \text{peak regurgitant jet velocity}$$

The peak regurgitant jet velocity can be measured using Doppler echocardiography using continuous wave (CW) Doppler whereby all velocities of blood along a single line of interrogation (placed through the mitral valve) is recorded on a graph of velocity against time. The Doppler signal can be restricted to a specific site using pulsed wave (PW) ultrasound.

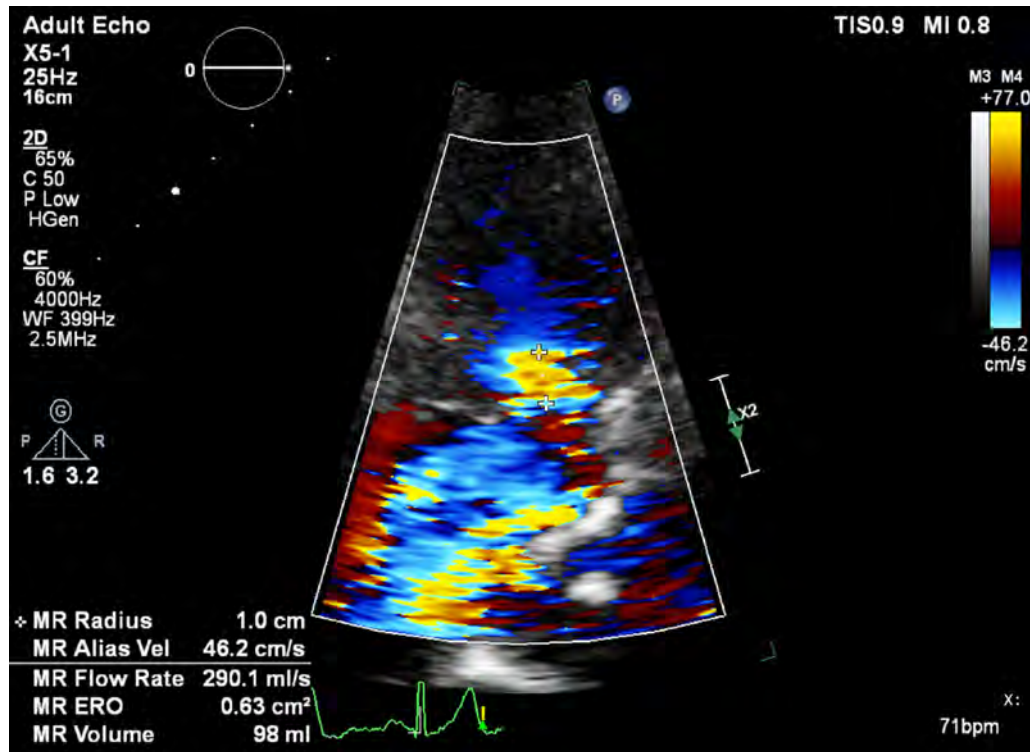
PW Doppler makes available an additional method for blood flow volumetric quantification where blood volume flow across a conduit:

$$\textit{Flow volume} = \textit{cross sectional area of conduit} \times \textit{time} \times \textit{blood velocity}$$

Blood velocity and the duration of flow can be readily quantified as the area under the curve on a PW Doppler trace (velocity time integral, VTI), and the equation can be applied for quantifying both aortic flow volume as well as mitral forward flow volume (the difference between the two would equal mitral regurgitant volume).

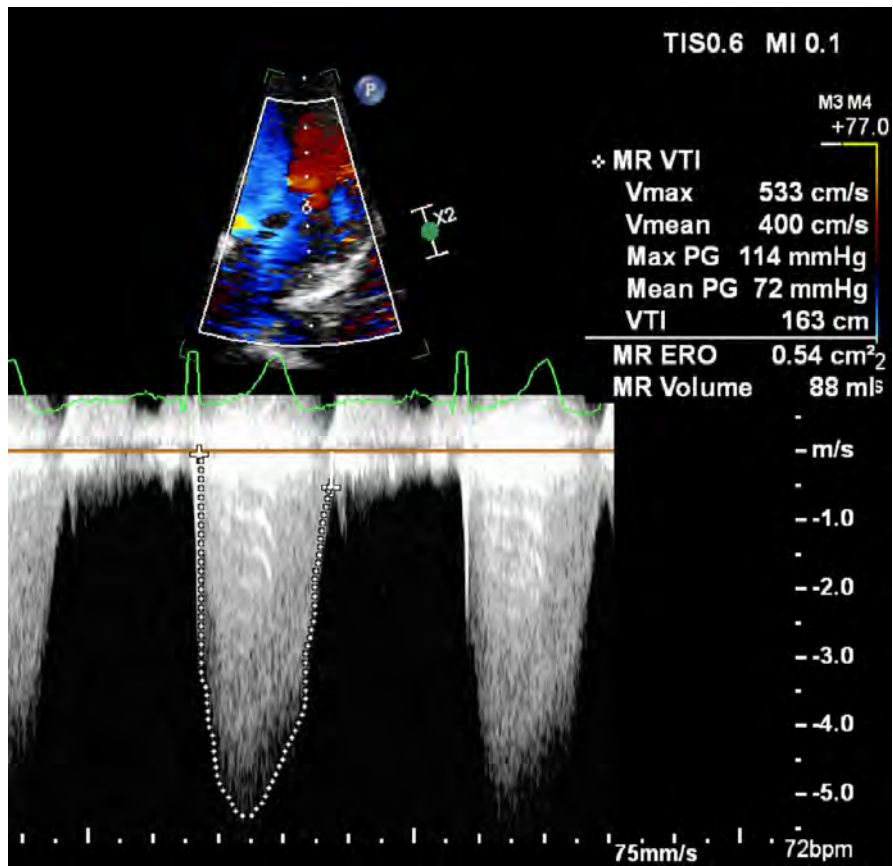
In addition to these “quantitative” methods of MR severity quantification, “qualitative” techniques are also employed, each with distinct cut-off points for defining mild, moderate and severe MR (**Table 1.2**).

Figure 1.6 Example of PISA on colour Doppler.



A PISA of 1.0cm is being measured proximal to the mitral valve regurgitant orifice at an aliasing velocity (Nyquist limit) of 46.2cm/s. Mitral regurgitant volume and EROA have been calculated automatically by the echocardiographic software.

**Figure 1.7** Example of continuous wave Doppler of the mitral regurgitation jet



Tracing around the Doppler profile allows quantification of the MR velocity time integral (VTI).

**Table 1.2** Grading the severity of primary chronic MR by echocardiography (43).

	<b>Mild</b>	<b>Moderate</b>	<b>Severe</b>
<b>Structural features</b>			
<b>MV morphology</b>	<i>*None or mild abnormality</i>	Moderate abnormality (thickening, tenting, prolapse, calcification)	<i>*Severe valve lesion (flail leaflet, ruptured papillary muscle, poor leaflet coaptation)</i>
<b>LV and LA size</b>	Normal	Normal / mildly dilated	Dilated
<b>Qualitative Doppler</b>			
<b>Colour flow jet area</b>	<i>*Small, central, narrow, often brief</i>	Variable	Large central jet (>50% of LA) or eccentric jet of variable size
<b>Flow convergence</b>	<i>*Not visible, transient, or small</i>	Intermediate size and duration	<i>*Large throughout systole</i>
<b>PISA size at Nyquist of 30-40cm/s)</b>	≤0.3cm		≥1.0cm
<b>CW Doppler jet</b>	Faint/partial/parabolic	Dense but partial or parabolic	Holosystolic/dense/ <i>*triangular</i>
<b>Semiquantitative</b>			
<b>VC (cm)</b>	<0.3cm		≥0.7cm average from 2 orthogonal views
<b>Pulmonary vein flow</b>	<i>*Systolic dominance</i>	Normal or systolic blunting	Minimal systolic flow / <i>*systolic flow reversal</i>
<b>Mitral inflow</b>	<i>*A-wave dominant</i>	Variable	E wave dominant
<b>Quantitative</b>			
<b>EROA</b>	<0.2cm <sup>2</sup>	0.2-0.39cm <sup>2</sup>	≥0.4cm <sup>2</sup>
<b>Regurgitant volume (ml)</b>	<30ml	30-59ml	≥60ml
<b>Regurgitant fraction (%)</b>	<30%	30-49%	≥50%

*\*Italic parameters are qualitative and semi-quantitative signs considered specific for their MR grade.*

There are recognised limitations in MR assessment by echo. PW Doppler methods require the combination of several parameters that carry intrinsic error, which increase as the root sum square. This means that even under research conditions, the volume bias and limits of agreement between observers for aortic stroke volume ( $4.7 \pm 29.1$  ml) and mitral stroke volume ( $2.9 \pm 19.6$  ml) are poor, with a tendency to under-estimation compared to thermodilution (44). Likewise, questions have been raised about the reliability of flow convergence even amongst experts from university institutions (45). For example, when grading MR as severe or non-severe, the overall inter-observer agreement was poor: 0.37 (95% CI: 0.16 to 0.58) for PISA measurements. Furthermore, there is evidence that certain jet characteristics will reduce the accuracy of echo-based quantification techniques, with very eccentric, late systolic, or multiple jets being particularly challenging for echo-based quantification (46). Despite the recommendation to quantify MR, a recent communication from the American College of Cardiology (ACC) recognised that inadequate quality of echo may be a barrier to optimal care of almost a quarter of patients with MR and that many decisions regarding severity of MR are still made on echo by visually estimating severity based on colour, with a minority of reports providing regurgitant volumes and fraction (47).

#### *1.4.3.2 Quantification by cardiac magnetic resonance*

In contrast to current guideline-based echocardiographic approaches, estimation of severity by CMR is reliant on a small number of quantitative methods that have been validated against other reference standards, including cardiac catheterisation (48), quantitative Doppler on TTE (49) and current 2D PISA-based methods (50).

LV stroke volume (LVSV) is calculated by taking away left ventricular end-systolic volume (LVESV) from left ventricular end-diastolic volume (LVEDV). Aortic flow ( $AV_f$ ) is measured directly with phase contrast mapping perpendicular to the proximal aorta, with mitral regurgitant volume equating to the difference between LVSV and  $AV_f$  (43).

Studies that compare the reproducibility of TTE and CMR however are limited. In a prospective study of 26 patients with a range of severity in MR, although regurgitant volume was similar between quantitative Doppler, flow convergence TTE and CMR, variability in measurements by all methods was poor between observers (Doppler -10ml (95% CI -76 to 56mls); PISA: -4ml (-21 to 13mls); CMR 0.7ml (-30 to 32mls) (50). Inter-observer variability of regurgitant fraction was significantly lower however by CMR than TTE in a retrospective study of 70 patients ( $0.1 \pm 7.3\%$  v  $-5.5 \pm 15\%$ ) across a range of severity of MR (51). Lower inter-observer variability was also achieved by CMR in a further retrospective study of 72 patients with an inter-observer coefficient of variation 3.7% for regurgitant volume, while the study also highlighted that quantification by echocardiography was often not achievable in practice (52).

Where an integrative approach to echo based MR severity grading has been applied as per American Society of Echocardiography (ASE) guidance, CMR based categorisation has been reported to possess an intra- and inter-observer disagreement of 5% and 10% respectively, versus 20% and 40% discordance with echocardiography (46). Furthermore, in this prospective observational study of 258 asymptomatic patients, a quarter of patients had a discrepant degree of severity diagnosed on CMR and echo, with the CMR classification offering superior prognostic value for predicting the composite end-point of



mortality or mitral valve surgery during the median follow-up of 5 years (46). In another study of 109 asymptomatic patients with severe MR defined as regurgitant volume >55ml or regurgitant fraction >40%, baseline CMR values were a good predictor for the development symptoms or other indications for surgery (53). With a mean follow-up of 2.5 years, subjects with a regurgitant volume of >55ml had a surgery-free survival rate of 21% at 5 years compared to 91% in those with regurgitant volume  $\leq$ 55ml. Meanwhile classification based on regurgitant fraction of  $\leq$ 40%, >40% and >50% led to surgery-free survival of 89%, 59%, and 16% respectively (53).

There are also however, limitations to quantifying MR severity by CMR, including the presence of non-compensated eddy-current-induced fields, variability in volumetric analysis according to placement of the basal slice and in phase velocity mapping according to the plane used for measuring aortic flow (54).

In summary, for the quantification of MR, echocardiography remains first-line albeit with recognised limitations. CMR quantification of MR is simple, feasible in a greater proportion of patients and from the limited comparative studies, may be more reproducible. However, CMR is more expensive, less widely available than echocardiography. CMR based outcome data also remain limited and present guidelines are derived from large echo-based outcome studies such that more data are needed which compare the primary analysis of newly acquired CMR datasets.

## 1.5 Management of primary mitral regurgitation

The treatment for symptomatic severe MR is surgery. When medically treated, MR is associated with excessive mortality and high morbidity (22). Conversely, current techniques for MV repair now allow restoration of normal life expectancy following surgery (4). There is no evidence-based medical therapy for patients with minimal or no symptoms (55). However, in patients with heart failure, angiotensin converting enzyme inhibitors (ACE-I), beta-blockers, and spironolactone should be considered in those unsuitable for surgery, or when symptoms persistent after surgery for palliation (24).

### 1.5.1 Mitral valve surgery

Mitral valve repair, rather than replacement, is widely recognised as the preferred treatment option with multiple registry and retrospective analyses demonstrating lower operative mortality, longevity comparable to that of mechanical valves, and improved long term survival without the risk of prosthetic valve-related complications such as thromboembolism, anticoagulation-related haemorrhage, endocarditis and structural valve degeneration (56-60). A variety of surgical techniques, including leaflet resection, implantation of artificial chordae, chordal transfer and annuloplasty, are at the surgeon's disposal to achieve restoration of normal valvular apparatus function (55). The technical difficulty of a successful mitral valve repair is increased with complex lesions such as extensive myxomatous degeneration, bileaflet prolapse and presence of annular calcification (5, 61). However, over 95% of degenerative mitral valves can be successfully repaired in expert hands, highlighting the importance of centralising expertise within Heart Valve Centres (24, 62).

## 1.5.2 International guidelines

### 1.5.2.1 Guideline format

Both European and American guidelines are categorised according to the class (strength) of recommendation, and the level (quality) of evidence (**Table 1.3 and 1.4**) (24, 25).

### 1.5.2.2 Current guideline recommendations

The current European and American guidelines (**Table 1.5**) recommend expectant management until class I indications for surgery are reached, namely the development of severe MR associated with the onset of symptoms, left ventricular systolic dysfunction (ejection fraction, LVEF,  $\leq 60\%$ ) or left ventricular end systolic dimension (LVESD)  $\geq 45\text{mm}$  (20, 24). These cut-off points have been determined by balancing the risk of surgery against the deterioration in prognosis reported by multiple retrospective and prospective observational studies (4, 63-65).

It has been also noted that the onset of atrial fibrillation (AF) (66, 67) and pulmonary hypertension (68, 69) are strong independent predictors of worsening postoperative morbidity and mortality in MR. These MR induced complications are recognised within guidelines as class II indications for surgery. However, with improvements in surgical technique and a reduction in surgical risk, work from multiple groups have pushed for earlier surgery within the asymptomatic severe mitral regurgitation cohort. This has given rise to controversy surrounding the timing of surgery for primary MR.

**Table 1.3** Classes of recommendations utilised by European and American guidelines

<b>Class of recommendation</b>	
Class I	Evidence or general agreement that treatment is beneficial, useful and effective. Treatment is recommended.
Class IIa	Weight of evidence is in favour of usefulness/efficacy. Treatment should be considered.
Class IIb	Usefulness/efficacy is less well established by evidence/opinion. Treatment may be considered.
Class III	Evidence/opinion that treatment is not useful/effective, and in some cases may be harmful. Treatment is not recommended.

**Table 1.4** Levels of evidence utilised by European and American guidelines

<b>Level of evidence</b>	
Level of evidence A	Data derived from multiple randomised clinical trials of meta-analyses.
Level of evidence B	Data derived from a single randomised clinical trial or large non-randomised studies.
Level of evidence C	Consensus opinion of experts and/or small studies, retrospective studies, registries.

**Table 1.5** Summary of current European (24) and American (20, 25) guidance on the timing of surgery for primary mitral regurgitation.

Recommendation		Class	Level
Patient factors	MV surgery is recommended for symptomatic patients with chronic severe primary MR and LVEF >30%	I	B
Valve factors	MV repair is recommended in preference to MV replacement when results are expected to be durable.	I	C
	MV replacement should not be performed for treatment of isolated severe primary MR limited to less than one half of the posterior leaflet unless MV repair has been attempted and was unsuccessful.	III	B
Ventricular status	MV surgery is recommended for asymptomatic patients with chronic severe primary MR and LV dysfunction (LVEF 30-60% and/or LVESD $\geq$ 45mm).	I	B
	Surgery should be considered in asymptomatic patients with preserved LV function (LVEF >60%, LVESD 40-44mm) when a durable repair is likely and surgical risk is low, and the presence of either 1) flail leaflet or 2) significant LA dilatation (volume index $\geq$ 60ml/m <sup>2</sup> ) in sinus rhythm.	IIa	B
	Mitral valve surgery is reasonable for asymptomatic patients who have preserved (LVEF >60%, LVESD <40mm) but progressive deterioration in LV function (increase in LV size or decrease in LVEF) on serial imaging.	IIa	C
	MV surgery may be considered in symptomatic patients with chronic severe primary MR and LVEF $\leq$ 30%	IIb	C
Complications related to MR	MV repair is reasonable in asymptomatic patients with chronic severe nonrheumatic primary MR and preserved LV function in whom there is a high likelihood of a successful and durable repair with 1) new onset AF or 2) resting pulmonary hypertension (sPAP >50mmHg).	IIa	B

### 1.5.3 Controversy in the timing of surgery

Given the adverse postoperative outcomes associated with the class I indications for surgery, together with the ability to restore long-term patient prognosis back to that of age and gender matched controls when operating before the onset of advanced symptoms (5), there is support for surgery to be offered earlier. In a single-centre prospective study of 610 consecutive patients with asymptomatic severe MR, outcomes were compared between those referred for early surgery on a class II (235 patients; 94% repair rate) and those referred with conventional class I indications (375 patients; 82% repair rate), with the decision made at the discretion of the referrer. At a follow-up of 12 years, the early surgery group had significantly lower cardiac mortality (HR 0.109; 95% confidence interval (CI) 0.014 to 0.836;  $p=0.033$ ) and cardiac event rates (HR 0.216; 95% CI 0.083 to 0.558;  $p=0.002$ ) (6).

In the absence of randomised controlled trials, a meta-analysis examined data from available observational studies to find that the patients who were offered early surgery on a class II indication had lower mortality rates and were more likely to have valve repair instead of replacement compared to patients who waited for the development of a class I indication (70).

Similarly, the multi-centre, multi-national Mitral Regurgitation International Database of 2097 consecutive patients with primary MR due to flail segments found improved survival at 10 years with lower rates of heart failure for those proceeding with early mitral repair compared with those managed medically until class I guidelines were triggered (71). These

data have led authors to suggest that current class I recommendations are criteria which do not promote optimal outcomes for patients with severe primary MR.

Despite the consistency of these reports, it is important to recognise that data supporting early surgery are mostly from single-centre, non-randomised studies and many findings are from retrospective registries. Selection bias is an important limitation of such observational studies as the decision for surgery are determined by the patients' primary physician. In practical terms, selection bias means that there may be prognostically important differences between one asymptomatic patient who is recommended early surgery, versus another asymptomatic patient of identical age and gender who is recommended watchful waiting. Whilst propensity score matching has been utilised to minimise differences in the observed covariates of these studies (6, 71), this statistical method does not account for the hidden biases of latent variables that remain after matching (72, 73). Finally, these observational studies have tended originate from high-volume centres with specialised, experienced surgeons performing large numbers of MV repairs. Such data on rates of repair and lower perioperative morbidity and mortality cannot always be extrapolated to lower volume centres (74, 75). Randomised prospective studies in mixed populations are lacking, although trials are under way (76). Furthermore, it can be difficult to persuade an asymptomatic patient in clinic to undergo major cardiothoracic surgery, as by definition, prophylactic surgery in asymptomatic individuals does not improve how they feel but does commit the patient to a period of rehabilitation and is associated with a minimum mortality risk of 1%, a risk which increases further if valve repair is unsuccessful and a replacement is performed instead (77). Additionally, MR still can recur after repair; in the most recent series, rates of recurrent MR were 13.3+1.2%



patients at 15 year follow up, with a reoperation rate of  $6.9 \pm 1.0\%$  (78). Finally, there are data that suggest careful outpatient care may deliver outcomes that are as good. In a study of 132 consecutive patients with asymptomatic severe MR, a programme of regular (3-12 monthly) reviews with referral based on Class 1 indications delivered outcomes equivalent to the general population over a follow-up period of  $62 \pm 26$  months (79). Mostly importantly, this had the added advantage that  $55 \pm 6\%$  of the cohort were able to avoid surgery altogether at 8 years follow-up without complication. Of equal importance, the surgical cohort reported excellent surgical outcomes with no compromise in symptom status or LV outcome from delay.

In summary, the first challenge with optimising the timing of surgery for primary MR lies with the accurate quantification of MR severity where echocardiography and CMR have been reported to generate a discordant severity assessment in one quarter of moderate or severe MR patients (46). Despite CMR severity assessments appearing to possess better outcome predictive powers compared to echocardiography in early observational studies, the use of CMR for MR remains in its infancy with the bulk of outcome data as well as current guidelines being based on echocardiography. Secondly, once asymptomatic severe MR has been confirmed, physicians have to confirm whether a valve may be repairable, even though many echo studies still do not identify aetiology or mechanism of MR (47). Thirdly, in the presence of confirmed severe asymptomatic primary degenerative MR, patients and physicians are faced with the conundrum of whether to undertake a potentially unnecessary operation with its associated mortality risks (79), or delaying surgery until the onset of a class I surgical indication with its associated outcome penalty (80). As a result of these challenges, the debate continues (81, 82), and in spite of clear guidelines on the

timing of surgery, a fifth of patients with severe primary MR continue to present postoperatively with reduced ejection fraction and an increased risk of congestive cardiac failure (83). These factors make the case for research into new biomarkers that can be used to improve the timing of surgery for MR.

## 1.6 Myocardial response to primary mitral regurgitation

It has been hypothesised that myocardial remodelling with the development of myocardial fibrosis in MR may be responsible for sub-clinical deteriorations in ventricular function, which becomes evident following MV repair as a result of the restoration of a normal afterload. These sub-clinical changes, if quantifiable, can represent novel biomarkers for optimising the timing of surgery. The myocardial response to valve disease has been well characterised in the pressure overloaded state of aortic stenosis (84), but less so in MR. This next section will summarise our current knowledge and its limitations on myocardial remodelling in MR.

### 1.6.1 The dynamic myocardial matrix

Myocytes are only responsible for two-thirds of muscle volume in the heart with the remaining volume comprising of fibroblasts, capillaries, nerve tissue, and an extracellular matrix (ECM) that is composed of fibrillar connective tissue and ground substance consisting of glycosaminoglycans and glycoproteins (85). The fibrillary connective tissue which predominantly consists of type I (85%) and type III (11%) collagen, with a small percentage of elastin, provides support and acts as a point of tether to cardiac myocytes, thereby protecting myofibrils against overstretch. It also provides a skeleton to improve

contraction, and is an important determinant of systolic and diastolic myocardial stiffness (85-89).

Myocardial collagen, which has an estimated half-life of 80-120 days, is regulated by resident cardiac fibroblasts and has a daily fractional synthesis rate of 0.5-0.9% (90, 91).

Under normal conditions, myocardial fibroblasts are quiescent and do not exhibit significant inflammatory or proliferative activity (92). Disruption of ECM homeostasis by ischaemia, toxins (e.g. alcohol), volume-overload (e.g. mitral or aortic regurgitation) or pressure-overload (e.g. AS or hypertension) states, as well as direct mechanical stimulation of myocardial fibroblasts themselves, results in development of proto-myofibroblasts which can be further stimulated to become pro-fibrotic myofibroblasts (93).

Multiple molecular pathways, including the upregulation of interleukin 1 $\beta$ , have been implicated in myofibroblast differentiation and alteration of the ECM (93, 94). These pathways ultimately lead to an imbalance in the ratio of metalloproteinases (MMP) to tissue inhibitor of metalloproteinases (TIMP)-1, which are important for modulating the degradation of matrix components and collagen synthesis (95, 96). Cardiac mast cells play a vital causative role in this ventricular remodelling process with MMP activity closely mirroring cardiac mast cell density. Furthermore, application of mast cell stabilising agents cromolyn and nedocromil sodium can successfully prevent both the increase in cardiac mast cell density and MMP activation, as well as reducing the degree of subsequent LV remodelling (97, 98). Transforming growth factor-beta1 (TGF- $\beta$ 1), which is released by mast cells, have been implicated in both the development of myocardial fibrosis with myofibroblasts differentiation (99) and cellular hypertrophy (100). To better characterise

the effects of these signalling pathways within the LV, animal models of volume overload have been studied.

### 1.6.2 Insight into ventricular remodelling from animal models

Animal models, primarily using rats, can be categorised into those of an whole-heart volume overload via the creation of an arterial-venous fistula (97, 101, 102), or LV specific volume-overload with the surgical disruption of the MV apparatus (103, 104). In rats with surgically induced infrarenal aorto-caval fistulae, one study reported that during an initial asymptomatic phase, there is progressive ventricular hypertrophy and dilatation over the first 8 postoperative weeks. LV end-diastolic pressure initially rises, before falling at 5 weeks to correspond with a significant decrease in LV stiffness (101). Meanwhile, collagen volume fraction (CVF) decreases during the first weeks, likely as a result of the concomitant rise in MMP activity (97), before CVF rises to normal or above-normal levels 2 weeks post fistula induction (101).

In MR, these initial myocardial changes can be seen to be adaptive as the more compliant and dilated ventricle allows maintenance of cardiac output by increasing stroke volume. One important point to note in these animal models is that different rats progressed at different rates before decompensating to overt congestive heart failure, reminiscent of how patients with similar degrees of MR may compensate for varying lengths of time during longitudinal follow-up. Additionally, increasing muscle hypertrophy was found to only occur over the first 8 weeks post fistula induction, demonstrating an upper limit to ventricular hypertrophy. As rats subsequently developed overt heart failure, there was further LV dilatation associated with additional rise in CVF and MMP activity. This

suggests that the development of heart failure may be the result of additional ventricular dilatation in the absence of concomitant muscle hypertrophy (102).

Mathematical modelling of ventricular dilatation suggests that stroke volume can be increased with increasing anatomical heart size to a fixed limit, beyond which stroke volume falls off (105); additionally, it is thought that the myocardium is required to generate a greater force when dilated in order to eject the same volume of blood (106). These together may explain the mechanism for decompensation in mitral regurgitation. Whilst other, more direct models of primary MR have been created with surgical rupture of chordae tendineae (103), or piercing of rat MV leaflets using a large bore needle inserted into the LV cavity via the apex (104), characterisation of LV remodelling in these models has been less extensive. In preliminary work, this latter group reported no significant increase in interstitial fibrosis in rats 14 weeks post MV perforation when LVEF were significantly lower compared to animals receiving a sham procedure (104). In all cases, it remains to be studied how accurately these animal models where volume overload is acutely induced surgically, reflect the physiological processes occurring with chronic mitral regurgitation in humans where regurgitant severity and volume overload tends to gradually worsens over many years.

### 1.6.3 Clinical models of ventricular response to primary mitral regurgitation

Supported by work on animal models, the response of the LV to MR has traditionally been conceptualised in well-defined stages (**Figure 1.8**) (107, 108). Initially, there is LV dilatation and eccentric hypertrophy but with preservation of systolic function as physiological compensation for chronic volume overload. This is followed by a

transitional stage with mild LV dysfunction that is reversible after surgical correction of the MR. Finally, there is decompensation with irreversible structural and functional changes. From this model and the results of LV remodelling after surgery, current guidelines provide us with predictive values of LVEF and end-systolic dimension (LVESd) to guide the timing of surgery (24). There are two broad categories of limitations when managing patients according to this model.

Firstly, the cut-off points set within these guidelines have their limitations. LVEF as a measure of LV contractility, is sensitive to the MR induced changes in pre-load and after-load. Pre-load is the end diastolic volume which stretches the LV to its greatest dimension; with MR, the regurgitant volume is retained within the heart organ by the temporary systolic displacement of blood from the LV into the LA. In diastole, this displaced volume re-joins the LV to produce a greater LVEDV. After-load is the pressure which the myocardium works against to eject blood during systole. In MR, the additional outlet created by MV incompetence reduces the total impedance for blood exiting the LV, and thereby lowers afterload (109), reducing the force necessary for the myocardium to contract. Increased pre-load and reduced after-load work in combination to maintain a normal range LVEF despite the ‘sub-clinical’ deterioration in contractile function, meaning that LVEF is a poor marker of contractility.

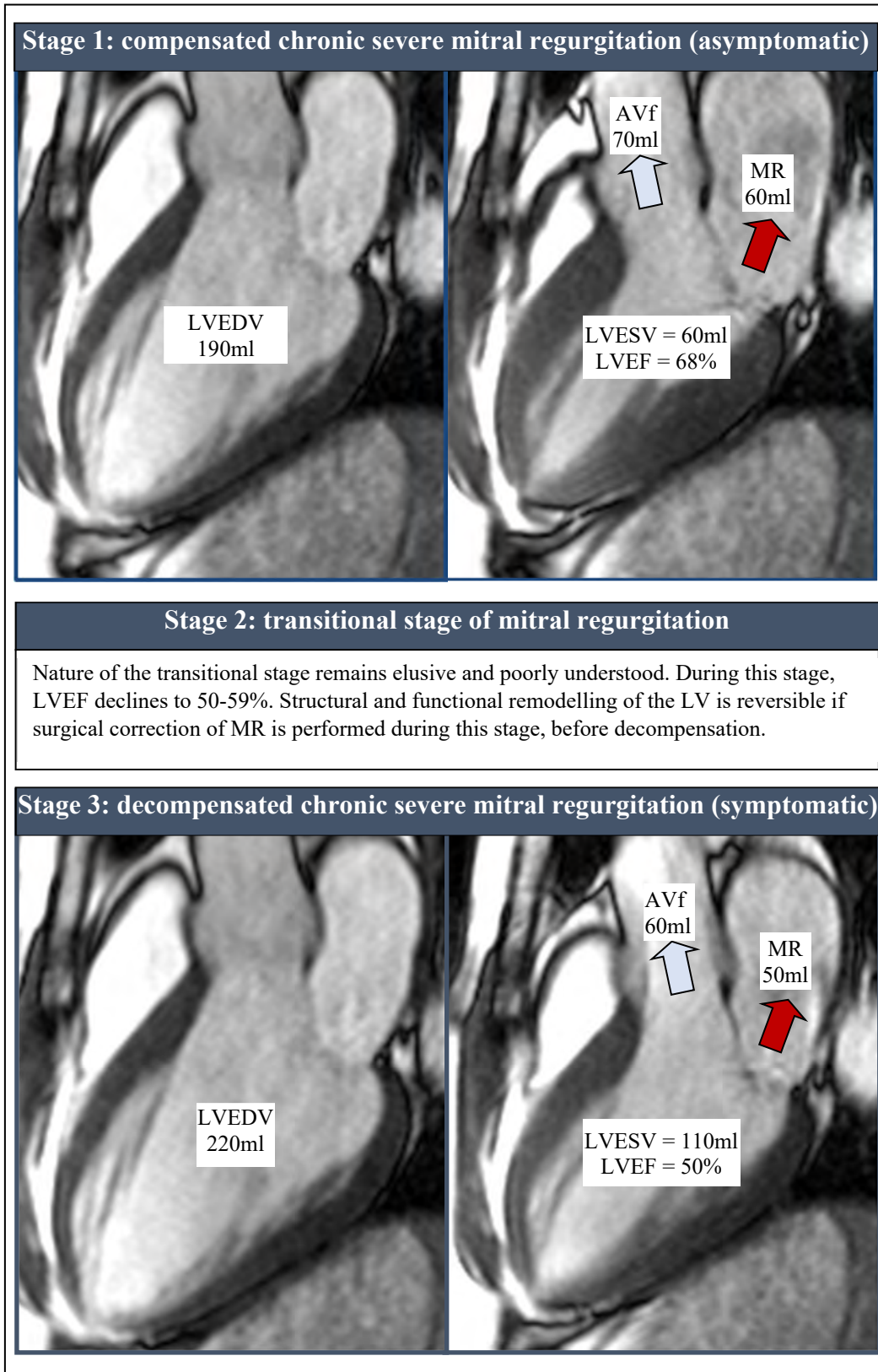
LVESd is similarly influenced by haemodynamic changes in MR as it is the result of interaction between LV end-diastolic dimension (LVEDd) and contractile function.

Furthermore, it has been demonstrated that the LV undergoes a preferential spherical remodelling process (**Figure 1.9**) at the apex and mid-ventricular level (110). This means

that when using LVEF and basal chamber dimensions as a decisive factor in timing of surgery, not all ventricles will normalise after surgery (111).

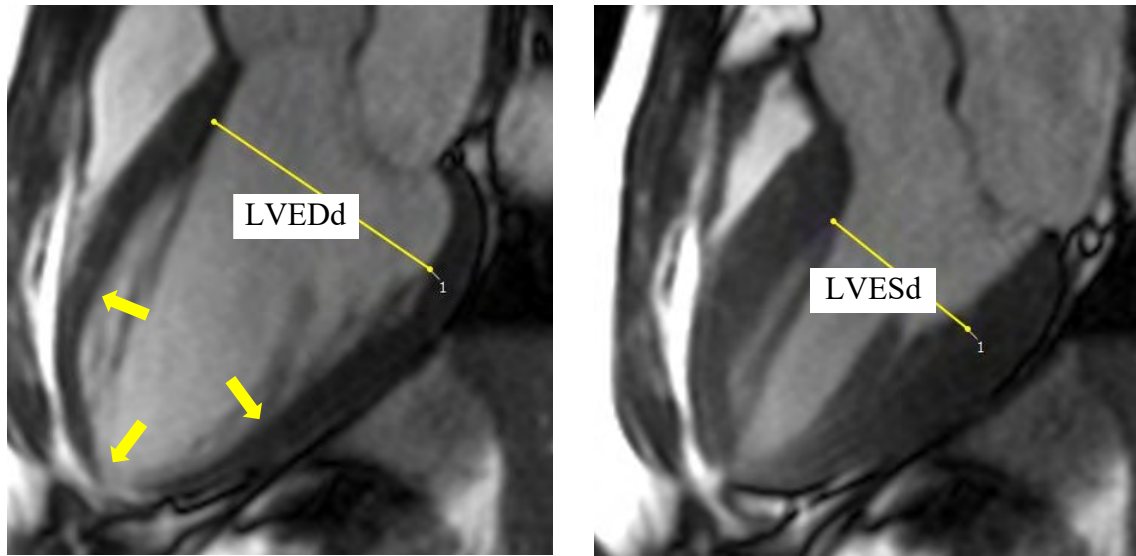
Secondly, there is growing evidence from clinical data that LV remodelling progresses as a spectrum of changes from the earliest stages of MR, with reductions in early myocardial relaxation velocity and global ventricular strain even in asymptomatic patients with normal ejection fraction (112-114). This sub-clinical reduction in contractility is in turn reflected in LA dilatation due to elevated LV end-diastolic pressure (115) and progressive secondary right ventricular (RV) failure (116). Sub-clinical LV dysfunction can be measured through change in myocardial strain via a number of methodologies, including tissue Doppler imaging (TDI), speckle tracking echocardiography (STE) and feature-tracking CMR (FT-CMR), and predicts both the onset of symptoms (113) and the degree of reverse LV remodelling following MV repair (117). Sub-clinical changes in LV systolic deformation, impaired diastolic relaxation and elevated LA pressure are frequently ascribed to the presence of interstitial fibrosis (89). There has been limited documentation of the histological changes that underlies LV remodelling in early asymptomatic severe MR. It is however known that MR does results in ventricular hypertrophy and an expansion of the extracellular volume (ECV) from a baseline of around 32% to 50% in MR patients with heart failure (118). Expansion of the ECV can now be measured on cardiac magnetic resonance (CMR) and is thought to reflect myocardial fibrosis across a range of cardiac pathologies (119, 120).

**Figure 1.8** Traditional model of left ventricular remodelling in mitral regurgitation.





**Figure 1.9** Apical spherical remodelling in MR.



Basal LV dimensions, which are recommended by current guidelines, do not account for the preferential apical remodelling in MR.

## 1.7 Non-invasive monitoring of myocardial fibrosis

As subclinical ventricular dysfunction has been attributed to the onset of myocardial fibrosis, there have been increasing attempts at non-invasive quantification and monitoring of myocardial fibrosis. These include the use of 1) serum biomarkers, 2) functional markers, and 3) direct measurement.

### 1.7.1 Serum biomarkers of myocardial fibrosis

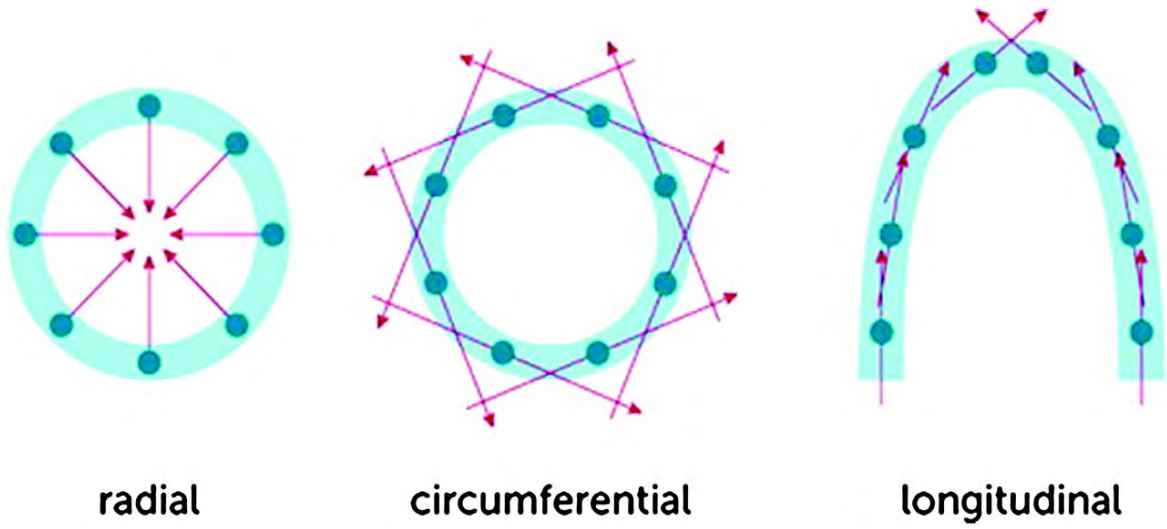
As described in section 1.6.1, the cardiac fibrillary connective tissue predominantly consists of type I (85%) and type III (11%) collagen. Procollagen type I amino-terminal peptide (P1NP) is cleaved from the procollagen precursor of type I collagen and released into the circulation during type I collagen synthesis and degradation, and similarly, procollagen type III amino-terminal peptide (P3NP) is released into the circulation during type III collagen synthesis and degradation. Elevations of both serum biomarkers are therefore markers of increased LV remodelling and have been reported to correlate with diastolic dysfunction in patients with coronary artery disease (121). Elevated P3NP has been associated with increased heart failure symptoms and reduced myocardial strain (122), as well as being an independent predictor of death and hospitalisation in chronic heart failure patients (123). The prognostic significance of P1NP and P3NP in MR have not been previously investigated and represents an area of great interest as it may provide insight into the ferocity of myocardial matrix remodelling activity across different disease severities.

### 1.7.2 Functional markers of myocardial fibrosis

There is growing evidence that the onset of myocardial fibrosis is the final common pathway responsible for development of subclinical LV systolic and diastolic dysfunction in patients across a range of cardiac pathologies (117, 124). TDI utilises the same Doppler principles as colour Doppler imaging, but is applied to myocardial tissue in order to quantify the degree of tissue movement in a single plane. For primary MR, TDI has been demonstrated to be of prognostic importance with one study reporting that a systolic mitral annular velocity (Sm) of  $\leq 10.5$  cm/s independently predicted a  $\geq 10\%$  deterioration in postoperative LVEF in patients who were preoperatively asymptomatic with LVEF  $> 60\%$  (112). Another group similarly reported that Sm of over 7 cm/s was an independent predictor of superior reverse LV remodelling following surgery as defined by  $\geq 20\%$  postoperative indexed LV mass (LVMI) regression (117).

Speckle tracking echocardiography (STE) is a deformation quantification technique that tracks the 2D movement of speckle artefacts in the myocardium, generated at random due to reflections, refraction, and scattering of echo beams (125). The degree of deformation, or strain that the myocardium undergoes is categorised into one of three directions – radial, circumferential and longitudinal (**Figure 1.10**). In patients with asymptomatic MR, global longitudinal strain (GLS) is lower compared to healthy controls, suggesting the presence of subclinical LV dysfunction (126), with a GLS of  $\geq -20\%$  predictive for the onset of cardiac events (hazard ratio (HR)=1.14, 95% confidence interval (CI) 1.04-1.26, P=0.007) (113).

**Figure 1.10** Sub-types of left ventricular myocardial wall strain.



Reproduced with permission from Blessberger & Binder 2010 (125).

Myocardial deformation imaging on CMR can also be performed on 2D images. Many dedicated deformation sequences exist, including spatial modulation of magnetization (SPAMM), harmonic phase (HARP), displacement encoding (DENSE) and strain encoding (SENC). These dedicated sequences are time consuming; the development of feature-tracking techniques are of growing interest as they allow strain to be derived from routine steady-state free precession (SSFP) cine images and negate the requirement to acquire additional sequences, offer rapid post-processing, while also delivering standard volumetric assessments of the LV (127, 128). However, all such 2D-based techniques suffer from through-plane loss of features in the third dimension. Furthermore, the assessment of myocardial strain from either a single, or even multiple 2D images may not be truly representative of global 3D myocardial function.

More recently, 3D feature tracking algorithms have been released commercially, which allows the tracking of LV deformation within a 3D ventricular model using adjacent stacks of 2D SSFP cine images (129). This is a novel technique which requires validation, the generation of reference ranges in the normal population (described in Chapter 3), before its use in disease processes can be advocated (see Chapters 5-7).

### 1.7.3 Direct myocardial fibrosis imaging

Direct myocardial fibrosis imaging with both ultrasound and CMR has been proposed. Ultrasound based myocardial characterisation can be performed using calibrated integrated backscatter (cIB) (130). With the onset of myocardial fibrosis, there is increased acoustic impedance at the intra-cellular and extra-cellular boundaries which in turn results in increased diffuse reflection of ultrasound waves. Comparative data between cIB and

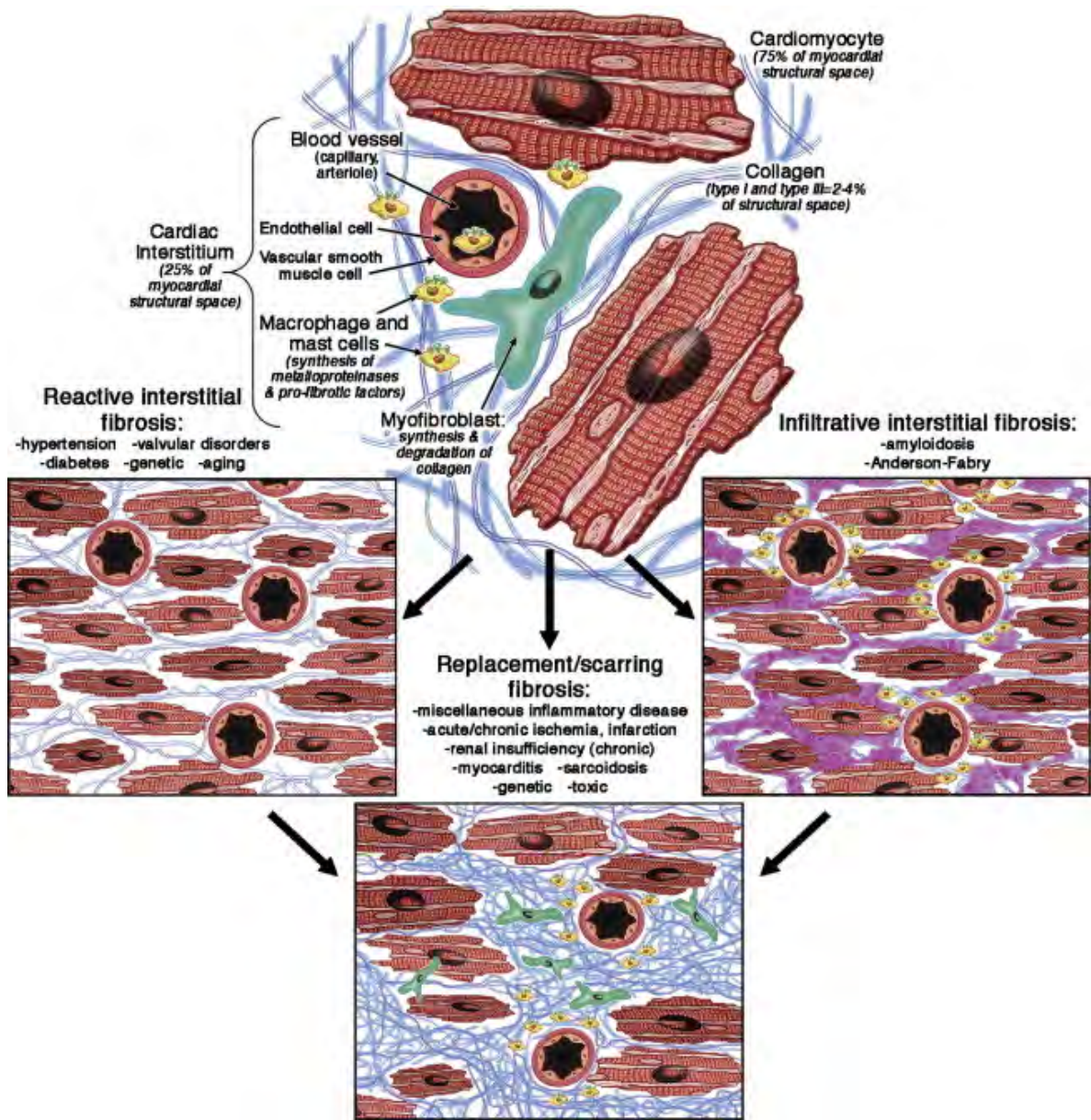
histological fibrosis remain limited. In one study of 25 patients undergoing cardiac transplantation, variation in myocardial collagen was estimated to be responsible for 20% of the observed variation in myocardial cIB (131). Meanwhile, a further study in coronary bypass patients did not find cIB to be a marker of increased myocardial fibrosis on LV biopsies. There are no specific data on the use of cIB in MR, however any echocardiography-based technique will be sensitive to the same limitations imposed by inadequate anatomical windows.

In contrast, there is a growing pool of evidence for the use of CMR based tissue characterisation in MR. Myocardial fibrosis can be classified into diffuse interstitial fibrosis where increased collagen deposition occurs in the absence of myocyte loss, or coarse replacement fibrosis in the presence of myocyte necrosis (93) (**Figure 1.11**), both of which have been observed in MR and can be imaged on CMR with T1 mapping and late gadolinium enhancement (LGE) techniques respectively (41, 132).

Gadolinium chelate is an extracellular contrast agent that quickly diffuses out of capillaries and into the extravascular space. Gadolinium is preferentially retained in areas of fibrosis or oedema where there is increased extravascular, extracellular space and slower diffusion kinetics. This higher concentration of gadolinium hastens the longitudinal relaxation time (T1) of hydrogen protons within the abnormal myocardium (133). This allows the CMR operator to visually select a 'time to inversion' in order to null the normal background myocardium, and highlights abnormal myocardium as white (134). The detection of myocardial LGE is widely used in clinical practice for characterisation of myocardial infarction (135) and focal scarring from non-ischaemic cardiomyopathy (136). There is a

direct correlation between the extent of LGE and coarse replacement fibrosis on histology with a dose-response relationship between LGE burden and adverse cardiovascular outcomes including heart failure and death (137).

Figure 1.11 Schematic diagram illustrating types of myocardial fibrosis.



Reproduced with permission from Mewton et al. 2011 (89).



As LGE relies upon a differential retention of contrast within areas of pathological myocardium which is then visualised by comparison between normal and abnormal myocardium, it cannot be relied upon to detect diffuse disease processes such as interstitial fibrosis where generalised contrast retention occurs and where there may be no 'normal' myocardial comparator. In such circumstances, extracellular volume (which expands from the development of interstitial fibrosis), can be calculated from pre- and post-contrast myocardial T1 (spin-lattice) relaxivity (138, 139).

ECV determined through T1 mapping on CMR has been shown to closely correlate with the histological quantification of diffuse interstitial myocardial fibrosis in a wide range of cardiac conditions including mitral regurgitation (119, 120, 140). The magnitude of ECV expansion has been found to be associated with worse prognosis and more advanced cardiac remodelling in patients with ischaemic heart disease cardiac and AS respectively (84, 141).

T2 (spin-spin) relaxivity is another biological parameter of CMR imaging which is lengthened in the presence of myocardial free water. T2 mapping has demonstrated utility in the detection of oedema following acute myocardial ischaemia (142), myocarditis (143), and cardiac allograft rejection (144). The utility of T2 mapping in MR remains unexplored, but given the volume overloaded nature of the LV in MR, T2 mapping may represent an additional non-invasive biomarker of ventricular remodelling in primary MR which can potentially capture the rate of non-fibrotic extracellular matrix expansion.

#### 1.7.4 Rationale for CMR-derived ECV as an early marker of ventricular remodelling in MR

To summarise our current knowledge of ventricular remodelling in MR (**Table 1.6**) – animal data have demonstrated that following the acute onset of volume overload, there is an initial reduction in myocardial extracellular collagen and a reduction in ventricular stiffness to allow ventricular dilatation (101). Early concomitant muscle hypertrophy aids the maintenance of ventricular function. Exhaustion of this compensatory response may be responsible for the development of overt heart failure in rats (102), but the evidence for this is less clear in humans (118). Clinical studies have detected both sub-clinical systolic and diastolic dysfunction whilst patients remain asymptomatic (89, 113, 145); these are thought to be secondary to the development of myocardial fibrosis. Finally, limited autopsy data have found the development of up to 33% patchy fibrosis within the myocardium of SCD victims with MVP (41), and a histologically measured interstitial space of up to 50% in MR patients with end-stage heart failure (118).

It is therefore evident that the prognosis of patients with MR seems intricately linked to the extent of LV remodelling. This may explain why current guideline-based management approaches that rely on the measurement of ventricular dimension and LVEF, produce suboptimal results where one fifth of patients continue to present postoperatively with reduced ejection fraction and an increased risk of congestive cardiac failure (83). This highlights the clear need to improve our clinical guidelines by comprehensively characterising the myocardial remodelling process across a range of MR severities and LV remodelling states in order to quantify the functional consequences and prognostic implications for patients.

T1 mapping on CMR allows the direct assessment of ventricular remodelling through ventricular size ECV quantification; ECV is reliably measured (146) and therefore represents an ideal non-invasive biomarker for optimising the timing of surgery. In a cross-sectional pilot study of 35 asymptomatic MR patients without class I indications for surgery, CMR derived ECV was increased compared to age- and gender-matched controls ( $0.32\pm 0.07$  vs  $0.25\pm 0.02$ ,  $P<0.01$ ) (147). Of importance, ECV was only elevated above normal control values in approximately half of the MR cases. Increasing ECV correlated with measures of systolic and diastolic dysfunction, and in the subset of 19 patients who underwent cardiopulmonary exercise testing (CPET), correlated with worsening exercise capacity. This raises the question of whether some patients have ventricles which are more susceptible to adverse remodelling than others and raises the question of whether those with increased ECV may benefit from early MV repair, whilst those with low ECV can be safely managed through a watchful-waiting approach.



## 1.8 Summary

Primary degenerative MR is an increasingly prevalent condition of the ageing population. Significant improvements in diagnostic imaging techniques and risk classification have improved patient outcomes by identifying those who clearly require surgery under class I indications on prognostic grounds. Despite this, a fifth of patients continue to present with de-novo ventricular dysfunction following surgery with higher rates of heart failure, morbidity and mortality. There has been a recent push towards early surgery once patients reach class II indications. However, concerns surrounding unnecessary surgery and its

associated morbidity and mortality risks remains a key conundrum in the management of asymptomatic severe MR patients.

Attention therefore needs to be diverted towards assessing the sub-clinical changes of the myocardium in mitral regurgitation, prior to the development of overt symptoms and decline in conventional measurements of ventricular function so that the timing of surgical intervention can be optimised. Whilst animal modelling has provided useful insight into the physiological and pathological processes that underlie the ventricular response to volume overload, the transferability of these processes to mitral regurgitation in humans, as well as the timing in onset of the hypothesised remodelling processes, remain unclear. From post-mortem and small biopsy studies, it is evident that both interstitial and replacement myocardial fibrosis can occur in primary MR with early imaging studies suggesting a role for fibrosis in ventricular dysfunction and arrhythmia (41). CMR has widely acknowledged advantages, particularly in repeatability of measurements of volume and ejection fraction, yet recent guidelines relegate its use to cases where there is discordant information or poor-quality imaging from echocardiography (43). Furthermore, continued developments in CMR with the advent of T1 and T2 mapping represent a unique opportunity to characterise the myocardium in attempt to unravel the individual myocardial response to chronic MR and help identify those “more vulnerable” to adverse remodelling.

**Table 1.6** Spectrum of adaptive processes in ventricular remodelling with primary mitral regurgitation and corresponding imaging observations. Text in bold highlights areas which this thesis investigates.

Spectrum of changes in left ventricular remodelling	Adaptive processes within the left ventricle in animal models	Imaging observations in humans	Current practice and future directions
<p>Initial LV response to volume overload</p> 	<p>LV dilatation in volume overload occurs due to increasing metalloproteinase activity and reduced collagen volume fraction, resulting in improved LV compliance (97, 101). In primary MR, this initial LV enlargement increases stroke volume to maintain cardiac output (105).</p>	<p>Initial increase and subsequent decrease in LV compliance on echo based deformation imaging with normal LVEF (148).</p>	<p>Current guidelines recommend regular echo surveillance of asymptomatic severe MR patients (24, 25).</p> <p><b>Novel techniques including 3D FT-CMR, CPET and exercise echo may be suited for assessing sub-clinical LV dysfunction.</b></p>
<p>“Compensated” chronic mitral regurgitation</p> 	<p><b>Increase in collagen volume fraction and reduction in metalloproteinase activity associated with continued muscle hypertrophy (101, 102).</b></p> <p>Variable duration of compensation among different hearts despite no change in burden of volume overload (101).</p>	<p><b>Expansion of ECV visualised on CMR (147). Subclinical systolic dysfunction as measured by myocardial strain on both echo and CMR thought to be secondary to myocardial fibrosis (149-151).</b></p> <p><b>Potential for myocardial fibrosis quantification to guide timing of surgery (152).</b></p> <p>Research required on kinetic energy and LV wall shear stress derived from intracardiac 4D flow, as well as ability for 4D flow to quantify MR in presence of multiple valvular incompetencies and intracardiac shunts (153).</p>	<p><b>Demand for imaging biomarkers of fibrosis and myocardial water to monitor continued LV remodelling during this “silent” asymptomatic stage, in order to improve the timing of surgery.</b></p> <p><b>Potential for serological biomarkers of collagen turnover and myocardial remodelling to guide the timing of surgery.</b></p>
<p>“Decompensated” chronic mitral regurgitation</p>	<p><b>Limit of cardiomyocyte hypertrophy reached, with additional rise in metalloproteinase activity resulting in further ventricular dilatation (102). Further ventricular dilatation no longer able to increase stroke volume and worsens myocardial efficiency (105, 106).</b></p>	<p>CMR gold standard for longitudinal measurement of ventricular volume. “Excess” LV dilatation can be expressed as a RVol/EDV ratio (154).</p> <p>Overt ventricular failure with symptom onset, LVEF &lt;60% and/or excessive LV dilatation on echocardiography (63-65).</p>	<p>Class I indications for surgery reached, associated with an adverse prognosis (24, 25).</p>

## 1.9 Aims and hypotheses

### Hypotheses:

1. In primary degenerative mitral regurgitation, patients develop myocardial fibrosis prior to the onset of symptoms and overt systolic dysfunction as defined by current class I surgical criteria (Chapter 5).
2. This fibrotic process can be indirectly quantified using CMR based tissue characterisation techniques (147), and exerts subclinical effects on myocardial contractility and relaxation (Chapter 4 and 5).
3. Continued fibrosis eventually leads to progression of symptoms, worsening exercise capacity (Chapter 5). The additional development of irreversible coarse replacement fibrosis will pose long lasting effects on patients' postoperative recovery and prognosis, explaining the previously reported cases of de-novo heart failure following MV surgery (Chapter 6 and 7).

### Principle aims:

1. Provide histological evidence that myocardial fibrosis develops prior to the onset of symptoms in patients with primary degenerative MR.
2. Validate the quantification of CMR-derived fibrosis against histology.
3. Comprehensively characterise the functional consequences of myocardial fibrosis in MR.

4. Assess if CMR-derived fibrosis impacts upon peri- and postoperative patient outcomes, thereby representing a non-invasive biomarker that can optimise the timing of surgery.

The primary endpoint of the prospective observational study described here is the difference in end-systolic volume index on CMR (as a measure of reverse LV remodelling) at 9 months following surgery, comparing those with ECV measured preoperatively above and below the median. Left ventricular end-systolic volume index (LVESVi) is a commonly measured outcome parameter for the quantification of reverse left ventricular remodelling in MR (68, 155).

Secondary end-points assess the difference in exercise performance, symptom status, postoperative recovery and ventricular contractility (measured by LVEF) between patients with an above and below-median ECV 9 months after MV surgery.

## CHAPTER 2

### **METHODS: ASSESSMENT OF FUNCTIONAL STATUS, BIOCHEMICAL MARKERS AND CARDIOVASCULAR STRUCTURE AND FUNCTION**

#### 2.1 Study design

In order to achieve the main aims of this thesis, a prospective, cross-sectional study of patients with primary degenerative MR before and after MV repair was developed. The study was abbreviated the Mitral FINDER study to reflect its goal of examining the role of myocardial Fibrosis IN patient outcome following MV surgery in patients with DEgenerative mitral Regurgitation. To establish the natural history of ECV in MR, an additional cohort of patients with asymptomatic severe MR who did not wish to consider early MV repair (via a class IIa surgical indication) was also studied. Overall study design is summarised in **Figure 2.1**.

This study was initially set up at University Hospital Birmingham. This Birmingham site was not only a heart valve centre featuring a specialist heart valve team (24), but additionally possessed research CMR facilities with well-established expertise in myocardial characterisation imaging, as well as a fully equipped CPET-echo department. Its historical annual rates of mitral valve repair meant that sufficient patient numbers would be recruited after two years, allowing for completion of postoperative investigations during the third year.

Following commencement of recruitment in August 2015, it became evident that recruitment numbers were less than expected due to an unforeseen delay in surgical waiting times at University Hospital Birmingham. This resulted in referring cardiology



centres diverting patient referrals to alternative heart valve centres within the West Midlands. The study was therefore extended with the addition of University Hospitals Coventry in December 2015 and New Cross Hospital in August 2016. All three surgical sites are specialist MV repair centres with high volume and good outcomes; together, they had the potential to capture the majority of surgical cases within the West Midlands.

### 2.1.1 Subjects

All patients with severe primary degenerative mitral regurgitation, diagnosed clinically, confirmed via echocardiography, were eligible for study inclusion. Exclusion criteria included concomitant moderate or severe aortic valve disease, non-incidental or symptomatic coronary artery disease, uncontrolled AF, and the inability to undergo CMR or CPET. Full inclusion and exclusion criteria have been published and are summarised in **Table 2.1** (152).

Patients under clinical care at University Hospital Birmingham were screened from the dedicated valvular heart disease clinic and mitral surgery waiting list. Patients under Coventry Hospital were screened from mitral valve surgeon clinics. Patients under New Cross hospital were screened from their electronic surgical clinic referral letters.

Patients with primary degenerative mitral regurgitation who were deemed eligible from available electronic notes were given a 'Patient Information Sheet' and provided a minimum of 24 hours to digest the study information. Following this, those who expressed written or verbal interest to join the study were contacted for a second study eligibility assessment by cross checking patients' clinical history and investigation results against the

screening criteria. Those confirmed to be eligible were invited to University Hospital Birmingham to provide written informed consent and undergo study investigations.

Contact details of a consultant cardiologist, independent from the study, were provided for unbiased advice if required by patients. Details of the study and contact details of the research team were formally provided to patients' general practitioner after written informed consent was obtained.

### 2.1.2 Ethics

The study protocol was approved by the East Midlands Research Ethics Committee (15/EM/0243), University Hospital Birmingham Research and Development committee (RRK5364) and was undertaken in accordance with the ethical guidelines of the 1975 Declaration of Helsinki of the World Medical Association. All patients gave written informed consent before entry into the study.

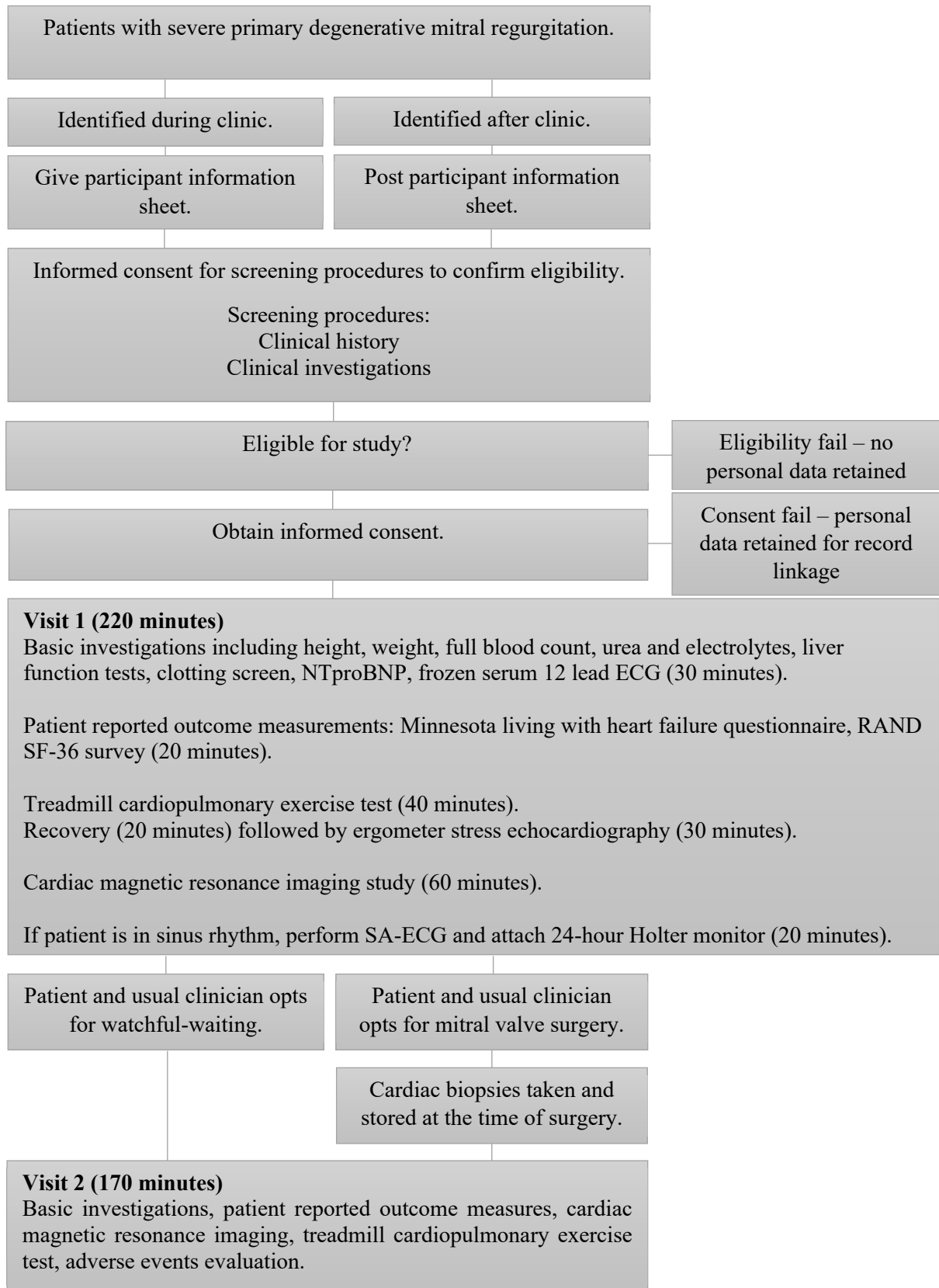
The study was supported by a British Heart Foundation project grant (PG/14/74/31056). The study was subjected to inspection and audit during April 2018 by University Hospital Birmingham NHS Foundation Trust under their remit as sponsor and was found to adhere to the principles of Good Clinical Practice.

### 2.1.3 Study promotion

To aid recruitment, study promotion was carried out by targeting cardiologists and cardiology departments with an interest in valvular heart disease from across the West Midlands. Study information and presentations were delivered to staff at Walsall Health

NHS Trust, Worcestershire Royal Hospital, University Hospital Birmingham, Heart of England NHS Foundation Trust and City and Sandwell Hospitals.

**Figure 2.1** Study design flowchart.



**Table 2.1** Study eligibility criteria (152).

<b>Inclusion criteria</b>
Age 18 and over
Primary degenerative MR (diagnosed and quantified according to the European Association of Echocardiography guidelines)
<b>Exclusion criteria</b>
Secondary mitral regurgitation
Primary mitral regurgitation not due to degenerative disease (including rheumatic disease)
Co-existing moderate or severe aortic valve disease
Congenital heart disease
Inherited or acquired cardiomyopathy
Non-incident or symptomatic coronary artery disease
Uncontrolled atrial fibrillation (resting heart rate >100/min)
Pregnancy
Unable to undergo CMR
Unable to undergo cardiopulmonary exercise test

## 2.2 Current and future strategies for risk stratification

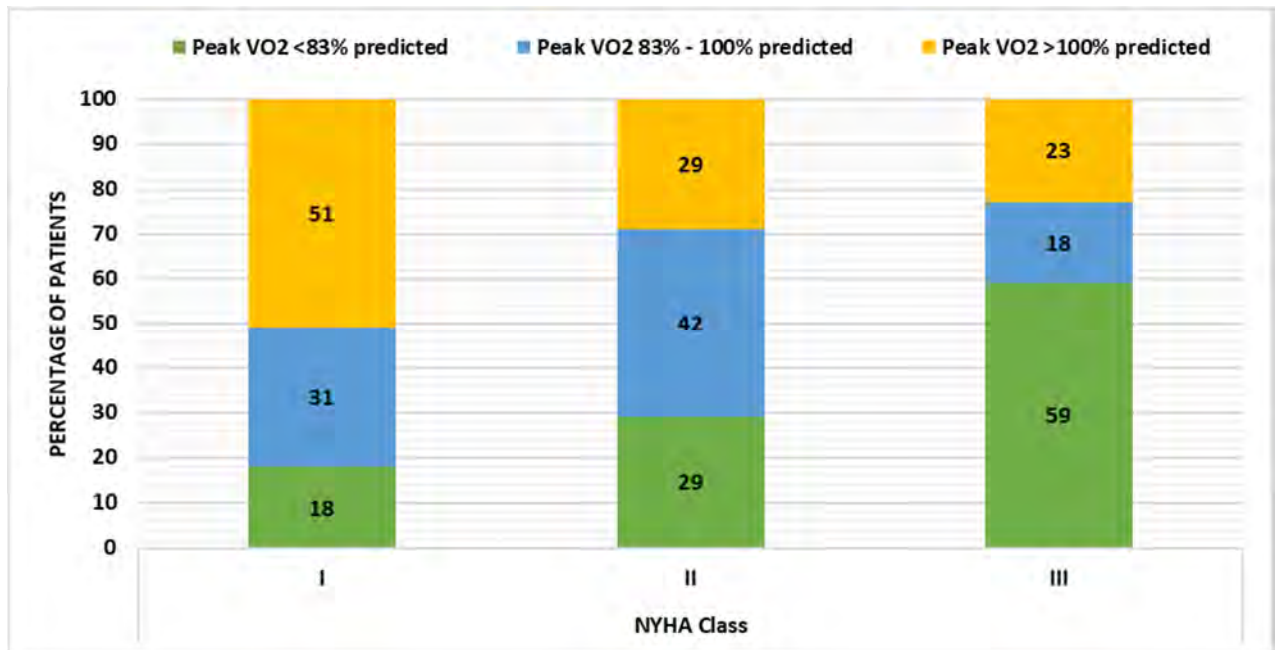
### 2.2.1 Symptomatology

The onset of symptoms in the form of exertional dyspnoea and associated decrease in exercise tolerance is a class I indication for surgery. Clear long-term postoperative survival advantages are present in those who are NYHA class I-II compared to NYHA class III-IV (4).

However, there can be significant variation in symptom reporting due to the subjective nature of symptoms, and anecdotally it is not uncommon for an asymptomatic patient to start reporting symptoms shortly after being informed of the worrying news that they have a leaky mitral valve which may require heart surgery in the future. In one study which compared the subjective and objective measures of exercise tolerance in AS patients, large disparities in subjective symptoms and actual fitness on ergometry testing was identified (156) (**Figure 2.2**).

Similarly, the categorisation of NYHA class amongst physicians is highly subjective. In one study where 113 clinicians assessed the NYHA class of 10 hypothetical pulmonary arterial hypertension patients, the intraclass correlation of NYHA classification was 0.649 with the majority of patients being categorised across two or three different NYHA classes (157). One potential method to overcome the limitations of the above widely used methodology is to assess patients' symptomatology in greater detail using Patient Reported Outcome Measures (PROMs).

**Figure 2.2** NYHA classification versus cardiopulmonary exercise test performance in patients with aortic stenosis (156).



The Minnesota Living with Heart Failure Questionnaire (MLHFQ) is one of the most widely used and recommended PROMs which contains 21 cardiac-specific questions split into a physical domain and an emotional domain (158). The MLHFQ has been found to possess good internal consistency (Cronbach's alpha = 0.85) in a study of patients with AF, with the ability to discriminate sharply between patients in NYHA class I vs class II-III with large effect sizes (159). More importantly, a medium effect (Cohen's effect size >0.50) was observed in patients completing the MLHFQ before and after AF ablation, thereby illustrating its validity for assessing changes in symptomatology during the longitudinal follow-up of cardiac patients (159).

The 36-item short-form survey (SF-36) is another validated PROM which consists of both physical and mental domains, thereby representing a more well-rounded quality of life assessment. The physical domain is sub-divided into physical functioning, physical role limitations, bodily pain, energy and general health perceptions; the mental domain is sub-divided into vitality, mental health, social functioning and emotional role limitations (160). In a large study of 7056 primary cardiac prevention patients, the physical domain of the SF-36 possessed superior predicative capability compared to traditional serum biomarkers for predicting mortality, with a low SF-36 physical domain score being associated with a 6-fold increase in mortality at 8 years follow-up (161). Furthermore, in a study of 663 undergoing mitral valve surgery, SF-36 was sensitive to postoperative left ventricular function and co-morbidities (162).

In this current study, patients' official symptom status and NYHA classification as judged by their referring consultant cardiologist were recorded. Additionally, all patients were

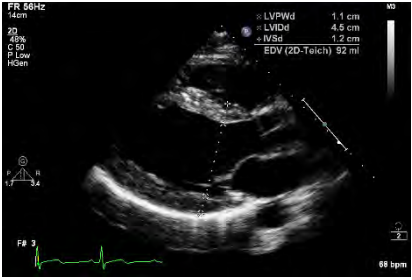
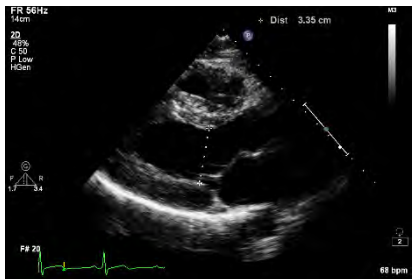




instructed to complete the MLHFQ and SF-36 PROMs in a quiet room without time pressure at baseline and follow-up visits.

### 2.2.2 Echocardiography

All patients underwent clinically indicated TTE and TOE performed by experienced echocardiographers accredited through the British Society of Echocardiography (BSE) for their initial MR diagnosis. Study data was collected from the most recent echocardiography study at the referring institution using information contained within raw echocardiography images as well as electronic reports. Study data, summarised in **Table 2.2**, included LV and RV dimensions, atrial dimensions, systolic and diastolic function as per minimum dataset requirements according to BSE guidelines (163, 164).

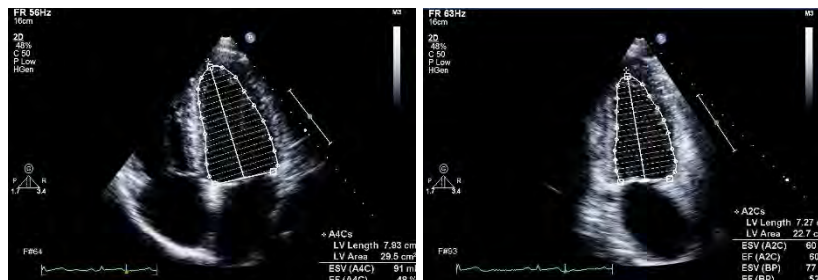
**Table 2.2** Baseline echocardiographic parameters collected from clinically indicated studies (163).

Parameter	Example images	Implications in mitral regurgitation
Left ventricular end-diastolic diameter ( LVEDd).		<p>LV dimensions are insensitive to the preferential spherical remodelling at the apex and mid-ventricular levels (111)</p>
Left ventricular end-systolic diameter ( LVESd).		
Left ventricular end-diastolic volume (LVEDV) calculated via biplane method of disks.	<div style="display: flex; justify-content: space-around;">   </div> <p>LV volume - LVEDV and LVESV via Simpson's Biplane method</p>	<p>Volumes on echocardiography are easy to acquire. This is the most widely adopted method of quantifying ventricular volumes. However, inadequate endocardial border definition is frequent, particularly in anterior and lateral endocardium</p>

Left ventricular end-systolic volume (LVESV) calculated via biplane method of disks.

Left ventricular ejection fraction (LVEF) can be calculated via the standard equation:

$$LVEF = \frac{(LVEDV - LVESV)}{LVEDV}$$



Left atrial volume (LA volume) recorded from the biplane area-length method.



LA volume of  $\geq 60\text{ml/m}^2$  is a recognised class II indication for surgery (24)

2D biplane makes assumptions on LA shape and echocardiography have been reported to underestimate LA volume compared to 3D CMR (165)

### 2.2.3 Cardiac magnetic resonance

CMR plays an increasingly important role in the diagnoses and management of cardiac pathologies, able to non-invasively quantify dimensions, volumes, systolic and diastolic function, as well as characterise myocardial tissue without the need for ionising radiation. In MR, as the current timing of surgery is dependent upon the extent and rate of progress of ventricular remodelling, the superior reproducibility of CMR impose significant advantages over echocardiography.

#### 2.2.3.1 Basic principles

CMR relies upon the principles of nuclear magnetic resonance. A permanent magnetic field with flux density of either 1.5Tesla (T) or 3T is generated using superconducting electromagnet immersed in liquid helium. This field aligns the normally random rotational axis (precession) of positively charged hydrogen nuclei (protons) to a low energy state parallel or high energy state anti-parallel to the direction of the magnetic field in the longitudinal plane (z-axis). Protons are abundant throughout the human body, particularly within water, fat and carbohydrate molecules.

At baseline, the majority of protons are in the low energy state, thereby resulting in net longitudinal magnetisation. Additionally, protons spin (precess) around the long axis of the primary magnetic field, with the rate of precession being proportional to the strength of the magnetic field. At baseline, protons precess independently, out of phase.

For image acquisition, radiofrequency (RF) coils within the scanner generates a RF pulse which energises low energy protons to high energy states, thereby decreasing the net

longitudinal magnetisation. Secondly, protons become synchronised and precess in-phase to result in net transverse magnetisation.

Following termination of the RF pulse, protons lose energy with release of a RF signal. This firstly results in transverse relaxation as protons no longer precess in-phase, with a reduction in net transverse magnetisation (T2 relaxation). Additionally, protons flip back to the low energy state parallel to the main magnetic field, with increased net longitudinal magnetisation (T1 relaxation).

A plot of net transverse relaxation against time results in magnetisation decreasing exponentially; this is termed the T2 curve. The rate of net transverse magnetisation loss varies dependent on tissue composition and structure, for example, water molecules move faster and thus have less field inhomogeneity than fat molecules. Therefore, T2 time for water molecules is longer than that of muscle or fat.

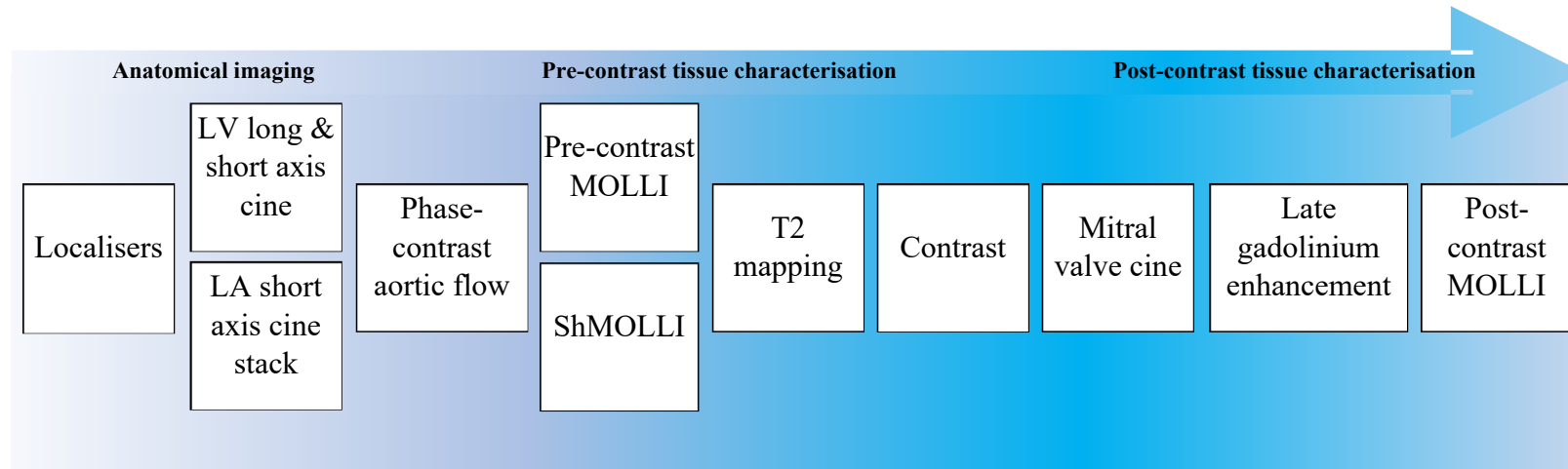
A plot of net longitudinal relaxation against time results in a logarithmic curve termed the T1 relaxation curve with the rate of re-magnetisation again dependent on underlying tissue characteristics. Water molecules move rapidly and do not flip into the low energy state quickly, therefore T1 relaxation takes longer compared to muscle or fatty tissue, resulting in a higher T1 time.

The changes in magnetic vector during relaxation induces an electrical signal which is received by the RF coils and stored within the K space. The Fourier transformation is then applied to the digital data stored within the K space to produce an analogue MRI image.

### 2.2.3.2 *Imaging protocol*

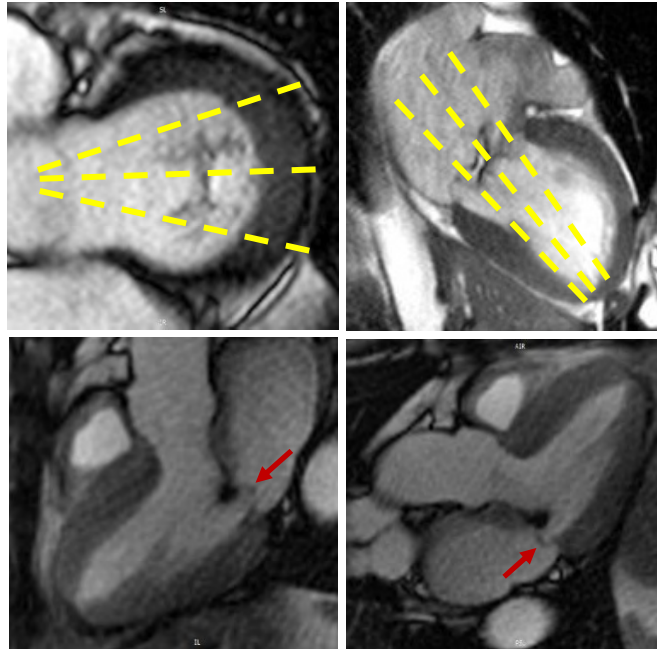
Strict safety standards were applied prior to patients entering the MRI scan room in order to exclude contraindications to MRI. All patients underwent multiparametric CMR (**Figure 2.3**) at University Hospital Birmingham (1.5 Tesla scanner Magnetom Avanto, Siemens). Vertical long axis (VLA), left ventricular outflow tract (LVOT), and horizontal long axis (HLA) steady-state free precession (SSFP) cine imaging (retrospective electrocardiographic gating) of the LV was performed to obtain apical 2- 3- and 4-chamber views respectively. These images were used to pilot the LV short axis (SAX) stack acquired using serial contiguous SAX cines (typical parameters to be achieved: temporal resolution 40–50ms, repetition time (TR) 46ms, echo time (TE) 1.17ms, flip angle 60, field of view (FoV) 300mm, in-plane resolution 1.4x1.4mm<sup>2</sup>, slice thickness 7mm with 3mm gap, minimum 25 phases per cardiac cycle) in accordance with previously validated methodology (166). MV anatomy were assessed using dedicated planes traversing the A1/P1 A2/P2 and A3/P3 scallops of the MV (**Figure 2.4**) (31). AV<sub>f</sub> was quantified from through-plane phase-contrast imaging at the level of the sinotubular junction (167). In the presence of AF, phase-contrast imaging was performed 5 times with mean AV<sub>f</sub> used within volumetric calculations. The research protocol took approximately 60 minutes per patient.

**Figure 2.3** Standard cardiac magnetic resonance imaging protocol.



T1 mapping sequences included 3(3)3(3)5 scheme Modified Look-Locker Inversion recovery (MOLLI) pulse sequence over 17 heart beats, and 5(1)1(1)1 Shortened Modified Look-Locker Inversion recovery (ShMOLLI) pulse sequence over 9 heart beats.

**Figure 2.4** Imaging planes for dedicated mitral valve views in a patient with P2 and P3 scallop prolapse.



Arrows denote the P2 (bottom left) and P3 scallops (bottom right).



#### *2.2.3.2.1 Delayed enhancement inversion recovery imaging*

For myocardial characterisation, LGE imaging was performed 7-10 minutes after

0.15mmol/kg gadolinium bolus (Gadovist Bayer Healthcare) was administered.

Gadolinium is a paramagnetic element which reduces T1 time. Following administration, Gadovist has a molecular size which allows it to distribute evenly in the extracellular space without becoming intracellular. In myocardial fibrosis, there is ECV expansion due to collagen deposition, thereby resulting in greater concentrations of gadolinium within fibrotic myocardium, which in turn experiences greater T1 shortening (168). These regions appear brighter on T1-weighted phase sensitive inversion recovery (PSIR) sequences, with signal from normal myocardium being suppressed using an initial inversion time (TI) identified with a Look-Locker sequence.

#### *2.2.3.2.2 T1 and T2 mapping*

Breath-held, ECG-gated T1 mapping was performed using the 3(3)3(3)5 scheme Modified Look-Locker Inversion recovery (MOLLI) pulse sequence over 17 heart beats (**Figure 2.5**) (169) and 5(1)1(1)1 Shortened Modified Look-Locker Inversion recovery (ShMOLLI) pulse sequence over 9 heart beats (139). MOLLI T1 myocardial and blood relaxation times pre- and 15 minutes post-gadolinium contrast administration were acquired at the basal and mid LV in the SAX plane and measured offline using cvi42® software as per European Society of Cardiology consensus statement for ECV quantification (170).

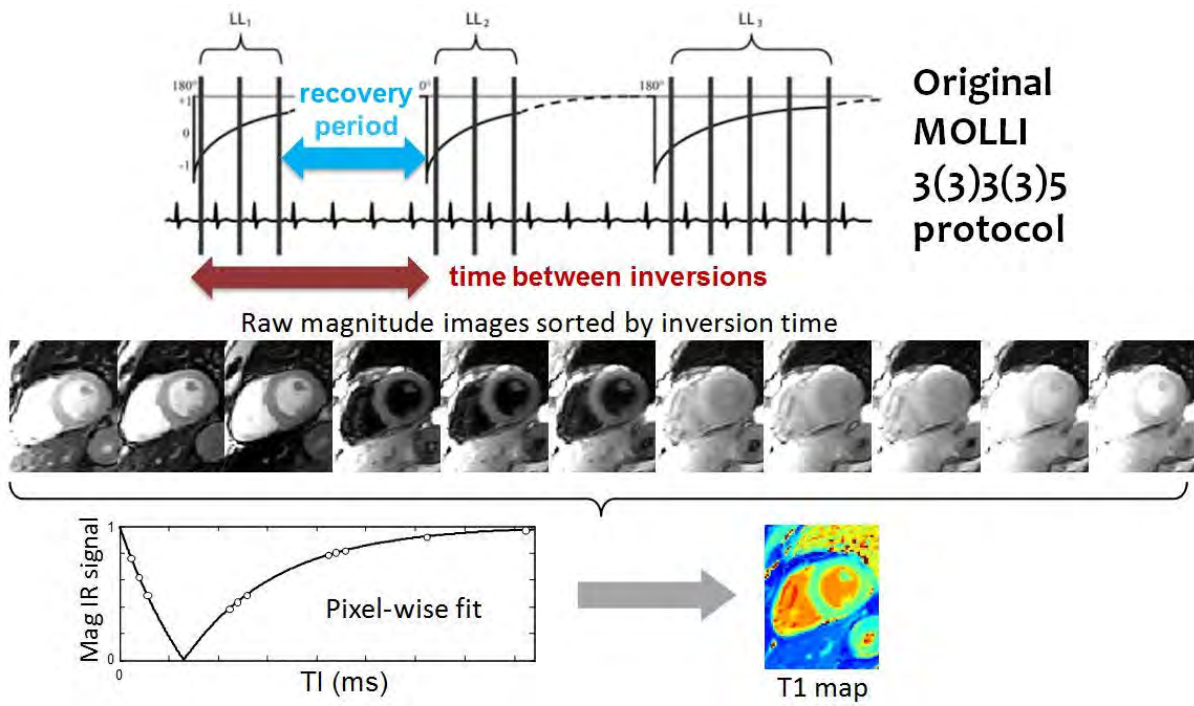
Typical ShMOLLI acquisition parameters were: TE 1.05ms, flip angle 35°, matrix size 192x144, in-plane resolution 1.9x1.9mm, slice thickness 7mm, FoV 300mm.

Typical MOLLI acquisition parameters were: TE = 1.1ms, flip angle=35°, matrix size 144x256, in-plane resolution 2.5x2.0mm, slice thickness 7mm, FoV 300mm.

Phantom studies were also undertaken to assess the stability of our T1 sequences. The T1 Mapping and ECV Standardisation (TIMES) phantom was scanned every 2 weeks for 6 months as part of the TIMES multicentre study, according to the user manual instructions distributed to centres, and as previously described (171). Analysis was done offline as previously described (171). 25 ShMOLLI and MOLLI phantom datasets were collected over the study period. The scanner room temperature was stable throughout the test period at  $21 \pm 1$  °C. Unadjusted for temperature, ShMOLLI and MOLLI T1 times across the 9 tubes were stable with coefficients of variation ranging between 0.5% to 1.6% and 0.4% to 0.9% respectively. Stability of both sequences improved further with temperature correction (0.5% to 1.5% and 0.4% to 0.9% respectively) as per our published data (172).

Breath-held, ECG gated T2 mapping was also performed at the basal and mid LV in the SAX plane with the following typical acquisition parameters: ECG triggered, TE=1.12ms, flip angle=70°, voxel size=2.2x1.8x6mm.

Figure 2.5 3(3)3(3)5 MOLLI scheme for T1 mapping in the heart (133).



### 2.2.3.3 CMR analyses

#### 2.2.3.3.1 Left ventricular volume, mass and function

Analysis of biventricular volume, function and LVM was performed with delineation of papillary muscles and trabeculations using thresholding (cvi42® version 5.3.6, Circle Cardiovascular Imaging, Canada). Measurements were made off-line using standard methodology on the contiguous short axis multi-slice acquisitions with delineation of atria/ventricles confirmed in matched long axis planes (166). For ventricular volume analysis, the endocardial border was detected with the largest and smallest cavity volumes defined as end-diastole and end-systole respectively. The endocardial border was defined as the boundary between blood pool and myocardium, with papillary muscles excluded from ventricular volume and included in ventricular mass. LVM was calculated as:

$$LVM (g) = (\text{end diastolic epicardial volume (ml)} \\ - \text{endocardial volume (ml)}) \times 1.05 (g/ml)$$

Volumes and masses were indexed to body surface area (BSA) calculated with the Mosteller formula:

$$BSA (m^2) = \sqrt{\frac{\text{weight (kg)} \times \text{height (cm)}}{3600}}$$

#### 2.2.3.3.2 MR quantification

Mitral regurgitant volume (MRV) was calculated as LVSV - AV<sub>f</sub>. Regurgitant fraction (RF) was calculated as RF (%) = (MRV / LVSV) x 100. If initial MR quantification analyses failed to pass quality assurance, then contours were edited to meet the specified criteria (Chapter 2.2.4.4).

### 2.2.3.3.3 ECV quantification

A non-linear least-square curve fitting was performed with the set of images acquired at different inversion times to generate a parametric pixel-wise colour T1 map for quantification of T1 relaxation time. Extracellular volumes were calculated using pre- and post-contrast myocardial and blood T1 values as per validated formulae (173), where ECV =  $\lambda * (1 - \text{haematocrit})$ :

$$\lambda = \frac{\frac{1}{T1_{myo\ post}} - \frac{1}{T1_{myo\ pre}}}{\frac{1}{T1_{blood\ post}} - \frac{1}{T1_{blood\ pre}}}$$

Haematocrit for ECV calculation was measured contemporaneously with the CMR study detailed in section 2.2.7.

There is no standardised off-line approach to measuring T1 myocardial relaxation times. Previous publications have employed either a manual contouring technique which quantified T1 relaxivity within a specific ‘region of interest’ (ROI) (147), or contoured the global endo- and epicardial boundaries before defining an automatic offset from these boundaries in order to reduce partial volume artefact from the blood pool and epicardium (84).

There is a sparsity of data on the optimal technique for patients with MR. Theoretically, a ROI approach has the advantage of being able to target regions containing focal disease processes and avoid regions deemed to contain artefact on visual assessment. However, a ROI approach may lower the reproducibility of results as ROIs are likely to vary across

observers, and if relatively small ROIs are chosen, ECV derived from such technique may not be reflective of generalised changes within the myocardium.

Conversely, a generalised contouring approach usually covers a larger proportion of the myocardium, therefore results may be more representative of diffuse disease processes. However, changes in T1 as a result of focal disease processes may be diluted when T1 relaxivity values are averaged across the entire myocardium. Furthermore, there are no guidelines on the appropriate level of endo- and epicardial offsets; a low offset will increase blood pool partial volume artefact, while increasing offsets will reduce the sensitivity of MRI to detect pathological conditions driving subendocardial and endomyocardial fibrosis. Finally, when a segment of the myocardium is influenced by artefacts such as susceptibility artefact arising from stomach contents or wrap artefact from the chest wall, these segments may need manual exclusion – introducing another source of interobserver variability.

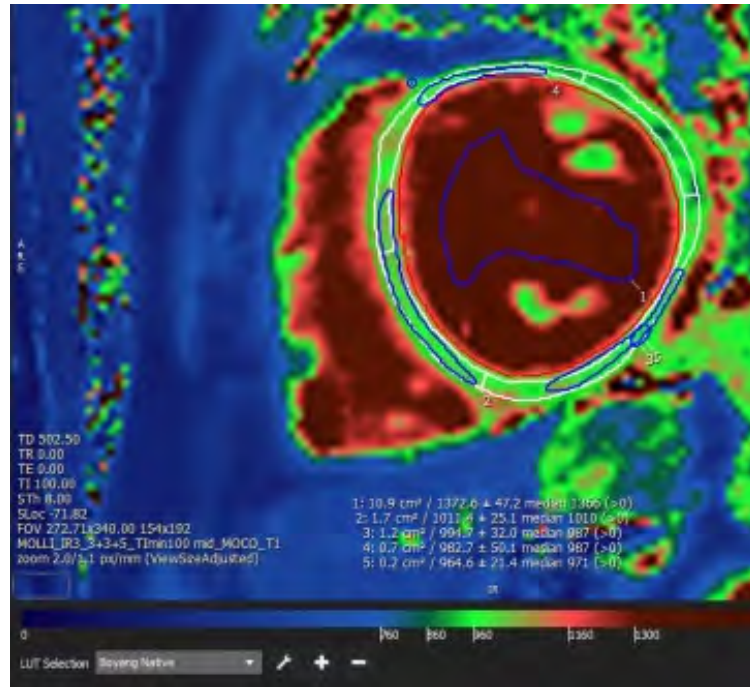
To test our methodology, a pilot study was set up to compare the variability and reproducibility of ECV derived from manual ROIs against different endocardial:epicardial offsets within our first 30 MR patients (174). ROIs were defined in the pre- and post-contrast T1 map in the LV septum, anterior, and posterior LV free wall to mirror the location of surgical biopsies (Section 2.3). For the global contouring approach, smooth endocardial and epicardial boundaries were defined on T1 maps, before applying a range of offsets. After defining the RV insertion point, segmental mean T1 values were recorded for 12 out of 16 American Heart Association (AHA) segments (175). T1 analyses were not

performed for the 4 apical segments due to increased partial volume artefact as the muscle become thinner towards the apex.

A 20:20 percent offset was chosen to provide T1 relaxivity of the myocardium, away from influences of the endocardium and epicardium. 0:50 offset was selected because it best coincides with myocardial regions reachable on surgical biopsy. Finally, 10:50 and 20:50 offsets were used to study the effects of a stepwise reduction in the influence of partial volume artefacts.

Within this pilot study, we found that a ROI approach (**Figure 2.6**) produced lower ECV compared to global contouring techniques. Within the global contour approaches, 0:50 offsets produced the highest ECV, whilst 20:20 offsets produced the lowest ECV (**Figure 2.7**) and the best interobserver reproducibility after 8% segmental exclusion (mean bias  $0.21 \pm 0.12\%$ , intraclass correlation, ICC 0.994) (174). Due to its superior reproducibility, the 20:20 offset technique was adopted for the main study.

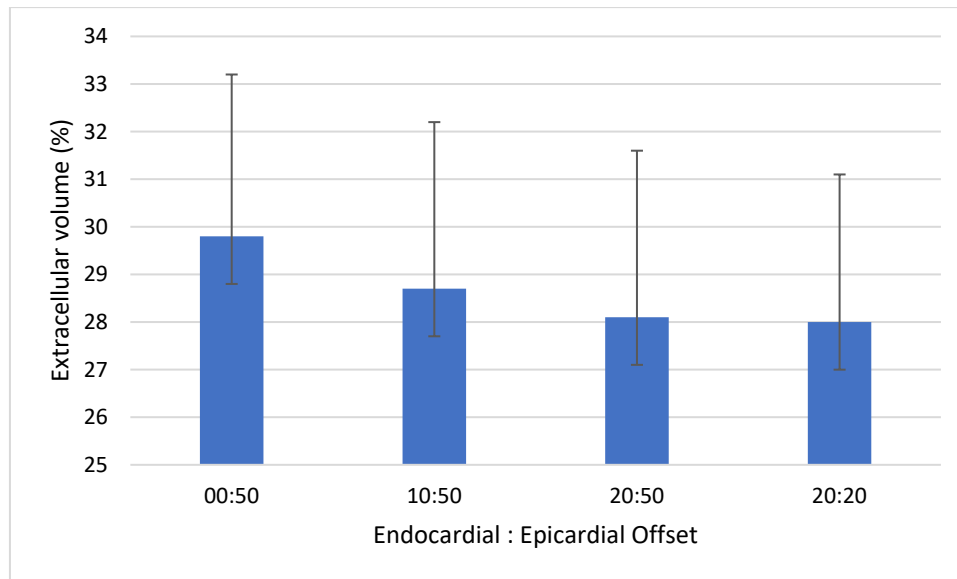
**Figure 2.6** Illustrative example of ROI and 20:20 offset approaches to T1 quantification in a native MOLLI sequence.



Colour scales have been defined with blue denoting lower T1 times, red denoting higher T1 times, with green in the middle.



**Figure 2.7** Effect of endocardial and epicardial offsets on calculated ECV.



Bars represent mean ECV, lines represent standard deviation (N=30). Lowest ECV values were obtained using the 20:20 offset approach.

### *Feature tracking*

Myocardial strain derived from feature-tracking of CMR cines (FT-CMR) represented a superior marker of systolic function when compared to LVEF and may have acted as a functional maker of fibrosis. For LV FT-CMR, both 2D and 3D techniques existed but we were unsure which was superior; this was therefore studied within Chapter 3.

LV myocardial deformation was assessed using feature-tracking on CMR (FT-CMR) using cvi42® (version 5.3.6, Circle Cardiovascular Imaging, Canada) as per our published methodology (176). 3D FT-CMR was performed using smoothed endocardial and epicardial borders in the end-diastolic frame of all short and long axis slices before defining the superior RV insertion points within the LV. Peak systolic strain, early diastolic strain rate and late diastolic strain rate were recorded in the circumferential, radial and longitudinal directions.

RV myocardial deformation was assessed using 2D FT-CMR from the RV free wall from HLA SSFP cine images as per our published methodology (177). The ventricular septum was not included within RV strain quantification in order clearly distinguish RV from LV dysfunction by eliminating influence from the interventricular septum. Furthermore, RV free wall longitudinal strain derived from speckle tracking echocardiography have been found to provide incremental prognostic value for predicting cardiac events in acute heart failure patients (178).

#### *2.2.3.4 Quality assurance*

All CMR studies were anonymised with unique computer-generated random identifiers by Dr A.P. who is an independent party from this study. All CMR analyses were subsequently

performed on anonymised studies. Unblinding was performed after completion of analyses.

For mass and volumetric assessment, manual contours were only accepted if: 1)  $AV_f$  is within 10ml of RV stroke volume (RVSV) in the absence of significant tricuspid regurgitation, and 2) LVM in diastole and systole are within 10% of each other.

For myocardial characterisation, all T1 and T2 maps were meticulously checked for the presence of breathing, susceptibility, motion correction and gating related artefacts at both scanning and analyses stages. Studies containing artefact were repeated following optimisation with localised shimming, adjustment of FoV, application of saturation bands and phase swapping during the scanning stage. Regions containing artefact were avoided when contouring; if avoidance was not possible then that specific LV segment would be excluded from the results.

For myocardial deformation quantification, inter- and intra-observer reproducibility of 3D FT-CMR were assessed in comparison with established 2D FT-CMR techniques (Chapter 3) (176).

#### 2.2.4 Cardiopulmonary exercise test

CPET was performed on a treadmill using an incremental RAMP protocol based on American Thoracic Society guidelines (179, 180).

Baseline resting haemodynamic parameters included heart rate (HR), systolic and diastolic blood pressure (BP); these parameters were monitored throughout the exercise and

recovery phases of the exercise protocol. A RAMP slope, based on gender, age, and estimated physical fitness of the subject was chosen with the aim of stimulating the patient to maximal exercise capacity during a test of approximately 8-12 minutes duration. Subjects wore a tight facemask to permit continuous measurements of ventilation, oxygen consumption ( $\text{VO}_2$ ), and carbon dioxide production ( $\text{VCO}_2$ ) in expired gas, from which estimates of peak oxygen consumption ( $\text{VO}_{2\text{peak}}$ ) and anaerobic threshold (AT) were obtained using a V-slope method (181). The ratio of minute ventilation (VE) to  $\text{VCO}_2$  ( $\text{VE}/\text{VCO}_2$ ) is an indicator of gas exchange efficiency; this was measured at the point of AT (182). Gas measurements were made on the commercially available CASE exercise testing system (GE Healthcare, Chicago, USA) fitted with PowerCube-ergo (SCHILLER, UK), where  $\text{O}_2$  were measured via micro fuel cell and  $\text{CO}_2$  via ultrasound sensors. ECG tracing were continuously monitored at rest, exercise and recovery for the assessment of arrhythmia burden. As part of quality assurance, the PowerCube-ergo system was calibrated on a daily basis for volumetric flow measurements using a 3L syringe,  $\text{CO}_2$  concentration using 0.15%  $\text{CO}_2$  calibration cylinder and baseline testing conditions including room temperature, humidity, altitude and atmospheric pressure.

$\text{O}_2$  pulse was automatically calculated as  $\text{VO}_2/\text{HR}$ . A cardiac limitation to exercise was defined as failure of systolic BP to increase by 20mmHg (183), the presence of chronotropic incompetence in the absence of non-cardiac limiting factors (184), plateauing or decrease in the  $\text{O}_2$  pulse curve in response to exercise (185).

A respiratory limitation to exercise was defined as the presence of a low breathing reserve (BR) at peak exercise coupled with exercise cessation due to dyspnoea; this may present

with associated exercise induced desaturation in pulse oximetry and low or plateauing ventilatory tidal volume (186). During exercise recovery, patients were required to indicate their level of perceived exertion intensity on the standard Borg scale (187).

#### 2.2.5 Exercise stress echocardiography

Exercise stress echocardiography (ESE) was performed at the initial study visit according to our published methodology (188). The aim of ESE was to investigate the presence of markers of poor postoperative prognosis in patients without pre-established class I surgical indication. These include exercise induced worsening in MR severity (189), pulmonary hypertension (190), and ventricular contractile reserve (191). ESE was therefore optional for patients with an established class I indication for MV surgery (including the presence of symptoms and echocardiographic evidence of systolic dysfunction), and compulsory for all others.

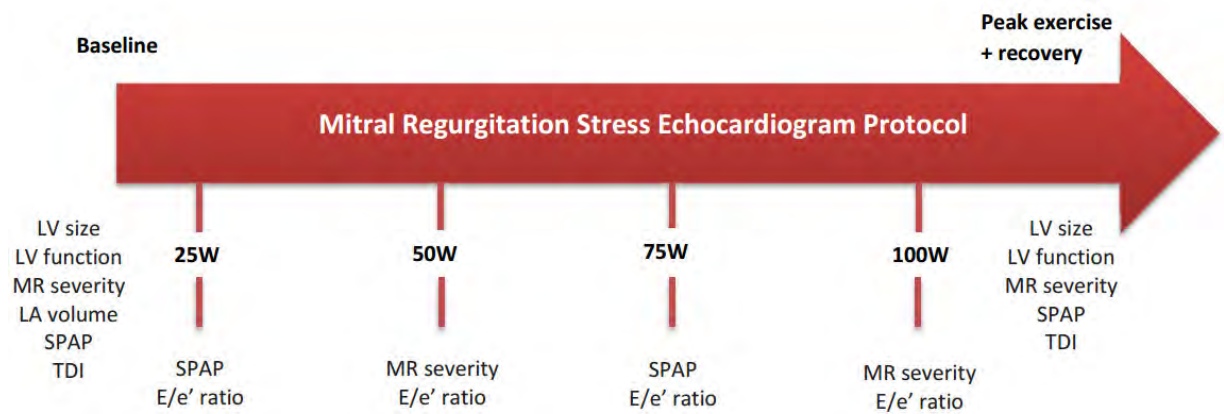
Following measurement of baseline echocardiography parameters (**Table 2.2**), patients were asked to exercise on a semi-supine bicycle ergometer at initial workloads of 20-25W for 2 minutes; the workload were then increased in steps of 15-30W every 2 minutes as decided according to the physical fitness and symptom status of the patient. This protocol (**Figure 2.8**) allowed time to perform additional measurements of MR severity and estimations of LV filling pressure and pulmonary artery pressure during each 2-minute period of exercise. LV size and systolic function were re-assessed at peak exercise. Global longitudinal strain was derived from the apical 2- 3- and 4-chamber views via speckle tracking at baseline and peak exercise (Epiq, Phillips). The quantification of MR was carried out using the integration of quantitative and qualitative approaches (43); ‘quantitatively’ by subtracting the stroke volume across the left ventricular outflow tract

(LVOT) from the stroke volume across the MV annulus, or the flow convergence method by proximal isovelocity surface area; and ‘qualitatively’ by visual assessment of the colour flow jet area and flow convergence zone.

The above methodology represented a revised research protocol which was adopted within a month of study initiation. An original research protocol planned to limit patients’ exercise requirements to only one exercise session by integrating VO<sub>2</sub>peak measurements into the stress echocardiography protocol. However, it soon became apparent that certain patients, who were self-reported asymptomatic from their MR, struggled to achieve a normal range VO<sub>2</sub>peak on ergometer.

Whilst previous studies have reported treadmill CPET to generally produce higher VO<sub>2</sub>peak compared to bicycle ergometer, it is recognised an individual’s familiarity with the exercise is a key factor (192). In practice, this means that a cyclist on an ergometer will be able to achieve a similar VO<sub>2</sub>peak as a runner on a treadmill. However, it was soon noted that a proportion of patients struggled more than others with the unfamiliarity of cycling in a left-tilted semi-supine position. The research protocol was therefore adapted into this revised format with an initial maximal exercise treadmill test, followed by a period of recovery and subsequent symptom-limited stress echocardiography where a minimum of  $\geq 80\%$  age predicted upper heart rate should be reached.

**Figure 2.8** Stress echocardiography protocol.



### 2.2.6 Haematology and biochemistry

10ml of whole blood was collected across one purple-top ethylenediaminetetraacetic acid blood tube, one gold-top serum separating tube, and one blue-top buffered sodium citrate blood tube in the Wellcome Clinical Research Facility, Birmingham. Routine haematological and biochemical assays were undertaken on venous samples in the departments of Haematology and Clinical Biochemistry, University Hospital Birmingham. Haematology tests included full blood count (haemoglobin, haematocrit, mean corpuscular volume, white cell count, platelet count) and international normalised ratio for clotting. Biochemistry analyses included measurement of urea, creatinine, electrolytes (sodium, potassium, calcium), liver function tests (alanine transaminase, alkaline phosphatase, bilirubin), C-reactive protein, N-terminal prohormone of brain natriuretic peptide (NTproBNP). Estimated glomerular filtration rate (eGFR) was calculated using the Modification of Diet in Renal Disease equation (193).

### 2.2.7 Inflammation and fibrosis markers

For each patient, an additional 8ml of whole blood was collected in two gold-top serum separating tubes, which were inverted five times to allow mixing of blood with clot activator. Blood was left to clot for 30-60 minutes in a vertical position until a dense clot was observed. The samples were then centrifuged at 1300g for 10 minutes in a swing-bucket rotor. Serum was then removed from the top down to avoid disturbing the gel plug. Two aliquots of 1ml serum were stored in cryovials at -80°C in the Wellcome Clinical Research Facility, Birmingham.

On completion of serum collection for the whole study cohort, serum was couriered in dry ice to external laboratories for analyses. TGF- $\beta$ 1 and IL- $\beta$  levels were measured using Bio-



Plex assays (Bio-Rad, Hercules, USA) by the Immunology department at the University of Birmingham. Amino terminal levels of type III procollagen (P3NP) and type I procollagen (P1NP) are markers of collagen turnover; these were measured with commercially available Roche Elecsys total P1NP immunoassay and Orion Diagnostica Uniq P3NP radioimmunoassay by the Royal Liverpool University Hospital Biochemistry Department.

### 2.3 Histology

Intraoperative myocardial biopsies were taken from the LV septum, anterior and posterior LV free wall. Biopsies were taken either with a Tru-Cut biopsy needle, or by scalpel, depending on access and surgeons' preference. Samples were immediately fixed in 10% buffered formalin and were subsequently embedded in paraffin at the histopathology department, University Hospital Birmingham. 4µm sections were stained for Elastic Van Gieson (EHVG) and Masson's trichrome (MT) for the assessment of myocardial fibrosis. All sections were anonymised by the histopathology department using a unique 7-character identifier before being processed for whole slide scanning at x20 magnification using an Axio Scan.Z1 slide scanner (ZEISS, Oberkochen, Germany). Scanned slides were reviewed and exported into tagged image file format (TIFF) images using ZEN software (Carl Zeiss Microscopy, Oberkochen, Germany).

CVF quantification on EHVG and MT sections were performed using Ilastik (version 1.3.0, Heidelberg, Germany) based analyses of TIFF files (**Figure 2.9**). Ilastik is an interactive machine-learning based, supervised object classification and segmentation tool (194). User supervised training was performed on a series of 15 scanned slides until the reliable classification of pixels belonging to 1) myocytes, 2) fibrous tissue, and 3) extra-

cellular space was obtained. A simple-segmentation map was then exported for pixel quantification in ImageJ for the calculation of CVF.

Sections were also stained with haematoxylin and eosin (H&E) for assessment of myocyte dimensions. Myofiber hypertrophy quantification was performed by manually quantifying the cross-sectional area of randomly selected myofibers via ZEN software (Carl Zeiss Microscopy). To ensure consistency and improve cross-comparison reliability, myofibers were only eligible for quantification when present in its axial orientation with visible nuclei present. A sample size of 50 myofibers per patient was chosen as per previously accepted methodology (195).

**Figure 2.9** User supervised training of CVF quantification using Ilastik.

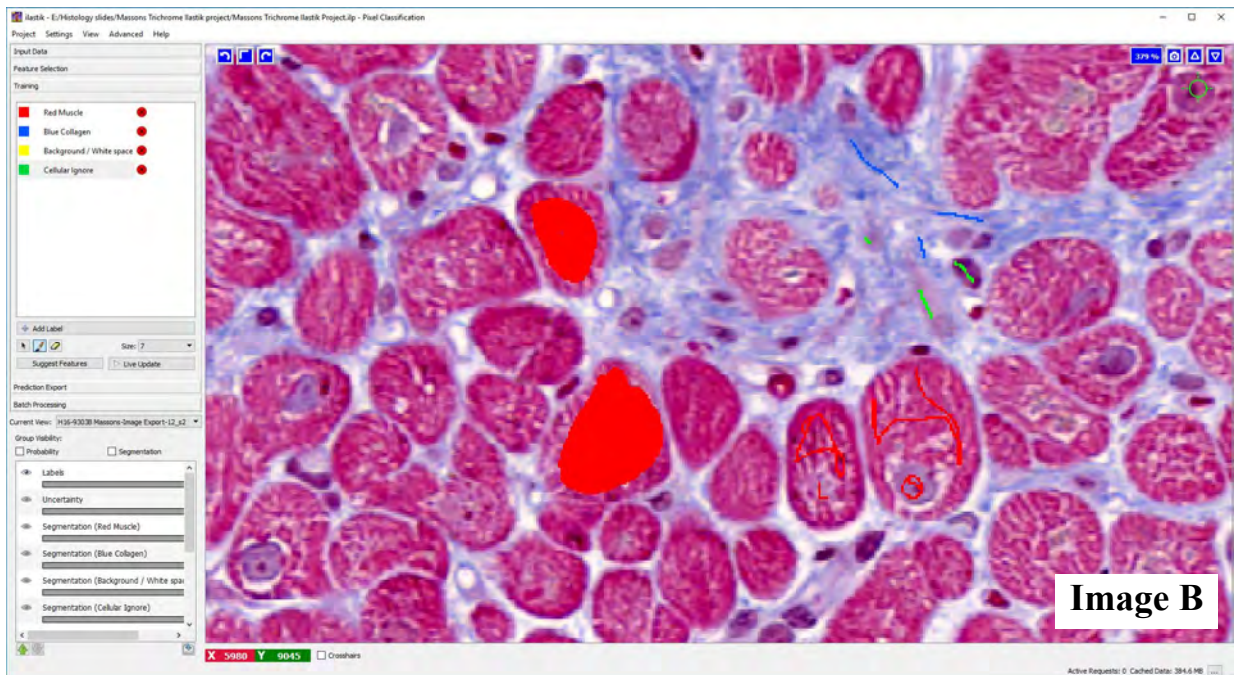
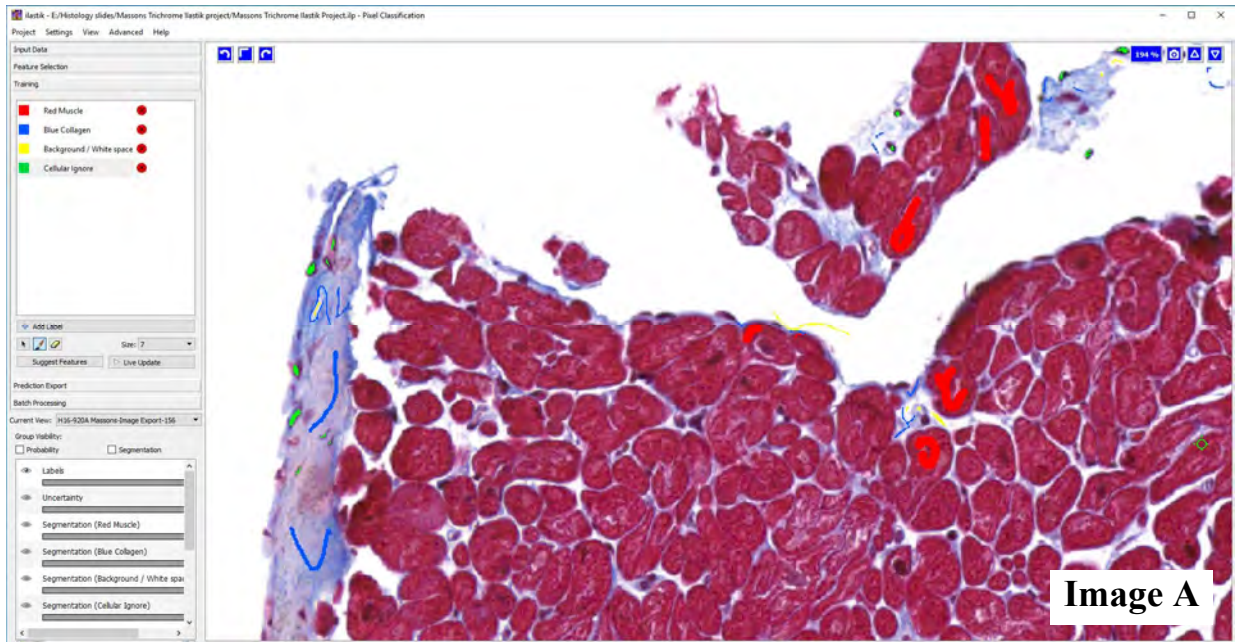
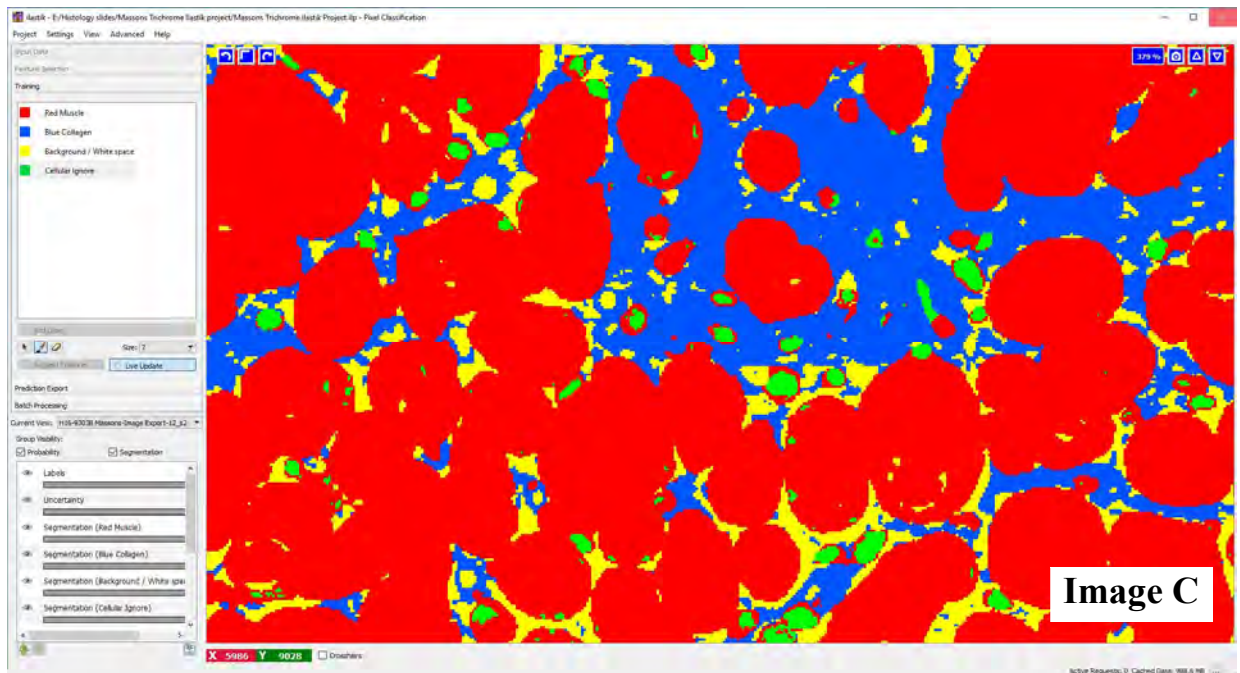


Figure 2.9 continued.



**Image A** illustrates providing Ilastik with the definitions 1) muscle (red), 2) collagen (blue), 3) background (yellow), and 4) other cellular matter (green) across one microscopy field. **Image B** demonstrates repetition of the training process across a different microscopy field, which is repeated across the entire slide for 15 slides. **Image C** illustrates the classification of pixels across microscopy field B, after completion of training.

### 2.3.1 Validation of collagen volume fraction quantification techniques

The clinical diagnosis and subjective quantification of histological fibrosis is routinely performed using EHVG and MT stains within the histopathology department of QEHB.

EHVG stains collagen pink, elastin purple and muscle brown. MT stains fibrous tissue blue, muscles red, and cytoplasm pink. Both stains offer the histopathologist good visual contrast for distinguishing fibrosis from muscle. However, it was not known which would allow more accurate semi-automated software quantification of fibrosis.

A validation study was setup comparing the accuracy of CVF between the two stains. For each stain, user supervised training was performed within Ilastik on a series of 15 full-slide TIFF images, until visually accurate classification of pixels into either 1) myocyte, 2) fibrous tissue, or 3) extracellular space was achieved across the 15 scanned slides (**Figure 2.10**).

After completion of training, the Ilastik algorithms were used to quantify the number of pixels identified as muscle or fibrosis tissue to allow calculation of CVF:

$$\text{Collagen Volume Fraction (CVF)} = \frac{\text{Fibrosis tissue pixels}}{\text{Fibrosis tissue pixels} + \text{Muscle tissue pixels}}$$

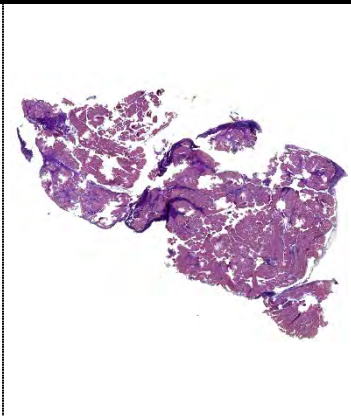
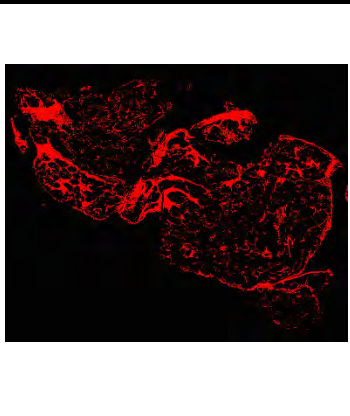
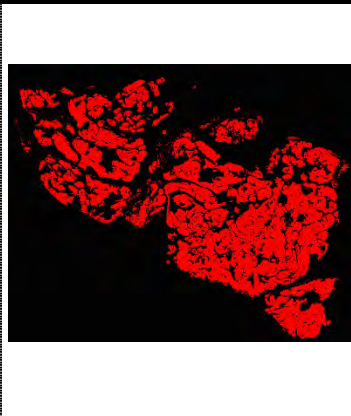
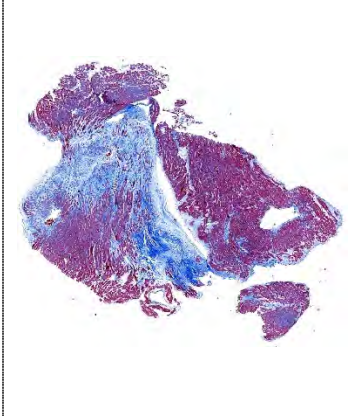

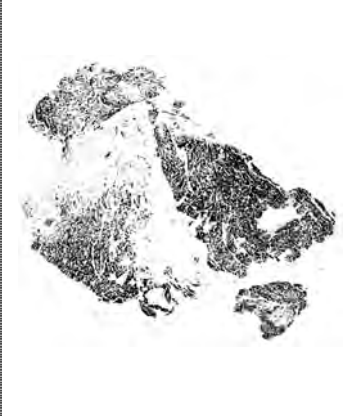
Validation of Ilastik quantification results on both EHVG and MT sections were carried out by correlating values against the subjective and semi-objective quantification of CVF as determined by an expert consultant cardiac histopathologist (Dr D.N.) who was blinded to the clinical details of each patient. 129 biopsy slides from the first 41 surgical patients

were included within this validation study. Semi-objective quantification was performed by manually tracing over areas of fibrosis over 5 representative field-of-views at x20 magnification.

Across these 129 biopsy slides, Ilastik classification of MT slides correlated well with expert quantification ( $R=0.82$ ,  $P<0.001$ ); conversely, Ilastik classification of EHVG slides correlated weakly with expert quantification ( $R=0.24$ ,  $P=0.006$ , **Figure 2.11**). Whilst a perfect correlation was not expected as the expert histopathologist only employed semi-quantitative methods across five fields-of-view which were subjectively representative of the whole slide, the Ilastik algorithms were noted to benefit from the greater colour contrast generated by MT staining. Upon visual inspection of classification results, Ilastik based EHVG classification was subject to under- and over-estimation of CVF. This may have been the result of slight alterations in section thickness, which can alter the colour intensity of stains.

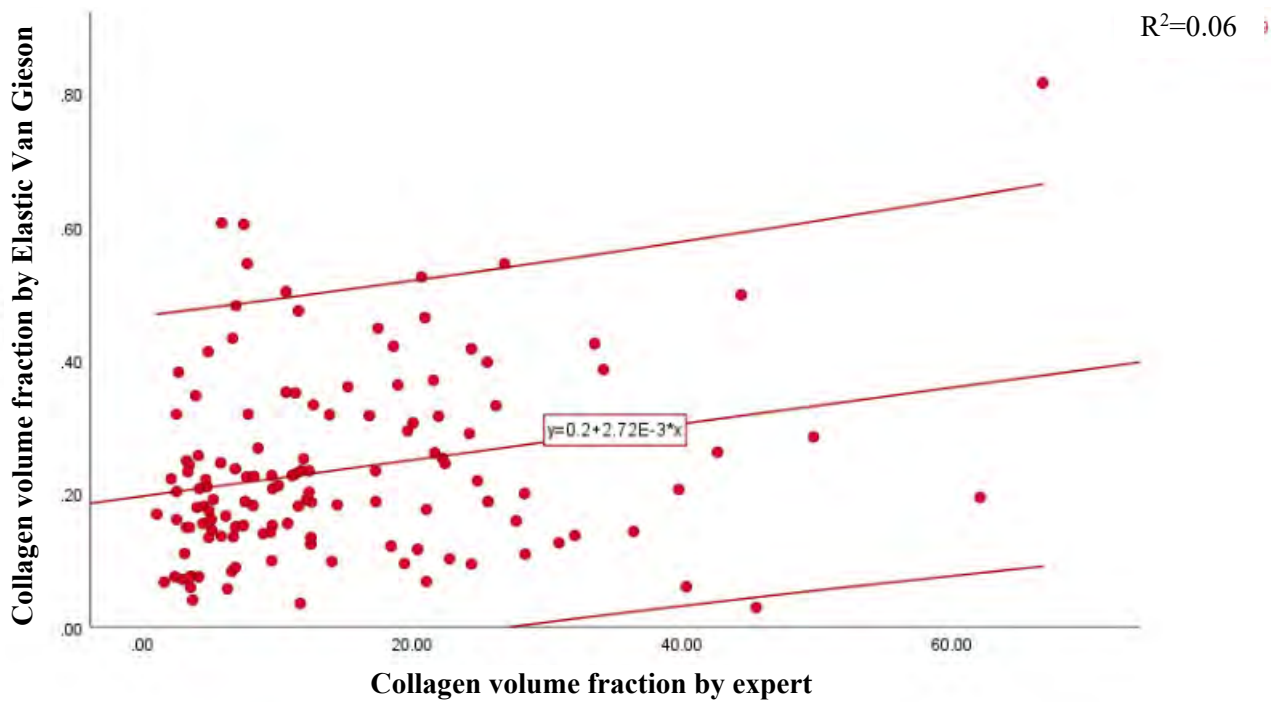
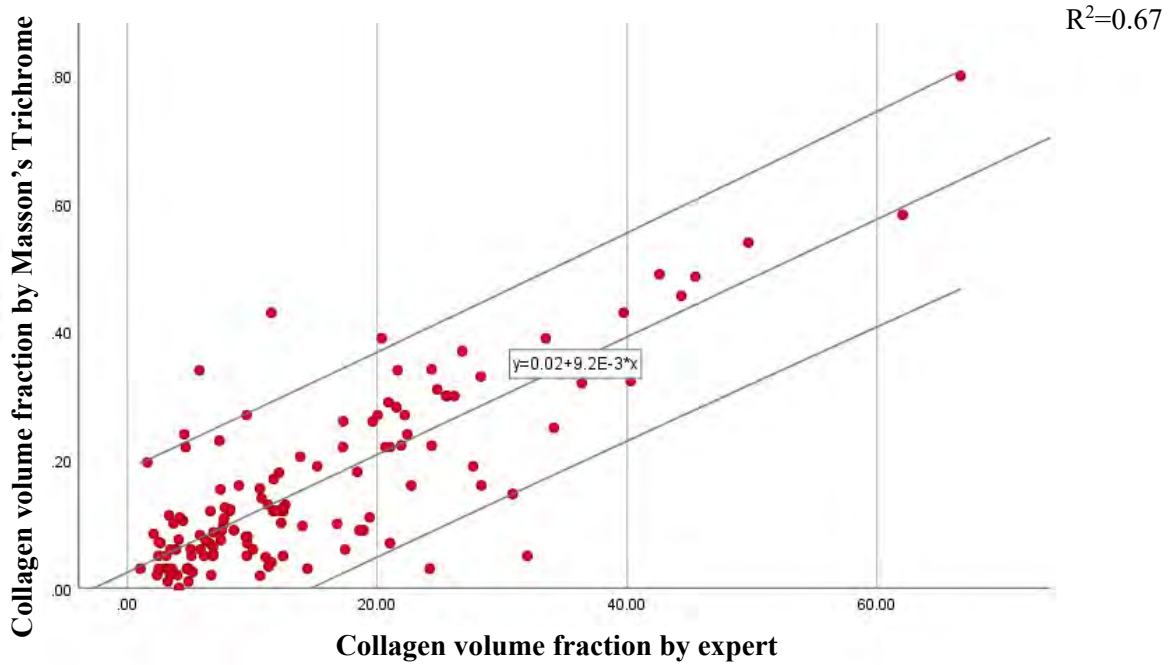
Based upon the results of this pilot study, Ilastik classification of MT stained sections possessed good correlation with that of a consultant cardiac histopathologist and was therefore utilised as the preferred CVF quantification technique in the main study (see Chapter 5).

**Figure 2.10** Visual illustration of the data output following the Ilastik based characterisation of EHVG and MT sections into fibrosis and muscle tissue.

	Scanned slides	Fibrosis tissue	Muscle tissue
Elastic Van Gieson			
Masson's Trichrome			

A higher degree of visual contrast between fibrosis and muscle tissue is subjectively present on Masson's Trichrome stained sections.

**Figure 2.11** Scatter plots demonstrating relationship of collagen volume fraction results between automated classification by Ilastik and expert quantification for Masson's Trichrome (top) and Elastic Van Gieson (bottom).





## 2.4 Perioperative outcomes and postoperative follow-up

Peri-operative outcomes were gathered from anaesthetic, perfusionist and operation notes.

Postoperative outcomes were collected from patients' electronic and paper health records.

For the peri-operative period, key measures including the duration of aortic clamping and cardiac bypass (as a measure of operative duration), and occurrence of intra-operative complications were recorded.

For the postoperative inpatient period, time to extubation and weaning off inotropic support, as well as need for renal replacement therapy and length of intensive care unit (ICU) and hospital stay were recorded. Competency of MV repair were confirmed by intra-operative TOE and postoperative inpatient TTE; patients with severe MR recurrence were excluded from subsequent analyses.

Patients were initially offered follow-up study visits 9-12 months following surgery. This 9-month period was selected as a balance between the intention to maximise follow-up duration within a feasible study completion period. Complications related to MV surgery were recorded from clinical history and review of patients' clinic records. Repeat CMR, treadmill CPET and PROMs were performed at this follow-up visit to quantify the degree of LV reverse remodelling and its functional consequences on patients' symptoms and exercise capacity.

There were significant delays to patients from the time of surgical referral to receiving their operation. Furthermore, recruitment at the beginning of the study period from QEHB was slower than expected. Therefore, during the final year of this study, the postoperative

follow-up period was shortened to 6 months in order to facilitate the completion of follow-up visits for all recruited patients. This adjustment to the follow-up period should not have significantly altered the observed degree of reverse remodelling within the cardiac chambers, as previous studies have reported the majority of volumetric changes within the heart to occur within 6 months following surgery (196, 197).

## 2.5 Statistical analyses and power calculation

The following methods were employed to examine data and statistical analysis using IBM SPSS Statistics (version 24, IBM Corp. NY. USA).

### 2.5.1 Power calculation

Based on pilot data and previously published reports (68, 147) the standard deviation of LVESVi in MR patients is 12ml. A survival advantage has previously been shown with a 7ml postoperative reduction in LVESVi (68). A volume difference of this magnitude was therefore chosen as a clinically significant difference when comparing patients with above- and below-median ECV. An independent T-test with 48 patients per group (96 total), and a within group standard deviation of 12ml yields a minimal detectable difference of 7ml at 80% power, with  $\alpha=0.05$ . This study aimed to recruit 115 surgical patients in total based on the assumption of a 15% dropout rate.

### 2.5.2 General data handling

Data distribution for continuous variables were assessed using normality plots and the Shapiro-Wilk test. Parametric data are presented as mean  $\pm$  standard deviation (SD), or absolute change  $\pm$  standard error of the mean (SEM), with 95% confidence interval (CI). Non-parametric data are expressed as median and interquartile range (IQR). Categorical

data are presented as frequency with percentage (%). Outlier data points were not excluded from statistical analyses.

### 2.5.3 Statistical methods

Continuous data were tested as appropriate using paired or independent two-tailed Student's T-test, or analysis of variance (ANOVA). Non-parametric data were log transformed where appropriate to achieve normality; if this was not suitable, then non-parametric testing (Mann Whitney U,  $\chi^2$  or Fisher's Exact Test as appropriate) was performed.

Categorical variables were assessed with the chi-squared test. Correlations of parametric data are expressed using Pearson's correlation co-efficient (R); Spearman's rank correlation coefficient (rho) was used for non-parametric data.

Statistical significance was taken as  $P < 0.05$  or as specified in each study in cases of Benjamini–Hochberg correction for multiple testing with a false discovery rate of 25%.

### 2.5.4 Regression models

Stepwise backward multivariable regression models were used to explore the relationship between dependent and independent variable(s). Multicollinearity between independent variables were detected using variance inflation factors.

Variables included in regression models were limited to ones known to influence the dependent variable from previous studies, as well as variables that were significant at the level of  $P < 0.10$  on simple linear regression. Regression models are assessed for goodness-of-fit using residual plots and reported with the coefficient of determination ( $r^2$ ). Associations found within regression analyses are reported with unstandardised  $\beta$  coefficient ( $\beta$ ) and standard error (SE). For regression models, gender is consistently coded as female = 0, male = 1.

#### 2.5.5 Assessment of reproducibility

Intra- and inter-observer agreement was tested by calculating mean absolute bias and 95% limits of agreement (CI) from Bland–Altman analyses, and intra-class correlation coefficient (ICC) for absolute agreement.

## 2.6 Summary

This study recruited consecutive patients with primary degenerative mitral regurgitation from referring cardiology departments and three established heart valve tertiary surgical centres within the West Midlands. Patients were comprehensively assessed with formal symptom quantification and cardiopulmonary testing. Their hearts were characterised anatomically with multiparametric CMR and functionally with exercise stress echocardiography. These results were corroborated against histological adaptations within the LV myocardium, and their implications for peri- and postoperative outcomes were determined.

## CHAPTER 3

### VALIDATION: NOVEL TECHNIQUES FOR MYOCARDIAL DEFORMATION ANALYSES

#### 3.1 Introduction

##### 3.1.1 Deformation imaging

The extent of myocardial deformation which occurs following application of contractile and relaxation forces can be quantified as strain and strain rate. This deformation represents a fundamental property of the tissue (198) and there is increasing evidence for a causative relationship between the development of myocardial fibrosis and a reduction in ventricular deformation across a range of conditions (199-201). Deformation imaging may, therefore, act as a functional imaging biomarker of myocardial fibrosis (149). Moreover, the correlation between fibrosis and strain has been established in patients with preserved ejection fraction, making strain a particularly promising prognostic biomarker in MR.

The gold standard technique for strain quantification is via the implantation of radiopaque materials (202) or ultrasound crystals (203) into the heart wall. However, the invasive nature of this technique has imposed severe limitations on its clinical applicability.

Non-invasive deformation analyses can be performed on CMR. Traditionally, 2-dimensional (2D) CMR “tagging” studies have been performed using one of many dedicated deformation sequences such as spatial modulation of magnetization (SPAMM), harmonic phase (HARP), displacement encoding (DENSE) and strain encoding (SENC). These sequences magnetise temporary tags into the myocardium which are prominent during systole and fades during diastole; these tags can be tracked throughout the cardiac cycle to highlight myocardial movement. The main disadvantage of dedicated deformation

CMR sequences is its time-consuming nature. To overcome this, it is possible to derive strain from feature tracking of steady-state free precession (SSFP) cine images. This latter technique has been labelled as a “double feature” as it negates the requirement to acquire additional sequences and offers rapid post-processing, while also delivering standard volumetric assessments of the LV (127, 128).

### 3.1.2 2D versus 3D feature tracking for the left ventricle

A recent meta-analysis generated normal ranges for feature tracking on CMR (FT-CMR) using the combined data of 659 participants pooled from 18 studies (204). However, this study also highlighted that previous attempts to define normal range values have employed 2D based techniques which either take the average of 3 long- or short-axis readings, or more frequently, record a single global longitudinal strain (GLS) value from the 4-chamber view, or a single global circumferential (GCS) and radial (GRS) strain value from the mid-LV level. Whilst assessing strain from either one or three short-axis (SAX; for circumferential and radial strain) and long-axis (LAX; for longitudinal strain) slices may be attractive due to its simplicity and low time requirement, it may not be truly representative of global myocardial function.

Recently, algorithms have been developed which permit 3D feature tracking of SSFP cine images, but there are no data comparing this technique with 2D analyses. In theory, 3D deformation analyses may overcome the through-plane loss of features in the third dimension and be less sensitive to inaccurate tracking within a single cine slice and hence improve the reproducibility of FT-CMR.

### 3.1.3 Right ventricular feature tracking in mitral valve disease

Reproducible and repeatable characterisation of RV systolic function is vital for monitoring patients with MR for multiple reasons. Firstly, the onset of overt heart failure symptoms in MR is a class I indication for surgery due to its significant association with postoperative outcome penalties (24, 25). For many decades, RV dysfunction is known to be an important determinant of exercise capacity in heart failure patients, including those with isolated valvular heart disease, and is independent of LV dysfunction (205, 206). Secondly, RV impairment is common in primary MR with one study reporting a preoperative prevalence of 30% (116). Its presence has been associated with a more complex postoperative recovery period as patients require longer ICU and hospital stays (207) as well as an increased rate of re-hospitalisation (208). Finally, the deleterious effects of preoperative RV dysfunction persist during long-term follow-up with multiple groups reporting higher rates of MR recurrence and increased cardiovascular mortality during follow-up to 10 years (116, 207, 208).

RV systolic function is traditionally quantified using the measurements of tricuspid annular plane systolic excursion (TAPSE), fractional area change (FAC) and right ventricular ejection fraction (RVEF) (209). However, tricuspid regurgitation (TR) is common, particularly in MR patients, meaning that these conventional markers of RV function face the same theoretical limitations of a double outlet ventricle as LVEF in MR. Furthermore, echocardiographic derived RV global longitudinal strain (RV  $E_{11}$ ) have been found to provide incremental prognostic value in patients with acute heart failure, myocardial infarction and pulmonary hypertension (178, 210, 211).

There are many challenges in the echocardiographic assessment of the right heart (209). RV FT-CMR offers the potential for rapid and sensitive quantification of RV function, with the advantage of high image quality not limited by the availability of an adequate acoustic window. However, RV FT-CMR remains a novel technique where limited data exists for defining what a normal strain value is, and if the technique is sufficiently reproducible (intraclass correlation, ICC >0.75) for clinical use (212, 213).

## 3.2 Aims and hypotheses

### 3.2.1 Hypotheses

- 1) We hypothesise that strain and strain rate derived from 3D FT-CMR has superior reproducibility compared to 2D FT-CMR.
- 2) Due to their mechanistic differences, the values of strain derived from 2D and 3D FT-CMR are not interchangeable, and new reference ranges are required.
- 3) Strain and strain rates derived from RV FT-CMR possess good intra- and inter-observer reproducibility, defined as ICC >0.75.

### 3.2.2 Aims

- 1) Determine and compare the inter- and intra-observer reproducibility of 2D and 3D FT-CMR.
- 2) Define reference values for 3D FT-CMR in a cohort of healthy volunteers.
- 3) Assess the reproducibility of RV FT-CMR.
- 4) Define reference values for RV FT-CMR.



This chapter aims to determine whether 3D feature-tracking offers superior reproducibility compared to 2D methodology. To allow meaningful interpretation of these novel FT-CMR techniques in diseased states, we will also define reference ranges for FT-CMR in a healthy cohort of volunteers.

### 3.2.3 Endpoints

The primary endpoints for this chapter are intra- and inter-observer intraclass correlation coefficients for 2D versus 3D FT-CMR in the LV, and 2D FT-CMR in the RV.

Secondary endpoints include mean bias on repeated strain measurement, and reference range values of peak strain and strain rate measurements.

## 3.3 Methods

### 3.3.1 Study population

Healthy subjects were originally identified from a prospective, controlled, observational CMR study examining the effects of living kidney donation on cardiovascular structure and function (NCT01028703) (214). For this study, baseline CMR examinations were included as previously described (127, 215), with the additional recruitment of 15 patients for construction of a cohort of 100 volunteers in a pre-determined, stratified fashion, to include 10 men and 10 women in each of 5 age deciles from 20 to 70 years. Only individuals in optimal health were included as defined by the absence of hypertension, diabetes, obesity, dyslipidaemia, or any cardiovascular, renal, hepatic, haematological and systemic inflammatory disease. Exclusion criteria included the presence of an abnormal full blood count, serum electrolytes, or resting 12-lead ECG. Demographic data were collected, including height, weight, body surface area, heart rate and office blood pressure

(normal <140/90mmHg). The study protocol conformed to the ethical guidelines of the 1975 Declaration of Helsinki and written informed consent was obtained from each subject.

### 3.3.2 CMR acquisition and analyses

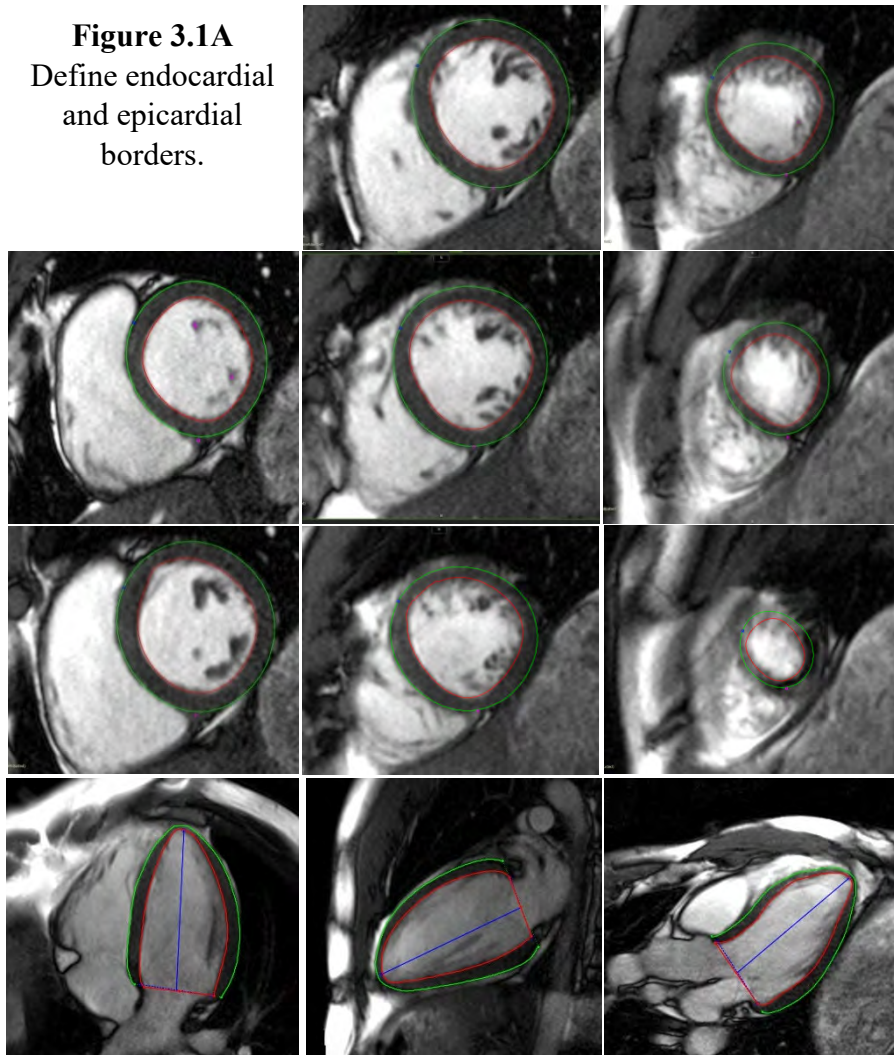
All patients underwent multiparametric CMR as described in section 2.2.4.3. Volumetric CMR assessment was performed as per section 2.2.4.3.1. All CMR studies were anonymised prior to strain analysis by randomly assigning studies with a unique ID ranging between 1 and 100 on Microsoft Excel.

#### 3.3.2.1 *Left ventricular feature tracking*

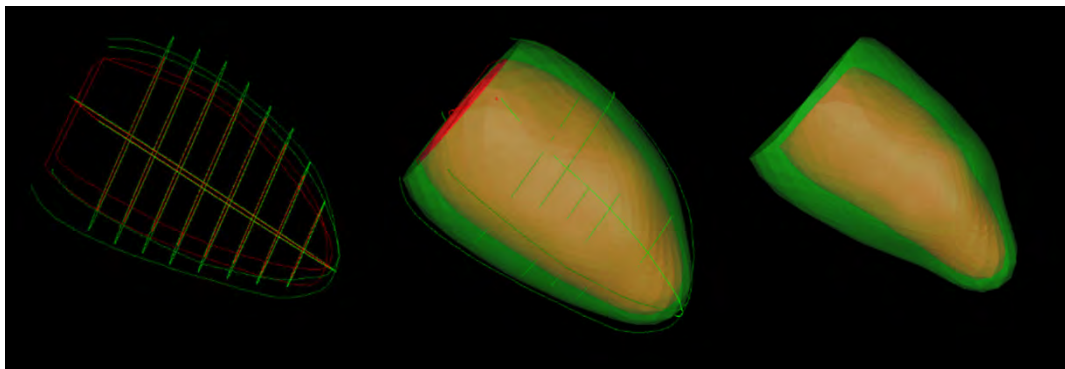
2D and 3D GCS, GRS, and GLS strain as well as strain rates (S' - peak systolic strain rate; E' – peak early diastolic strain rate; A' – peak late diastolic strain rate) were obtained using cvi42® (version 5.3.6, Circle Cardiovascular Imaging, Canada). Smoothed endocardial and epicardial borders were drawn in the end-diastolic frame. For 2D strain analysis, circumferential (Ecc) and radial (Err) strain and strain rates were obtained at the mid LV in the short axis view, 2D longitudinal strain (Ell) and strain rates were obtained from the HLA image (127). The level of the mid LV was determined and recorded by the primary investigator (BL) in order for the secondary investigator (AD) to replicate analyses at the same level. 3D feature tracking was performed by defining contours in the end-diastolic frame of all short and long axis slices before defining the superior RV insertion points within the LV (**Figure 3.1**).

**Figure 3.1** Steps taken for 3D FT-CMR.

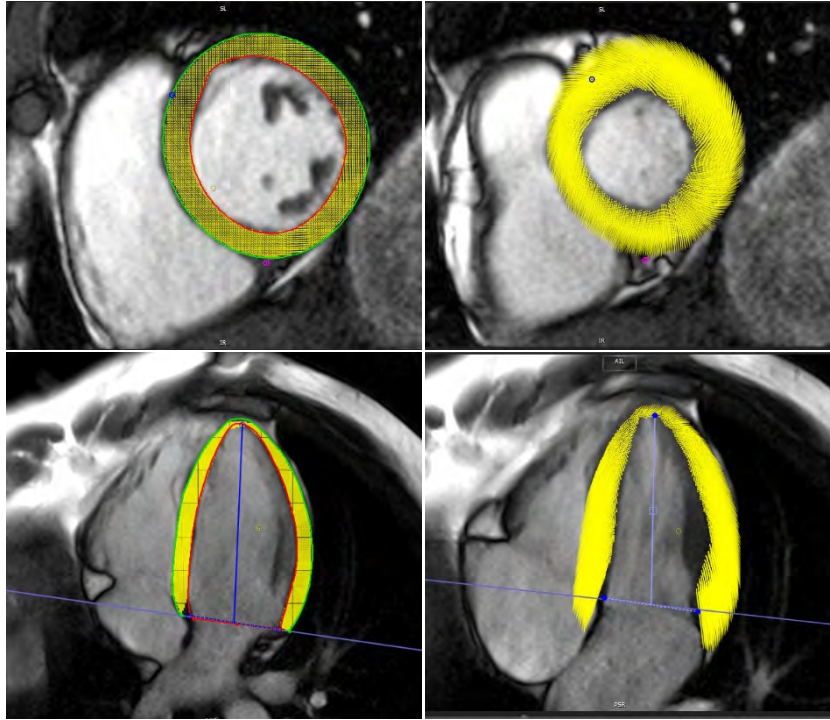
**Figure 3.1A**  
Define endocardial  
and epicardial  
borders.



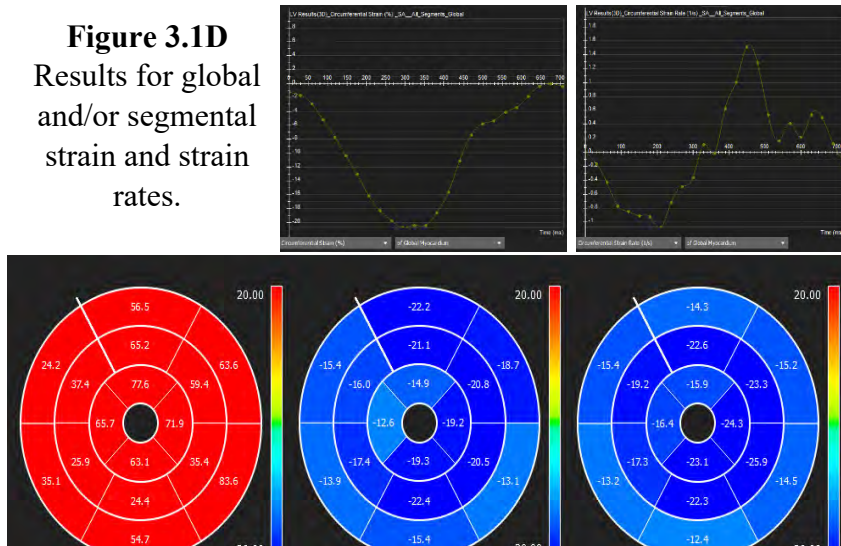
**Figure 3.1B** 3D construct of endocardial and epicardial borders are used to generate a 3D model of the myocardium in diastole which is tracked through to systole.



**Figure 3.1C** Ensure good quality tracking



**Figure 3.1D**  
Results for global  
and/or segmental  
strain and strain  
rates.



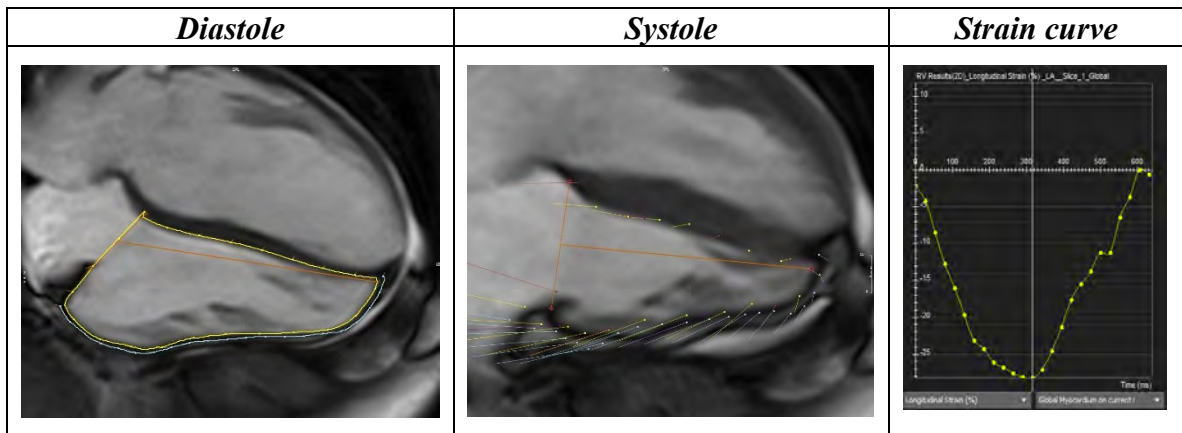
Feature tracking on cvi42® derives myocardial strains by fitting a nearly incompressible deformable 2D model to individual 2D cine slices over the cardiac cycle. Similarly, in 3D feature tracking, a 3D deformable model of the myocardium is generated in the end-diastolic phase by interpolating the endo- and epicardial boundaries tracked by the 2D algorithm. The basis of these algorithms has been previously described and their validity demonstrated (216, 217). The accuracy of feature tracking was manually checked following automated strain analysis on the 2D and 3D CMR models by assessing the tracking of the endocardial and epicardial borders; however, to minimize variability, a maximum of two user adjustments were allowed in the event of significant mis-tracking.

#### *3.3.2.2 Right ventricular feature tracking*

RV FT-CMR was performed using cvi42® (version 5.3.6, Circle Cardiovascular Imaging, Canada) as per our published methodology (218, 219). From the horizontal long-axis view, right ventricular free wall longitudinal (E11) strain, as well as strain rates (peak systolic strain rate SRS'; peak early diastolic strain rate SRE'; peak late diastolic strain rate SRA'), were defined in the region of interest between the endocardial and epicardial borders (**Figure 3.2**) drawn in the end-diastolic frame (defined as phase 1 out of 25). RV peak strain was taken as the highest strain irrespective of time during systole.

The accuracy of feature tracking for both endocardial and epicardial RV borders was visually checked following automated strain analysis on the CMR model, and good quality tracking was obtained in all subjects following a maximum of two user adjustments.

**Figure 3.2** Contouring for RV strain, with the timing of peak strain interpretation on the strain curve.



RV E11 was defined as the peak in the strain curve irrespective of the time in the cardiac cycle.

### 3.3.3 Reproducibility Studies

For LV intra-observer variability, the primary investigator (BL) performed feature tracking analyses for all 100 subjects, with a second complete analysis repeated after a 1-month interval in every subject. For inter-observer variability, AD independently feature tracked a randomly generated set of 45 scans. These subject numbers were chosen as they mirrored the methodology of well-established reference range studies (204, 215).

For RV FT-CMR intra- and inter-observer repeatability, a sample size of 10 CMR studies were selected as this would detect a minimum ICC of 0.7 with power = 80% and alpha = 0.05 (220). For intra-observer variability, observer AD performed tissue tracking analysis for all 100 subjects, with a second analysis repeated in a randomly generated subset of 10 patients after a 1-month interval. For inter-observer variability, observer BL independently feature tracked the randomly selected set of 10 scans.

### 3.3.4 Comparison of strain with other measures of systolic function

To compare the strain results derived from 3D FT-CMR on cvi42®, 3D strain parameters were correlated with LVEF.

### 3.3.5 Statistical analyses

Paired t-tests were used to compare the size of biases between 2D and 3D derived strain. Independent samples t-test was used to explore gender differences amongst strain and strain rates. One-way ANOVA were used to assess the relationship between image quality and reproducibility bias. Linear regression analysis was used to explore the relationship between strain and baseline variables. Variables reaching a P-value of <0.10 were included in stepwise backward multivariable regression models. Intra- and inter-observer agreement was tested by calculating mean bias and 95% limits of agreement from Bland–Altman

analyses, and ICC for absolute agreement from a single measurement. Mean segmental GCS was compared across the 16 segments using a repeated measures ANOVA with Huynh-Feldt adjustment.

### 3.4 Results

#### 3.4.1 Demographics, ventricular volumes and ejection fraction

Baseline demographics are illustrated in **Table 3.1**. 85 subjects had a 10-year QRISK-2 score of <10% and all subjects had a 10-year QRISK-2 score of <20% (221). There were 8 current smokers and 19 ex-smokers. Cardiac volumes, mass and function according to each age decile are listed in **Table 3.2**; values were within normal limits for all participants (166). On linear regression analyses, there were no significant correlations between age and the parameters of height, weight, BSA, or eGFR. Meanwhile, increasing age correlated with increasing LVEF ( $r=0.4$ ,  $P<0.001$ ), RVEF ( $r=0.2$ ,  $P=0.03$ ), and decreasing indexed biventricular volumes (LVEDVi  $r=-0.4$ ,  $P<0.001$ ; LVESVi  $r=-0.45$ ,  $P=<0.001$ ; RVEDVi  $r=-0.3$ ,  $P=0.001$ ; RVESVi  $r=-0.3$ ,  $P=0.001$ ). There was no association between age and indexed LVM. There were no significant differences between men and women for indexed biventricular volumes or function but men had higher indexed LVM compared to women (**Table 3.1**).

#### 3.4.2 Left ventricular reproducibility

Intra- and inter-observer variability are listed in **Table 3.3**; intra- and inter-observer limits of agreement are illustrated in the Bland-Altman analyses of **Figure 3.3** and **3.4** respectively. Reproducibility biases were significantly lower for almost all strain and strain rates when derived from 3D FT-CMR. Similarly, 3D feature tracking had superior ICC



compared to 2D models for the majority of peak strain and strain rate parameters. For peak strain, 3D GCS has the highest reproducibility, followed by GRS and GLS.

**Table 3.1** Baseline demographics of 100 healthy subjects.

	<b>Female</b> (n=50)	<b>Male</b> (n=50)	<b>Overall</b> (n=100)	<b>P</b>
<b>Age (years)</b>	44.8±14.3	44.7±14.3	44.8±14.3	0.98
<b>Height (cm)</b>	163.8±5.6	178.2±8.6	171.2±10.2	<0.001
<b>Weight (kg)</b>	69.9±11.7	80.9±12.8	75.5±13.4	<0.001
<b>BSA (m<sup>2</sup>)</b>	1.8±0.2	2.0±0.2	1.9±0.2	<0.001
<b>LVEF (%)</b>	70.5±6.7	70.8±6.7	70.7±6.7	0.81
<b>LVEDVi (ml/m<sup>2</sup>)</b>	64.1±13.1	65.5±11.6	64.8±12.3	0.57
<b>LVESVi (ml/m<sup>2</sup>)</b>	19.4±7.5	19.6±7.0	19.5±7.2	0.88
<b>LVMi (kg/m<sup>2</sup>)</b>	52.1±9.9	62.9±12.1	57.4±12.2	<0.001
<b>RVEF (%)</b>	67.5±8.4	66.3±7.1	66.9±7.8	0.46
<b>RVEDVi (ml/m<sup>2</sup>)</b>	63.4±13.2	68.4±14.2	65.8±13.9	0.07
<b>RVESVi (ml/m<sup>2</sup>)</b>	21.0±8.0	23.7±9.5	22.3±8.8	0.14
<b>Haemoglobin (g/L)</b>	13.1±0.8	14.5±1.0	13.8±1.2	<0.001
<b>eGFR (mL/min)</b>	85.1±13.5	88.8±12.7	86.8±13.2	0.18

**Table 3.2** Ventricular volumes and function according to age decile.

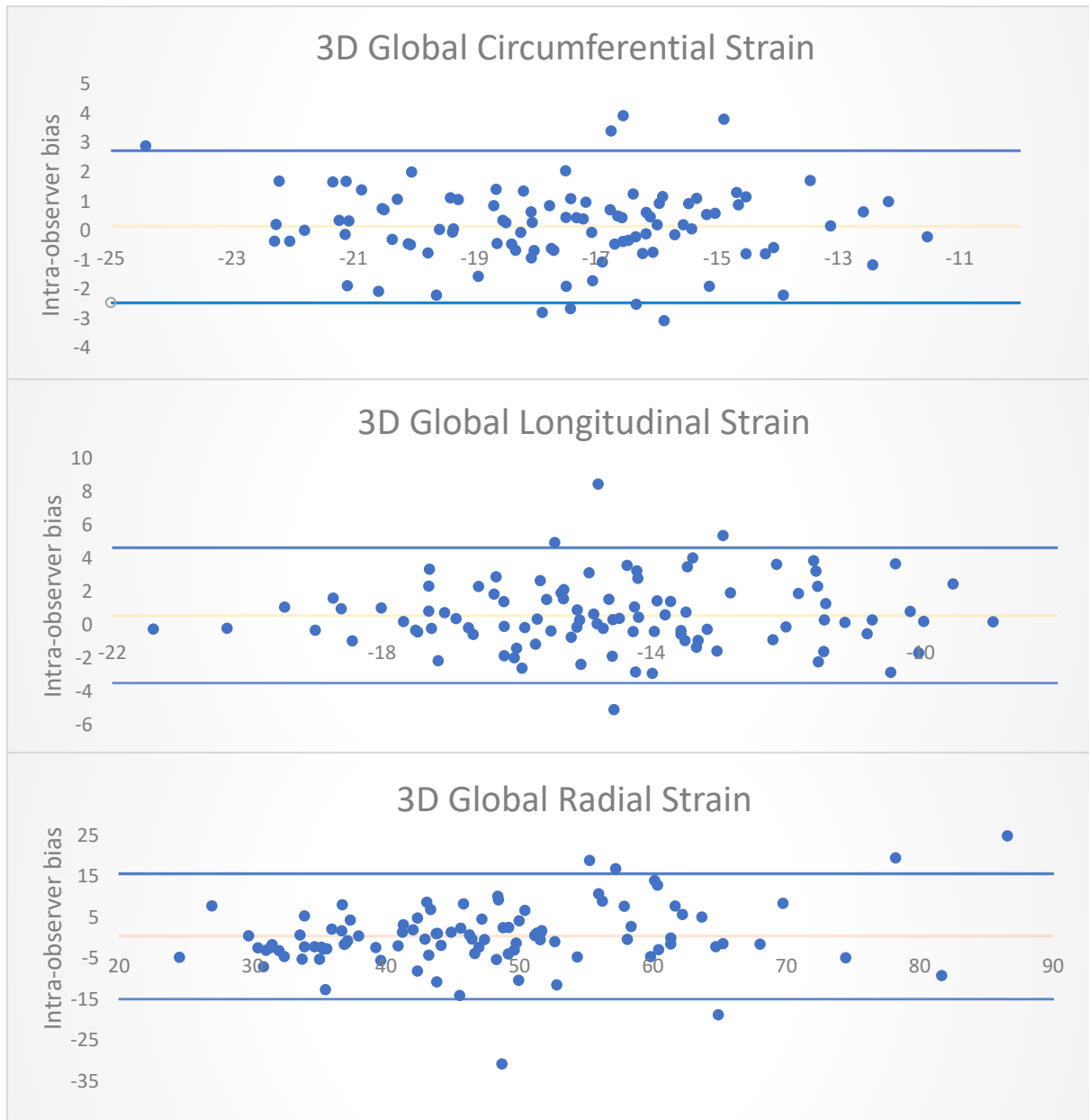
	<b>Age</b>				
	20-29 years	30-39 years	40-49 years	50-59 years	60-69 years
<b>LVEF (%)</b>	68±6	68±5	70±6	73±6	75±8
<b>LVEDVi (ml/m<sup>2</sup>)</b>	71±15	69±12	66±9	62±13	57±7
<b>LVESVi (ml/m<sup>2</sup>)</b>	23±7	22±7	20±6	17±8	15±6
<b>LVMi (g/m<sup>2</sup>)</b>	52±14	62±13	62±14	56±9	55±9
<b>RVEF (%)</b>	65±7	66±9	66±6	69±7	69±10
<b>RVEDVi (ml/m<sup>2</sup>)</b>	73±17	68±15	67±11	59±12	62±10
<b>RVESVi (ml/m<sup>2</sup>)</b>	26±9	24±9	24±9	18±6	20±9

**Table 3.3** 2D vs 3D intra- and inter-observer reproducibility for peak strain and strain rates.

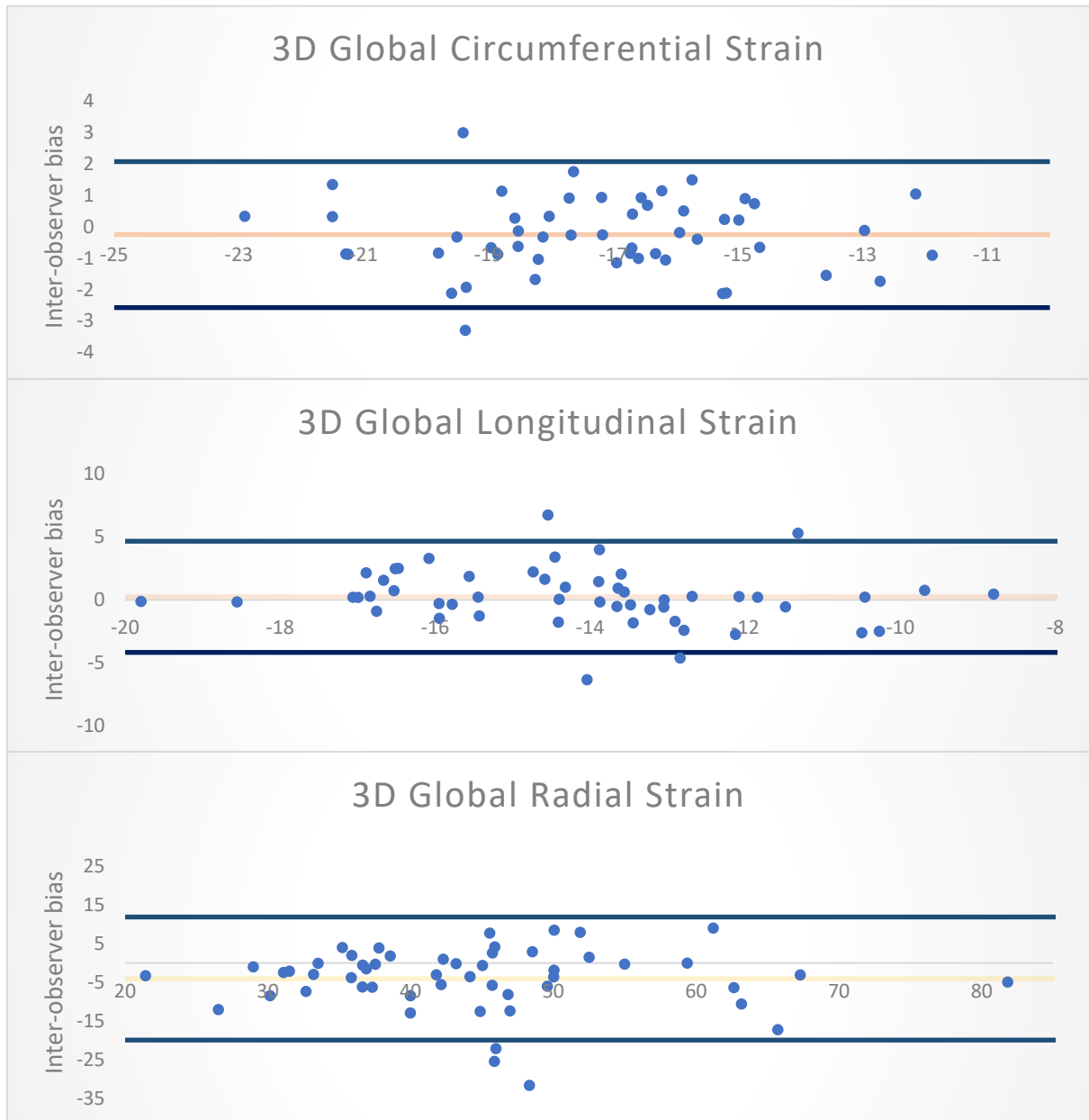
		Intra-observer reproducibility		Inter-observer reproducibility	
		Mean absolute bias	ICC (95% CI)	Mean absolute bias	ICC (95% CI)
Circumferential	3D GCS	1.04±0.83	0.88 (0.83 to 0.92)	0.94±0.71	0.88 (0.79 to 0.93)
	2D GCS	1.73±1.52*	0.82 (0.75 to 0.88)	2.18±1.77*	0.66 (0.45 to 0.79)
	3D GCS S'	0.09±0.09	0.81 (0.73 to 0.87)	0.09±0.11	0.67 (0.47 to 0.80)
	2D GCS S'	0.26±0.34*	0.44 (0.27 to 0.59)	0.26±0.27*	0.41 (0.14 to 0.62)
	3D GCS E'	0.16±0.13	0.64 (0.51 to 0.75)	0.15±0.16	0.72 (0.54 to 0.84)
	2D GCS E'	0.49±0.45*	0.27 (0.08 to 0.45)	0.52±0.56*	0.00 (-0.27 to 0.29)
	3D GCS A'	0.04±0.05	0.93 (0.90 to 0.95)	0.04±0.04	0.93 (0.88 to 0.96)
	2D GCS A'	0.13±0.11*	0.74 (0.63 to 0.82)	0.17±0.13*	0.58 (0.35 to 0.75)
Longitudinal	3D GLS	1.45±1.21	0.76 (0.66 to 0.84)	1.29±1.12	0.74 (0.57 to 0.85)
	2D GLS	1.91±1.51†	0.66 (0.53 to 0.76)	1.83±1.31^	0.70 (0.52 to 0.83)
	3D GLS S'	0.15±0.16	0.36 (0.18 to 0.52)	0.11±0.11	0.62 (0.40 to 0.77)
	2D GLS S'	0.20±0.17†	0.48 (0.31 to 0.62)	0.18±0.14*	0.62 (0.40 to 0.77)
	3D GLS E'	0.20±0.23	0.50 (0.33 to 0.63)	0.14±0.15	0.54 (0.30 to 0.72)
	2D GLS E'	0.22±0.19	0.53 (0.37 to 0.66)	0.23±0.16†	0.48 (0.22 to 0.68)
	3D GLS A'	0.05±0.06	0.80 (0.71 to 0.86)	0.05±0.06	0.80 (0.66 to 0.89)
	2D GLS A'	0.17±0.20*	0.66 (0.53 to 0.76)	0.19±0.18*	0.54 (0.30 to 0.72)
Radial	3D GRS	5.32±5.55	0.82 (0.75 to 0.88)	5.18±5.15	0.79 (0.61 to 0.89)
	2D GRS	7.43±8.36*	0.74 (0.63 to 0.82)	8.38±9.00	0.42 (0.16 to 0.63)
	3D GRS S'	0.56±0.60	0.75 (0.65 to 0.83)	0.50±0.49	0.73 (0.55 to 0.85)
	2D GRS S'	1.02±1.23*	0.57 (0.24 to 0.69)	1.31±1.60*	0.14 (-0.12 to 0.39)
	3D GRS E'	0.71±0.63	0.67 (0.54 to 0.76)	0.65±0.65	0.49 (0.22 to 0.68)
	2D GRS E'	1.29±1.24*	0.42 (0.24 to 0.57)	1.65±1.31*	0.11 (-0.10 to 0.35)
	3D GRS A'	0.10±0.12	0.85 (0.78 to 0.90)	0.10±0.09	0.86 (0.76 to 0.92)
	2D GRS A'	0.20±0.22*	0.64 (0.51 to 0.75)	0.21±0.17*	0.70 (0.51 to 0.83)

Statistical significance: \*denotes paired T test  $P < 0.001$ , ^denotes  $P < 0.01$ , † denotes  $P < 0.05$  when comparing the size of bias derived from 2D vs 3D feature tracking on paired t-test. ICC = intra-class correlation for single measures.

**Figure 3.3** Bland-Altman plots for intra-observer bias for 3D peak GCS, GRS, and GLS.



**Figure 3.4** Bland-Altman plots for inter-observer bias for 3D peak GCS, GRS, and GLS.



### 3.4.3 Reference values for left ventricular global strain and strain rate

Good quality tracking was obtained for all subjects following a maximum of two editions.

Reference ranges for strain and strain rates derived from 3D vs. 2D FT-CMR were not interchangeable. Peak strains obtained via 3D feature tracking were lower than corresponding 2D peak strains for GLS and GCS but not for GRS (**Table 3.4**). Similarly, peak systolic (S'), early diastolic peak (E') and late diastolic peak (A') strain rates obtained from 3D were generally lower than those obtained with 2D feature tracking.

3D FT-CMR normal range values for the whole cohort are listed in **Table 3.5** and were defined as the 95% confidence interval of the whole cohort regardless of age. The borderline zones were defined as the upper and lower ranges where measured value lay outside the 95% confidence interval for at least one age group. The abnormal zones were defined by the range where measured values lay outside the 95% confidence interval for any age group.

Abnormally low and high refer to the lower and upper reference limits are defined as measurements which lie outside the 95% confidence interval at all age groups. Borderline zone values should be looked up in the age-specific tables (**Table 3.6 (a)** and **(b)**). The borderline zone was defined as the upper and lower ranges where the measured value lay outside the 95% prediction interval for at least one age group.

**Table 3.4** Comparison of 2D vs. 3D FT-CMR strains and strain rates.

		<i>2D</i>	<i>3D</i>	<i>P</i>
<i>Circumferential</i>	Peak strain (%)	-20.9±3.6	-17.6±2.6	<0.001
	S' (1/s)	-1.21±0.34	-0.92±0.19	<0.001
	E' (1/s)	1.48±0.44	0.96±0.22	<0.001
	A' (1/s)	0.57±0.22	0.48±0.16	<0.001
<i>Radial</i>	Peak strain (%)	47.6±15.4	47.4±12.9	0.86
	S' (1/s)	3.11±1.72	2.93±1.10	0.18
	E' (1/s)	-3.76±1.40	-3.04±1.05	<0.001
	A' (1/s)	-0.70±0.32	-0.68±0.26	0.29
<i>Longitudinal</i>	Peak strain (%)	-19.8±2.9	-14.6±2.7	<0.001
	S' (1/s)	-1.16±0.22	-0.74±0.25	<0.001
	E' (1/s)	1.08±0.27	0.79±0.31	<0.001
	A' (1/s)	0.74±0.29	0.42±0.15	<0.001

*Values are mean + SD. P values are derived from paired t-test.*



**Table 3.5** Reference values for 3D FT-CMR.

	Abnormally low		Normal zone		Abnormally high
<b>Strain</b>					
<b>GCS</b>	> -11.5	Borderline zone	-13 to -23	Borderline zone	< -24.8
<b>GLS</b>	> -8.5		-9 to -20		< -21.5
<b>GRS</b>	< 21.2		22 to 73		> 86.3
<b>Strain rates</b>					
<b>GCS S'</b>	> -0.45	Borderline zone	-0.53 to -1.31	Borderline zone	< -1.38
<b>GCS E'</b>	< 0.44		0.47 to 1.45		> 1.45
<b>GCS A'</b>	< 0.15		0.17 to 0.79		> 0.96
<b>GLS S'</b>	> -0.37	Borderline zone	-0.43 to -1.09	Borderline zone	< -1.45
<b>GLS E'</b>	< 0.29		0.36 to 1.30		1.51
<b>GLS A'</b>	< 0.16		0.18 to 0.68		> 0.79
<b>GRS S'</b>	< 0.73	Borderline zone	0.77 to 5.1	Borderline zone	> 6.76
<b>GRS E'</b>	> -0.42		-1.0 to -5.1		< -5.61
<b>GRS A'</b>	> -0.19		-0.17 to -1.2		< -1.54

#### 3.4.4 Factors influencing left ventricular 3D FT-CMR

There was no relationship between gender and strain or strain rate, with the exception that  $E'$  was more negative in females than males. 3D peak strains increased with age, with a more noticeable change after the age of 50, although the correlation was weak (GLS =  $12.73 + 0.04 \times \text{age}$ ,  $R^2=0.06$ ,  $R=0.24$ ; GCS =  $14.52 + 0.07 \times \text{age}$ ,  $R^2=0.15$ ,  $R=0.38$ ; GRS =  $35.07 + 0.28 \times \text{age}$ ,  $R^2=0.10$ ,  $R=0.32$ ) (**Table 3.6 (a)**). Increasing age was related to higher peak systolic and late diastolic strain rates (**Table 3.6 (b)**). Increasing age was also associated with a reduction in early diastolic strain rate for circumferential and longitudinal, but not radial directions. There were no interaction effects between age and gender for the prediction of strain on multivariable regression analyses.

#### 3.4.5 Segmental Strain

The normal range values and reproducibility of GCS were calculated when the myocardium was split according to a modified American Heart Association left ventricular model with omission of the apical cap (**Figure 3.4**) (175). Repeated-measures ANOVA demonstrated significant regional variations in GCS ( $P<0.001$ ), with reproducibility being generally good or excellent in the basal and mid segments but lower in the apical segments. Segmental peak strain in the longitudinal and radial direction was poorly reproducible compared to the circumferential direction; these results are illustrated in **Figures 3.5 and 3.6** respectively.

**Table 3.6**

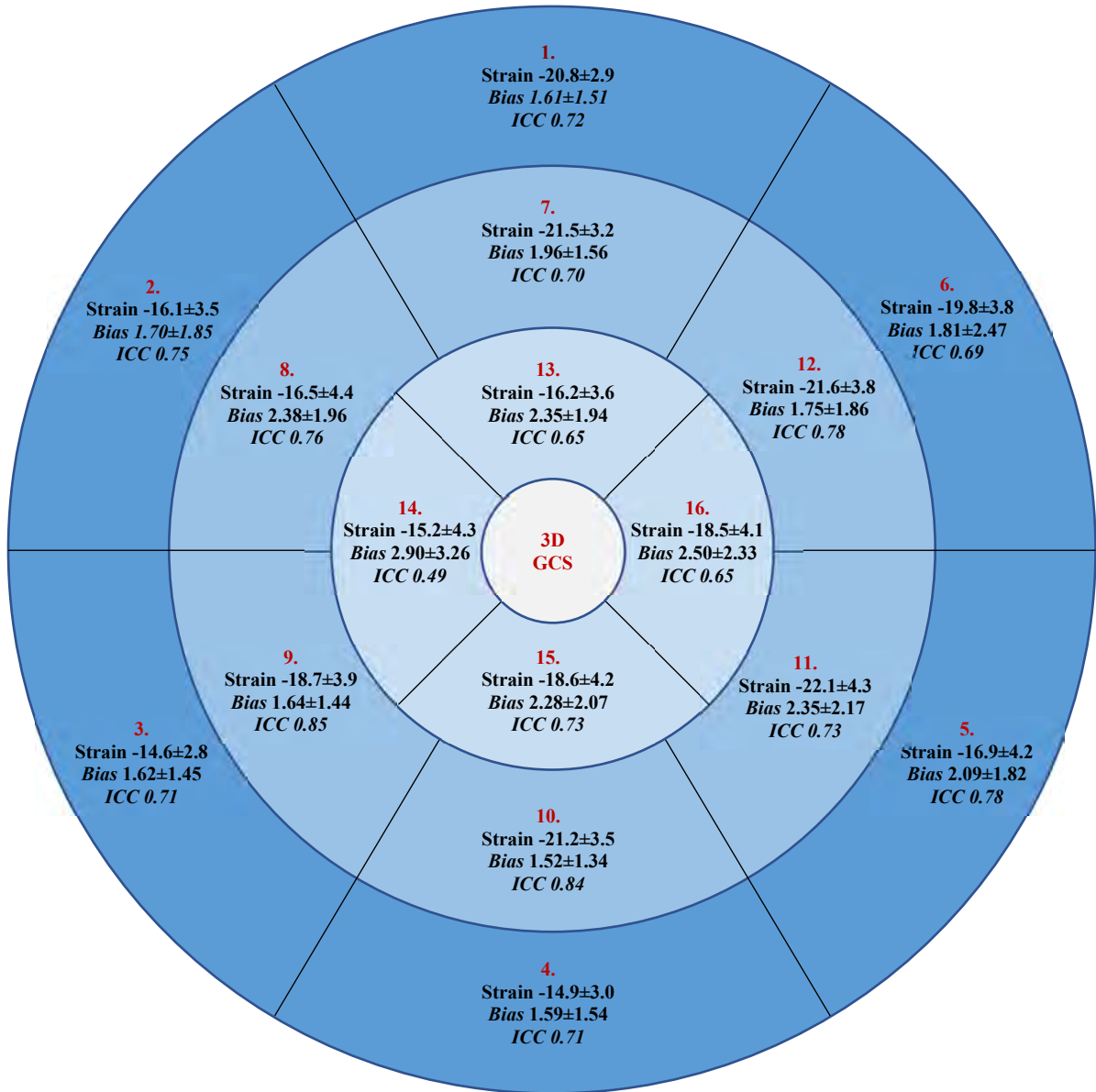
(a) 3D peak strain across age deciles.

Strain by Age Decile (%)					
	20-29 yr	30-39 yr	40-49 yr	50-59 yr	60-69 yr
<b>GCS</b>	-16.9±2.1	-16.8±2.3	-16.4±2.4	-18.2±2.0	-19.7±2.6
<b>GLS</b>	-14.8±2.1	-13.4±2.3	-14.0±2.8	-14.9±2.2	-16.2±2.7
<b>GRS</b>	45.9±12.0	43.9±9.8	42.4±10.8	47.9±9.0	57.5±14.7

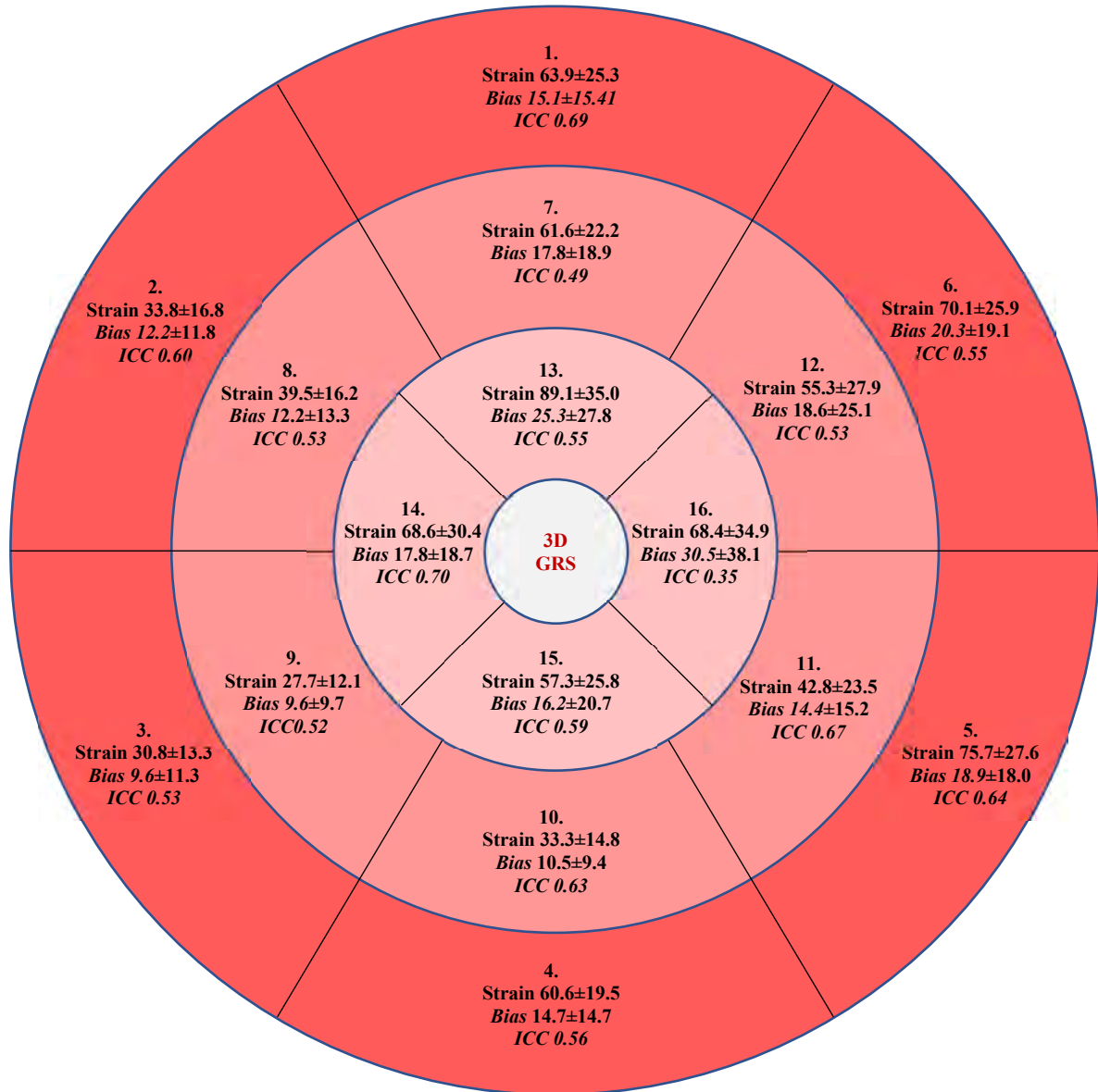
(b) Age adjusted 3D peak strain rates and results of linear regression analyses on the relationship between age and strain rate.

	Strain rate by Age Decile (1/s)					Statistical analyses			
	20-29 yr	30-39 yr	40-49 yr	50-59 yr	60-69 yr	R	R <sup>2</sup>	β	P
<b>GCS S'</b>	-0.87±0.13	-0.86±0.19	-0.90±0.23	-0.92±0.18	-1.03±0.18	0.26	0.07	0.003	<b>0.009</b>
<b>GCS E'</b>	1.06±0.19	0.98±0.24	0.95±0.22	0.91±0.24	0.88±0.20	-0.26	0.07	-0.004	<b>0.008</b>
<b>GCS A'</b>	0.36±0.09	0.37±0.11	0.44±0.08	0.55±0.12	0.69±0.14	0.74	0.55	0.008	<b>&lt;0.001</b>
<b>GRS S'</b>	2.79±0.84	2.63±0.95	2.61±0.96	2.89±0.72	3.80±1.51	0.29	0.09	0.023	<b>0.003</b>
<b>GRS E'</b>	-3.30±1.18	-2.85±0.90	-2.85±1.24	-3.06±0.88	-3.16±1.02	-0.12	0.00	-0.001	0.906
<b>GRS A'</b>	-0.50±0.12	-0.52±0.17	-0.62±0.16	-0.79±0.23	-0.97±0.29	0.66	0.43	0.012	<b>&lt;0.001</b>
<b>GLS S'</b>	-0.74±0.12	-0.69±0.16	-0.77±0.20	-0.76±0.15	-0.82±0.18	0.26	0.07	0.005	<b>0.009</b>
<b>GLS E'</b>	0.98±0.26	0.81±0.24	0.90±0.31	0.73±0.16	0.74±0.17	-0.30	0.01	-0.005	<b>0.002</b>
<b>GLS A'</b>	0.34±0.09	0.34±0.08	0.40±0.09	0.49±0.10	0.59±0.10	0.69	0.47	0.007	<b>&lt;0.001</b>

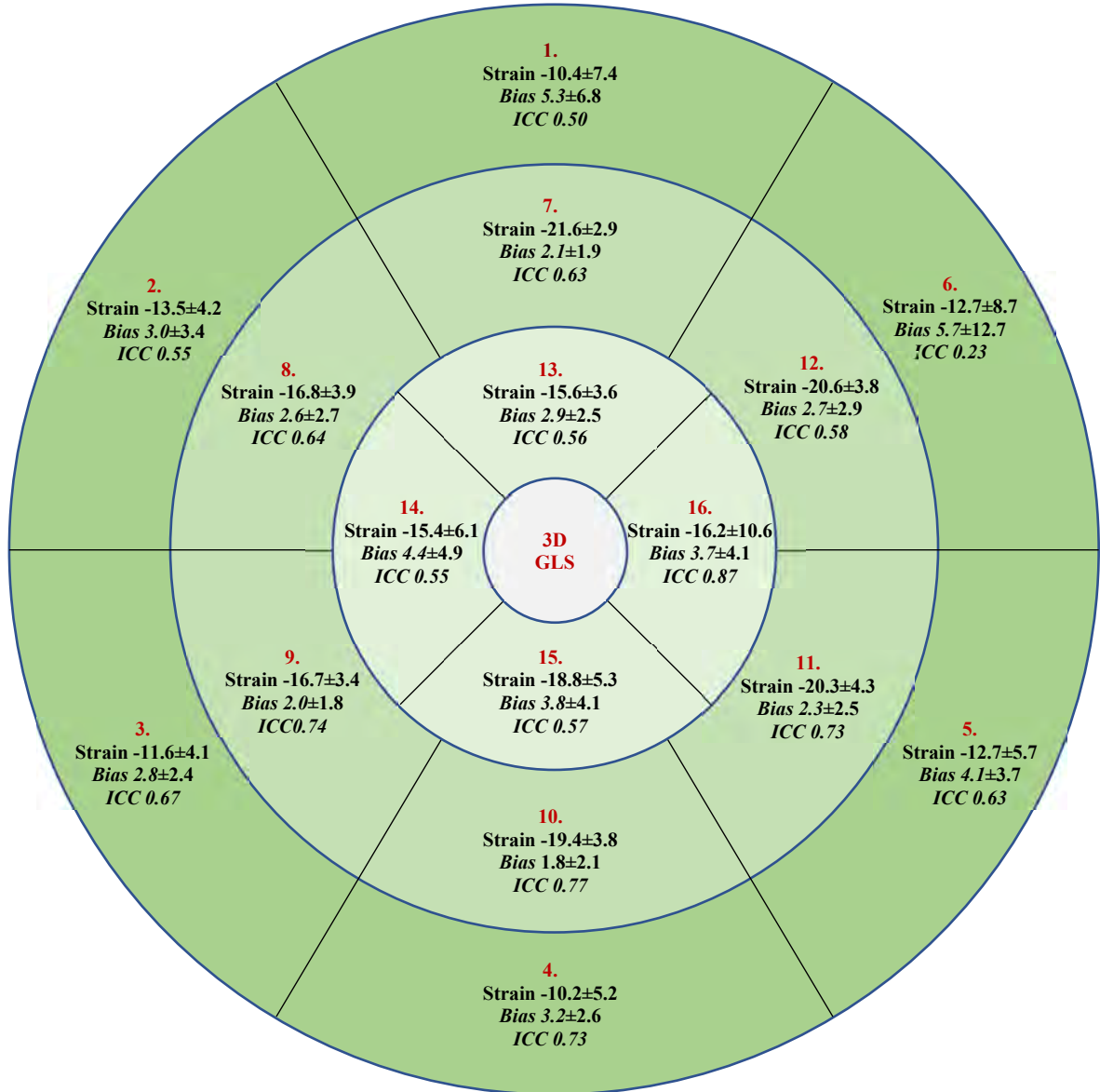
**Figure 3.5** 16 segment model illustrating peak GCS±SD with mean intra-observer absolute bias±SD and ICC.



**Figure 3.6** 16 segment model illustrating peak GRS±SD with mean absolute intra-observer bias±SD and ICC.



**Figure 3.7** 16 segment model illustrating peak GLS±SD with mean absolute intra-observer bias±SD and ICC.



#### 3.4.6 Comparison of strain with other measures of systolic function

To act as external validation, we correlated peak strain by 3D FT-CMR against LVEF.

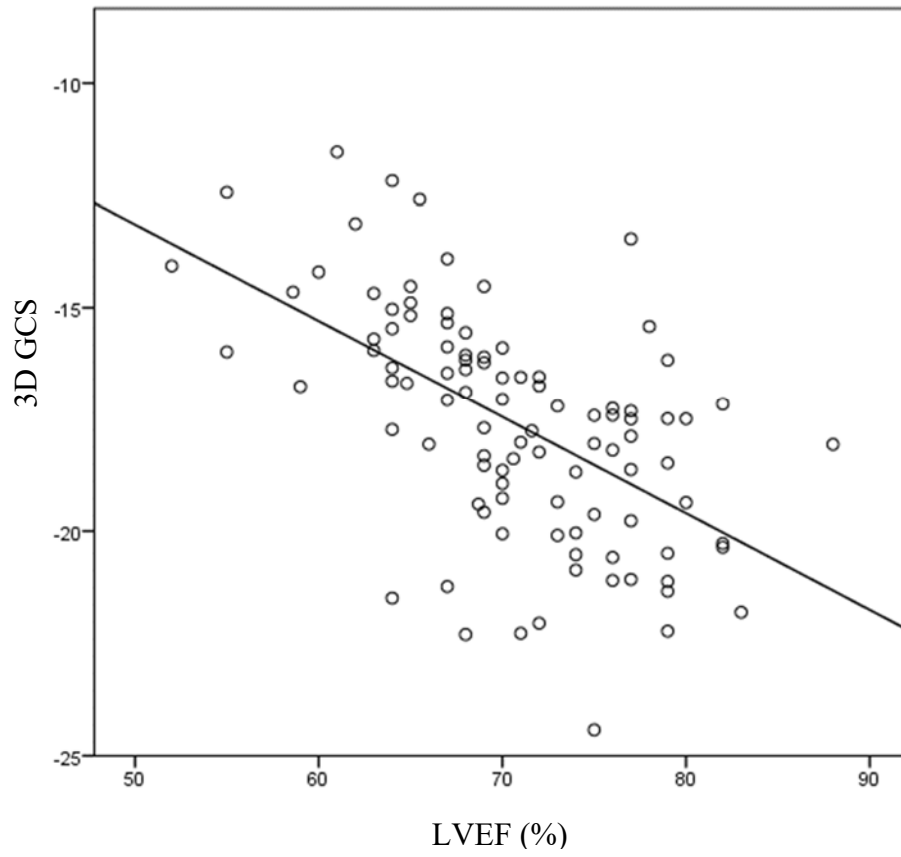
LVEF significantly correlated with (but was not identical to) 3D GCS (**Figure 3.8**,  $r=0.56$ ,  $P<0.001$ ), GRS ( $r=0.60$ ,  $P<0.001$ ) and GLS ( $r=0.42$ ,  $P<0.001$ ).

#### 3.4.7 Right ventricular reproducibility

Intra- and inter-observer reproducibility studies for RV FT-CMR are presented in **Table**

**3.7** The magnitude of biases is presented graphically on Bland Altman plots (**Figure 3.9**).

**Figure 3.8** Correlation of 3D GCS against LVEF.

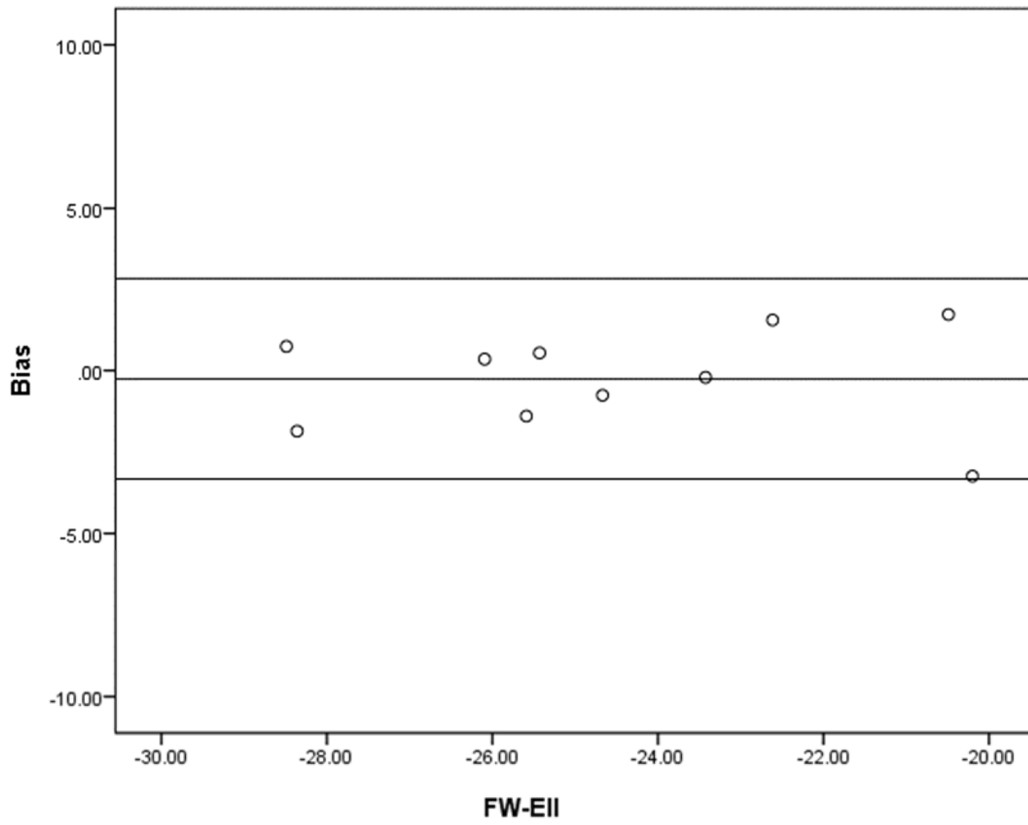




**Table 3.7** Reproducibility studies for RV free-wall deformation.

	<b>Variability</b>	<b>Mean bias <math>\pm</math> SD</b>	<b>Limits of agreement</b>	<b>ICC (95% CI)</b>
RV E <sub>II</sub>	<i>Intra-observer</i>	1.08 $\pm$ 0.97	-1.85 to 1.93	0.92 (0.61 to 0.98)
	<i>Inter-observer</i>	1.23 $\pm$ 1.57	-2.71 to 2.19	0.87 (0.57 to 0.97)
SR <sub>S</sub> '	<i>Intra-observer</i>	0.22 $\pm$ 0.25	-0.37 to 0.61	0.28 (-0.28 to 0.74)
	<i>Inter-observer</i>	0.19 $\pm$ 0.33	-0.56 to 0.69	0.38 (0.9 to 0.89)
SR <sub>E</sub> '	<i>Intra-observer</i>	0.17 $\pm$ 0.24	-0.45 to 0.37	0.71 (0.18 to 0.92)
	<i>Inter-observer</i>	0.17 $\pm$ 0.22	-0.38 to 0.49	0.69 (0.17 to 0.91)
SR <sub>A</sub> '	<i>Intra-observer</i>	0.25 $\pm$ 0.25	-0.68 to 0.30	0.64 (0.047 to 0.89)
	<i>Inter-observer</i>	0.25 $\pm$ 0.29	-0.73 to 0.45	0.64 (0.2 to 0.94)

**Figure 3.9** Bland-Altman plot illustrating inter-observer bias for RV E<sub>II</sub>.



Mean x-axis represents mean right ventricular free wall strain, y-axis represents the magnitude of inter-observer bias.

#### 3.4.8 Reference values for RV strain and strain rate

Reference ranges values for RV strain and strain rates according to age deciles are listed in

**Table 3.8.** Good quality tracking was obtained in all subjects following a maximum of two editions. On linear regression analyses, there was no correlation between strain or strain rate values and the parameters of age, gender, height, weight, body mass index or body surface area (data not shown).

Considering the absence of a consistent impact of age and gender on strain and strain rate, overall cohort values are presented in the highlight section of **Table 3.8.**

**Table 3.8** Reference values for RV strain and strain rate strain.

	Age deciles					Regression analysis				Overall cohort
	≥20 to <30	≥30 to <40	≥40 to <50	≥50 to <60	≥60 to <70	R	R <sup>2</sup>	β	P	
<b>Ell</b>	-23.9 ±3.54	-23.2 ±3.42	-24.6 ±3.54	-25.4 ±2.94	-23.9 ±4.36	0.10	0.01	-0.02	0.35	-24.2±3.59
<b>SR S'</b>	-1.5±0.34	-1.5±0.39	-1.6±0.39	-2.6±4.27	-1.6±0.49	0.12	0.01	-0.02	0.13	-1.7±1.95
<b>SR E'</b>	1.1±0.27	1.0±0.33	1.0±0.34	1.0±0.25	1.0±0.45	0.10	0.01	-0.002	0.31	1.0±0.33
<b>SR A'</b>	1.1±0.33	1.0±0.35	1.1±0.32	1.1±0.31	1.1±0.37	0.08	0.01	0.002	0.43	1.1±0.33

Values are mean±SD; RV Ell = right ventricular peak longitudinal strain; SR<sub>S'</sub> = peak systolic strain rate; SR<sub>E'</sub> = peak early diastolic strain rate, SR<sub>A'</sub> = peak late diastolic strain rate. Values for the overall cohort are highlighted in red.

### 3.5 Discussion

#### 3.5.1 Left ventricular feature tracking

This is the first study to compare 2D with 3D deformation analysis using the same FT-CMR package, as well as the first to offer reference range values for 3D FT-CMR. 3D FT-CMR consistently delivered superior intra- and inter-observer repeatability for deformation analysis compared to 2D FT-CMR. Optimal reproducibility with 3D deformation analysis was achieved when measuring circumferential strain and strain rates, with more variability observed in indices of radial and long axis function.

In this population of age-stratified healthy volunteers, 3D FT-CMR strain and strain rate reference ranges are not interchangeable with 2D FT-CMR. Therefore, a new set of reference ranges have been established for 3D FT-CMR. Peak strain values from 3D FT-CMR possessed good correlation with LVEF, suggesting that peak strain values are a valid measure of systolic function. However, this correlation is not perfect, providing scope for peak strain to be a superior imaging biomarker of sub-clinical dysfunction in MR patients with normal range LVEF.

In the majority of measurements, there were benefits in terms of reduced intra- and inter-observer variability with 3D FT-CMR. The largest improvement in reproducibility can be seen for radial strain and strain rates (215). Feature tracking in the radial direction is perhaps most sensitive to through-plane feature loss since it is dependent upon the software tracking subtle twist along the endo- and epicardial borders. Unlike the measurement of Ell where through plane loss of the original segment of the mitral annulus is replaced by an adjacent segment of mitral annulus which is positioned identically for continued tracking, the through-plane loss of a subtle myocardial feature along the radial

direction results in complete information loss and hence the potential for larger degrees of mistracking.

Our results mirror the findings of 3D echocardiography which have demonstrated that absolute values are generally lower than those obtained via 2D methods, regardless of the exact tracking technique (222). 3D echocardiography for measurement of strain and strain rate however, has been adversely affected by both poor spatial and temporal resolution, leading to coarser speckle patterns and a higher speckle decorrelation between subsequent volumes. Moreover, the need to stitch together volumes to achieve adequate frame rates for analysis at higher heart rates has limited the clinical application of this technique. In contrast to 3D echocardiography, 3D FT-CMR has high feasibility and was possible in all subjects in the current study with the main requirement being a minimum of 25 phases per cine study.

Two-dimensional strain analysis is troubled by the through-plane loss of features into the third dimension. As the LV twists during contraction, the out of plane motion of one segment exaggerates the perceived degree of muscle shortening, thereby resulting in the over-estimation of myocardial movement (223). 3D FT-CMR is able to overcome this limitation and therefore produces lower absolute value strain and strain rates that may be a closer reflection of the underlying myocardial mechanics. This phenomenon mirrors how a normal ventricle can be seen undergoing a 40% reduction in 2D diameter (the transition from end diastole to end systole) with only a 15-20% reduction in actual muscle fibre length (224).

No difference was found in strain between genders, which replicates findings from a large meta-analysis that included 2D echocardiography studies (225). By contrast, small sex related differences in strain were described in a 3D echocardiography study of 303 healthy subjects; however, these were considered sufficiently small to be clinically irrelevant and not worthy of producing sex-specific reference ranges (226). The same study identified a weak relationship between strain, strain rate and age which was also considered too weak to be of clinical significance. Likewise, this current study documented a weak relationship between strain, strain rate and age that was directionally different, and that showed a small increase from 50 years. It is possible that this weak relationship reflects the smaller sample size of the deciles within this study and may be an issue with sampling, as no disparities were found either between sexes in conventional measures of indexed ventricular size or function in our study (227).

Segmental strain analysis has been proposed as a useful method for the diagnosis of regional myocardial disease, and will be of particular interest in MR where fibrosis has been reported to be more prevalent in the inferolateral LV segments (41). In a study comparing the diagnostic accuracy of 1D, 2D and 3D strain in a porcine model of myocardial infarction, 3D strain provided incremental diagnostic information when delineating dysfunctional and non-viable myocardium compared to 1D or 2D methods of strain analyses (228). We have provided segmental GCS reference ranges based upon the modified 16-segment AHA model and have demonstrated that the majority of basal and mid-ventricular segments have good reproducibility, but reproducibility is poor at the apex. This effect is likely due to the thinning of the ventricular wall and increased blurring of the endocardium-blood pool boundary. Reproducibility for segmental strain is poor,

particularly for GLS and GRS. Therefore, these were excluded from use in our main MR study.

### 3.5.2 Right ventricular feature tracking

We present one of the first reports of reference values for RV myocardial E<sub>II</sub> using FT-CMR from a group of healthy volunteers across a balanced stratification of age and sex.

The reproducibility of RV E<sub>II</sub> was good, but poor for RV strain rates, which are differential quantities that are derivatives of the former.

The lower limit of normal RV E<sub>II</sub> from this current study was -17.8% (defined as 1.96 standard deviations below the mean). This is comparable to that of previous smaller healthy volunteer cohorts (229, 230).

In contrast to our work on LV GLS, we did not demonstrate any relationship between age and RV E<sub>II</sub> (176). Of interest, the widely reported relationship between increasing age and conventional measures of chamber size and function, such as decreasing RV volumes with increasing RV ejection fraction are present (231). In a smaller RV FT-CMR on 50 patients (229), and a larger RV speckle tracking echocardiography study containing 219 healthy subjects, there were no relationship between strain and age (232). In contrast, a further speckle tracking study of 276 healthy volunteers found a statistically significant decline in RV E<sub>II</sub> with age that was felt too small to be of clinical importance (233) and a significant difference between genders. The values obtained in this latter study are much higher than those reported in our study and it is possible these are due to differences in the procedures used for calculation of the physical quantities, not only in terms of algorithms. Such issues have bedevilled echocardiography and are likely to be greater between modalities (234).



### 3.5.3 Limitations

While the clinical utility of 2D strain is well supported in the literature, our data demonstrating lower 3D values have only been acquired in a normal population; it is therefore not yet possible to determine whether 3D FT-CMR will provide incremental value in disease cohorts. While recent data have emphasised the incremental value of 2D deformation analysis on echocardiography across a range of populations and cardiovascular disease, including subjects from the community with preserved and impaired ventricular function (235), the clinical benefit of 3D analysis on feature-tracking has yet to be explored. In theory, the ability to measure true 3D myocardial motion should provide a better view of myocardial mechanics, with improved reproducibility, in comparison to echocardiography which produces a composite measure of GLS from 2D images in the apical four chamber, two chamber and long axis.

At the time of study initiation and publication, only 2D FT-CMR for the RV was available on commercially available versions of cvi42®. 3D FT-CMR for the RV is in development with one group publishing their results in a cohort of 50 patients (229), however, this 3D algorithm remains a developmental prototype. Theoretically, 3D FT-CMR for the RV will overcome barriers imposed by through-plane data loss. However, unlike the well defined walls of the LV, the thinner RV wall may be more difficult to track accurately in clinically indicated CMR studies. Finally, for LV FT-CMR, endo- and epicardial contours are recycled from those used for LVM quantification; conversely RV epicardial contours are not part of routine clinical practice – posing additional time requirements.

#### 3.5.4 Summary

In summary, 3D FT-CMR with its distinct reference ranges, has superior reproducibility compared to its 2D equivalent and should be the preferred methodology of myocardial strain analyses. 3D FT-CMR was therefore utilised within this thesis to investigate sub-clinical LV dysfunction in MR.

RV E11 derived from FT-CMR is a novel technique that is reproducible and allows rapid measurement of RV myocardial deformation without the limitation of acoustic window or need for additional CMR sequence acquisition. We have provided reference range values for RV FT-CMR in a healthy cohort of age and gender stratified volunteers. These normal ranges can be used in the assessment of any congenital or acquired cardiovascular disease. However, specifically for this thesis, they allowed us to investigate the use of preoperative RV E11 to explain the onset of symptoms, deterioration in exercise capacity and the postoperative prognostic stratification of patients with primary degenerative MR.

## CHAPTER 4

### CHARACTERISATION OF THE PRIMARY DEGENERATIVE MITRAL REGURGITATION DISEASE PROCESS – THE MITRAL FINDER STUDY

#### 4.1 Introduction

MR is a prevalent condition affecting 2.5% of the general population (1). Due to the incompetency of this single valve, a diverse range of physiological and pathological changes can occur at the level of the heart, circulation and patient.

Whilst previous studies have characterised some of these changes, the tendency has been to focus on a specific facet of the MR disease process. Therefore, cardiac volumetric adaptations (53), myocardial tissue remodelling (147), and objective measures of patients' exercise capacity (236) have all been reported in isolation. Furthermore, whilst there is growing interest in the wider adoption of PROMS in patients undergoing heart valve surgery to quantify patients' symptom burden in both clinical and research settings, data within MR remains very limited (237). The comprehensive multi-modality characterisation of the Mitral FINDER patients, as a single 'real-world' MR cohort is of interest as it facilitates the exploration of associative relationships between cardiac volumetric measurements made via gold-standard CMR, with non-invasive tissue characterisation and patients' subjective and objective symptom burden.

Furthermore, detailed characterisation of the baseline Mitral FINDER cohort will facilitate subsequent studies on histological changes in MR and predictors of postoperative outcomes in later chapters. The purpose of such studies is to identify novel biomarkers which can help us to optimise the timing of surgery in asymptomatic severe MR patients. As there is a growing trend in the UK for patients to be referred early under class II

indications, prior to the onset of symptoms. The makeup of the Mitral FINDER cohort should ideally reflect this with a preponderance for asymptomatic patients - a pertinent feature as it is within the asymptomatic patient population where novel surgical timing biomarkers will make the most prognostic impact on clinical practice.

Lastly, longitudinal study of patients with severe asymptomatic MR opting for conservative, non-surgical therapy is of interest as it allows exploration of real-world differences between patients opting for conservative versus surgical therapy. Whilst current cross-sectional studies report an increase in myocardial fibrosis as detected on CMR based ECV quantification (147), there is no longitudinal data on whether ECV expansion continues over time, nor the speed of this expansion. Clinically, this latter consideration is of importance when considering the “safety” of a ‘watchful waiting’ management approach in severe MR.

## 4.2 Aims

This study aimed to:

1. Present baseline data for the cohort recruited to Mitral FINDER;
2. Explore differences between those selecting early invasive surgery and those patients preferring a non-invasive, ‘watchful waiting’ approach;
3. Examine differences over time in ECV and other non-invasive imaging markers of fibrosis in ‘watchful waiting’ patients.

## 4.3 Methods

Methodology are as detailed in Chapter 2. In brief, this was a multi-centre prospective observational cross-sectional comparison of patients, before and after surgery for chronic

severe primary degenerative MR (clinicaltrials.gov NCT02355418) (152). In order to establish the natural history of ECV in MR, an additional cohort of MR patients who did not wish for surgery were followed.

Classification into fibroelastic deficiency (FED) versus Barlow's disease (BD), and establishing the presence or absence of mitral annular disjunction (MAD) was based on blinded independent review of echocardiographic and CMR imaging by two experienced imaging cardiologists (RS, NE), and confirmed on surgery.

#### 4.4 Results

As this chapter aimed to assess differences between surgical and non-surgical patients, only clinical data for these two main cohorts are presented here, with further sub-cohort comparisons of surgical symptomatic versus surgical asymptomatic patients being presented within Chapter 5.

##### 4.4.1 Recruitment

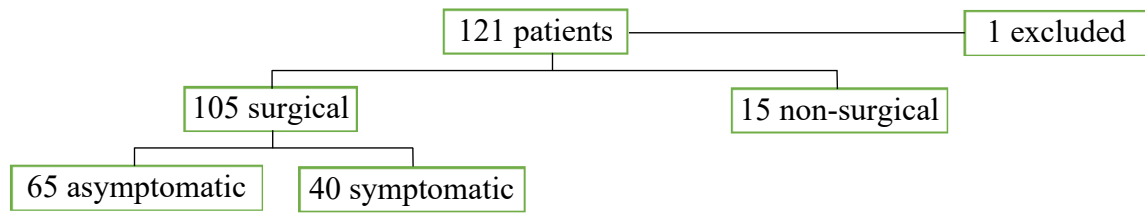
Following the exclusion of 1 patient whose CMR and stress echocardiography diagnosed MR due to a non-degenerative (Carpentier type I) mechanism, 120 patients (73% male, mean age  $63.1 \pm 13.4$  years) were included into the Mitral FINDER study (**Figure 4.1**).

##### 4.4.2 Baseline demographics

Surgical patients were predominantly overtly asymptomatic (NYHA class I N=65), with only eight patients possessing marked limitation of physical activity (NYHA class III). Non-surgical patients were statistically older and possessed lower eGFR than surgical patients; no significant differences in co-morbidities were present between the two groups

(Table 4.1). Despite a significant difference in NYHA classification, the two groups possessed similar symptom burden when quantified via PROMs.

**Figure 4.1** Mitral FINDER study patient recruitment summary.



121 patients with severe MR were recruited. One patient was subsequently excluded for possessing non-degenerative MR. NYHA class I patients were categorised asymptomatic, NYHA class II-III patients were categorised as symptomatic.

**Table 4.1** Baseline clinical characteristics of surgical versus non-surgical patients.

	Surgical		Non-surgical		P
	N	Value	N	Value	
<b>Demographics</b>					
Age (years)	105	63.1±13.4	15	73.6±9.5	<b>0.004</b>
Male gender (n, %)	105	77 (73%)	15	8 (53%)	0.133
NYHA classification	105		15		<b>0.002</b>
○ Class I		65 (62%)		15 (100%)	
○ Class II-III		40 (38%)		0 (0%)	
BMI (kg/m <sup>2</sup> )	105	25.5±4.5	15	23.9±3.3	0.167
Atrial fibrillation (n, %)	105		15		0.221
○ Paroxysmal		23 (22%)		6 (40%)	
○ Permanent		7 (7%)		0 (0%)	
Diabetes Mellitus (n, %)	105	2 (2%)	15	0 (0%)	1.000
Treated hypertension (n, %)	105	33 (31%)	15	8 (53%)	0.143
Treated hypercholesterolaemia (n, %)	105	20 (19%)	15	3 (20%)	1.000
Current smoker (n, %)	105	5 (5%)	15	2 (13%)	0.212
MR subtype	105		15		0.333
○ Fibroelastic deficiency		60 (57%)		6 (40%)	
○ Indeterminant/other		10 (10%)		3 (20%)	
○ Barlow's disease		35 (33%)		6 (40%)	
<b>SF-36</b>					
Physical functioning	105	75 (45-95)	15	75 (60-90)	0.910
Role limitations due to physical health	105	75 (0-100)	15	75 (0-100)	0.263
Role limitation due to emotional problems	105	100 (67-100)	15	100 (33-100)	0.730
Energy / fatigue	105	55 (40-75)	15	60 (40-70)	0.805
Emotional well-being	105	76 (60-88)	15	80 (76-96)	0.626
Social function	105	75 (50-100)	15	88 (75-100)	0.676
Pain	105	80 (68-100)	15	90 (78-100)	0.953
General health	105	65 (50-75)	15	65 (55-75)	0.859
<b>MLHFQ</b>					
Physical dimension score	104	6 (1-20)	15	6 (0-10)	0.307
Emotional dimension score	104	3 (1-10)	15	1 (0-7)	0.777
Total score	104	13 (4-41)	15	8 (0-21)	0.172
<b>Serum markers</b>					
eGFR (μmol/L)	105	75.0±14.8	15	62.7±22.5	<b>0.006</b>
NTproBNP pg/ml	103	174 (101-389)	15	423 (169 – 1159)	0.047
P1NP μg/L	104	54 (43-71)	14	55 (37-68)	0.471
P3NP μg/L	104	3.5 (2.9-4.6)	14	3.8 (3.5-4.5)	0.331
P1NP:P3NP ratio	104	15.6 (11.3-19.3)	14	12.5 (9.9-16.0)	0.503
TGF-β1 ng/ml	104	44.9±12.5	14	40.0±12.3	0.158
Interleukin 1α pg/ml	104	0.3 (0-2.1)	14	0.0 (0.0 – 0.3)	0.989
Interleukin 1β pg/ml	104	0 (0-0.2)	14	0.0 (0.0 – 0.0)	0.605

Data are reported as N (%), with p-values from Fisher's exact tests or  $\chi^2$  test when more than two variables; median (interquartile range), with p-values from Mann-Whitney U tests; or as mean±SD, with p-values from independent samples t-tests, as applicable. P-values in bold are significant after correction for multiple testing with the Benjamini–Hochberg procedure.



#### 4.4.3 Imaging characterisation of primary degenerative MR

CMR based imaging characterisation of the surgical and non-surgical groups are summarised in **Table 4.2**. Patients opting for conservative therapy possessed less severe MR compared to those undergoing surgery, with associated differences in end-diastolic and systolic volumes. Pertinently, whilst there was no statistical difference between the surgical guideline biomarkers of LVEF and LVESd, non-surgical patients possessed significantly smaller LVESVi.

One-third of patients possessed paroxysmal or permanent AF. The beat-to-beat variation in heart rate associated with AF created challenges for the retrospective gated acquisition and analyses of cine and T1 maps. Cines images may be blurred if acquired during a period with significant beat-to-beat variability, and T1 maps may contain images of the LV captured in both diastole and systole.

In order to improve the quality of acquired images and the reliability of analyses results, cines were repeated until sequence acquisition could be completed during a period when beat-to-beat variation was minimal. The Siemens Magnetom Avanto scanner divides a cine sequence into an industry-standard 25 phases to illustrate a single cardiac cycle. As an additional quality reassurance step, during the volumetric analyses of cine images, each cine slice forming the LV stack were individually analysed to ensure that end-systolic image (denoted by peak LV contraction) was captured on identical phases of the cardiac cycle. In situations where end-systole occurred on different phases, images were manually reorganised within cvi42® in order to avoid the overestimation of LVESVi from gating artefacts. For ECV quantification, T1 maps were visually inspected following each acquisition to ensure that all eleven raw inversion magnitude images were captured in end-

diastole, with the sequence repeated until gating artefacts were absent. Finally, for the measurement of  $AV_f$  from phase-contrast imaging, sequences were repeated five times with mean  $AV_f$  used within volumetric calculations.

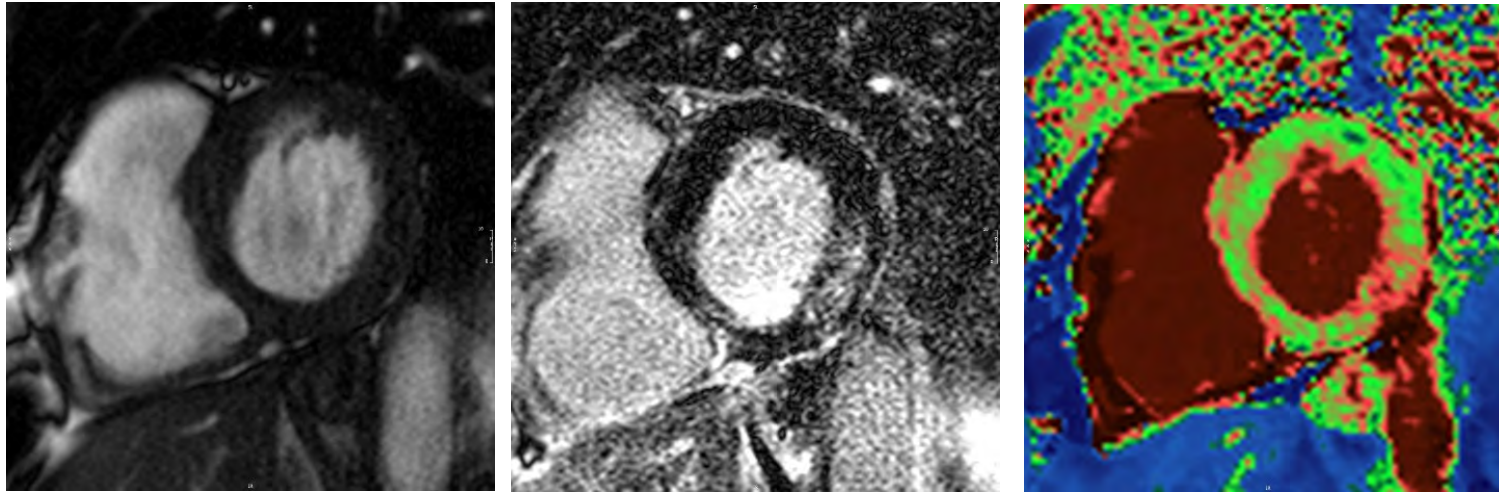
LGE was identified in approximately one-third of patients (typical appearance of LGE illustrated in **Figure 4.2**; two patients did not have gadolinium contrast due to claustrophobia which led to early termination of the CMR protocol; one patient was excluded due to embolic infarct pattern LGE). Patients with LGE possessed similar exercise capacity ( $\%PredVO_2$   $91.9\pm 22.4$  vs  $92.8\pm 21.1$ ,  $P=0.826$ ), systolic function (LVEF  $69.9\pm 6.4$  vs  $67.9\pm 8.9\%$ ,  $P=0.211$ ), and symptom burden (MLHFQ 11 [2-38] vs 13 [5-37],  $P=0.353$ ) to those without LGE. However, the presence of LGE was associated with more severe MR ( $69.7\pm 33.3$  vs  $55.5\pm 27$ ml,  $P=0.0.15$ ) in the overall cohort.

**Table 4.2** Cardiac magnetic resonance characteristics of surgical and non-surgical patients.

	Surgical		Non-surgical		P
	N	Value	N	Value	
LVEF (%)	105	68.3±8.2	15	70.5±7.4	0.323
LVEDVi (ml/m <sup>2</sup> )	105	104.0±21.8	15	86.3±23.7	<b>0.004</b>
LVESVi (ml/m <sup>2</sup> )	105	33.3±11.9	15	25.6±9.9	<b>0.019</b>
LVEDd (cm)	102	5.7±0.7	14	5.3±0.5	<b>0.035</b>
LVESd (cm)	99	3.7±0.7	14	3.4±0.7	0.090
LVMi (g/m <sup>2</sup> )	105	69.3±13.3	15	61.2±13.2	<b>0.029</b>
AV <sub>flow</sub> (ml)	103	70.8±20.2	13	66.9±21.4	0.524
AV <sub>flow</sub> indexed for BSA (ml/m <sup>2</sup> )	103	37.4±9.6	13	36.1±10.4	0.654
RVEF (%)	105	56.2±8.4	13	57.5±8.8	0.581
RVEDVi (ml/m <sup>2</sup> )	105	71.0±15.1	15	67.4±18.1	0.406
RVESVi (ml/m <sup>2</sup> )	105	31.6±10.3	15	28.5±9.5	0.284
MR volume (ml)	105	63.9±30.4	15	40.3±16.8	<b>0.004</b>
MR fraction (%)	105	46±15	15	36±12	<b>0.016</b>
LA volume (ml)	103	90.5±44.7	15	76.6±30.5	0.246
LGE presence (n, %)	102	35 (34%)	15	5 (33%)	1.000
LGE mass (g)	102	0.00 (0.00-0.38)	15	0.00 (0.00-1.60)	0.646
ECV (%)	101	27.4±3.2	14	27.7±2.1	0.687
Pre-contrast T1 relaxivity (ms)	104	985.4±25.2	14	995.7±29.3	0.163
Post-contrast T1 relaxivity (ms)	102	460.9±28.8	14	452.5±37.8	0.328
T2 relaxivity (ms)	76	53.4±3.4	8	54.0±2.6	0.584
GCS (s <sup>-1</sup> )	103	-17.6±3.2	15	-17.9±3.3	0.758
GLS (s <sup>-1</sup> )	103	-15.5±3.0	15	-16.0±4.6	0.555
RV E <sub>11</sub> (s <sup>-1</sup> )	105	-21.5±4.7	14	-20.8±5.9	0.596

Data are reported as N (%), with p-values from Fisher's exact tests or  $\chi^2$  test when more than two variables; median (interquartile range), with p-values from Mann-Whitney U tests; or as mean±SD, with p-values from independent samples t-tests, as applicable. Bold p-values are significant at p<0.05.

**Figure 4.2** Illustrative example of the appearance of myocardial fibrosis on CMR.



*Left:* cine sequence provides anatomical information; *centre:* LGE highlighting myocardial fibrosis in the basal inferolateral LV segment; *right:* native MOLLI T1 map (colour coding: blue represents low T1 values, green represents normal range T1 values, and red represents elevated T1 values) highlighting increased T1 values in regions corresponding with LGE, but also patchy areas of more subtle T1 elevation, not visualised on LGE.

#### 4.4.4 Exercise capacity in primary degenerative MR

104 surgical and 15 non-surgical patients underwent maximal CPET for the objective quantification of exercise efficiency and exercise capacity (**Table 4.3**). 1 asymptomatic surgical patient was unable to undergo CPET due to time commitment.

Patients contributed similar exercise efforts regardless of surgical and symptomatic status, as illustrated by the consistent peak RER and Borg scale of perceived exertion across both groups. Peak exercise capacity (%PredVO<sub>2</sub>peak) and ventilatory efficiency (VE/VCO<sub>2</sub>) were similar between surgical and non-surgical groups.

**Table 4.3** Cardiopulmonary exercise test parameters

	Non-surgical		Surgical		P
	N	Value	N	Value	
VO <sub>2</sub> peak (ml/kg/min)	15	20.7±5.6	104	22.7±7.8	0.338
%PredVO <sub>2</sub> AT (%)	15	64.4±10.3	104	59.6±16.7	0.279
%PredVO <sub>2</sub> peak (%)	15	98.2±18.7	104	91.2±22.4	0.248
Peak O <sub>2</sub> pulse (ml/beat)	15	9.9±4.1	104	12.0±4.0	0.068
%PredO <sub>2</sub> pulse (%)	15	85.8±21.8	104	87.5±23.6	0.791
%PredHRpeak (%)	15	107.2±18.1	104	97.6±16.4	<b>0.038</b>
VE/VCO <sub>2</sub>	14	33.3±4.5	104	32.8±6.7	0.783
Borg score	15	14.9±1.6	98	15.7±1.9	0.153
Peak RER	15	1.1±0.1	104	1.1±0.1	0.889

Data are reported as mean±SD, with p-values from independent samples t-tests. Bold p-values are significant at p<0.05.

4.4.5 Exercise stress echocardiographic characterisation of primary degenerative MR  
Exercise stress echocardiography was performed to assess the dynamic response of the ventricle, MR jet and pulmonary arterial pressures to exercise. Across the entire study, an increase in LVEF ( $62.7\pm 5.6\%$  vs  $67.0\pm 8.4\%$ ,  $P<0.001$ ) and decrease in LVESV ( $27.2\pm 9.3\text{ml/m}^2$  vs  $23.0\pm 11.0\text{ml/m}^2$ ,  $P<0.001$ ) was observed with ergometry.

With peak exercise, we found the technical feasibility of LV  $E_{II}$  measurements to significantly deteriorate due to a combination of tachycardia, tachypnoea and shifting echocardiographic windows. Therefore, adequately tracked peak exercise  $E_{II}$  was only recorded in 30 patients. Exercise  $E_{II}$  was therefore excluded from the results summary (**Table 4.4**). MR response was classified as “unable to determine” in instances of insufficient visualisation of the MR jet.

No significant differences to exercise were noted between surgical and non-surgical cohorts in terms of ventricular contractile response, MR severity or estimated systolic pulmonary artery pressure (sPAP) values. A ‘normal LV response to exercise’ was defined as objectively or subjectively determined increase in LVEF and reduction in LVESV at peak exercise. Symptomatic and asymptomatic surgical patients possessed similar proportions of abnormal response to exercise ( $P=0.788$ ).

Within the surgical cohort, 65 patients were NYHA class I and underwent surgery with a class IIa indication. It has been suggested that exertion mediated deterioration in MR severity, sPAP or LV function, may represent additional adverse prognostic markers in asymptomatic patients. We have therefore identified these patients (11 [19%] with

deteriorating MR, 7 [12%] with exertional sPAP >60mmHg, and 14 [25%] with deteriorating LV function) for future postoperative prognostic studies.



**Table 4.4** Exercise stress echocardiography parameters at rest and peak exercise.

		Non-surgical		Surgical		P
		N	Value	N	Value	
Rest	LVEF	14	64.9±8.0	82	63.1±5.9	0.309
	LVESV	14	23.2±7.6	82	28.3±9.3	0.053
	Echo E <sub>II</sub>	10	19.1±2.5	70	20.0±2.9	0.331
Peak	LVEF	8	68.9±5.6	60	66.6±9.4	0.504
	LVESV	8	16.7±5.2	60	26.1±11.5	<b>0.027</b>
Interpretation	MR response to exercise	13		82		0.628
	○ No change		10 (77%)		62 (76%)	
	○ Increases		3 (23%)		15 (18%)	
	○ Unable to determine		0 (0%)		5 (6%)	
	Ventricular response to exercise	13		79		0.725
	○ Normal		11 (85%)		60 (72%)	
	○ Abnormal		2 (15%)		19 (23%)	
	sPAP response to exercise	13		83		0.469
	○ No change		6 (46%)		42 (52%)	
	○ Increases to ≤60mmHg		6 (46%)		26 (35%)	
○ Increases to >60mmHg		1 (8%)		15 (12%)		

Data are reported as N (%), with p-values from Fisher's exact tests or  $\chi^2$  test when more than two variables; or as mean±SD, with p-values from independent samples t-tests, as applicable. Bold p-values are significant at p<0.05.

#### 4.4.6 Sub-cohort analyses of asymptomatic patients

As overt symptoms are a class I indication for surgery, symptomatic patients were excluded from sub-cohort analyses aimed at exploring the differences between patients opting for conservative vs surgical management, when both are reasonable options.

We found that patients opting for conservative therapy were statistically older than those opting for early surgical intervention, with a trend for higher proportions of female gender (**Table 4.5**). Of importance, non-surgical patients had similar levels of symptom burden and achieved a similar level of predicted exercise capacity, whilst MR severity was statistically lower than the surgical cohort.

**Table 4.5** Sub-cohort analyses between NYHA class I patients opting for surgical and non-surgical management.

	Surgical		Non-surgical		P
	N	Value	N	Value	
<b>Demographics</b>					
Age (years)	65	62.2±14.3	15	73.6±9.5	<b>0.004</b>
Male gender (n, %)	65	50 (77%)	15	8 (53%)	0.065
BMI (kg/m <sup>2</sup> )	65	24.9±4.2	15	23.9±3.3	0.376
Atrial fibrillation (n, %)	65		15		0.087
○ Paroxysmal		10 (15%)		6 (40%)	
○ Permanent		2 (3%)		0 (0%)	
MR subtype	65		15		0.201
○ Fibroelastic deficiency		38 (58%)		6 (40%)	
○ Indeterminant/other		3 (5%)		3 (20%)	
○ Barlow's disease		24 (37%)		6 (40%)	
<b>SF-36</b>					
Physical functioning	65	90 (65-95)	15	75 (60-90)	0.102
Role limitations due to physical health	65	100 (50-100)	15	75 (0-100)	0.218
Role limitation due to emotional problems	65	100 (100-100)	15	100 (33-100)	0.088
Energy / fatigue	65	65 (55-80)	15	60 (40-70)	0.334
Emotional well-being	65	84 (64-92)	15	80 (76-96)	0.298
Social function	65	88 (75-100)	15	88 (75-100)	0.824
Pain	65	90 (78-100)	15	90 (78-100)	0.814
General health	65	70 (60-80)	15	65 (55-75)	0.465
<b>Minnesota living with heart failure questionnaire</b>					
Physical dimension score	65	2 (0-8)	15	6 (0-10)	0.313
Emotional dimension score	65	2 (0-4)	15	1 (0-7)	0.500
Total score	65	0 (0-4)	15	8 (0-21)	0.590
<b>Cardiopulmonary exercise test</b>					
VO <sub>2</sub> peak (ml/kg/min)	64	25.5±7.5	15	20.7±5.6	<b>0.023</b>
%PredVO <sub>2</sub> AT (%)	64	63.3±15.2	15	64.4±10.3	0.775
%PredVO <sub>2</sub> peak (%)	64	98.6±19.8	15	98.2±18.7	0.951
Peak O <sub>2</sub> pulse (ml/beat)	64	12.7±4.0	15	9.9±4.1	<b>0.017</b>
%PredO <sub>2</sub> pulse (%)	64	92.3±21.1	15	85.8±21.8	0.291
%PredHRpeak (%)	64	99.9±13.7	15	107.2±18.1	0.087

VE/VCO <sub>2</sub>	64	31.2±5.4	14	33.3±4.5	0.179
Borg score	59	15.7±1.8	15	14.9±1.6	0.130
Peak RER	64	1.15±0.12	15	1.13±0.08	0.683
<b>Cardiac magnetic resonance</b>					
LVEF (%)	65	69.5±7.9	15	70.5±7.4	0.631
LVEDVi (ml/m <sup>2</sup> )	65	105.0±22.1	15	86.3±23.7	<b>0.005</b>
LVESVi (ml/m <sup>2</sup> )	65	32.5±12.5	15	25.6±9.9	<b>0.049</b>
LVMi (g/m <sup>2</sup> )	65	71.4±13.0	15	61.2±13.2	<b>0.008</b>
AV <sub>flow</sub> (ml)	63	75.0±18.4	13	66.9±21.4	0.163
AV <sub>flow</sub> indexed for BSA (ml/m <sub>2</sub> )	63	40.0±8.4	13	36.1±10.4	0.152
RVEF (%)	65	57.3±8.1	13	57.5±8.8	0.917
RVEDVi (ml/m <sup>2</sup> )	65	71.1±13.2	15	67.4±18.1	0.249
RVESVi (ml/m <sup>2</sup> )	65	31.0±8.8	15	28.5±9.5	0.337
MR volume (ml)	65	62.0±29.6	15	40.3±16.8	<b>0.004</b>
MR fraction (%)	65	44.3±11.8	15	36.4±11.6	<b>0.021</b>
LA volume (ml)	63	87.5±43.8	15	76.6±30.5	0.364
LGE presence (n, %)	64	22 (34%)	15	5 (33%)	0.939
LGE mass (g)	64	0.00 (0.00-0.37)	15	0.00 (0.00-1.60)	0.834
ECV (%)	63	26.8±3.1	14	27.7±2.1	0.329
Pre-contrast T1 relaxivity (ms)	65	981.4±23.9	14	995.7±29.3	0.054
Post-contrast T1 relaxivity (ms)	63	466.4±28.5	14	452.5±37.8	0.125
T2 relaxivity (ms)	41	52.9±2.7	8	54.0±2.6	0.262
GCS (s <sup>-1</sup> )	64	-18.2±3.0	15	-17.9±3.3	0.731
GLS (s <sup>-1</sup> )	64	-15.9±2.7	15	-16.0±4.6	0.853
RV E <sub>II</sub> (s <sup>-1</sup> )	65	-21.6±4.5	14	-20.8±5.9	0.530

Data are reported as N (%), with *p*-values from Fisher's exact tests or  $\chi^2$  test when more than two variables; or as mean±SD, with *p*-values from independent samples *t*-tests, as applicable. Bold *p*-values are significant at *p*<0.05.

#### 4.4.7 Longitudinal changes following conservative management

Longitudinal CMR studies were performed in 12 out of 15 conservatively managed patients following a mean period of  $10.8 \pm 1.9$  months; 3 patients were lost to follow-up.

During this follow-up period, all patients remained NYHA class I with no significant change in subjective and objective measures of symptom burden. On CMR, there were no statistically significant changes in biventricular size or function, and no significant increase in ECV (**Table 4.6**). There were no new cases of LGE detection.

**Table 4.6** Longitudinal CMR parameters in conservatively managed asymptomatic MR patients (N=12).

	Visit 1	Visit 2	P
<b>CMR parameters</b>			
ECV (%)	28.0±2.3	27.2±1.3	0.229
LVEF (%)	70.4±8.3	70.3±10.4	0.964
LVEDVi (ml/m <sup>2</sup> )	87.2±25.8	88.9±29.3	0.513
LVESVi (ml/m <sup>2</sup> )	26.0±10.9	26.8±15.4	0.768
LVMi (g/m <sup>2</sup> )	61.8±13.1	62.1±16.2	0.906
MR volume (ml)	41.5±18.2	45.7±22.7	0.174
MR fraction (%)	36.7±11.8	40.1±16.9	0.249
RVEF (%)	57.0±9.6	53.8±9.6	0.286
RVEDVi (ml/m <sup>2</sup> )	67.6±17.8	76.3±28.6	0.146
RVESVi (ml/m <sup>2</sup> )	29.2±10.2	36.5±23.0	0.225
GCS (s <sup>-1</sup> )	-17.5±3.2	16.7±3.3	0.239
GLS (s <sup>-1</sup> )	16.0±4.9	-15.3±2.8	0.395
RV E <sub>II</sub> (s <sup>-1</sup> )	-20.6±4.8	-18.8±5.7	0.423
<b>Symptom burden</b>			
MLHFQ total	8.5 (0.8 – 19.5)	4 (2.0-10.8)	0.529
%PredVO <sub>2</sub> peak (%)	102.6±13.0	101.8±14.1	0.876

*Data are reported as mean±SD or median (interquartile range); with p-values from paired samples t-tests or related-samples Wilcoxon signed rank test. Bold p-values are significant at p<0.05.*

## 4.5 Discussion

### 4.5.1 Cohort representation

The Mitral FINDER study represents one of the most comprehensive characterisations of a single cohort of patients with severe primary degenerative MR to date, featuring gold-standard cardiac volume and tissue characteristic measurements, along with in-depth symptom burden and exercise capacity profiling. We intended the Mitral FINDER cohort to reflect current trends in surgical referrals with a preponderance for asymptomatic patients, so that we can study the postoperative prognostic impact of preoperative biomarkers in patients where the indications for surgery are less robust. This was achieved as highlighted by 62% of patients being NYHA class I and the overall surgical cohort possessing low symptom burden on PROMs and good exercise capacity on CPET.

The Mitral Regurgitation International Database (MIDA) is a multicentre registry of degenerative MR patients enrolled from 6 tertiary centres across Europe and the United States of America; it contains the largest published dataset of primary degenerative MR patients undergoing MV surgery (238). The make-up of the Mitral FINDER surgical cohort, with its mean age of 63 years and male preponderance of 73%, are similar to the mean of 65 years and male gender of 74% in the 1709 patients within the MV repair cohort of the MIDA registry, as well as the mean age of 63-65 years reported by the UK National Adult Cardiac Surgery Audit (77). Furthermore, the proportions of symptomatic patients in the MIDA registry and the Mitral FINDER study are similar, albeit a more stringent criteria of NYHA  $\geq$ II was utilised to define the presence of symptoms in the current study, compared to NYHA III-IV in the MIDA registry. These factors, together with similar incidences of comorbidities including diabetes mellitus, hypertension and AF, suggest that it is reasonable to extrapolate findings on histological fibrosis and

postoperative outcomes within the Mitral FINDER study to that of the wider MR population.

#### 4.5.2 Comparison of surgical and non-surgical study arms

As an observational study, the decision for surgery vs conservative therapy was left to the participants of the Mitral FINDER study and their usual cardiologists. When both management options were reasonable choices, we found that patients opting for conservative therapy were statistically older than those opting for surgical intervention. This finding highlights the point that as the population ages, patients may increasingly wish to avoid surgery unless it becomes a necessity. With data to suggest that 55% of asymptomatic severe MR patients may remain symptom free at 8 years of follow-up (79), the odds a person remaining untroubled by MR-related symptoms for the duration of their life can be quite favourable in the older patient.

Finally, interests in minimally invasive valve intervention have been catapulted by recent successes with transcatheter aortic valve implantation (TAVI) (239). Whilst the development of equivalent minimally invasive techniques for MV disease remains in relative infancy, early experiences with systems such as the MitraClip (240), thoracoscopic or robot-assisted mitral valve surgery (241) offer hope to current asymptomatic MR patients that they may be eligible for a minimally invasive procedure should they eventually develop symptoms over the next decade.



#### 4.5.3 Longitudinal changes in ECV with conservative management

Within our conservatively managed cohort, whilst mean values of MR volume and fraction increased by 4.2ml / 3.4% during the follow-up period, the magnitude of this increase did not reach statistical significance. One previous study have reported a mean increase in MR severity of 7.4ml or 2.9% per year, however, there can be a high degree of variability across individuals with a reduction in MR burden being possible in patients following reductions in blood pressure (afterload) (18).

More importantly, symptom burden, measures of biventricular size and function remained stable with no statistically significant change in ECV. The stability in CMR parameters reassures us that it is reasonable to delay surgery in patients without class I surgical indications, provided that they are “truly” asymptomatic as assessed subjectively via PROMs and objectively via CPET. This stability provides mechanistic insight into why some research groups have reported continued symptom-free status in over half of their cohort at 8 years follow-up (79). Whilst CPET requires specialised equipment and expertise to perform, the prognostic value of routine PROMs, which can be completed whilst patients are sitting in the waiting room for their annual MR surveillance review, is of future research interest.

#### 4.5.4 Limitations

Being an observational study, we did not interfere with patients’ decision for surgery vs conservative therapy. Whilst this allowed us to explore the real-world characteristics of each cohort, it did produce a small non-surgical sample size. Despite this, the main

purpose of the Mitral FINDER study was to investigate the postoperative outcomes of surgical patients – an aim which is facilitated by the larger surgical cohort.

AF is common in MR patients and poses a unique set of problems for reliable CMR results. The steps taken within this study to overcome the beat-to-beat variation in heart rate in AF patients are time consuming, which may limit its wider adoption within the routine clinical setting.

#### 4.5.5 Summary

The Mitral FINDER cohort is representative of real-world patients with severe primary degenerative MR. This cohort has been comprehensively characterised both structurally on CMR, and functionally through self-reported questionnaire and CPET. We found that asymptomatic patients opting for conservative therapy are statistically older than those opting for early surgery. Reassuringly, despite no intervention, no significant changes in non-invasive tissue characterisation parameters were identified following a median follow-up of 10.8 months.

## CHAPTER 5

### HISTOLOGICAL QUANTIFICATION OF FIBROSIS IN PRIMARY MITRAL REGURGITATION

#### 5.1 Introduction

The currently available histological characterisation of myocardial fibrosis in primary degenerative MR remains extremely limited. Understanding this MR induced LV fibrotic process is important because symptoms and exercise capacity in MR are determined not only by the severity of regurgitation, but also by the myocardial response of the volume overloaded ventricle (107). Fibrosis is thought to be responsible for the onset of sub-clinical deterioration in ventricular function (117, 124), and is likely the cause of de-novo LV dysfunction following MV repair (83). To understand, and to be able to non-invasively monitor this LV remodelling process will be crucial for optimising the management of MR.

##### 5.1.1 Histological characterisation of the myocardium in primary degenerative MR

Early autopsy studies on symptomatic patients late in the MR disease process highlighted a stepwise increase in myocardial fibre hypertrophy and interstitial spacing between patients with moderate symptoms and LV dysfunction, compared to those with severe symptoms and LV dysfunction (118). However, it remains unclear what myocardial changes are present prior to overt cardiac failure. A significant proportion of our understanding has been indirectly derived from rat models of volume overload (section 1.6.2), although these models have tended to be in the form of aorto-caval fistulae rather than direct valvular pathology. Data from these models suggest that the development of heart failure may be the result of additional ventricular dilatation in the absence of concomitant muscle hypertrophy (102).

Biopsy studies in humans are challenging but there has been a growth of studies using CMR imaging for non-invasive myocardial characterisation in asymptomatic moderate and severe MR. Coarse replacement fibrosis detected on LGE (32) and diffuse interstitial fibrosis quantified with T1 mapping and ECV calculation (147) have both been demonstrated in asymptomatic MR. Further studies have suggested that LV involvement in mitral valve prolapse may not simply be secondary to volume overload alone, with more extensive LGE found in patients with MVP (242). Interest has heightened with evidence that LGE, ECV and change in T1 mapping may reflect the development of a substrate for arrhythmogenesis in MVP (243), with more extensive LGE in those with mitral-annular disjunction (244). However, evidence for the association between increased T1, ECV and the presence of interstitial fibrosis in MR remains sparse (140), and these techniques, being influenced by both oedema and fibrosis, are non-specific for the underlying histological pattern. The validation of these techniques has primarily been performed in primary or ischaemic cardiomyopathies, with a recent meta-analysis identifying only two studies that correlates CMR-derived ECV and histological quantification of fibrosis in MR (245) where one study contained four cases of primary MR, and the other ten (119, 140). Furthermore, given the differences in pathophysiology between ischaemia, pressure overload and volume overloaded states, direct histological characterisation in MR remains of great interest.

Finally, several post-mortem studies on sudden cardiac death (SCD) victims with MVP have consistently reported fibrosis involving papillary muscles and basal inferolateral LV, independent of the severity of MR (41, 246, 247). However, the quantification of fibrosis

from SCD victim may not be directly transferrable to the majority of patients with MR because 1) only a small percentage of MR and MVP patients suffer from life threatening arrhythmias, 2) a significant proportion of cases within these studies only possessed mild MR (41, 246), and 3) there is invariably myocardial injury, necrosis and additional scar development from cardiac arrest and prolonged cardiopulmonary resuscitation (248).

## 5.2 Aims and hypotheses

A knowledge gap exists for the quantification of myocardial fibrosis in primary MR. We hypothesise that histological evidence of myocardial fibrosis develops in MR, prior to the onset of symptoms and overt heart failure. Its accumulation is responsible for sub-clinical deteriorations in systolic and diastolic function, and is contributory towards the gradual development of symptoms.

The aims of this prospective study of patients with asymptomatic and symptomatic primary degenerative MR were to assess: i) the histological changes within the myocardium in response to chronic severe MR; ii) the association between histological extent of fibrosis and myocardial structure, function and tissue characterisation on CMR; iii) the relationship between extent of myocardial remodelling (histology; CMR), symptoms and exercise capacity.

## 5.3 Methods

Methods are as detailed in Chapter 2. In brief, this was a prospective multicentre observational study (clinicaltrials.gov NCT02355418) (152) of patients with moderate or severe primary degenerative MR. For this study, patients with moderate MR on referral

echocardiography were excluded from analyses, as only severe MR cases were eligible for mitral valve surgery (30).

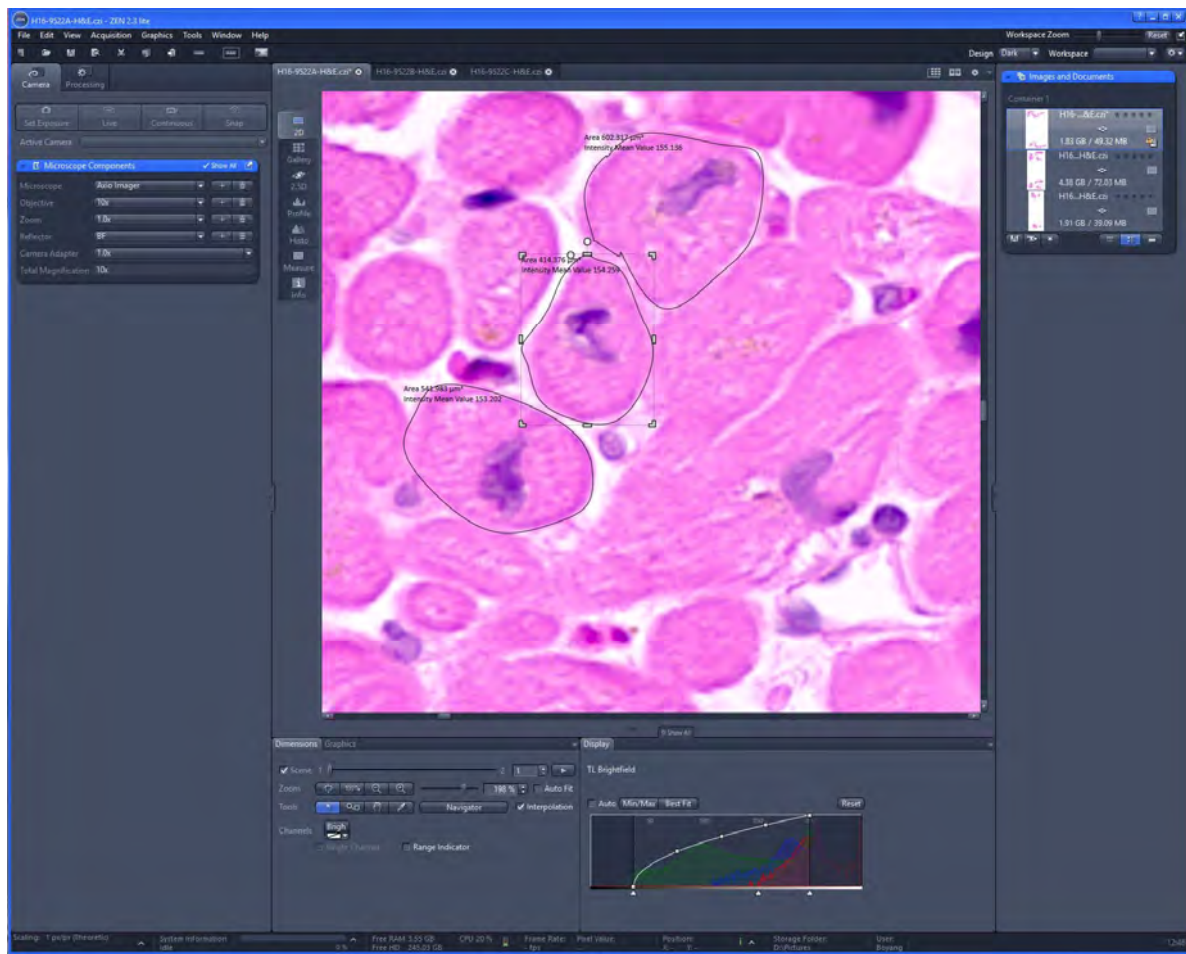
### 5.3.1 Histological techniques

LV biopsies were harvested during MV surgery from the LV septum, anterior and posterior free wall with a 14G TruCut needle or scalpel. Histological analyses were performed blinded to clinical and imaging data (DN; BL). Myocardial fibrosis was analysed on x20 whole-slide scanned MT sections (Axio Scan.Z1 ZEISS, Oberkochen, Germany). CVF was quantified with Ilastik machine-learning software. CVF<sub>mean</sub> represents the mean, and CVF<sub>max</sub> represents the highest CVF across the three biopsy sites.

Control myocardial samples were obtained from autopsies of 8 subjects (5 male, all Caucasian, age  $59 \pm 6.9$  years) from our collaboration with the Center for Applied Medical Research, University of Navarra Pamplona, Spain who died of non-cardiac causes showing no signs of macroscopic or microscopic cardiac lesions.

Blinded myofiber hypertrophy quantification was performed by manually quantifying the cross-sectional area (CSA) of 50 randomly selected myofibers via ZEN software (Carl Zeiss Microscopy). To ensure consistency, only myofibers found in its mid-axial orientation were eligible for quantification (**Figure 5.1**).

**Figure 5.1** Manual quantification of myofiber cross sectional area using ZEN.



For each patient, fifty randomly selected myocytes in its mid-axial orientation (highlighted by the presence of a central nucleus) were quantified for the assessment of myofiber hypertrophy.

### 5.3.2 Statistical analyses

In addition to general statistical principles listed in section 2.5, the goodness of fit of regression models was assessed graphically, with logarithmic transformations applied where either poor fit or heteroscedasticity was identified. For regression models where the dependent variable was log-transformed, the resulting coefficients were anti-logged, and converted into percentage changes, in order to simplify interpretation.

## 5.4 Results

In total, 120 patients with severe primary degenerative mitral regurgitation were recruited, of whom 105 were referred for mitral valve repair. One of these surgical patients was excluded from analyses, due to a history of previous percutaneous coronary intervention with stenting, leaving N=104. The 15 patients that declined surgery all had a class IIa indication for repair but opted to be treated conservatively with a ‘watchful waiting strategy’. Comparing those patients choosing repair rather than watchful waiting, the former were significantly younger, with higher eGFR and greater LVESVi, LVMi and MR severity (**Table 5.1**).



**Table 5.1** Clinical characteristics of conservative and surgical patients.

	N	Management		P-Value
		Conservative	Surgical	
<b>Clinical characteristics</b>				
Age (years)	119	74±9	63±13	<b>0.004</b>
Male sex (n, %)	119	8 (53%)	76 (73%)	0.206
Treated hypertension	119	8 (53%)	32 (31%)	0.084
BMI (kg/m <sup>2</sup> )	119	24±3	26±5	0.170
Atrial fibrillation	119			0.227
None		9 (60%)	74 (71%)	
Paroxysmal (n, %)		0 (0%)	7 (7%)	
Permanent (n, %)		6 (40%)	23 (22%)	
eGFR (ml/min/1.73m <sup>2</sup> )	117	56 (43–79)	75 (64–84)	<b>0.023</b>
Degeneration subtype	119			0.347
Barlow's		6 (40%)	35 (34%)	
Indeterminant		3 (20%)	10 (10%)	
Fibroelastic deficiency		6 (40%)	59 (57%)	
NTproBNP	117	423 (169-1159)	233 (110-567)	0.100
MLHFQ score	119	8 (0-21)	13 (4-41)	0.201
%PredVO <sub>2</sub> max (%)	118	98±19	91±22	0.253
Echocardiography E/e'	102	9.2 (6.2-11.1)	8.0 (6.9-11.8)	0.861
Resting sPAP (mmHg)	99	41±16	35±15	0.184
Ventricular ectopy burden (%)	60	0.3 (0.0-0.4)	0.1 (0.0-1.2)	0.876
<b>Cardiac magnetic resonance characteristics</b>				
LVESVi (ml/m <sup>2</sup> )	119	25.6±9.9	33.3±11.9	<b>0.018</b>
LVEF (%)	119	70.5±7.4	68.3±8.2	0.324
GCS	117	-17.9±3.3	-17.6±3.2	0.752
GLS	117	-16.0±4.6	-15.5±3.0	0.542
LVMi (g/m <sup>2</sup> )	119	61.2±13.2	69.4±13.3	<b>0.028</b>
RVESVi (ml/m <sup>2</sup> )	119	28.5±9.5	31.6±10.3	0.285
RVEF (%)	119	57.5±8.8	56.3±8.8	0.599
RV E <sub>II</sub>	118	-20.8±5.9	-21.6±4.7	0.561
Aortic forward flow (ml)	115	66.9±21.4	70.9±20.3	0.512
MR volume (ml)	119	40.3±16.8	63.9±30.5	<b>0.004</b>
MR fraction (%)	119	36.4±11.6	46.0±14.8	<b>0.017</b>
ECV (%)	115	27.7±2.1	27.3±3.2	0.687
Native T1 (ms)	117	995.7±29.3	985.0±24.9	0.143
LGE presence (n,%)	117	5 (33%)	34 (33%)	1.000
LGE quantification (g)	118	0.00 (0.00-1.60)	0.00 (0.00-0.35)	0.631

Data are reported as N (%), with p-values from chi<sup>2</sup> tests; median (interquartile range), with p-values from Mann-Whitney U tests; or as mean±SD, with p-values from independent samples t-tests, as applicable. Bold p-values are significant at p<0.05.

#### 5.4.1 Histology of surgical myocardial biopsies

Of the 104 patients treated surgically, biopsies were collected from 86 (83%). Of these, 67 patients had biopsies taken from all three sites (LV septum, anterior and posterior free wall), with N=14 having two biopsies, and N=5 a single biopsy (N=234 biopsies in total). Biopsies were not feasible across all biopsy sites in all patients due to limited visualisation or safe instrument access to the ventricular myocardium from the left atrial incision at the time of surgery. In addition, two patients chose to undergo surgery at institutions external to the study sites, where biopsies were not taken. For the eight control patients, a single whole-heart autopsy section was available for analysis.

*Cellular Hypertrophy:* Direct histological quantification of cardiomyocyte hypertrophy was performed via haematoxylin and eosin (H&E) stained slides. MR patients were found to possess marked muscle hypertrophy compared to controls (cardiomyocyte CSA  $853\pm 230\mu\text{m}^2$  vs  $124\pm 26\mu\text{m}^2$ ,  $P<0.001$ , **Figure 5.2A**) with histological quantification correlating significantly with CMR derived LVMI ( $R=0.33$ ,  $P=0.002$ ).

*Myocardial Fibrosis:* MR patients had a median  $\text{CVF}_{\text{mean}}$  of 14.6% [IQR 7.4-20.3]; and  $\text{CVF}_{\text{max}}$  of 22.2% [10.2-31.8], both of which were significantly higher than control CVF values (3.3% [2.6-6.1],  $P<0.001$ , **Figure 5.2B**). For MR patients, there were no significant gender differences in  $\text{CVF}_{\text{mean}}$  (men 14.1% [7.3-18.5] vs. women 16.1% [11.4-24.6],  $P=0.163$ ).

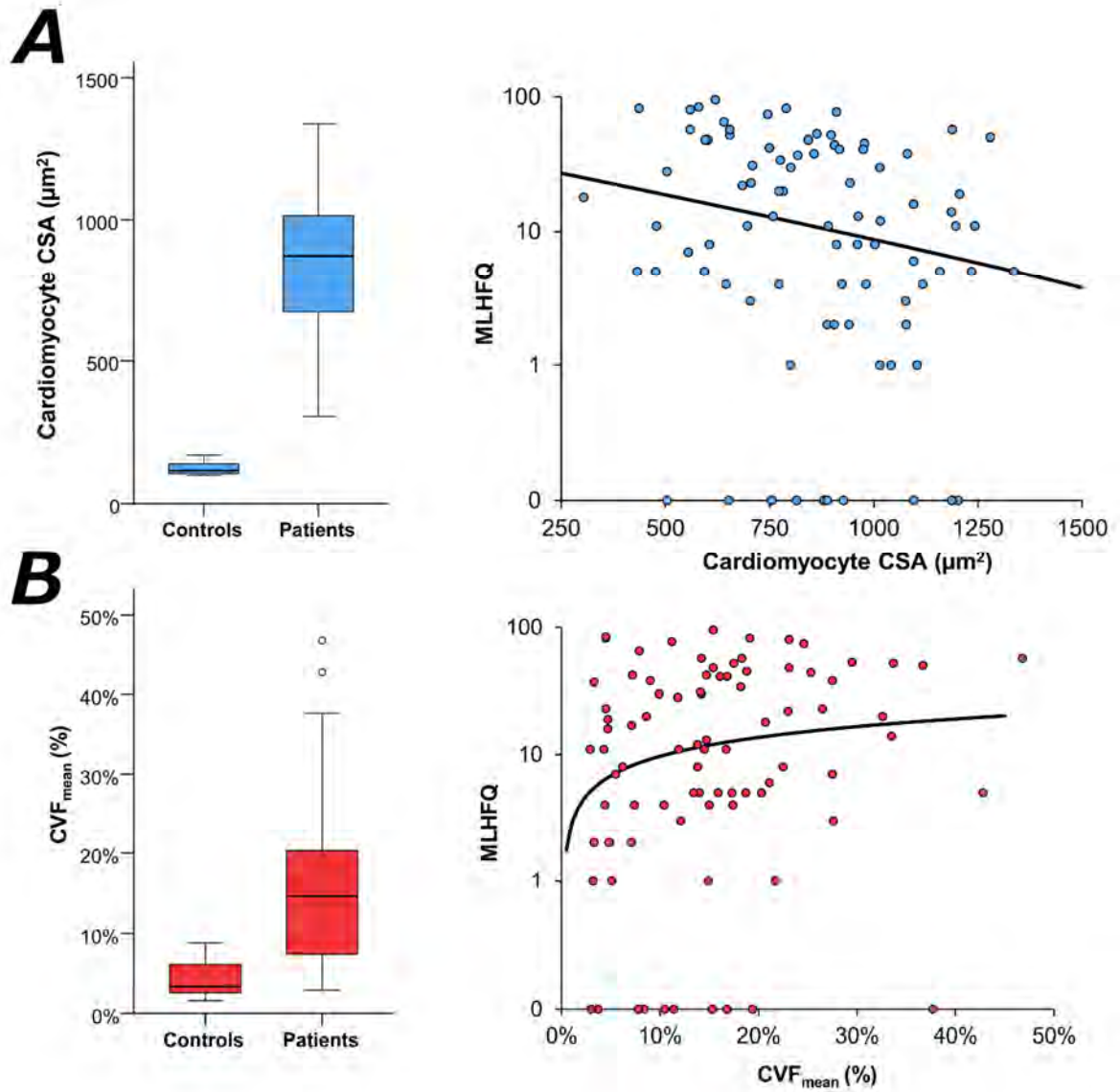
124 myocardial biopsies contained endocardium (median thickness  $100\mu\text{m}$  [58-181]), whilst 111 biopsies contained only myocardium. Biopsies with endocardium showed higher CVF than those without endocardium (16.7% [10.4-27.1] vs. 6.6% [3.5-12.3],

P<0.001). There was a significant correlation between mean endocardial thickness and CVF ( $\rho = 0.35$ ,  $P < 0.001$ ), consistent with endocardial thickening and subendocardial scar. The pattern of fibrosis varied between participants and within the myocardium, including diffuse interstitial fibrosis, perivascular fibrosis and areas of replacement fibrosis (**Figure 5.3**).

There was no clear pattern to the distribution of fibrosis within each individual biopsy sample; although CVF in samples with endocardium was approximately twice that of mid-myocardial samples, no clear endocardial-epicardial gradient could be seen within individual biopsy samples. In the 67 patients who had 3 biopsies, the heterogeneity was reflected in a low intraclass correlation coefficient (ICC) for fibrosis across the three biopsy sites (ICC=0.23, 95% CI 0.08-0.39,  $P=0.001$ ; **Figure 5.4**).

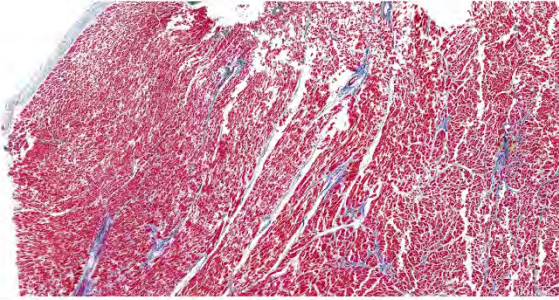
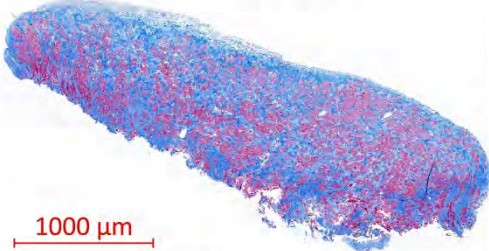
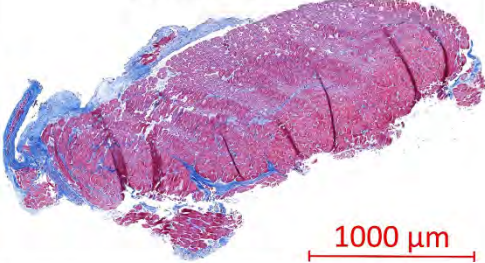
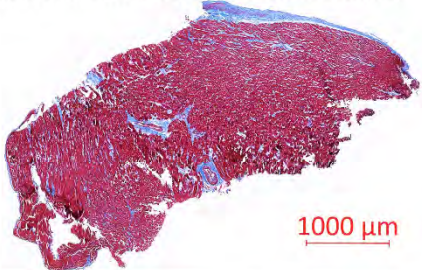
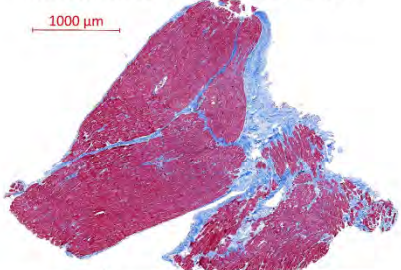
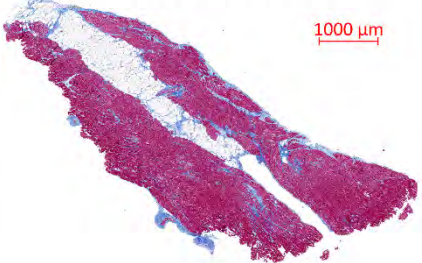
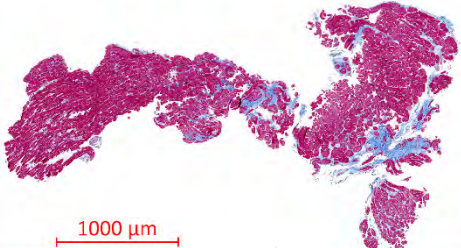
*Fatty Infiltration:* Biopsies were assessed by an experienced cardiac histopathologist, who gave a blinded subjective quantification of fatty infiltration on a scale of 0 (no fat infiltration) to 3 (prominent fat infiltration). Of the 79 biopsies assessed, 27 (34%) contained some degree of fat infiltration. Across the 79 biopsies, fatty infiltration was found to increase significantly with  $CVF_{\text{mean}}$  ( $\rho=0.23$ ,  $P=0.045$ ), and to have a near-significant correlation with age ( $\rho=0.22$ ,  $P=0.056$ ). No significant correlations, however, were present with CMR parameters.

**Figure 5.2** Distribution of A) cardiomyocyte CSA and B) CVF, in controls and MR patients (left), and their relationship with increasing symptoms in MR patients (right).



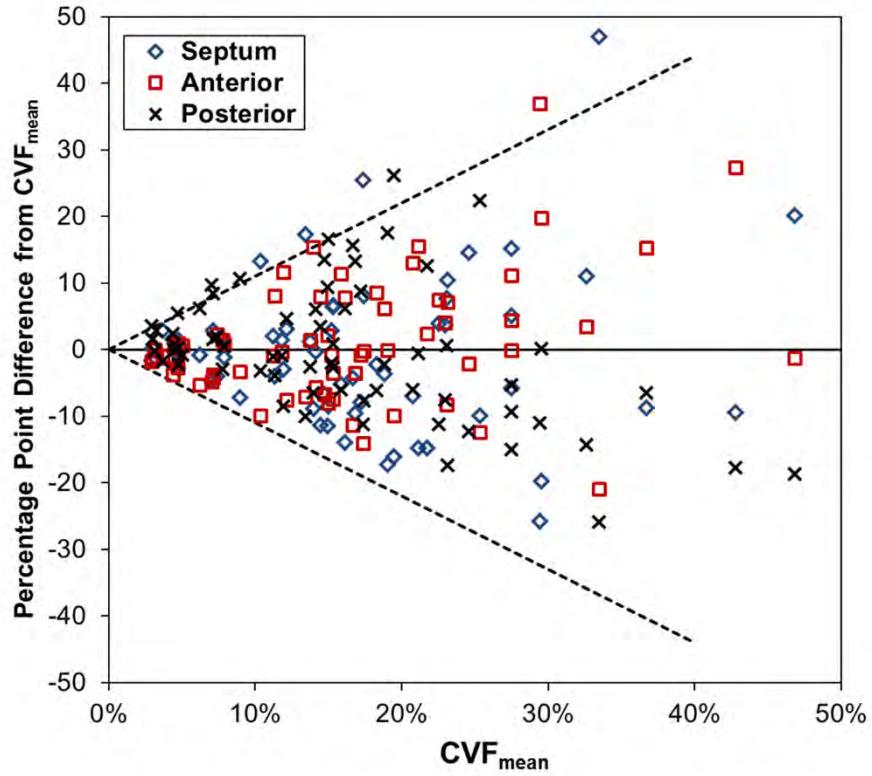
An inverse correlation is present between MLHFQ and cardiomyocyte CSA ( $R=-0.24$ ,  $P=0.030$ ), whereas each two-fold increase in CVF<sub>mean</sub> resulted in a 37% ( $p=0.034$ ) increase in MLHFQ. Trendlines are as per statistical model in Table 5.5.

**Figure 5.3** Histological specimens from mitral regurgitation patients and controls.

<p>Control 44 ♂</p>	<p>Autopsy myocardial specimen with 8.4% CVF consisting of predominantly perivascular fibrosis with mild interstitial fibrosis.</p> 	
<p>75 ♂ NYHA I, no comorbidities. LVEF 65%, ECV 26.8%</p>	<p>Anterior ventricular free wall biopsy. 70% CVF. Severe interstitial and replacement fibrosis with mild endocardial thickening.</p> 	<p>Posterior ventricular free wall biopsy. 25% CVF. Predominantly interstitial fibrosis with mild endocardial thickening.</p> 
<p>68 ♂, NYHA 2, AF, LVEF 65%, ECV 25.4%</p>	<p>Anterior ventricular free wall biopsy. 15% CVF. Moderate endothelial thickening, perivascular fibrosis and mild diffuse interstitial fibrosis.</p> 	<p>Posterior ventricular biopsy. 24% CVF. Endothelial thickening with certain areas containing prominent interstitial and endocardial fibrosis.</p> 
<p>86 ♂, NYHA 2, paroxysmal AF, LVEF 80%, ECV 29.6%</p>	<p>Ventricular septum biopsy. 16% CVF. Moderate patchy interstitial and replacement fibrosis with prominent lipid infiltration.</p> 	<p>Posterior ventricular biopsy. 12% CVF. Moderate patchy interstitial and replacement fibrosis with no fatty infiltration.</p> 

Sections are stained with Masson Trichrome highlighting fibrous tissue as blue and myocytes as purple-red. Histological fibrosis is patchy with little congruence in fibrosis burden across different biopsy sites. ECV can provide an overall estimation of myocardial status but fails to account for endocardial fibrosis.

**Figure 5.4** Modified Bland-Altman plot of the consistency of CVF by biopsy site.



Only those patients with biopsies at all three sites (N=67) were included in the analysis. For these, the percentage point difference between the CVF at each site and the average CVF across the three sites ( $CVF_{\text{mean}}$ ) was plotted against the  $CVF_{\text{mean}}$ . The broken lines represent the 95% prediction intervals, namely  $\pm 110\%$ . For example, for a patient with  $CVF_{\text{mean}}$  of 20%, the CVF of individual biopsies would be expected to be within the range 0-42%.

#### 5.4.2 Impact of Fibrosis on Ventricular Structure and Function

The extent of histological fibrosis, as quantified by  $CVF_{\text{mean}}$ , was not found to be significantly associated with biventricular volumes, ejection fraction, LV mass, LV longitudinal and circumferential strain, or diastolic function ( $E/e'$ ) (**Table 5.2**). Although CVF did not significantly correlate with systolic or diastolic function, a significant correlation was present between ECV and parameters of both systolic (LVEF, LVESVi, GCS, GLS) and diastolic ( $E/e'$ ) function, as well as NTproBNP (**Figure 5.5**). However, there were no significant association between CVF or ECV and MR severity (**Table 5.2**).

LGE was present in 34 (33%) out of 103 patients who received gadolinium-based contrast agent, and was identified in the basal inferolateral LV segment, as well as the papillary muscles (median LGE 0.98g [0.33-2.47]). LGE quantification was not significantly associated with either the MLHFQ score ( $\rho=0.030$ ,  $p=0.764$ ) or ECV ( $\rho=0.06$ ,  $p=0.568$ ). Patients with LGE were characterised by more severe MR ( $74.6\pm 32\text{ml}$  vs.  $57.5\pm 27.8\text{ml}$ ,  $P=0.006$ ) and diastolic dysfunction ( $E/e'$  median: 9.7 [IQR: 7.6-13.8] vs. 7.9 [6.2-10.6],  $p=0.018$ ); there was no significant difference in measures of LV systolic function according to LGE status.

Fibrosis on biopsy ( $CVF_{\text{mean}}$ ) was not found to be significantly correlated with ECV ( $\rho=0.18$ ,  $P=0.101$ , **Figure 5.6**), native T1 ( $\rho=0.04$ ,  $P=0.714$ ), or the amount of LGE ( $\rho=-0.09$ ,  $P=0.402$ ).

In view of more recent reports suggesting that patients with BD may have a different tissue response to MR than those with fibro-elastic deficiency, a sub-group analysis was performed in these patients. BD patients possessed higher degrees of histological fibrosis

compared to FED patients (CVF<sub>mean</sub> 15.4% [12.1-25.3] vs. 14.0% [5.5-19.1], P=0.071; CVF<sub>max</sub> 28.0% [16.7-42.8] vs. 20.2% [7.5-29.4], P=0.009), despite having similar biventricular volumes, ejection fraction, LVMi and MR severity; there was no evidence of a significant difference in ECV or incidence of LGE according to sub-type of primary MR (Table 5.3).



**Table 5.2** Correlation of histological fibrosis against non-invasive preoperative imaging parameters.

	Correlation with $CVF_{\text{mean}}$			Correlation with ECV		
	<i>N</i>	<i>Rho</i>	<i>P</i>	<i>N</i>	<i>Rho</i>	<i>P</i>
NTproBNP	84	0.35	<b>0.001</b>	99	0.54	<b>&lt;0.001</b>
Echocardiography E/e'	72	0.09	0.460	87	0.25	<b>0.022</b>
sPAP (mmHg)	71	0.14	0.232	82	0.14	0.209
Degeneration Subtype (Barlow's)*	77	0.21	0.070	91	0.13	0.208
LVEF (%)	86	-0.15	0.178	101	-0.22	<b>0.029</b>
GCS (%)	84	0.14	0.221	99	0.31	<b>0.002</b>
GLS (%)	84	0.12	0.271	99	0.29	<b>0.003</b>
LVESVi (ml/m <sup>2</sup> )	86	0.07	0.541	101	0.22	<b>0.025</b>
LVMi (g/m <sup>2</sup> )	86	-0.12	0.261	101	-0.05	0.640
RVEF (%)	86	-0.06	0.579	101	-0.14	0.170
RV E <sub>II</sub>	86	0.09	0.411	101	0.30	<b>0.003</b>
RVESVi (ml/m <sup>2</sup> )	86	-0.10	0.381	101	0.21	<b>0.037</b>
MR volume (ml)	86	0.04	0.714	101	-0.07	0.471
MR fraction (%)	86	0.16	0.147	101	0.02	0.868
ECV (%)	83	0.18	0.101	-	-	-
Native T1 (ms)	85	0.04	0.714	101	0.62	<b>&lt;0.001</b>
LGE Presence*	84	-0.07	0.514	101	0.06	0.535

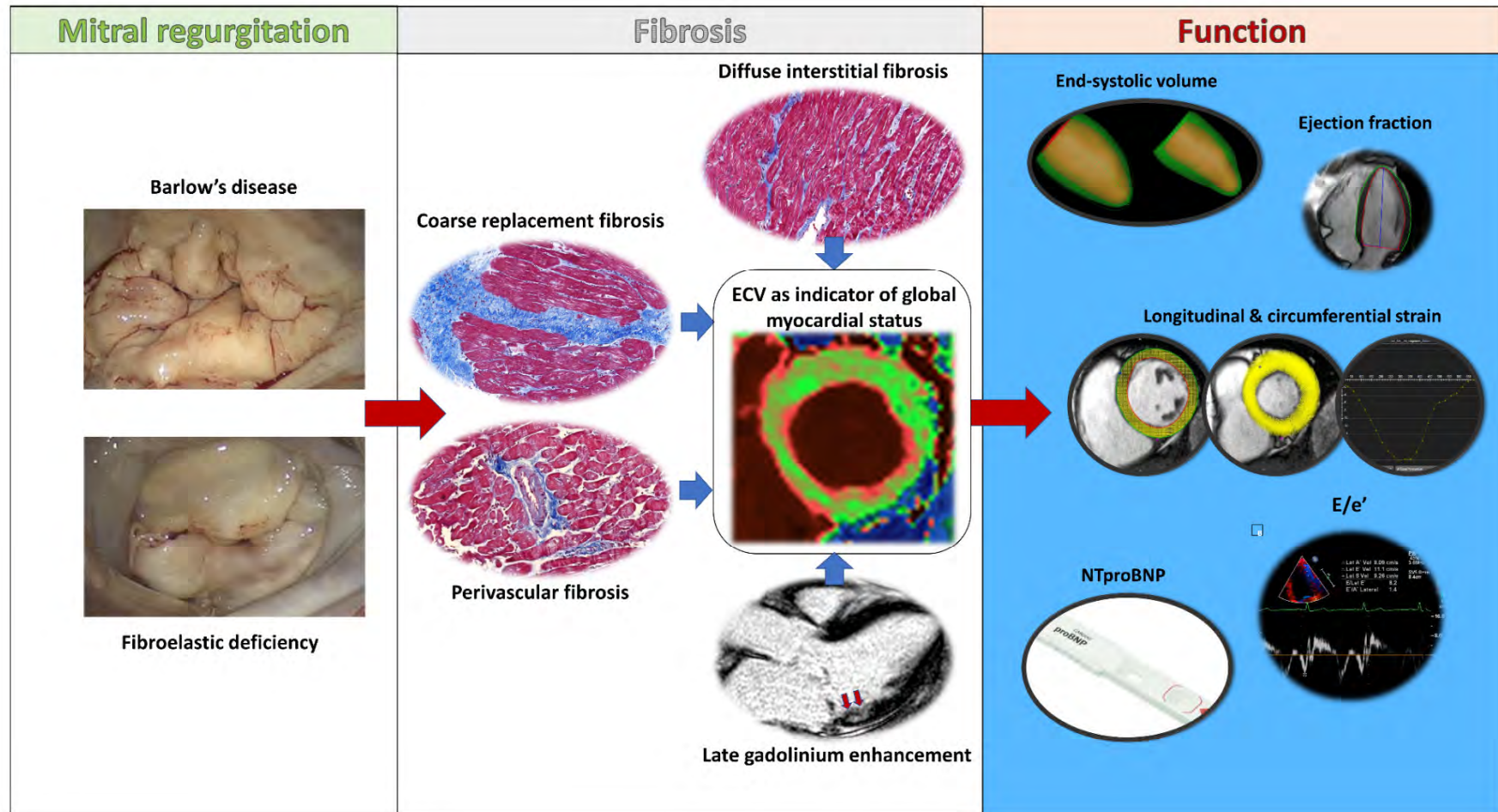
Results are from Spearman's (*Rho*) correlation coefficients. Bold *p*-values are significant at  $p < 0.05$ . \*Dichotomous variables

**Table 5.3** Cardiac magnetic resonance parameters according to the sub-type of MR.

	Fibroelastic deficiency	Barlow's disease	P
	N=59	N=35	
LVESVi (ml/m <sup>2</sup> )	33.4±11.3	32.8±13.6	0.833
LVEF (%)	68.2±8.6	69.3±8.0	0.554
LVMi (g/m <sup>2</sup> )	71.4±12.9	67.8±13.8	0.213
RVESVi (ml/m <sup>2</sup> )	30.7±9.7	33.0±10.5	0.294
RVEF (%)	57.0±9.0	55.1±8.0	0.316
Aortic forward flow (ml)	73.9±22.2	68.0±17.4	0.182
MR volume (ml)	65.5±31.6	65.3±29.6	0.975
MR fraction (%)	45.9±15.2	47.5±14.2	0.614
LGE presence (n,%)	21 (37%)	11 (31%)	0.597
ECV (%)	27.0±3.4	27.8±3.1	0.276
Native T1 (ms)	981.2±23.0	991.6±25.4	<b>0.045</b>

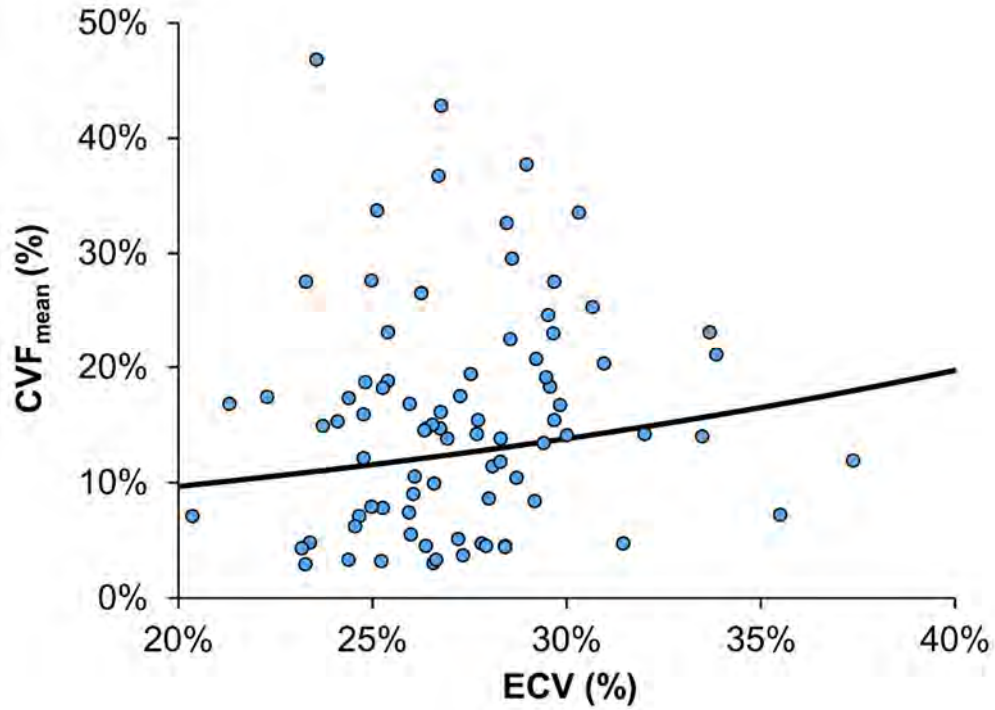
Data are reported as mean±SD, with p-values from independent samples t-tests, or as N (%), with p-values from chi<sup>2</sup>-tests, as applicable. Bold p-values are significant at p<0.05.

**Figure 5.5** Impact of myocardial fibrosis in primary degenerative mitral regurgitation.



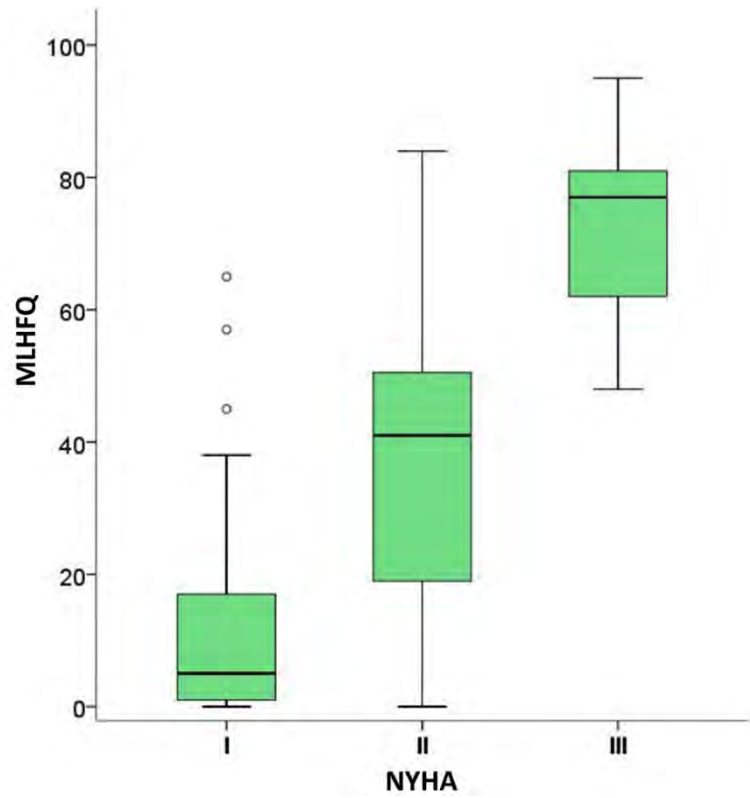
Primary MR of different aetiology induces myocardial fibrosis. Fibrosis, whether diffuse or coarse, can be quantified with CMR derived ECV. ECV, in turn, is associated with multiple markers of systolic and diastolic dysfunction.

**Figure 5.6** Relationship between ECV and histological evidence of interstitial fibrosis on biopsy ( $CVF_{\text{mean}}$ ).



The trendline is based on a regression model, with ECV as the independent variable, and  $\text{Log}_2 CVF_{\text{mean}}$  as the independent variable. This relationship was not found to be statistically significant ( $\text{Rho}=0.18$ ,  $P=0.101$ ).

**Figure 5.7.** Box plot illustrating the distribution of patient symptoms according to NYHA class.



A wide range of symptom scores is present in each NYHA class, with significant degrees of overlap across different classes.

### 5.4.3 Clinical Impact of Fibrosis on Symptoms and Exercise Capacity

Symptom burden was quantified using two difference approaches, namely NYHA

classification and MLHFQ scoring. In total, N=65/31/8 surgical patients were classified as NYHA class I/II/III, respectively, whilst the median MLHFQ score was 13 [IQR: 4-41].

Although there was a significant stepwise increase in MLHFQ scoring with increasing NYHA class ( $\rho=0.66$ ,  $P<0.001$ ), considerable variability in MLHFQ scores was present within each class, with a range of 0-65 observed in NYHA class I (**Figure 5.7**). As such, the MLHFQ scoring was used in preference to NYHA classification for statistical analyses, as this also had the benefit of greater granularity. However, the analysis was also repeated using NYHA, with the results reported in **Table 5.4**.

Exploration of potential parameters which may affect symptom burden, as quantified by MLHFQ, is reported in **Table 5.5**. Histological fibrosis predicted symptom burden (**Figure 5.2B**), with each two-fold increase in  $CVF_{\text{mean}}$  resulting in a 37% ( $p=0.034$ ) increase in MLHFQ scoring; meanwhile, no significant relationship was present for ECV ( $p=0.058$ ) or LGE ( $p=0.357$ ). Increasing symptom burden was significantly associated with the presence of AF, diastolic function, sPAP, and a reduction in CMR-derived indexed LV mass ( $LVM_i$ ;  $R=-0.28$ ,  $P=0.005$ ) as well as histologically quantified cellular hypertrophy ( $R=-0.24$ ,  $P=0.030$ ) (**Figure 5.2A**).

All surgical patients underwent cardiorespiratory symptom-limited CPET; 4 were excluded from analyses for substantial sub-maximal exercise, due to non-cardiorespiratory causes (severe osteoarthritis and anxiety). Although the two parameters were not interchangeable, a significant correlation was present between percentage predicted  $VO_2$  ( $\%PredVO_{2\text{max}}$ ) and symptom burden (**Table 5.6**). In those who exercised, the mean peak

VO<sub>2</sub> was 23.2±7.4ml/kg/min, giving a %PredVO<sub>2</sub>max of 92.9±20.5%, at an age-predicted heart rate of 99.0±14.8%; VE/VCO<sub>2</sub> was 32.9±6.9. On linear regression, formally tested exercise capacity quantified as %PredVO<sub>2</sub> was significantly associated with ECV, markers of biventricular systolic function, E/e', the presence of AF, and sPAP, but not with CVF (**Table 5.5**).

#### 5.4.4 Fibrosis and Biomarkers

The ability of serum biomarkers to reflect histological myocardial fibrosis was studied; NTproBNP showed the strongest correlation against CVF<sub>mean</sub> (rho=0.29, P=0.007) and ECV (rho=0.54, P<0.001); remaining significant even when restricting analyses to NYHA class I patients. Type III procollagen peptide (P3NP) showed weaker correlation with ECV (rho=0.24, P=0.017), whilst type I procollagen peptide (P1NP) was not found to be significantly associated with either CVF or ECV (**Table 5.7**).

**Table 5.4** Baseline characteristics of surgical patients according to symptom status.

	N	NYHA I	NYHA II-III	P-Value
<b><i>Clinical characteristics</i></b>				
Age (years)	104	62±14	64±12	0.428
Male sex	104	50 (77%)	26 (67%)	0.254
BMI (kg/m <sup>2</sup> )	104	25±4	27±5	0.065
Treated hypertension	104	20 (31%)	12 (31%)	1.000
eGFR (ml/min/1.73m <sup>2</sup> )	104	75 (65–84)	72 (60–82)	0.401
Atrial fibrillation	104			<b>0.008</b>
<i>None</i>		53 (82%)	21 (54%)	
<i>Paroxysmal</i>		2 (3%)	5 (13%)	
<i>Permanent</i>		10 (15%)	13 (33%)	
Degeneration subtype	104			0.076
<i>Barlow's</i>		24 (37%)	11 (28%)	
<i>Indeterminant</i>		3 (5%)	7 (18%)	
<i>Fibroelastic deficiency</i>		38 (58%)	21 (54%)	
MLHFQ score	103	5 (1-17)	43 (30-57)	<b>&lt;0.001</b>
%PredVO <sub>2</sub> max (%)	103	99±20	79±22	<b>&lt;0.001</b>
Resting sPAP (mmHg)	85	33±10	38±20	0.071
Ventricular ectopy burden (%)	54	0.1 (0.0–1.0)	0.5 (0.0-1.4)	0.356
<b><i>Cardiac magnetic resonance characteristics</i></b>				
LVESVi (ml/m <sup>2</sup> )	104	32.5±12.5	34.8±10.9	0.342
LVEF (%)	104	69.5±7.9	66.4±8.6	0.065
GCS (%)	102	-18.2±3.0	-16.6±3.5	<b>0.017</b>
GLS (%)	102	-15.9±2.7	-14.8±3.3	0.099
LVMi (g/m <sup>2</sup> )	104	71.4±13.0	66.0±13.2	<b>0.045</b>
RVESVi (ml/m <sup>2</sup> )	104	31.0±8.8	32.5±12.6	0.474
RVEF (%)	104	57.3±8.1	54.5±9.6	0.122
RV E <sub>II</sub>	104	-21.6±4.5	-21.4±5.0	0.811
MR volume (ml)	104	62.0±26.9	67.2±35.9	0.410
MR fraction (%)	104	44.3±11.8	48.9±18.6	0.121
ECV (%)	101	26.8±3.1	28.2±3.3	<b>0.045</b>
Native T1 (ms)	103	981.4±23.9	991.2±25.8	0.054
LGE presence (n,%)	102	22 (34%)	12 (32%)	0.830

Data are reported as N (%), with p-values from  $\chi^2$  tests; median (interquartile range), with p-values from Mann-Whitney U tests; or as mean±SD, with p-values from independent samples t-tests, as applicable. Bold p-values are significant at  $p < 0.05$ .



**Table 5.5** Linear regression analyses of symptom burden against histology, cardiac imaging and pulmonary pressures.

	Relationship with MLHFQ				Relationship with %PredVO2max			
	<i>N</i>	<i>R</i>	Coefficient (95% CI)	<i>P</i> -Value	<i>N</i>	<i>R</i>	Coefficient (95% CI)	<i>P</i> -Value
Age (per year)	103	-0.08	-0.8% (-2.8%, 1.3%)	0.442	100	0.05	0.08 (-0.22, 0.38)	0.598
Gender (Female)**	103	0.19	79.6% (-2.8%, 231.8%)	0.061	100	-0.01	-0.31 (-9.43, 8.80)	0.946
BMI (kg/m <sup>2</sup> )	103	0.21	6.9% (0.7%, 13.6%)	<b>0.030</b>	100	-0.01	-0.03 (-1.01, 0.95)	0.945
Treated hypertension (Yes)**	103	0.05	15.9% (-35.9%, 109.7%)	0.623	100	0.04	1.75 (-7.09, 10.59)	0.695
Permanent AF (Yes)**	103	0.21	100.5% (5.2%, 282.1%)	<b>0.035</b>	100	-0.32	-15.60 (-24.97, -6.23)	<b>0.001</b>
Log <sub>2</sub> CVFmean (%)*	86	0.23	37.0% (2.5%, 83.3%)	<b>0.034</b>	83	-0.18	-3.82 (-8.45, 0.82)	0.105
Log <sub>2</sub> CVFmax (%)*	86	0.19	26.0% (-3.1%, 63.8%)	0.084	83	-0.11	-2.20 (-6.42, 2.03)	0.304
Cardiomyocyte CSA (um <sup>2</sup> )	85	-0.24	-0.1% (-0.3%, 0.0%)	<b>0.030</b>	83	0.13	0.01 (-0.01, 0.03)	0.245
Echocardiography E/e'	88	0.22	7.5% (0.5%, 15.0%)	<b>0.036</b>	87	-0.36	-1.60 (-2.49, -0.70)	<b>0.001</b>
sPAP (mmHg)	84	0.24	2.4% (0.3%, 4.5%)	<b>0.026</b>	81	-0.28	-0.43 (-0.76, -0.10)	<b>0.012</b>
Degeneration Subtype (Barlow's)**	93	-0.06	-16.7% (-54.0%, 50.6%)	0.541	91	0.02	0.77 (-8.18, 9.72)	0.865
LVEF (%)	103	-0.03	-0.6% (-3.9%, 2.8%)	0.728	100	0.23	0.57 (0.09, 1.05)	<b>0.021</b>
GCS (%)	101	0.10	4.5% (-4.0%, 13.9%)	0.305	98	-0.26	-1.64 (-2.87, -0.42)	<b>0.009</b>
GLS (%)	101	0.00	0.2% (-8.7%, 10.0%)	0.965	98	-0.32	-2.19 (-3.50, -0.87)	<b>0.001</b>
LVESVi (ml/m <sup>2</sup> )	103	-0.02	-0.3% (-2.6%, 2.0%)	0.805	100	-0.20	-0.34 (-0.67, -0.01)	<b>0.045</b>
LVMi (g/m <sup>2</sup> )	103	-0.28	-2.9% (-4.9%, -0.9%)	<b>0.005</b>	100	0.03	0.05 (-0.26, 0.36)	0.739
RVEF (%)	103	-0.07	-1.1% (-4.2%, 2.0%)	0.466	100	0.41	0.96 (0.54, 1.39)	<b>&lt;0.001</b>
RV E <sub>II</sub>	103	0.06	1.8% (-4.0%, 8.0%)	0.548	100	-0.20	-0.84 (-1.69, 0.01)	0.051
RVESVi (ml/m <sup>2</sup> )	103	0.00	0.0% (-2.6%, 2.7%)	0.994	100	-0.23	-0.44 (-0.83, -0.06)	<b>0.024</b>
MR volume (ml)	103	0.06	0.3% (-0.6%, 1.2%)	0.540	100	-0.19	-0.13 (-0.26, 0.00)	0.057
MR fraction (%)	103	0.11	1.1% (-0.8%, 3.0%)	0.253	100	-0.40	-0.55 (-0.80, -0.30)	<b>&lt;0.001</b>
ECV (%)	100	0.19	8.9% (-0.3%, 19.0%)	0.058	98	-0.22	-1.37 (-2.60, -0.13)	<b>0.030</b>
Native T1 (ms)	102	0.07	0.4% (-0.8%, 1.5%)	0.508	100	-0.07	-0.06 (-0.22, 0.10)	0.471
LGE Presence (Yes)**	101	0.09	31.1% (-26.6%, 134.2%)	0.357	99	0.01	0.33 (-8.42, 9.08)	0.941

Results are from Pearson's (*R*) correlation coefficients and univariable regression models, with LnMLHFQ or %PredVO2max as the dependent variable. For LnMLHFQ, the resulting coefficients were then antilogged, and converted to percentage increases associated with a one unit increase in the factor. *P*-values <0.05 have been highlighted in bold. CSA=cross-sectional area. \*Factors were log<sub>2</sub>-transformed to improve model fit, hence coefficients are relative to a two-fold increase in the factor. \*\*Factors are dichotomous; hence the coefficient represents the difference in the outcome between the stated category and the reference category.

**Table 5.6** Spearman's correlation between NYHA class, MLHFQ and %PredVO2max.

	<b>MLHFQ</b>	<b>%PredVO2max</b>
<b>NYHA</b>	N= 103, Rho = 0.66, <b>P&lt;0.001</b>	N=103, Rho = -0.42, <b>P&lt;0.001</b>
<b>MLHFQ</b>	-	N=102, Rho = -0.50, <b>P&lt;0.001</b>

*Results are from Spearman's (rho) correlation coefficients; bold p-values are significant at  $p < 0.05$*

**Table 5.7** Correlation of serum biomarkers against histological and imaging measures of myocardial fibrosis.

	Average	CVF <sub>mean</sub> (%)			ECV (%)			LGE (g)		
		<i>N</i>	<i>Rho</i>	<i>p-Value</i>	<i>N</i>	<i>Rho</i>	<i>p-Value</i>	<i>N</i>	<i>Rho</i>	<i>p-Value</i>
NTproBNP (µg/mL)	233 (110, 567)	84	0.29	<b>0.007</b>	99	0.54	<b>&lt;0.001</b>	100	0.16	0.115
P1NP (ng/mL)	57±21	85	0.08	0.462	100	0.03	0.751	101	0.10	0.342
P3NP (ng/mL)	3.8±1.4	85	0.19	0.087	100	0.24	<b>0.017</b>	101	-0.01	0.923

*Averages are reported as median (interquartile range) or mean±SD, as applicable. Correlation analyses were performed using Spearman's (Rho) correlation coefficients, and bold p-values are significant at p<0.05*

## 5.5 Discussion

This is the most comprehensive study to characterise myocardial changes in patients with chronic primary severe MR, combining CMR based assessment of structural changes with detailed invasive histological profiling, for the identification of functional correlates. Our work provides definitive histological evidence for the presence of myocardial fibrosis, even in asymptomatic MR patients with normal range CMR volumetric parameters and good exercise capacity. We noted complex morphology and topography of fibrosis with three main patterns: thickened endocardium with increased fibrosis in biopsies containing subendocardium; cellular hypertrophy and increased fibrosis compared to controls; and a variable degree of fat infiltration. Despite the increase in fibrosis compared to control subjects without MR, the extent of fibrosis on myocardial biopsy at the time of surgery was not related to LV or RV volume, mass, EF, global longitudinal strain, diastolic function or MR severity on CMR. Biopsy and CMR offered complementary information however because patterns of fibrosis proved variable, and CMR-derived ECV and LGE were not able to capture the subendocardial changes highlighted on histology. Hence, while the extent of fibrosis on myocardial biopsy was related to symptoms but was not related to LV function, non-invasive tissue characterisation with ECV was associated with changes in both systolic and diastolic function.

Fibrosis quantified by ECV is of consequential importance across the spectrum of LVEF in heart failure patients (141). Specifically for asymptomatic severe MR, it can independently predict patients' subsequent decompensation (249). Our study data provide mechanistic insight into this phenomenon with ECV expansion correlating positively with LVESVi, RVESVi, NTproBNP,  $E/e'$ , and negatively with LVEF, GCS, GLS and RV EII.

The range of ECV observed within our surgical cohort ( $27.3\pm 3.2\%$ ) is only mildly raised compared to the mean ECV of 25.9% (95% CI 25.5% – 26.3%) within a recent pooled analysis of 3872 participants (250), and is lower than the median of 28.1% reported within a consecutive series of 1172 clinically indicated CMRs (141). This suggests that the burden of fibrosis quantified on ECV is relatively low for the general cardiology setting. The narrower range of global fibrosis quantified by ECV may have weakened our ability to detect correlations, where a broader range always favours the likelihood of obtaining significant results.

Our histology findings are inconsistent with an early autopsy study that quantified interstitial tissue and myocardial fibre hypertrophy in 4 groups of patients: 1) 22 normal hearts, 2) 20 hearts from patients with MR (NYHA class II-III) who died early after mitral valve replacement from causes other than cardiac failure, 3) 22 hearts from patients with MR (NYHA class III-IV) who died early after mitral valve replacement from cardiac failure with low cardiac output syndrome, and 4) 22 hearts from patients with hypertensive heart disease (NYHA class II-III). In this whole heart study, the expansion of the interstitial space was similar in NYHA II-III patients compared to normal hearts, whereas NYHA III-IV patients possessed significantly larger interstitial spacing (118). Conversely, multiple groups have reported the presence of more extensive myocardial fibrosis in MVP patients who were studied at autopsy following malignant arrhythmias (41, 243, 246). In these latter cases, the severity of MR was frequently mild or moderate, and the patients were asymptomatic. Our study also did not show a relationship between fibrosis on histology, or with fibrosis measured indirectly by T1 mapping or ECV. It is thought that mechanical stress as a result of volume overload is the major driver of fibrogenesis in MR,

which stimulates the differentiation of latent proto-myofibroblasts, induces cardiomyocyte hypertrophy and fibrogenesis (93). However, this process is likely mediated by additional factors. For example, in BD, MAD and papillary muscle traction have been proposed as independent sources of mechanical stress (244, 251). Furthermore, disease duration is likely to be a key factor, which remains difficult to quantify, yet may contribute to the lack of association between MR severity and fibrosis in our study.

Despite evidence that high native T1, elevated ECV, and LGE measure diffuse interstitial fibrosis and replacement fibrosis in other diseases, we found no correlation between CVF and CMR measures of fibrosis (140, 252, 253). This is consistent with surgical data in aortic stenosis, which also failed to correlate non-invasive CMR data with myocardial biopsy, even when performed during surgery at multiple sites (84). There are several potential reasons for this. Firstly, similar to previous reports (242), LGE was found in 34% cases of primary MR, but the most common location was in the basal inferolateral LV wall and associated papillary muscles. Although the inferolateral wall was one of the three pre-specified targets to be biopsied, the focal nature of the fibrosis means this could have been missed – this situation is best exemplified by the low sensitivity of myocardial biopsy in the diagnoses of cardiac sarcoidosis (254). Additionally, the low ICC of CVF from multiple biopsy sites within the same heart confirmed that histological fibrosis was patchy, further contributing to the lack of consistency between ECV and CVF; this observation is reminiscent of the large coefficient of variation of 43% reported for interstitial fibrosis (but only 3% for cardiomyocyte CSA) in dilated cardiomyopathy (255). This may also help to explain why ECV – a measure of global myocardial status, correlated with CMR measures of biventricular systolic function and echo derived E/e, highlighting the potential value of

ECV as a marker of LV remodelling in MR. Finally, avoidance of the endocardium during quantification of ECV to prevent blood pool contamination may also contribute to the discordant results with histology (84). However, ECV in itself has limitations including cross over of ranges between health and disease (250), practical limitations of movement with respiration, and further research is needed on whether ECV offers incremental prognostic value over traditional cardiac biomarkers.

### 5.5.1 Limitations

This study was observational and therefore no causation can be inferred. Patients opting for surgery were significantly younger than those opting for conservative therapy. This selection bias means that results are only applicable to patients undergoing surgery, and so may not be generalizable to the population as a whole. Although pre-specified, invasive myocardial biopsy was not performed in all patients with symptomatic and asymptomatic MR who went forward to surgery due to technical difficulties. Despite this, we provide the largest histologic characterisation of patients with severe primary MR, with comprehensive characterisation of symptoms by validated questionnaires and CPET. Secondly, invasive measurement of pulmonary artery pressures was performed at the clinician's discretion and was not a requirement of this study. Although assessment by echocardiography was performed, there were cases inevitably without enough tricuspid regurgitation for sPAP to be measured. Finally, we recognise that E/e' may be less reliable as a measure of diastolic dysfunction in severe MR, however other parameters such as deceleration time of the early mitral inflow are similarly affected by heart rate dependence.

### 5.5.2 Conclusions

Histological evidence of diffuse interstitial and replacement myocardial fibrosis, along with concomitant cardiomyocyte hypertrophy is present in asymptomatic MR, in the presence of normal LV volume and ejection fraction. Fibrosis is patchy and highly variable within the heart, which may contribute to the lack of correlation with T1 mapping, ECV and LGE. ECV, as a marker of global myocardial status, correlated well with multiple measures of systolic and diastolic function in MR. Further studies are warranted to investigate whether latent fibrosis detected using T1, ECV or LGE offer incremental value in predicting outcome in asymptomatic patients with severe primary MR.



## CHAPTER 6

### PREOPERATIVE PREDICTORS OF PERI-OPERATIVE SURGICAL OUTCOMES

#### 6.1 Introduction

Early surgical outcomes are determined by 1) surgery type – whether repair or replacement, 2) complexity of the lesion, 3) experience of the surgeon and the heart valve team, and 4) the preoperative status of the patient (55).

Valvular repair is associated with lower operative mortality compared to replacement and avoids prosthetic valve-specific complications such as thromboembolism, anticoagulation-related haemorrhage, endocarditis and structural valve degeneration (56-60, 238).

Advanced myxomatous degeneration of the valve has been linked with increased MR recurrence and overall mortality (256, 257). Finally, the probability of a successful repair and postoperative complication rates are improved if surgery is performed within a specialised Heart Valve Centre, by a specialised mitral surgeon; this leads to the development of strict definitions for a ‘Centre of Excellence in Mitral Valve Repair’ (258, 259).

The stepwise inclusion of the above recommendations within successive European and American guidelines is partly responsible for the observed improvement in patient outcomes over the past decades (24, 25). However, the identification and validation of prognostic biomarkers that can provide insight into the preoperative status of patients and aid in the optimisation of surgical timing, represents one of the remaining challenges facing patients and clinicians (188).

The onset of preoperative symptoms is a class I surgical indication, and is widely associated with an increased incidence of postoperative low cardiac output states, longer intensive care stays and increased operative mortality (4, 64, 145). However, there are limited data on the prognostic significance of other preoperative biomarkers.

Early studies have found that the other class I (LVEF and LVESd) and class II (presence of AF) guideline indications for surgery do not confer any postoperative prognostic value (64, 145). However, it remains unclear whether the lack of association between systolic dysfunction and postoperative outcomes is simply a reflection of the reliance upon 2D echocardiography rather than 3D CMR imaging (29), or the delayed response of LVEF and LVESd in the “double outlet” state of MR (260). Support for the latter hypothesis arises from reports where sub-clinical LV dysfunction was detected via echocardiographic GLS and this offered incremental prognostic value for the prediction of postoperative mortality and prolonged inotropic dependency in both primary and secondary MR (261, 262).

As discussed in Chapter 3, the reduction in GLS is felt to reflect myocardial fibrosis across a range of cardiac pathologies (199-201); we have also demonstrated in Chapter 5 that a significant myocardial fibrosis burden is present even in asymptomatic MR patients, with fibrosis burden correlating with symptom burden. This creates a great deal of interest in exploring the operative prognostic implications of myocardial fibrosis in MR.

## 6.2 Aims and hypotheses

We hypothesised that adverse ventricular remodelling in the form of increasing myocardial fibrosis would be associated with more frequent low cardiac output states in the peri-

operative period. Increased burden of fibrosis would be associated with reduced myocardial contractility, leading to increased peri-operative inotrope dependency, worse renal function, longer intensive care unit stay (ICU LoS), and would cause patients to be more susceptible to cardiovascular complications.

This chapter aimed to:

- 1) Quantify the peri-operative and short-term ( $\leq 30$  day) postoperative complication rates within our three Heart Valve Centres of Excellence to facilitate comparison with National outcomes.
- 2) Explore the relationship between patients' preoperative status and operative outcomes, with particular focus on the significance of myocardial fibrosis burden.

The primary endpoints for this study included the duration of inotropic support, requirement for renal replacement therapy, length of intensive care unit stay (ITU LoS), and cardiovascular complication rate. These parameters were selected as they are likely to be influenced by low cardiac output states and are the commonly utilised markers of peri-operative outcome amongst surgical trials (263).

### 6.3 Methods

This chapter utilises the surgical cohort of the Mitral FINDER study, a prospective multicentre observational study on patients with primary degenerative mitral regurgitation. Detailed patient recruitment and data collection methodology have been described in Chapter 2. All patients received comprehensive preoperative characterisation with multi-parametric CMR and CPET.

Cardiovascular complications were defined as myocardial infarction, decompensated heart failure, significant arrhythmia, significant pericardial effusion or tamponade requiring drainage, and stroke (264, 265). Operative mortality was defined as death within 30 days or during the same hospitalisation. Acute kidney injury (AKI) was defined as a 1.5-fold increase in baseline creatinine (266).

Surgical and postoperative complications were collected from patients' paper, electronic and discharge summary records. Clinical letters were screened for complications arising after hospital discharge, but within 30 days of the surgery date. Surgical findings, operative duration and complications were extracted from surgical and perfusionist notes. The type and duration of inotropic and mechanical organ support requirements were gathered from ICU notes. Laboratory test results and weight measurements were obtained from clinical reporting and observation charting systems.

Postoperative inpatient TTE protocols varied based on surgical site and patient requirements. When available, data including postoperative biventricular function, MR severity and early outpatient complications were recorded. For this chapter, only inpatient and early outpatient complications ( $\leq 30$  days from date of surgery) were included.

### 6.3.1 Statistical analyses

Overall statistical principles have been described in Section 2.5. For this Chapter, log transformation for NTproBNP, length of stay in the intensive care unit (ITU) and hospital were performed to allow parametric statistical testing. The Benjamini–Hochberg procedure was used to correct for multiple testing.

### 6.3.2 Missing data

As this was an observational study, not all patients possessed sufficient clinical indications to undergo a right heart catheterisation study for the invasive measurement of sPAP. In those without right heart catheterisation, estimated sPAP was utilised where available, however, this was not feasible for patients without tricuspid regurgitation. Under these circumstances, sub-cohort analyses were performed utilising the data available.

## 6.4 Results

### 6.4.1 Baseline clinical data

To summarise the baseline clinical data, 105 patients underwent mitral valve surgery.

There were no significant differences in age or gender across symptom categories (**Table 6.1**). Symptomatic patients scored worse than asymptomatic patients across both physical and emotional dimensions of PROM scoring.

Symptomatic patients possessed lower LVMI, higher ECV, higher pre-contrast T1 and lower post-contrast T1. The severity of MR, biventricular volumes and ejection fraction were similar between symptomatic and asymptomatic cohorts. Of note, GCS was the only quantifier of systolic function to demonstrate a significant difference between symptomatic and asymptomatic patients across our cohorts (**Table 6.1**). On serum biomarker analyses, the presence of symptoms was associated with higher NTproBNP, P3NP and interleukin 1 $\beta$  concentrations.

All patients underwent symptom-limited CPET. Asymptomatic patients achieved higher %PredVO<sub>2</sub> peak compared to symptomatic patients with more efficient ventilatory efficiency (VE/VCO<sub>2</sub>).

**Table 6.1** Comparison of clinical parameters between asymptomatic and symptomatic surgical patients.

	Asymptomatic N=65	Symptomatic N=40	P
<b>Demographics</b>			
Age (years)	62±14	64±12	0.398
Male gender (n, %)	50, 77%	27, 68%	0.289
BMI kg/m <sup>2</sup>	24.9±4.2	26.6±4.8	0.065
Permanent AF (n, %)	2, 3%	5, 13%	<b>0.036</b>
Diabetes mellitus (n, %)	2, 3%	0, 0%	0.524
Treated hypertension (n, %)	20, 31%	13, 33%	0.854
Current smoker (n, %)	3, 5%	2, 5%	1.000
<b>Functional testing</b>			
%PredVO <sub>2</sub> max (%)	98.6±19.8	79.4±21.3	<b>&lt;0.001</b>
VE/VCO <sub>2</sub>	31.2±5.4	35.4±7.7	<b>0.002</b>
Resting sPAP (mmHg)	33±10	38±20	0.071
<b>RAND symptom score</b>			
Physical functioning	90 (65-95)	40 (20-63)	<b>&lt;0.001</b>
Role limitations due to physical health	100 (50-100)	0 (0-50)	<b>&lt;0.001</b>
Role limitation due to emotional problems	100 (100-100)	67 (0-100)	<b>&lt;0.001</b>
Energy / fatigue	65 (55-80)	38 (20-53)	<b>&lt;0.001</b>
Emotional well-being	84 (64-92)	68 (52-84)	<b>&lt;0.001</b>
Social function	88 (75-100)	50 (25-81)	<b>&lt;0.001</b>
Pain	90 (78-100)	78 (40-90)	<b>&lt;0.001</b>
General health	70 (60-80)	50 (35-63)	<b>&lt;0.001</b>
<b>MLHFQ symptom score</b>			
Physical dimension score	2 (0-8)	23 (15-30)	<b>&lt;0.001</b>
Emotional dimension score	2 (0-4)	10 (5-15)	<b>&lt;0.001</b>
Total score	5 (1-17)	42 (25-55)	<b>&lt;0.001</b>
<b>Serum results</b>			
Haemoglobin (g/L)	139±12	131±16	<b>0.007</b>
eGFR	76±14	74±15	0.673
NTproBNP	186 (76-474)	373 (195-998)	<b>0.006</b>
PINP µg/L	56±20	58±22	0.721

P3NP $\mu\text{g/L}$	3.5 $\pm$ 1.0	4.5 $\pm$ 1.7	<b>&lt;0.001</b>
TGF- $\beta$ 1	44.8 $\pm$ 12.4	45.2 $\pm$ 13.0	0.871
Interleukin 1 $\alpha$ pg/ml	0.03 (0.00-2.06)	0.56 (0.04-3.66)	0.064
Interleukin 1 $\beta$ pg/ml	0 (0.00-0.09)	0.07 (0.00-0.38)	<b>0.028</b>
<b>Cardiac magnetic resonance</b>			
LVEF (%)	69.5 $\pm$ 7.9	66.4 $\pm$ 8.5	0.841
LVEDVi (ml/m <sup>2</sup> )	105.0 $\pm$ 22	102.4 $\pm$ 21.4	0.561
LVESVi (ml/m <sup>2</sup> )	32.5 $\pm$ 12.5	34.5 $\pm$ 10.9	0.398
LVEDd (cm)	5.7 $\pm$ 0.6	5.7 $\pm$ 0.7	0.967
LVESd (cm)	3.7 $\pm$ 0.7	3.8 $\pm$ 0.6	0.379
LVMi (g/m <sup>2</sup> )	71.4 $\pm$ 13.0	65.8 $\pm$ 13.1	<b>0.037</b>
AVflow (ml)	75.0 $\pm$ 18.4	64.0 $\pm$ 21.3	<b>0.006</b>
AVflow indexed for BSA (ml/m <sup>2</sup> )	33.3 $\pm$ 10.1	40.0 $\pm$ 8.4	<b>&lt;0.001</b>
RVEF (%)	57.3 $\pm$ 8.1	54.4 $\pm$ 9.5	0.104
RVEDVi (ml/m <sup>2</sup> )	72.1 $\pm$ 13.2	69.1 $\pm$ 17.8	0.317
RVESVi (ml/m <sup>2</sup> )	31.0 $\pm$ 8.8	32.5 $\pm$ 12.4	0.480
MR volume (ml)	62 $\pm$ 27	67 $\pm$ 35	0.433
MR fraction (%)	44 $\pm$ 12	49 $\pm$ 18	0.098
LA volume (ml)	88 $\pm$ 44	95 $\pm$ 46	0.392
LGE			
Presence (N, %)	22 of 64 (34%)	13 of 39 (33%)	0.914
Mass (g)	1.7 $\pm$ 1.5	1.5 $\pm$ 1.4	0.761
ECV (%)	26.9 $\pm$ 3.1	28.2 $\pm$ 3.3	<b>0.045</b>
Pre-contrast T1 relaxivity (ms)	980 $\pm$ 24	991 $\pm$ 26	<b>0.029</b>
T2 relaxivity (ms)	52.98 $\pm$ 2.7	53.9 $\pm$ 4.0	0.174
GCS (s <sup>-1</sup> )	-18.2 $\pm$ 3.0	-16.6 $\pm$ 3.4	<b>0.019</b>
GLS (s <sup>-1</sup> )	-15.9 $\pm$ 2.7	-14.9 $\pm$ 3.3	0.119
RV Ell (s <sup>-1</sup> )	-20.9 $\pm$ 7.5	-21.3 $\pm$ 5.1	0.745

Data are reported as N (%), with p-values from chi<sup>2</sup> or Fisher's exact test as appropriate; median (interquartile range), with p-values from Mann-Whitney U tests; or as mean $\pm$ SD, with p-values from independent samples t-tests, as applicable. P-values represent comparisons between symptomatic and asymptomatic cohorts; values <0.05 are highlighted in bold.



#### 6.4.2 Operative outcomes

There were no operative mortalities. Successful MV repair was achieved in all but one patient who received mechanical valve replacement. 15 patients received concomitant coronary artery bypass graft (CABG) for asymptomatic coronary disease incidentally discovered at the time of preoperative coronary angiography. These CABG cases were included within the main analyses because patients did not suffer from symptomatic coronary disease as determined by the absence of preoperative angina, exercise ECG negative for inducible ischaemia and the absence of infarct pattern LGE on CMR. 16 patients required concomitant tricuspid valve repair and 20 required AF ablation, both with a preponderance for the symptomatic cohort (**Table 6.2**). Two patients required returning to theatre a second time for management of operative complications (excessive bleeding from sternotomy and iatrogenic aortic regurgitation).

For the peri-operative stage, 4 patients experienced intra-operative complications which required immediate intervention. These included 2 cases of intracardiac excessive bleeding, 1 case of air embolus, and 1 case of neo-chord induced tethering of a leaflet. On weaning off cardiopulmonary bypass, the majority of patients possessed no residual MR on peri-operative TOE; none had possessed more than mild MR. 1 patient with FED developed moderate MR on pre-discharge TTE.

ITU charts were not available or incomplete for 6 patients, 3 of whom had surgery at external institutions. From the available data, 71% were extubated on the same day of surgery, 77% required <24hours of inotropic support, and 56% were discharged from ITU within 48 hours. 4 patients required mechanical blood pressure support in the form of

intra-aortic balloon pump (IABP). Whilst 8 patients developed AKI, only 1 required renal replacement therapy. The median hospital stay was 7 [6-10] days.

41 (39%) patients experienced a cardiac rhythm disturbance in the form of new-onset postoperative AF (31), other atrial tachycardia (5), conservatively managed bradycardia/heart block (4) and ventricular tachycardiac (1). Temporary arrhythmic disturbances were not included within cardiovascular complications unless it resulted in a permanent consequence for the patient (such as implantation of a permanent pacemaker).

Cardiovascular complications occurred in 5% of patients and included clinically significant RV failure as diagnosed by their primary physician (2), ischaemic stroke (1), pericardial effusion requiring drainage (1), and complete heart block requiring permanent pacing (1).

Non-cardiovascular complications occurred in 16% of patients and consisted of infections (4), pneumothoraces (5), pleural effusion requiring chest drainage (2), prolonged respiratory weaning (1), excessive bleeding or high drain output (2), gastrointestinal bleeding (1), and prolonged post-op delirium (2).

**Table 6.2** Summary of operative and postoperative parameters in the Mitral FINDER cohort.

	Overall	Asymptomatic	Symptomatic	P
<b>Operative details</b>				
Leaflets repaired (n=101):				
Isolated anterior	11 (11%)	4 (6%)	7 (18%)	0.103
Isolated posterior	54 (54%)	38 (60%)	16 (42%)	0.068
Bileaflet	36 (36%)	21 (33%)	15 (39%)	0.677
Annuloplasty ring models (n=101):				
Edwards Physio II	54	34	20	0.976
LivaNova Memo 3D	25	15	10	
Medtronic CG Future Band	18	12	6	
Other	4	2	2	
Coronary bypass grafting (n=104)	15 (14%)	9 (14%)	6 (15%)	0.889
Tricuspid valve repair (n=104)	18 (17%)	6 (9%)	12 (31%)	<b>0.001</b>
AF ablation (n=104)	21 (21%)	8 (12%)	12 (30%)	0.044
Peri-operative complications (n=104)	4 (4%)	3 (5%)	1 (3%)	1.000
Aortic cross-clamp duration (n=100)	99±36	98±37	102±35	0.774
Cardiopulmonary bypass duration (n=100)	125±45	124±47	127±42	0.619
Inotropic requirement coming off bypass (n=100)	23 (23%)	12 (19%)	11 (29%)	0.269
MR severity on TOE on sternotomy closure (n=83)				
None	67	40	27	0.671
Trivial	11	6	5	
Mild	5	2	3	
<b>Postoperative recovery</b>				
Duration of inotropic support (days) (n=99)	1 (0-1)	1 (0-1)	1 (0-2)	0.614
Intra-aortic balloon pump requirement (n, %) (n=99)	4 (4%)	2 (3%)	2 (5%)	0.642
Time to extubation (days) (n=97)	0 (0-1)	0 (0-1)	0 (0-1)	0.607
ITU length of stay (days) (n=101)	2 (1-3)	2 (1-3)	2 (1-3)	0.471

Acute kidney injury (n, %) (n=101)	8 (8%)	4 (6%)	4 (10%)	0.479
Renal replacement therapy (n, %) (n=102)	1 (1%)	0 (0%)	1 (3%)	0.392
New rhythm disturbance (n, %) (n=104)	42 (42%)	27 (43%)	15 (39%)	0.836
Cardiovascular complication (n, %) (n=104)	5 (5%)	1 (3%)	4 (11%)	0.071
LV impairment on inpatient TTE (n, %) (n=82)	39 (48%)	24 (49%)	15 (15%)	0.827
Change in haemoglobin on discharge (g/L) (n=101)	-40.2±16.4	-42.1±14.6	-37.1±18.7	0.110
Hospital length of stay (days) (n=101)	7 (6-10)	7 (6-9)	7 (6-11)	0.141
Weight change at discharge (kg) (n=82)	-0.4±2.6	-0.4±2.9	0.4±2.3	0.924
Weight change at 6 weeks follow-up (kg) (n=60)	-0.1±3.4	-0.3±3.4	0.1±3.5	0.695

Data are reported as N (%), with p-values from  $\chi^2$  or Fisher's exact test as appropriate; median (interquartile range), with p-values from Mann-Whitney U tests; or as mean±SD, with p-values from independent samples t-tests, as applicable. P-values represent comparisons between symptomatic and asymptomatic cohorts. P-values highlighted in bold are significant after correction for multiple testing with the Benjamini–Hochberg procedure.

### 6.4.3 Risk factor analyses

#### 6.4.3.1 *Significance of myocardial fibrosis*

We have established in Chapter 5 that histological fibrosis is patchy in MR; it was, therefore, important to utilise histological, imaging and serum markers of myocardial fibrosis when exploring the relationship between fibrosis burden and study endpoints. We identified a weak relationship between inotrope duration, ICU LoS and pre-contrast T1 relaxivity. However, this relationship does not remain statistically significant after correction for multiple testing (**Table 6.3**). The exclusion of 15 patients who underwent CABG from statistical analyses did not alter final analyses outcomes (data not shown).

To explore whether only severe myocardial fibrosis may exert a negative prognostic effect, patients in the highest quartile of fibrosis, determined via the different modalities, have been compared to those in the lower three-quartiles (**Table 6.4**). No significant relationships between fibrosis burden and peri-operative outcomes were identified by this additional analysis. Whilst a borderline P value was present between LGE mass and ICU LoS, this does not remain significant if correcting for multiple testing and is unlikely to be of clinical significance when the overall presence of LGE does not impact on perioperative outcomes (**Table 6.3**).

**Table 6.3** Risk factor exploration for primary endpoints.

	Inotrope duration			ICU LoS			Cardiovascular complications		
	N	Rho	P	N	Rho	P	N	Exp( $\beta$ )	P
<b>Fibrosis burden</b>									
ECV (%)	95	0.15	0.145	97	0.09	0.383	100	1.10	0.464
Pre-contrast T1 (ms)	98	0.21	0.045	100	0.22	0.032	103	1.02	0.246
Post-contrast T1 (ms)	96	0.10	0.329	98	0.10	0.331	101	1.01	0.738
LGE (g)	98	-0.07	0.484	99	-0.09	0.450	102	0.79	0.682
LGE presence	97	-0.03	0.780	99	-0.13	0.207	102	0.46	0.499
CVF <sub>mean</sub> (%)	82	0.13	0.242	84	-0.11	0.327	85	0.98	0.778
CVF <sub>max</sub> (%)	82	0.16	0.160	85	0.09	0.417	85	0.99	0.712
NTproBNP ( $\mu$ g/ml)	97	0.16	0.127	99	0.14	0.171	102	1.00	0.613
P1NP (ng/mL)	98	0.06	0.539	100	-0.16	0.122	103	0.96	0.150
P3NP (ng/mL)	98	0.09	0.392	100	0.07	0.480	103	0.98	0.943
TGF- $\beta$ 1 (ng/ml)	98	0.13	0.202	100	-0.01	0.897	103	1.02	0.494
<b>Symptom burden</b>									
NYHA class	99	0.09	0.375	101	-0.03	0.790	104	4.62	0.019
MLHFQ	98	-0.00	0.980	100	-0.21	0.036	103	1.04	0.054
<b>Clinical characteristics</b>									
Age (years)	99	-0.12	0.239	101	0.14	0.159	104	0.97	0.251
BMI (kg/m <sup>2</sup> )	99	0.01	0.945	101	0.06	0.575	104	1.00	0.968
Gender (Female)	99	-0.11	0.264	101	-0.12	0.216	104	0.67	0.722
Permanent AF	99	0.22	0.029	101	0.21	0.037	104	2.48	0.338
Echo GLS (s <sup>-1</sup> )	66	0.02	0.852	69	-0.13	0.300	70	0.91	0.676
Normal LV response to exercise	74	-0.02	0.885	77	0.12	0.307	79	0.31	0.410
Echo E/e'	84	0.04	0.732	86	0.06	0.603	89	0.99	0.962
sPAP (mmHg)	82	0.00	1.000	83	-0.05	0.632	85	1.02	0.525
%PredVO <sub>2</sub> peak (%)	98	-0.16	0.119	101	-0.06	0.583	103	0.98	0.245
LESVi (ml/m <sup>2</sup> )	99	0.17	0.092	101	0.16	0.117	104	1.04	0.219
LVEF (%)	99	-0.18	0.068	101	-0.25	0.013	104	0.89	0.036
LVMi (g/m <sup>2</sup> )	99	0.03	0.803	101	0.11	0.298	104	0.98	0.503
Indexed AV <sub>flow</sub> (ml/m <sup>2</sup> )	97	-0.19	0.062	99	-0.03	0.790	102	0.88	0.047

MR volume (ml)	99	0.12	0.230	101	-0.10	0.329	104	1.00	0.991
MR fraction (%)	99	0.17	0.095	101	-0.08	0.422	104	1.01	0.716
RVESVi (ml/m <sup>2</sup> )	99	0.05	0.630	101	0.01	0.953	104	1.10	0.007
RVEF (%)	99	-0.17	0.089	101	-0.07	0.486	104	0.84	0.008
GCS (s <sup>-1</sup> )	97	0.23	0.024	99	0.25	0.013	102	1.18	0.210
GLS (s <sup>-1</sup> )	97	0.10	0.320	99	0.19	0.055	102	1.13	0.392
RV GLS (s <sup>-1</sup> )	99	0.13	0.207	101	0.06	0.577	104	1.03	0.801
<b>Surgical factors</b>									
MR subtype (Barlow's)	89	0.14	0.197	91	0.01	0.947	94	0.88	0.895
Bileaflet involvement	98	0.29	0.004	100	0.04	0.710	102	1.24	0.822
Concomitant CABG	98	0.08	0.450	100	0.25	0.011	103	1.50	0.725
Concomitant TV repair	98	0.07	0.067	100	0.01	0.963	103	3.42	0.197
Concomitant AF ablation	98	0.15	0.145	100	0.11	0.261	103	6.24	0.053
Annuloplasty ring size	96	0.15	0.134	98	0.01	0.897	100	1.05	0.732

*Rho denotes Spearman's rank correlation coefficient.  $Exp(\beta)$  denotes odds ratio derived from binary logistic regression. P values <0.05 have been highlighted in green; however, all P values lost statistical significance after correction for multiple testing with the Benjamini–Hochberg procedure.*

**Table 6.4** Summary of sub-cohort analyses for determination of primary endpoints

	<b>Inotrope duration</b>		<b>ICU LoS</b>		<b>Cardiovascular complications</b>		
	<b>N</b>	<b>P</b>	<b>N</b>	<b>P</b>	<b>N</b>	<b>Exp(<math>\beta</math>)</b>	<b>P</b>
Highest Quartile ECV	80	0.889	82	0.810	84	1.07	0.954
Highest Quartile CVF <sub>mean</sub>	71	0.605	73	0.389	73	0.00	0.998
Highest Quartile CVF <sub>max</sub>	71	0.246	73	0.754	73	0.00	0.998
Highest Quartile LGE	82	0.058	<b>84</b>	<b>0.044</b>	86	1.19	0.886

*P values derived from Mann-Whitney U Test for continuous dependent variables and logistic binary regression for binary dependent variables. P values <0.05 have been highlighted in bold.*



#### *6.4.3.2 Significance of symptoms*

There was no statistical difference in the duration of inotropic support and ICU LoS between symptomatic and asymptomatic cohorts (**Table 6.3**). However, a trend was present between symptom burden and the development of cardiovascular complications.

#### *6.4.3.3 Other preoperative biomarkers*

A trend was present between the parameters of permanent AF, LVEF, GCS, bileaflet repair, requirement for concomitant CABG, and the study endpoints of inotropic requirements and ICU LoS. However, none of these associations remained significant after correction for multiple testing. Similarly, a relationship between RV systolic dysfunction and cardiovascular complications was present, however, this did not remain statistically significant following correction for multiple testing (**Table 6.3**).

### **6.5 Discussion**

The assessment of biventricular function plays an important role in predicting mortality and complications following cardiac surgery (24, 25, 261, 267). In MR, there have been multiple lines of evidence to suggest that the development of ventricular dysfunction may be secondary to the onset of myocardial fibrosis (199-201). However, there are limited data correlating direct fibrosis quantification against cardiac surgery outcomes.

In one study, the presence of mid-wall LGE was found to be associated with higher ICU readmission rates following MV repair. However, a direct comparison between this study and our current study is difficult as it featured a smaller study cohort of 48 patients, and contained a combination of primary and secondary MR cases (268).

Expanding our inclusion criteria to that of other valvular conditions, the presence of LGE in 63 aortic valve replacement patients was reported as a predictor of 30-day cerebrovascular accident and cardiac conduction blockade (269). We did not detect such associations, possibly due to the low incidences of cardiovascular complications within our current study.

We aimed to quantify the contemporary risks of MV surgery at three specialised Heart Valve Centres. Recognising that previous studies have predominantly employed 2D based echocardiographic parameters (270), we aimed to assess the value of preoperative biomarkers in predicting postoperative recovery parameters, with particular focus on markers of myocardial fibrosis.

In this study of 105 patients, there were no operative mortalities – this compares favourably with the operative mortality of larger registries (238) as well as the approximately 1% mortality rate for isolated MV surgery found within the Society for Cardiothoracic Surgery database (77). MV repair was feasible in 99% of our cases, with patients spending a median time of 1 day in ITU and 7 days in hospital. Similarly, our rate of cardiovascular complications was low at 5%.

Contrary to previous reports, we did not identify a statistically significant association between NYHA classification (4, 64, 145) or exercise capacity (271, 272) and postoperative outcome; this may be a consequence of our cohort consisting predominantly of overtly asymptomatic patients. Despite this, a statistical trend was present between increasing NYHA classification and the risk of developing cardiovascular complications.

In a previous study consisting of 425 patients undergoing cardiac surgery, GLS derived from echocardiography was found to offer incremental prognostic value over TTE derived LVEF for predicting early postoperative mortality and prolonged inotropic dependency (261). As reductions in GLS is felt to reflect the development of myocardial fibrosis, we were interested to explore whether more direct fibrosis quantification techniques would provide a stronger relationship with postoperative outcomes. Within this current study, a statistical trend was noted between CMR derived GCS, LVEF, and ITU requirements. However, neither histological, imaging nor serum biomarkers of fibrosis were significantly associated with patient outcomes.

Finally, it may be the case that myocardial fibrosis may only be of prognostic significance in the longer term - a recent meta-analysis found LGE to predicted long term all-cause mortality following AV surgery (273). This highlights our continued interest in the longer-term postoperative implications of myocardial fibrosis in MR.

## 6.6 Limitations

Study size represents the main limitation of this study, which becomes particularly pertinent as the use of multiple-testing correction can increase the probability of type 2 errors. Our study is significantly smaller than the prognostic biomarker study from the MIDA registry, which contained 2D echocardiographic data on 3666 patients with isolated MR (270). However, the strengths of our current study lie in its more comprehensive characterisation of each participant, and final recruitment numbers compare favourably against those of other published studies (126, 208).

LV functional reserve, defined as an improvement in GLS with exercise echocardiography, has been highlighted as a promising predictor of postoperative LV recovery in MR (126). Despite our studies being performed by two experienced BSE accredited cardiac imaging consultants, GLS during exercise was feasible in less than half of the study participants. This limited our ability to explore exercise GLS as a prognostic biomarker.

Finally, 3 patients underwent surgery at external surgical institutions due to individual preferences, therefore operative complications were limited to information available within clinical letters.

## 6.7 Summary

Operative mortality and cardiovascular complication risks were low within our three specialised Heart Valve Centres, and compare favourably with UK statistics.

Markers of cardiac fibrosis were not associated with operative outcome in MR.

Meanwhile, symptom burden, preoperative AF, and markers of biventricular systolic function demonstrated a statistical trend towards increased ITU demand and cardiovascular complications.

## CHAPTER 7

### DETERMINANTS OF MEDIUM TERM POSTOPERATIVE VENTRICULAR REMODELLING AND PATIENT OUTCOMES

#### 7.1 Introduction

The optimal management of chronic severe primary MR is to repair the valve, but the timing of surgery remains controversial. Current guidelines (**Table 1.5**) recommends a ‘watchful waiting’ approach until the onset of symptoms or left ventricular dysfunction, but have been criticised for promoting ‘rescue surgery’ as patients delaying surgery until a class I indication have higher operative mortality and increased rates of postoperative heart failure (80).

Chronic volume overload is a stimulus for adverse adaptive LV remodelling. Subclinical reduction in LV strain before MV repair predicts reduced LVEF following surgery and is thought to reflect interstitial myocardial fibrosis (151).

Recent advances in CMR imaging have provided a method to track changes in interstitial fibrosis. ECV derived from T1 measurements using a MOLLI sequence before, and 15-minutes postcontrast correlated well with histologically derived CVF (120). In a pilot study of 24 MR patients without class I indications for surgery, significant increases in ECV were present compared to age- and gender-matched controls and correlated with both exercise capacity and global longitudinal strain (147). The prognostic value of ECV and other CMR- and CPET-based non-invasive biomarkers remains of great interest in the prediction of postoperative reverse LV remodelling and patient recovery.

## 7.2 Aims and hypotheses

We hypothesise that expansion of the ECV on preoperative CMR is associated with impaired LV recovery following surgery, resulting in reduced LV reverse remodelling, more symptoms and lower exercise capacity at 6-9 months follow-up.

The aims of this chapter include:

- 1) Quantifying the intermediate-term postoperative outcome of MR patients.
- 2) Identification of non-invasive biomarkers which could provide prognostic information for the optimisation of surgical timings.

Change in LVESVi is a frequently utilised measure of ventricular remodelling and myocardial contractility (68, 274). The primary endpoint of this chapter is the change in postoperative LVESVi on CMR, comparing those with ECV above and below the median at 6-9 months following surgery.

Secondary endpoints include 1) exercise capacity measured as %PredVO<sub>2</sub> peak on CPET (180), 2) cardiac-specific symptoms measured with MLHFQ (275-280), and 3) ventricular systolic dysfunction measured by postoperative LVEF (126, 281, 282).

## 7.3 Methods

Methodology is as detailed in Chapter 2. In brief, this was a multi-centre prospective cross-sectional comparison of MR patients before and after surgery for chronic severe primary degenerative MR (clinicaltrials.gov NCT02355418) (152). To establish the natural history of ECV in MR, an additional cohort of MR patients who did not wish to undergo early surgery were followed. Analyses followed the principles of intention to treat

analysis; if a patient did not attend for postoperative follow-up investigations, clinical information including long term postoperative complications and mortality were gathered from clinical documentation and community General Practitioner records.

### 7.3.1 Statistical analyses

#### 7.3.1.1 Power calculation

Based on pilot data and previously published reports (68, 147) the standard deviation of LVESVi in MR patients is 12ml. A survival advantage has previously been shown with a 7ml postoperative difference in LVESVi (68). A volume difference of this magnitude was therefore chosen as a clinically significant difference when comparing patients with above- and below-median ECV. An independent T-test with 48 patients per group (96 total), and a within-group standard deviation of 12ml yields a minimal detectable difference of 7ml at 80% power, with  $\alpha=0.05$ .

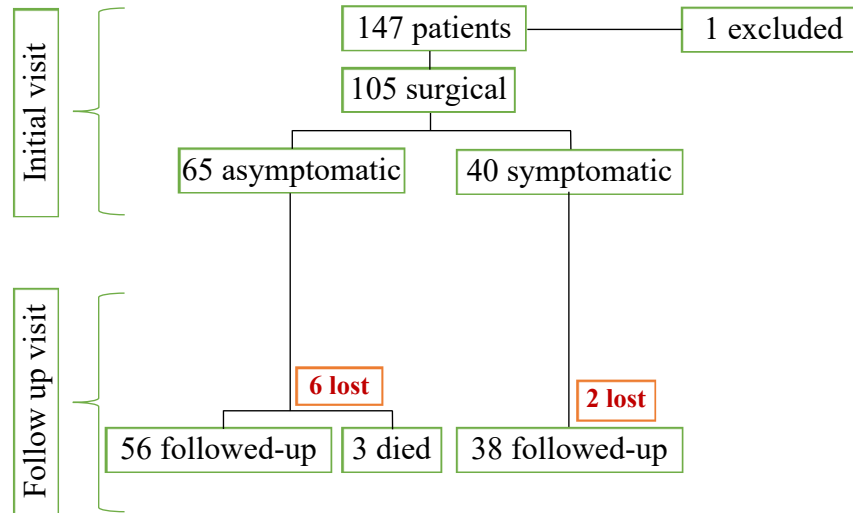
## 7.4 Results

### 7.4.1 Recruitment and follow-up

147 patients were recruited into the Mitral FINDER study. 1 was excluded following study investigations diagnosed a Carpentier type I mechanism. 105 patients underwent surgery whilst 41 were managed conservatively (**Figure 7.1**). 94 surgical patients attended for postoperative investigations; 12 non-surgical cases attended for longitudinal follow-up.

Median time from study enrolment to surgery was 3.4 [1.3-6.0] months. Postoperatively, surgical patients received follow-up investigations at 8.6 [7.4-10.5] months.

**Figure 7.1** Flow diagram summarising patient recruitment and follow-up.





#### 7.4.2 Baseline clinical data

An overview of the Mitral FINDER cohort has been provided within previous chapters. To summarise, there were no significant differences in age or gender between patients with and without overt symptoms within the surgical cohort (**Table 6.1**). Overtly symptomatic patients were characterised by reduced GCS, LVMi and increased ECV.

#### 7.4.3 Surgical outcomes following hospital discharge

An outpatient TTE was identified for 62 patients following a mean postoperative period of  $4.5 \pm 2.9$  months. One patient developed recurrent moderate MR on inpatient TTE; all others possessed no or mild MR at the time of hospital discharge. 3 patients died during the follow-up period. The causes of death were community-acquired pneumonia, aspiration pneumonia following meningococcal meningitis on a background of previous stroke, and hydropneumothorax secondary to previous asbestos exposure.

The incidence of adverse events during the post-discharge follow-up period were similar between symptomatic and asymptomatic patients (**Table 7.1**,  $\chi^2=2.0$ ,  $P=0.574$ ).

Cardiac related adverse events included two cases of atrial flutter, one case of new-onset AF requiring DC cardioversion. Recurrent severe MR occurred in 1 patient due to neochordal rupture, which required transcatheter valve implantation following the onset of symptoms. One patient developed severe asymptomatic MR, whilst two others developed moderate MR; these patients did not require further intervention.

**Table 7.1** Summary of the incidences of adverse events during postoperative follow-up in symptomatic and asymptomatic MR patients.

	<b>Asymptomatic</b>	<b>Symptomatic</b>
No adverse events	55 (85%)	36 (90%)
Non-cardiac adverse events	3 (5%)	2 (5%)
Cardiac adverse events	4 (6%)	2 (5%)
Death	3 (5%)	0 (0%)

*Data are reported as N (%).*

Non-cardiac adverse events included one case of pleural effusion requiring drainage and a sternal wound infection requiring surgical cleaning. Two patients underwent MV repair via a mini-thoracotomy technique; one was complicated by an incisional hernia and the other by a unilateral phrenic nerve injury. In patients undergoing median sternotomy, there were two cases of pleural effusion requiring drainage.

#### 7.4.4 Imaging characterisation following mitral valve surgery

93 out of 94 surgical patients who attended follow-up study visits underwent postoperative CMR; one was unable to CMR due to the presence of a non-CMR compatible pacemaker. A statistically significant postoperative reduction in MR severity and biventricular volumes was noted (**Table 7.2**).

Pertinently, a postoperative reduction in ECV was also observed, with the magnitude of ECV reduction unaffected by preoperative symptom status (asymptomatic  $-0.5 \pm 2.7\%$  vs  $-1.4 \pm 4.0\%$ ,  $P=0.209$ ) or LGE presence (absent  $-0.6 \pm 3.0\%$  vs present  $-1.3 \pm 4.0\%$ ,  $P=0.345$ ). Instead, the magnitude of ECV reduction correlated well with preoperative ECV ( $R=-0.64$ ,  $P<0.001$ , **Figure 7.2A**).

Overall postoperative systolic function was good across the cohort with a mean postoperative LVEF of  $63.3 \pm 8.3$ ; only 6 (6%) patients had LVEF  $<50\%$ .

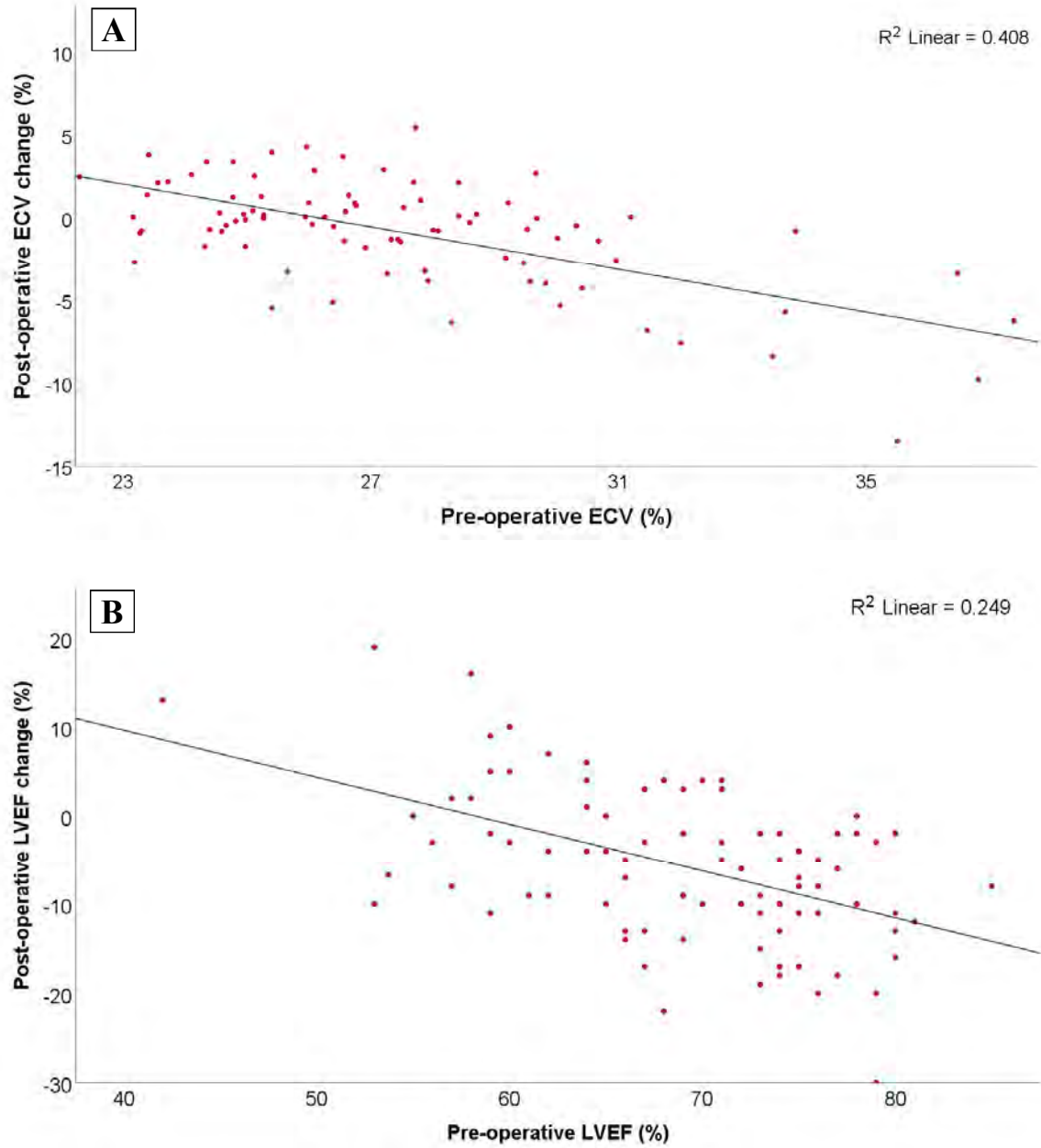
33 out of 93 patients had  $\geq 10\%$  drop in postoperative LVEF, with preoperatively asymptomatic patients undergoing an overall larger reduction compared to symptomatic patients ( $-7.2 \pm 7.1\%$  vs  $-3.4 \pm 9.9\%$ ,  $P=0.030$ , **Figure 7.2B**).

**Table 7.2** Comparison of CMR parameters before and after surgery.

	<b>N</b>	<b>Preoperative</b>	<b>Postoperative</b>	<b>P</b>
LVEF (%)	93	69.1±8.0	63.3±8.3	<b>&lt;0.001</b>
LVEDVi (ml/m <sup>2</sup> )	93	102.9±22.4	71.8±16.6	<b>&lt;0.001</b>
LVESVi (ml/m <sup>2</sup> )	93	32.2±11.8	26.9±10.8	<b>&lt;0.001</b>
LVMi (g/m <sup>2</sup> )	93	68.6±13.5	60.2±11.3	<b>&lt;0.001</b>
MR volume (ml)	93	63.3±30.3	14.6±8.6	<b>&lt;0.001</b>
MR fraction (%)	93	46.1±15.0	17.1±9.4	<b>&lt;0.001</b>
RVEF (%)	93	56.4±8.7	56.8±7.1	0.654
RVEDVi (ml/m <sup>2</sup> )	93	71.0±15.0	68.0±13.6	<b>0.026</b>
RVESVi (ml/m <sup>2</sup> )	93	31.2±10.0	29.5±8.3	<b>0.036</b>
ECV (%)	89	27.4±3.3	26.6±2.8	<b>0.027</b>
T2 (ms)	61	53.5±3.6	52.4±2.4	<b>0.005</b>

*Data are reported as mean±SD with p-values from paired samples t-tests. Bold p-values are significant at p<0.05.*

**Figure 7.2** Scatter plot demonstrating the relationship between preoperative and magnitude of change in postoperative CMR parameters for A) ECV and B) LVEF.



Patients with higher preoperative ECV and LVEF experienced larger postoperative reductions in ECV and LVEF.

#### 7.4.5 Symptom burden and exercise capacity following mitral valve surgery

Successful MV surgery resulted in significant improvements in  $O_2$ pulse and  $VE/VCO_2$ .

However, statistically significant improvements in peak exercise capacity were observed only in symptomatic patients (**Table 7.3**).

Similarly, objective quantification of symptoms (available in 93 out of 94 patients) revealed that improvements in physical functioning (SF36) and MLHFQ Physical domains only occurred in symptomatic patients (**Table 7.4**). Of significance, a reduction in emotional burden was still observed in the asymptomatic sub-group.

Despite the postoperative improvements in symptom burden and exercise capacity in symptomatic individuals, this sub-group of patients failed to achieve the same level of fitness and symptom-free status as preoperatively asymptomatic patients ( $\%PredO_2peak$   $92.2\pm 18.8\%$  vs  $102.9\pm 21.1\%$ ,  $P=0.017$ , MLHFQ 12 [5-26] vs 3 [0-10],  $P<0.001$ ).

**Table 7.3** Changes in exercise parameters following surgery according to preoperative symptom status (N=89).

		<b>Pre-operation</b>	<b>Post-operation</b>	<b>P</b>
<b>O<sub>2</sub>pulse</b> (ml/beat)	<i>Asymptomatic</i>	12.9±4.0	14.0±4.1	<b>0.002</b>
	<i>Symptomatic</i>	10.9±4.0	12.9±3.3	<b>0.007</b>
<b>VE/VCO<sub>2</sub></b>	<i>Asymptomatic</i>	31.7±5.4	29.0±5.7	<b>0.002</b>
	<i>Symptomatic</i>	35.2±8.2	30.6±5.5	<b>&lt;0.001</b>
<b>%PredO<sub>2</sub>peak</b> (%)	<i>Asymptomatic</i>	99.2±19.9	102.9±21.1	0.122
	<i>Symptomatic</i>	80.8±20.6	92.2±18.8	<b>&lt;0.001</b>

**Table 7.4** Changes in objective measures of symptom burden following surgery according to preoperative symptom status (N=94).

		Pre-operation	Post-operation	P
SF36 physical functioning	<i>Asymptomatic</i>	90 (70-95)	90 (75-100)	0.985
	<i>Symptomatic</i>	40 (20-60)	75 (60-90)	<b>&lt;0.001</b>
SF 36 physical role limitations	<i>Asymptomatic</i>	100 (63-100)	100 (50-100)	0.655
	<i>Symptomatic</i>	0 (0-50)	75 (25-100)	<0.001
MLHFQ Physical	<i>Asymptomatic</i>	2 (0-8)	2 (0-8)	0.310
	<i>Symptomatic</i>	24 (17-30)	7 (3-15)	<b>&lt;0.001</b>
MLHFQ Emotional	<i>Asymptomatic</i>	2 (0-5)	0 (0-2)	<b>0.049</b>
	<i>Symptomatic</i>	10 (6-15)	3 (1-8)	<b>&lt;0.001</b>
MLHFQ Total	<i>Asymptomatic</i>	5 (1-16)	3 (0-10)	<b>0.004</b>
	<i>Symptomatic</i>	42 (30-53)	10 (5-22)	<b>&lt;0.001</b>

Data are reported as median (interquartile range), with p-values from Wilcoxon Signed Ranks Test. Bold p-values are significant at  $p < 0.05$ .



#### 7.4.6 Postoperative determinants of reverse left ventricular remodelling

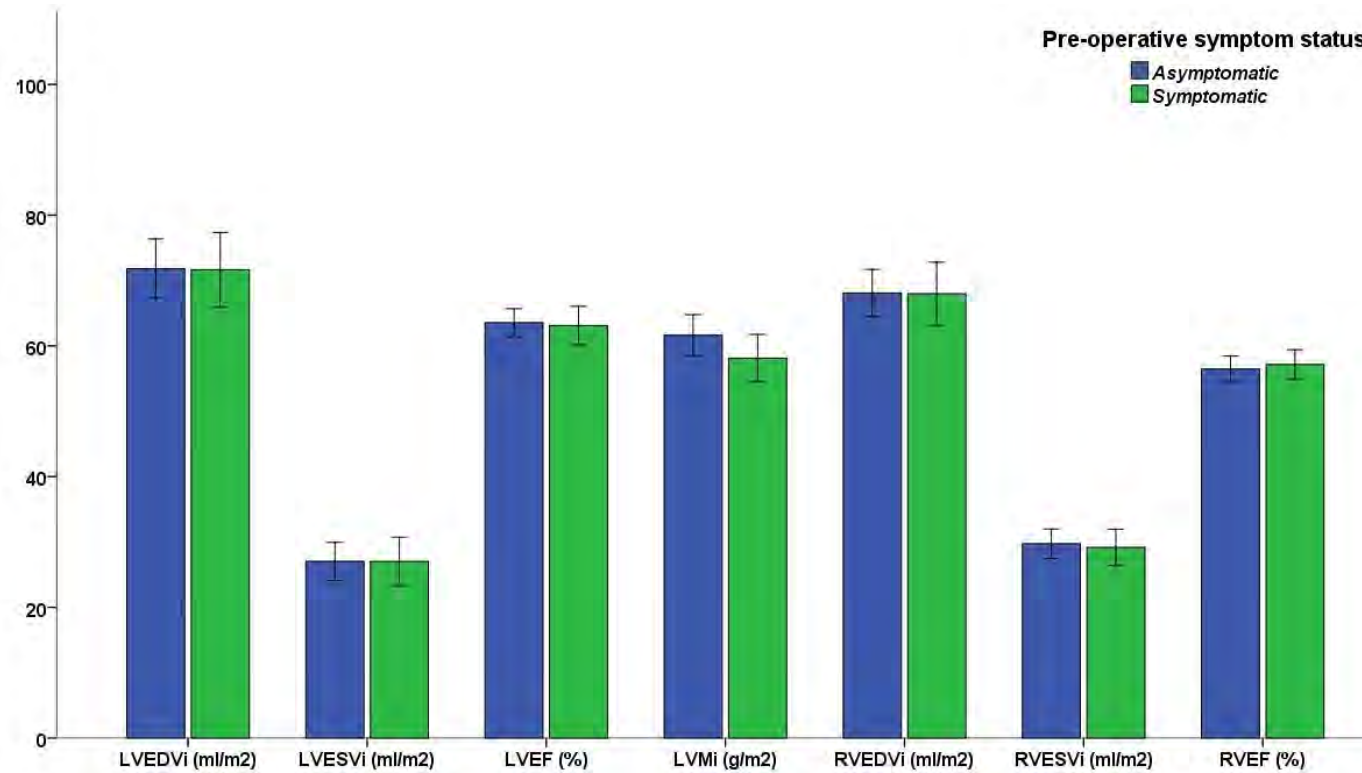
To investigate the impact of preoperative symptoms on postoperative reverse remodelling, postoperative CMR parameters were split according to preoperative symptom status; no statistically significant differences were identified across the two sub-groups (**Figure 7.3**, all P values >0.05).

Preoperative ECV has been identified as a potential prognostically important imaging biomarker. Its influence on postoperative reverse remodelling was therefore assessed by comparing postoperative systolic function markers in patients with above- and below-median preoperative ECV.

We found no statistically significant difference in measures of postoperative systolic function between patients with above- and below-median preoperative ECV (LVESVi  $26.1 \pm 9.7$  vs  $28.2 \pm 12.2$  ml/m<sup>2</sup>, P=0.363; LVEF  $62.8 \pm 8.3$  vs  $64.1 \pm 8.2$ %, P=0.454).

Similarly, the presence or absence of preoperative LGE did not influence postoperative volumetric CMR parameters (LVESVi  $26.2 \pm 9.5$  vs  $27.4 \pm 11.6$  ml/m<sup>2</sup>, P=0.607; LVEF  $63.1 \pm 5.7$  vs  $63.6 \pm 9.3$ %, P=0.778).

**Figure 7.3** Clustered bar chart showing mean postoperative CMR values based on preoperative symptom status.



Whiskers represent 95% confidence interval. P values on paired T-testing for all illustrated CMR parameters remained statistically non-significant at  $P > 0.05$ .

#### 7.4.7 Determinants of a favourable postoperative outcome

Determinants of a favourable postoperative outcome were assessed by correlating parameters against secondary outcomes (**Table 7.5**). No single parameter correlated significantly with all three secondary outcomes. Postoperative systolic function correlated with multiple preoperative CMR parameters, whilst postoperative exercise capacity and MLHFQ scores tended to correlate with preoperative exercise fitness and symptom burden.

ECV and  $CVF_{\text{mean}}$  correlated significantly with postoperative symptoms, but not with exercise capacity or LVEF; the presence of LGE was not associated with any secondary outcomes.

Historically, an LVEF of <50% after surgical correction of MR has been identified as deleterious to long-term survival (126, 281, 282). Within our study, six (6.5%) patients possessed postoperative LVEF <50% on CMR. Of these, three were NYHA class I prior to surgery; their preoperative LVEF ranged from 53 to 79%,  $MR_{\text{fraction}}$  ranged between 22 to 57%, NTproBNP between 34 and 2258pg/ml, and ECV between 23.7 and 37.4%; only one patient possessed LGE, and histological  $CVF_{\text{mean}}$  ranged between 5.1 and 36.7%. Five out of these six patients required three or more days of ITU support and had above-median length-of-stay in hospital.

In a backwards linear regression model which contained all preoperative parameters that were found to significantly correlate with postoperative LVEF, GCS and LVEDd remained an independent predictor of LVEF >50% ( $R^2=0.284$ ,  $P<0.001$ ). Preoperative GCS

remained an independent predictor of postoperative LVEF when limiting analyses to preoperatively NYHA class I patients.

**Table 7.5** Correlations between preoperative parameters and secondary outcomes.

Preoperative parameters	Postoperative outcomes								
	N	LVEF		%PredVO <sub>2</sub> peak			MLHFQ		P
		Rho	P	N	Rho	P	N	Rho	P
<b>Demographics</b>									
Age (years)	93	0.02	0.855	89	0.02	0.871	93	0.01	0.951
Female gender	93	0.13	0.202	89	-0.09	0.412	93	0.24	0.020
BMI (kg/m <sup>2</sup> )	93	-0.08	0.425	89	-0.02	0.852	93	-0.01	0.918
Permanent atrial fibrillation	93	-0.13	0.214	89	-0.15	0.159	93	0.17	0.096
Degeneration subtype (Barlow's)	93	-0.16	0.134	89	-0.09	0.412	85	0.00	0.971
NTproBNP	91	-0.13	0.230	87	-0.15	0.152	91	0.18	0.089
<b>Symptom and functional status quantification</b>									
MLHFQ score	92	0.09	0.373	88	-0.28	0.008	92	0.58	<0.001
%PredVO <sub>2</sub> peak (%)	92	0.09	0.390	89	0.68	<0.001	92	-0.32	0.002
VE/VCO <sub>2</sub>	92	-0.13	0.228	89	-0.31	0.003	92	0.06	0.574
Resting sPAP (mmHg)	75	-0.02	0.888	72	-0.20	0.088	75	0.00	1.000
Exercise induced MR worsening	74	0.01	0.419	71	-0.13	0.292	73	0.03	0.828
Exercise induced LV deterioration	72	-0.06	0.615	69	-0.38	0.001	71	0.32	0.007
Exercise induced sPAP >60mmHg	75	0.03	0.806	72	0.16	0.186	74	0.08	0.518
<b>Imaging</b>									
LVEDd	91	-0.42	<0.001	87	0.11	0.295	91	-0.18	0.094
LVESd	89	-0.45	<0.001	85	0.12	0.270	89	0.02	0.835
LVEDVi (ml/m <sup>2</sup> )	93	-0.39	<0.001	89	0.13	0.233	93	-0.21	0.039
LVESVi (ml/m <sup>2</sup> )	93	-0.56	<0.001	89	0.02	0.869	93	-0.04	0.693
LVEF (%)	93	0.43	<0.001	89	0.10	0.342	93	-0.10	0.330
GCS (%)	91	-0.42	<0.001	87	-0.16	0.137	91	0.07	0.541
GLS (%)	91	-0.22	0.034	87	-0.24	0.023	91	-0.01	0.961

LVMi (g/m <sup>2</sup> )	93	-0.26	0.011	89	0.08	0.454	93	-0.29	0.004
RVEDVi (ml/m <sup>2</sup> )	93	-0.16	0.122	89	0.17	0.121	93	-0.11	0.309
RVESVi (ml/m <sup>2</sup> )	93	-0.27	0.008	89	-0.03	0.746	93	-0.11	0.299
RVEF (%)	93	0.22	0.037	89	0.27	0.009	93	0.02	0.827
RV E <sub>II</sub>	93	-0.17	0.094	89	-0.07	0.519	93	-0.12	0.238
MR volume (ml)	93	-0.21	0.047	89	-0.11	0.297	93	-0.21	0.046
MR fraction (%)	93	-0.17	0.109	89	-0.30	0.004	93	-0.08	0.453
ECV (%)	91	-0.02	0.858	87	-0.08	0.483	91	0.26	0.015
T2 (ms)	66	-0.13	0.302	63	-0.14	0.271	66	0.06	0.621
LGE presence (n,%)	93	-0.09	0.413	89	-0.05	0.635	93	-0.07	0.530
E/e'	81	-0.12	0.293	76	-0.27	0.017	80	0.10	0.363
<b>Histology</b>									
CVF <sub>mean</sub>	75	-0.13	0.277	72	-0.13	0.283	75	0.27	0.018
CVF <sub>max</sub>	75	-0.12	0.321	72	-0.08	0.531	75	0.21	0.068

Data reported represents the results of Spearman's rank correlation. Correlations highlighted green are significant at  $p < 0.05$ , remaining significant after correction for multiple testing with the Benjamini–Hochberg procedure.

## 7.5 Discussion

This is the first multimodality study to characterise postoperative changes following MR surgery, featuring multiparametric CMR to quantify reverse LV remodelling, as well as detailed symptom and functional exercise capacity characterisation. Within a predominantly asymptomatic cohort of patients, we found long-term postoperative complications to be uncommon.

104 out of 105 patients underwent MV repair rather than replacement, this compares favourably with the 89% incidence of MV repair reported by the MIDA registry (238). At follow-up, only one patient required further surgical intervention for recurrent MR.

Our patients experienced a significant degree of reverse LV remodelling, with 94% possessing preserved postoperative systolic function defined as LVEF >50% on CMR. ECV contraction also occurred following surgery; reassuringly a linear relationship was present between the magnitude of ECV reduction and preoperative ECV. This suggests, at least within a relatively asymptomatic cohort, that the largest reduction in myocardial fibrosis occurs in patients who had accumulated the most fibrosis.

Successful MV surgery in asymptomatic patients did not significantly improve their physical symptom burden but did relieve emotional symptoms. Meanwhile, successful surgery reduced both physical and emotional symptom burden in NYHA II-III patients – however, these patients remained more symptomatic compared those who were preoperatively NYHA class I. This pattern is also present when measuring exercise capacity where NYHA II-III patients failed to regain their lost exercise capacity and achieve the same %PredVO<sub>2</sub>peak as NYHA I patients. These findings provide mechanistic

insight into why previous studies have reported higher long-term mortality rates when patients delay surgery after the onset of symptoms (80).

Invasive histological  $CVF_{\text{mean}}$  and non-invasive ECV provide insight into the degrees of myocardial fibrosis – both parameters correlated significantly with postoperative symptom burden, suggesting that irreversible myocardial fibrosis may be contributing to the persistence of postoperative symptoms. However, the magnitude of the correlation between fibrosis and post-operative symptom burden was exceeded by the correlation between pre- and post-operative symptoms. Additionally, fibrosis burden was not predictive of postoperative  $\%PredVO_{2\text{peak}}$ , further suggesting that fibrosis may not be prognostically important within the MR patient population. Whilst it may be argued that predicted  $VO_{2\text{peak}}$  values are population averages rather than the patients' true baseline exercise capacity, and  $\%PredVO_{2\text{peak}}$  calculated using patients' historical  $VO_{2\text{peak}}$  may have produced a significant correlation with myocardial fibrosis; as CPETs are much cheaper and simpler than CMRs to perform, such a finding would be more supportive for a baseline CPET to be performed in routine clinical practice when asymptomatic patients first commence their regular surveillance programme.

We explored the association between the secondary outcomes of postoperative LVEF, exercise capacity and symptom burden with a wide range of preoperative clinical parameters. No single preoperative parameter was significantly associated with all three factors. We previously reported ECV as a promising non-invasive biomarker which correlated with multiple markers of systolic and diastolic dysfunction (Chapter 5). However, contrary to our primary hypothesis, we were unable to identify a significant



association between preoperative ECV and postoperative LV systolic function. This suggests that ECV is not a prognostically important biomarker in our cohort of predominantly asymptomatic MR patients. An overall favourable stage of LV remodelling within the Mitral FINDER cohort may have contributed to this outcome – a hypothesis which is supported by the lower observed rate of postoperative LV dysfunction when compared to previous studies (83, 283). We discussed in Chapter 1 (section 1.6.2) that early stages of myocardial fibrosis in MR are likely a reversible physiological, rather than irreversible pathological process. This mirrors our observation of a correlation between preoperative ECV expansion, and its postoperative reduction. ECV may still be of prognostic value in patients with more advanced degrees of pathological LV remodelling.

Although ECV was not predictive of postoperative systolic parameters, preoperative myocardial strain strongly predicted postoperative systolic function. As discussed in Chapter 3, the development of fibrosis is believed to be associated with a reduction in myocardial strain. Impaired myocardial deformation, as a downstream consequence of adverse myocardial remodelling, may have a more direct association with postoperative ventricular status.

Pertinently, even within a cohort of patients with favourably remodelled myocardium, postoperative exercise fitness and symptom burden in our symptomatic cohort failed to improve back to a level that was comparable with the preoperatively asymptomatic cohort. We have identified a positive correlation between pre- and postoperative symptom burden and exercise capacity, highlighting that symptom development, much like systolic dysfunction, is not a binary parameter. Instead, the accumulation of symptoms and

exercise limitation are continuous parameters with prognostic importance. These findings support the benefits of early surgery before class I indications are met (80), and highlights the potential value of surveillance PROMs and exercise testing to detect “sub-clinical” progression of symptom burden in patients whom early surgery on class II surgical indication is not clinically appropriate.

## 7.6 Limitations

A major limitation of this current study is the under recruitment of surgical patients with 92 out of the required 96 patients undergoing postoperative CMR. Patient recruitment was a challenge which we had identified and attempted to address early following initiation of the study. Whilst historical rates of MV repair at University Hospital Birmingham suggested that this single recruitment centre would have been sufficient to attain recruitment targets, our recruitment was hindered by unforeseen delays in surgical waiting times. To overcome this limitation, we successfully applied for ethical approval revisions to include two additional cardiac surgery centres and maximised patient recruitment as well as retention by having the research fellow attend each surgical clinic in person. This process allowed the patients’ primary surgeons to introduce them to a single source of contact for the research project, reassuring patients with a familiar contact who would be present throughout the preoperative, operative and postoperative process.

For this study’s original hypothesis and power calculation to be realised, patients with above-median ECV would require  $7\text{ml}/\text{m}^2$  or higher LVESVi when compared to patients with below-median ECV. Instead, the direction of our data is reversed with higher ECV patients possessing a non-significantly lower postoperative LVESVi, suggesting that a larger patient cohort would not have made a difference to our study outcomes. It is

possible that studying patients with more advanced LV remodelling and higher incidences of postoperative LV dysfunction would have increased the prognostic power of preoperative ECV. However, such a study is not required as we have demonstrated a prognostic benefit when operating early, before deteriorations in exercise capacity or subtle increases in symptom burden.

This study provided a relatively short postoperative CMR follow-up in comparison to previously published long-term echocardiographic outcome studies. A further follow-up study of the Mitral FINDER cohort 3-5 years following surgery remains of interest. There was a median delay of 3.4 months between preoperative assessment and MV surgery. This may have allowed time for further ECV expansion to take place and thereby reducing the ability of preoperative ECV to predict postoperative outcomes. However, our longitudinal ECV data presented within Chapter 4 in conservatively managed patients suggests that this is unlikely to be significant.

## 7.7 Summary

With a predominantly asymptomatic cohort of primary degenerative MR patients, the incidence of postoperative complications following MV surgery at our three expert centres was low, and most patients possessed preserved LV systolic function at a median follow-up period of 8.6 months. Neither histologically quantified fibrosis nor CMR derived ECV predicted postoperative cardiac function, suggesting that ECV is unlikely to possess incremental value over existing biomarkers for optimising the timing of MR surgery. Following surgery, there was a contraction of ECV, proportionate to the extent of its preoperative expansion, suggesting that patients with the highest fibrosis burden will also undergo the most amount of regression. Despite this, and the higher magnitude of

improvement in symptom burden and exercise capacity, preoperatively symptomatic patients did not recover to the same baseline as overtly asymptomatic patients. These findings support the benefits of early surgery for MR; for patients in whom early surgery is not clinically appropriate (e.g. patient preference), longitudinal GCS, MLHFQ and CPET may detect “sub-clinical” LV dysfunction and symptom progression.

## CHAPTER 8

### CONCLUSIONS – FUTURE DIRECTIONS

#### 8.1 Summary of thesis findings

The work within this thesis primarily aimed to examine the postoperative implications of myocardial fibrosis in patients with primary degenerative mitral regurgitation. Secondary aims included providing histological evidence that myocardial fibrosis develops in MR, validating CMR based fibrosis quantification against histological findings, and the comprehensive characterisation of functional consequences of fibrosis, both for the heart and the patient.

In the most comprehensive study to characterise myocardial changes in patients with chronic primary severe MR, this thesis provides definitive histological evidence for the presence of myocardial fibrosis, even in asymptomatic MR patients with normal range ejection fraction. In Chapter 5, I demonstrated this fibrosis to correlate significantly with patients' symptom burden; but being a patchy process, it does not correlate with ECV. Conversely, a significant correlation was present between ECV and multiple markers of systolic and diastolic function. The peri-operative and medium-term postoperative prognostic implications of ECV was therefore investigated in Chapters 6 and 7; I found patients with above- and below-median ECV to possess similar postoperative LVESVi, as well as other markers of systolic function. Conversely, traditional pre-operative measures of systolic function best correlated with post-operative LV systolic function. Therefore, within a predominantly asymptomatic cohort of MR patients, ECV was not a useful prognostic biomarker of patient outcome.

The overall ECV measured fibrosis burden was low in our study cohort when compared to other cardiac conditions, and it is possible for ECV to become prognostically important in patients with more fibrosis and advanced degrees of heart failure symptoms. However, given the clear surgical indication in patients with overt symptoms, and the significant overlap of ECV values between asymptomatic MR patients and the general population, ECV is unlikely to become a useful clinical tool in routine practice.

The robustness of my study outcomes is supported by good study methodology. Described in Chapter 2, MR related cardiac changes were assessed using multi-parametric CMR. This offered the gold-standard assessment of volumetric status and tissue characteristics. Furthermore, all CMR studies were independently blinded by an external researcher, before being analysed by me to negate bias and inter-observer variability during longitudinal follow-up.

The detailed characterisation of myocardial function and patient symptoms were a key component of the study design. Myocardial deformation imaging has been touted as a functional imaging biomarker of myocardial fibrosis. However, my initial experience with traditional 2D based tissue tracking methods on CMR produced unreliable results due to poor reproducibility. In Chapter 3, I investigated and validated a novel 3D FT-CMR technique which offered superior reproducibility compared to 2D FT-CMR, with 3D GCS possessing an ICC of 0.88. This suggested that 3D FT-CMR possesses very good reproducibility – one of the traits necessary for the adoption of a test within clinical practice (213).

Similarly, symptom burden, traditionally categorised by physicians according to the NYHA classification, has been criticised for being non-robust with poor inter-observer reproducibility (284). This may have contributed to the contradictory evidence on whether delaying surgery until after the onset of overt symptoms produces better patient outcomes (79, 80). In Chapter 4 and 5, I demonstrated that even within NYHA class I patients, there are wide ranges of subjectively quantified symptom scores and objectively quantified exercise capacities. This suggests that NYHA classification, whilst prognostically important, may result in the over-simplification of patients' symptoms by allowing an external observer (the physician) to categorise a continuous variable (symptom burden) into a binary category (presence or absence). This study overcomes the limitations imposed by physician-assigned NYHA classification, with the detailed quantification of patient-reported symptom burden and objective quantification of cardiac fitness across study participants. This point is reinforced in Chapter 7 where I demonstrated that preoperatively symptomatic patients fail to recover fully from a physical-symptom and fitness perspective even following successful MV repair, with preoperative symptom scoring and exercise capacity correlating significantly with postoperative symptom scoring and exercise capacity. Therefore, symptom scoring with PROMS and cardiac fitness quantification with CPET may be more sensitive methods of monitoring for symptom progression, with the potential to act as useful adjuncts in patients' annual clinical surveillance reviews.

Patient under-recruitment became a concern shortly following study initiation. I addressed this by expanding the study into two additional surgical centres and by raising awareness of the study amongst cardiology departments of the region's referral hospitals.

Furthermore, extension of the study's data collection period by six months allowed the postoperative follow-up of patients who were affected by prolonged surgical waiting times. Despite these steps, I needed an additional four patients to attend postoperative follow-up CMR. However, as discussed in Chapter 7, increasing the postoperative CMR follow-up rate from 93 to 96 patients as per pre-study power calculation is unlikely to have altered final study outcomes. The lack of association between ECV and postoperative prognosis is likely secondary to the favourable LV remodelling state of the Mitral FINDER cohort. Only 6% of study patients developed a postoperative LVEF of <50%, contrasting with the 16-18% reported in previous studies (83, 283). Similarly, the range of ECV observed within this study's surgical cohort ( $27.3 \pm 3.2\%$ ) is only mildly raised compared to the mean ECV of 25.9% (95% CI 25.5% – 26.3%) within a recent pooled analysis of 3872 participants (250), and is lower than the median of 28.1% reported within a consecutive series of 1172 clinically indicated CMRs (141). This suggests that the burden of fibrosis quantified on ECV within the Mitral FINDER cohort is relatively low for the general cardiology setting, and patients' ventricles may not be sufficiently scarred to impose a significant prognostic penalty. Whether ECV becomes prognostically important in patients with more advanced fibrosis burden remains uncertain, and could be studied if the focus of recruitment was shifted towards patients presenting with decompensated heart failure. However, there is little indication for such a study as I have demonstrated superior patient outcomes with early surgery, both in terms of subjective symptom burden and objective exercise capacity. Conversely, if an elderly but overtly asymptomatic severe MR patient has stably good exercise capacity and low symptom burden during annual surveillance, then they may be reassured that surgery is not yet necessary.



Even though ECV did not correlate with postoperative outcomes, I have demonstrated in Chapter 5 that GCS and GLS obtained from 3D FT-CMR significantly correlated with preoperative ECV. In Chapter 7, I reported that postoperative systolic function was independently predicted by preoperative GCS. It is therefore conceivable that whilst preoperative ECV does not predict postoperative myocardial function, impaired myocardial deformation, as a downstream consequence of adverse myocardial remodelling, can more directly predict postoperative ventricular status. Further work is required to investigate 3D FT-CMR as a prognostic imaging biomarker in asymptomatic MR.

## 8.2 Future directions

### 8.2.1 How do we manage asymptomatic patients not wishing for early surgery?

Data described in this thesis have proposed that myocardial fibrosis is not a key determinant of postoperative prognosis in a cohort of patients predominantly with asymptomatic severe MR. I have, however, demonstrated the benefits of intervention prior to the onset of overt symptoms, as symptomatic patients often fail to fully achieve symptom-free status despite successful MV repair. As highlighted by our non-surgical cohort, not all asymptomatic patients wish to undergo early surgery. This is particularly true since increasing age is associated firstly with an increased probability of remaining symptom-free for life (as a result of a shorter life expectancy), and secondly with higher surgical risks.

For NYHA class I patients who prefer not to undergo early surgery, there is the need to provide further guidance on the safety of a ‘watchful-waiting’ management approach. The

results of this thesis suggest that PROMs and CPET are more sensitive methods of quantifying symptom status, with a wide range of ‘sub-clinical symptom burden’ present even in NYHA class I patients. A large randomised clinical outcome study assessing the sensitivity and specificity of serial PROMs and CPET, to detect sub-clinical symptom progression, is therefore needed in older NYHA class I patients who prefer initial non-surgical therapy.

#### 8.2.2 Does fibrosis evaluation using imaging have a role in symptomatic severe MR patients, who are later in their disease process?

LGE and ECV imaging are currently at the forefront of research in aortic stenosis, aiming to optimise the timing of surgery. Both the presence of LGE (285) and expansion of ECV (286) have been identified as independent predictors of post-intervention mortality. This has led to the ongoing EVOLVED trial, in which patients are randomised to different therapeutic techniques according to their LGE status (287).

MR and aortic stenosis are both valvular diseases triggering myocardial fibrosis. Given their similarities, an important question is whether fibrosis imaging has a role in the management of symptomatic severe MR patients, who are later in their disease process? The Mitral FINDER cohort was comprised primarily of asymptomatic (NYHA I) patients, with a smaller proportion of NYHA II and III patients. It is of interest to evaluate if severely symptomatic MR patients with impaired LV function have a higher burden of fibrosis, and if this would contribute to poorer outcomes in patients with a delayed presentation to medical services. From a clinical perspective, however, the management of such patients is unlikely to be altered as they will have a clear indication for surgical intervention.

### 8.2.3 Why does late gadolinium enhancement develop in MR and is it of prognostic importance?

It remains unclear why some MR patients develop LGE, and others do not. Whilst the prevalence and severity of LGE in aortic stenosis appear proportionate to the severity of the valve disease (288), this is not the case in MR. LGE has been widely reported to be present in patient cohorts containing mild and moderate MR (32, 41, 289). These same studies have proposed that there is increased tendency for LGE to develop in MR patients with Barlow's disease due to increased mechanical traction forces arising from the prolapsing leaflets, and that LGE is of prognostic importance as it represents a proarrhythmic substrate that increases the risk of ventricular arrhythmia.

These pertinent research questions fall outside the remit of the original Mitral FINDER study. However, as an initial effort to tackle these questions, I acquired additional data on the Mitral FINDER cohort with the aim of investigating: 1) the cause of LGE in MR and 2) whether LGE increases arrhythmic risk. The results of these pilot studies are presented in Appendix I. The risk of ventricular arrhythmia was found to be low in the Mitral FINDER patients. I was also unable to delineate a clear relationship between MR subtype, mitral valve prolapse and LGE. Further research is therefore needed to investigate why LGE develop in MR. One theory, akin to how blood flow turbulence in aortic stenosis results in dilatation of the aorta (290), is that turbulent blood flow may increase left ventricular wall shear stress in a subgroup of MR patients. Increased shear stress in turn may stimulate focal LGE development. Recent developments in 4D phase-contrast CMR have allowed us to visualise intra-ventricular blood flow with quantification of its kinetic

energy (291, 292). This technique offers an avenue for future research on patients' differential vulnerability to develop myocardial fibrosis in MR.

### 8.3 Conclusion

The Mitral FINDER study provides definitive histological evidence for the presence of myocardial fibrosis in primary degenerative mitral regurgitation, before the development of symptoms or deterioration in cardiac function. Due to its patchy nature within the myocardium, ECV on CMR, but not fibrosis on histology, is a better marker of preoperative myocardial function and symptom status.

Contrary to our original hypothesis, biomarkers of fibrosis do not predict postoperative medium-term outcomes in patients with no or minimal symptoms.

Instead, we have identified additional support for the benefits of early surgery, with overtly symptomatic patients failing to reach completely symptom-free status despite successful repair. Findings from this study suggest that early surgery before the onset of symptoms is beneficial for patients. For older patients who are less willing and less likely to develop symptoms during their lifetime, there is cautious optimism that close surveillance, with detailed subjective and objective symptom burden quantification techniques, may provide adequate prognostic information for individualised clinical decision making.

## REFERENCES

1. Nkomo VT, Gardin JM, Skelton TN, Gottdiener JS, Scott CG, Enriquez-Sarano M. Burden of valvular heart diseases: a population-based study. *Lancet* (London, England). 2006;368(9540):1005-11.
2. Iung B, Baron G, Butchart EG, Delahaye F, Gohlke-Barwolf C, Levang OW, et al. A prospective survey of patients with valvular heart disease in Europe: The Euro Heart Survey on Valvular Heart Disease. *Eur Heart J*. 2003;24(13):1231-43.
3. Enriquez-Sarano M, Avierinos JF, Messika-Zeitoun D, Detaint D, Capps M, Nkomo V, et al. Quantitative determinants of the outcome of asymptomatic mitral regurgitation. *The New England journal of medicine*. 2005;352(9):875-83.
4. Tribouilloy CM, Enriquez-Sarano M, Schaff HV, Orszulak TA, Bailey KR, Tajik AJ, et al. Impact of preoperative symptoms on survival after surgical correction of organic mitral regurgitation - Rationale for optimizing surgical indications. *Circulation*. 1999;99(3):400-5.
5. David TE, Armstrong S, McCrindle BW, Manlihot C. Late Outcomes of Mitral Valve Repair for Mitral Regurgitation Due to Degenerative Disease. *Circulation*. 2013;127(14):1485-92.
6. Kang DH, Park SJ, Sun BJ, Cho EJ, Kim DH, Yun SC, et al. Early Surgery Versus Conventional Treatment for Asymptomatic Severe Mitral Regurgitation. *J Am Coll Cardiol*. 2014;63(22):2398-407.
7. Standring S, Gray H. *Gray's anatomy : the anatomical basis of clinical practice*. 39th ed. Standring S, editor: Churchill Livingstone/Elsevier; 2005.
8. Carpentier A. Cardiac-Valve Surgery - The French Correction. *J Thorac Cardiovasc Surg*. 1983;86(3):323-37.
9. Grewal J, Suri R, Mankad S, Tanaka A, Mahoney DW, Schaff HV, et al. Mitral Annular Dynamics in Myxomatous Valve Disease New Insights With Real-Time 3-Dimensional Echocardiography. *Circulation*. 2010;121(12):1423-31.
10. Ho SY. Anatomy of the mitral valve. *Heart*. 2002;88:5-10.
11. Walmsley T. The heart. In: Sharpey-Schafer E, Symington J, Bryce TH, eds. *Quain's Elements of Anatomy*. 11th ed. London: Longmans, Green & Co; 1929. 152 p.
12. Degandt AA, Weber PA, Saber HA, Duran CMG. Mitral valve basal chordae: Comparative anatomy and terminology. *Annals of Thoracic Surgery*. 2007;84(4):1250-5.
13. Rusted IE, Scheifley CH, Edwards JE, Kirklin JW. Guides to the commissures in operations upon the mitral valve. *Proceedings of the Staff Meetings of the Mayo Clinic*. 1951;26(16):297-305.
14. Asgar AW, Mack MJ, Stone GW. Secondary Mitral Regurgitation in Heart Failure Pathophysiology, Prognosis, and Therapeutic Considerations. *J Am Coll Cardiol*. 2015;65(12):1231-48.
15. Adams DH, Rosenhek R, Falk V. Degenerative mitral valve regurgitation: best practice revolution. *Eur Heart J*. 2010;31(16):1958-66.
16. Carpentier A, Lacourgayet F, Camilleri JP, Dubost C. Fibroelastic dysplasia of the mitral-valve - an anatomical and clinical entity. *Circulation*. 1980;62(4):207-.
17. Barlow JB, Pocock WA. The significance of late systolic murmurs and mid-late systolic clicks. *Maryland state medical journal*. 1963;12:76-7.

18. Enriquez-Sarano M, Basmadjian AJ, Rossi A, Bailey KR, Seward JB, Tajik AJ. Progression of mitral regurgitation - A prospective Doppler echocardiographic study. *J Am Coll Cardiol.* 1999;34(4):1137-44.
19. Viar WN, Harrison TR. Chest pain in association with pulmonary hypertension - its similarity to the pain of coronary disease. *Circulation.* 1952;5(1):1-11.
20. Nishimura RA, Otto CM, Bonow RO, Carabello BA, Erwin JP, 3rd, Guyton RA, et al. 2014 AHA/ACC guideline for the management of patients with valvular heart disease: a report of the American College of Cardiology/American Heart Association Task Force on Practice Guidelines. *J Am Coll Cardiol.* 2014;63(22):e57-185.
21. Selzer A, Katayama F. Mitral regurgitation: clinical patterns, pathophysiology and natural history. *Medicine.* 1972;51(5):337-66.
22. Ling LH, EnriquezSarano M, Seward JB, Tajik AJ, Schaff HV, Bailey KR, et al. Clinical outcome of mitral regurgitation due to flail leaflet. *N Engl J Med.* 1996;335(19):1417-23.
23. Dziadzko V, Clavel MA, Dziadzko M, Medina-Inojosa JR, Michelena H, Maalouf J, et al. Outcome and undertreatment of mitral regurgitation: a community cohort study. *Lancet (London, England).* 2018;391(10124):960-9.
24. Baumgartner H, Falk V, Bax JJ, De Bonis M, Hamm C, Holm PJ, et al. 2017 ESC/EACTS Guidelines for the management of valvular heart disease The Task Force for the Management of Valvular Heart Disease of the European Society of Cardiology (ESC) and the European Association for Cardio-Thoracic Surgery (EACTS). *Eur Heart J.* 2017;38(36):2739-+.
25. Nishimura RA, Otto CM, Bonow RO, Carabello BA, Erwin JP, Fleisher LA, et al. 2017 AHA/ACC Focused Update of the 2014 AHA/ACC Guideline for the Management of Patients With Valvular Heart Disease. *J Am Coll Cardiol.* 2017;70(2):252-89.
26. d'Arcy JL, Coffey S, Loudon MA, Kennedy A, Pearson-Stuttard J, Birks J, et al. Large-scale community echocardiographic screening reveals a major burden of undiagnosed valvular heart disease in older people: the OxVALVE Population Cohort Study. *Eur Heart J.* 2016.
27. Lancellotti P, Tribouilloy C, Hagendorff A, Popescu BA, Edvardsens T, Pierard LA, et al. Recommendations for the echocardiographic assessment of native valvular regurgitation: an executive summary from the European Association of Cardiovascular Imaging. *Eur Heart J-Cardiovasc Imaging.* 2013;14(7):611-2.
28. Chikwe J, Adams DH, Su KN, Anyanwu AC, Lin HM, Goldstone AB, et al. Can three-dimensional echocardiography accurately predict complexity of mitral valve repair? *Eur J Cardio-Thorac Surg.* 2012;41(3):518-24.
29. Liu B, Edwards NC, Pennell D, Steeds RP. The evolving role of cardiac magnetic resonance in primary mitral regurgitation: ready for prime time? *European heart journal cardiovascular Imaging.* 2019;20(2):123-30.
30. Vahanian A, Alfieri O, Andreotti F, Antunes MJ, Baron-Esquivias G, Baumgartner H, et al. Guidelines on the management of valvular heart disease (version 2012). *Eur Heart J.* 2012;33(19):2451-96.
31. Chan KMJ, Wage R, Symmonds K, Rahman-Haley S, Mohiaddin RH, Firmin DN, et al. Towards comprehensive assessment of mitral regurgitation using cardiovascular magnetic resonance. *Journal of Cardiovascular Magnetic Resonance.* 2008;10.
32. Han Y, Peters DC, Salton CJ, Bzymek D, Nezafat R, Goddu B, et al. Cardiovascular magnetic resonance characterization of mitral valve prolapse. *JACC Cardiovascular imaging.* 2008;1(3):294-303.

33. Gabriel RS, Kerr AJ, Raffel OC, Stewart RA, Cowan BR, Occleshaw CJ. Mapping of mitral regurgitant defects by cardiovascular magnetic resonance in moderate or severe mitral regurgitation secondary to mitral valve prolapse. *Journal of Cardiovascular Magnetic Resonance*. 2008;10:7.
34. Stork A, Franzen O, Ruschewski H, Detter C, Mullerleile K, Bansmann PM, et al. Assessment of functional anatomy of the mitral valve in patients with mitral regurgitation with cine magnetic resonance imaging: comparison with transesophageal echocardiography and surgical results. *Eur Radiol*. 2007;17(12):3189-98.
35. Salgo IS, Gorman JH, Gorman RC, Jackson BM, Bowen FW, Plappert T, et al. Effect of annular shape on leaflet curvature in reducing mitral leaflet stress. *Circulation*. 2002;106(6):711-7.
36. Obase K, Jeevanandam V, Saito K, Kesner K, Barry A, Hollatz A, et al. Visualization and Measurement of Mitral Valve Chordae Tendineae Using Three-Dimensional Transesophageal Echocardiography from the Transgastric Approach. *J Am Soc Echocardiogr*. 2015;28(4):449-54.
37. Sanfilippo AJ, Harrigan P, Popovic AD, Weyman AE, Levine RA. Papillary-muscle tracking in mitral-valve prolapse - quantitation by 2-dimensional echocardiography. *J Am Coll Cardiol*. 1992;19(3):564-71.
38. Fattouch K, Murana G, Castrovinci S, Mossuto C, Sampognaro R, Borruso MG, et al. Mitral valve annuloplasty and papillary muscle relocation oriented by 3-dimensional transesophageal echocardiography for severe functional mitral regurgitation. *J Thorac Cardiovasc Surg*. 2012;143(4):S38-S42.
39. Han YC, Peters DC, Kissinger KV, Goddu B, Yeon SB, Manning WJ, et al. Evaluation of Papillary Muscle Function Using Cardiovascular Magnetic Resonance Imaging in Mitral Valve Prolapse. *Am J Cardiol*. 2010;106(2):243-8.
40. Kılıçgedik A. Papillary Muscle Free Strain in Patients with Severe Degenerative and. 2017;108(4):339-46.
41. Basso C, Marra MP, Rizzo S, De Lazzari M, Giorgi B, Cipriani A, et al. Arrhythmic Mitral Valve Prolapse and Sudden Cardiac Death. *Circulation*. 2015;132(7):556-66.
42. Gornick CC, Tobler HG, Pritzker MC, Tuna IC, Almquist A, Benditt DG. Electrophysiological effects of papillary-muscle traction in the intact heart. *Circulation*. 1986;73(5):1013-21.
43. Zoghbi WA, Adams D, Bonow RO, Enriquez-Sarano M, Foster E, Grayburn PA, et al. Recommendations for Noninvasive Evaluation of Native Valvular Regurgitation: A Report from the American Society of Echocardiography Developed in Collaboration with the Society for Cardiovascular Magnetic Resonance. *Journal of the American Society of Echocardiography : official publication of the American Society of Echocardiography*. 2017.
44. Thavendiranathan P, Liu SZ, Datta S, Rajagopalan S, Ryan T, Igo SR, et al. Quantification of Chronic Functional Mitral Regurgitation by Automated 3-Dimensional Peak and Integrated Proximal Isovelocity Surface Area and Stroke Volume Techniques Using Real-Time 3-Dimensional Volume Color Doppler Echocardiography In Vitro and Clinical Validation. *Circ-Cardiovasc Imaging*. 2013;6(1):125-33.
45. Biner S, Rafique A, Rafii F, Tolstrup K, Noorani O, Shiota T, et al. Reproducibility of Proximal Isovelocity Surface Area, Vena Contracta, and Regurgitant Jet Area for Assessment of Mitral Regurgitation Severity. *Jacc-Cardiovascular Imaging*. 2010;3(3):235-43.

46. Penicka M, Vecera J, Mirica DC, Kotrc M, Kockova R, Van Camp G. Prognostic Implications of Magnetic Resonance-Derived Quantification in Asymptomatic Patients With Organic Mitral Regurgitation: Comparison With Doppler Echocardiography-Derived Integrative Approach. *Circulation*. 2018;137(13):1349-60.
47. Wang A, Grayburn P, Foster JA, McCulloch ML, Badhwar V, Gammie JS, et al. Practice gaps in the care of mitral valve regurgitation: Insights from the American College of Cardiology mitral regurgitation gap analysis and advisory panel. *Am Heart J*. 2016;172:70-9.
48. Hundley WG, Li HF, Willard JE, Landau C, Lange RA, Meshack BM, et al. Magnetic-resonance-imaging assessment of the severity of mitral regurgitation - comparison with invasive techniques. *Circulation*. 1995;92(5):1151-8.
49. Kizilbash AM, Hundley WG, Willett DL, Franco F, Peshock RM, Grayburn PA. Comparison of quantitative Doppler with magnetic resonance imaging for assessment of the severity of mitral regurgitation. *Am J Cardiol*. 1998;81(6):792-5.
50. Cawley PJ, Hamilton-Craig C, Owens DS, Krieger EV, Strugnell WE, Mitsumori L, et al. Prospective Comparison of Valve Regurgitation Quantitation by Cardiac Magnetic Resonance Imaging and Transthoracic Echocardiography-3. *Circ-Cardiovasc Imaging*. 2013;6(1):48-57.
51. Lopez-Mattei JC, Ibrahim H, Shaikh KA, Little SH, Shah DJ, Maragiannis D, et al. Comparative Assessment of Mitral Regurgitation Severity by Transthoracic Echocardiography and Cardiac Magnetic Resonance Using an Integrative and Quantitative Approach. *Am J Cardiol*. 2016;117(2):264-70.
52. Aplin M, Kyhl K, Bjerre J, Ihlemann N, Greenwood JP, Plein S, et al. Cardiac remodelling and function with primary mitral valve insufficiency studied by magnetic resonance imaging. *European heart journal cardiovascular Imaging*. 2016;17(8):863-70.
53. Myerson SG, d'Arcy J, Christiansen JP, Dobson LE, Mohiaddin R, Francis JM, et al. Determination of Clinical Outcome in Mitral Regurgitation With Cardiovascular Magnetic Resonance Quantification. *Circulation*. 2016;133(23):2287-96.
54. Bertelsen L, Svendsen JH, Kober L, Haugan K, Hojberg S, Thomsen C, et al. Flow measurement at the aortic root - impact of location of through-plane phase contrast velocity mapping. *Journal of cardiovascular magnetic resonance : official journal of the Society for Cardiovascular Magnetic Resonance*. 2016;18(1):55.
55. De Bonis M, Al-Attar N, Antunes M, Borger M, Casselman F, Falk V, et al. Surgical and interventional management of mitral valve regurgitation: a position statement from the European Society of Cardiology Working Groups on Cardiovascular Surgery and Valvular Heart Disease. *Eur Heart J*. 2016;37(2):133-9.
56. Zhou YX, Leobon B, Berthoumieu P, Roux D, Glock Y, Mei YQ, et al. Long-term outcomes following repair or replacement in degenerative mitral valve disease. *The Thoracic and cardiovascular surgeon*. 2010;58(7):415-21.
57. Suri RM, Schaff HV, Dearani JA, Sundt TM, 3rd, Daly RC, Mullany CJ, et al. Survival advantage and improved durability of mitral repair for leaflet prolapse subsets in the current era. *The Annals of thoracic surgery*. 2006;82(3):819-26.
58. Gillinov AM, Blackstone EH, Nowicki ER, Slisatkorn W, Al-Dossari G, Johnston DR, et al. Valve repair versus valve replacement for degenerative mitral valve disease. *The Journal of thoracic and cardiovascular surgery*. 2008;135(4):885-93, 93.e1-2.
59. Vassileva CM, Mishkel G, McNeely C, Boley T, Markwell S, Scaife S, et al. Long-term survival of patients undergoing mitral valve repair and replacement: a longitudinal analysis of Medicare fee-for-service beneficiaries. *Circulation*. 2013;127(18):1870-6.



60. Enriquez-Sarano M, Akins CW, Vahanian A. Mitral regurgitation. *Lancet* (London, England). 2009;373(9672):1382-94.
61. Braunberger E, Deloche A, Berrebi A, Abdallah F, Celestin JA, Meimoun P, et al. Very long-term results (more than 20 years) of valve repair with Carpentier's techniques in nonrheumatic mitral valve insufficiency. *Circulation*. 2001;104(12):I8-I11.
62. Castillo JG, Anyanwu AC, Fuster V, Adams DH. A near 100% repair rate for mitral valve prolapse is achievable in a reference center: implications for future guidelines. *The Journal of thoracic and cardiovascular surgery*. 2012;144(2):308-12.
63. David TE, Ivanov J, Armstrong S, Rakowski H. Late outcomes of mitral valve repair for floppy valves: Implications for asymptomatic patients. *J Thorac Cardiovasc Surg*. 2003;125(5):1143-52.
64. EnriquezSarano M, Tajik AJ, Schaff HV, Orszulak TA, Bailey KR, Frye RL. Echocardiographic prediction of survival after surgical-correction of organic mitral regurgitation. *Circulation*. 1994;90(2):830-7.
65. Tribouilloy C, Grigioni F, Avierinos JF, Barbieri A, Rusinaru D, Szymanski C, et al. Survival Implication of Left Ventricular End-Systolic Diameter in Mitral Regurgitation Due to Flail Leaflets A Long-Term Follow-Up Multicenter Study. *J Am Coll Cardiol*. 2009;54(21):1961-8.
66. Ngaage DL, Schaff HV, Mullany CJ, Barnes S, Dearani JA, Daly RC, et al. Influence of Preoperative atrial fibrillation on late results of mitral repair: Is concomitant ablation justified? *Annals of Thoracic Surgery*. 2007;84(2):434-43.
67. Szymanski C, Magne J, Fournier A, Rusinaru D, Touati G, Tribouilloy C. Usefulness of Preoperative Atrial Fibrillation to Predict Outcome and Left Ventricular Dysfunction After Valve Repair for Mitral Valve Prolapse. *Am J Cardiol*. 2015;115(10):1448-53.
68. Kang DH, Kim JH, Rim JH, Kim MJ, Yun SC, Song JM, et al. Comparison of Early Surgery Versus Conventional Treatment in Asymptomatic Severe Mitral Regurgitation. *Circulation*. 2009;119(6):797-804.
69. Barbieri A, Bursi F, Grigioni F, Tribouilloy C, Avierinos JF, Michelena HI, et al. Prognostic and therapeutic implications of pulmonary hypertension complicating degenerative mitral regurgitation due to flail leaflet: A Multicenter Long-term International Study. *Eur Heart J*. 2011;32(6):751-9.
70. Goldstone AB, Patrick WL, Cohen JE, Aribeara CN, Popat R, Woo YJ. Early surgical intervention or watchful waiting for the management of asymptomatic mitral regurgitation: a systematic review and meta-analysis. *Ann Cardiothorac Surg*. 2015;4(3):220-9.
71. Suri RM, Vanoverschelde JL, Grigioni F, Schaff HV, Tribouilloy C, Avierinos JF, et al. Association Between Early Surgical Intervention vs Watchful Waiting and Outcomes for Mitral Regurgitation Due to Flail Mitral Valve Leaflets. *Jama-Journal of the American Medical Association*. 2013;310(6):609-16.
72. Shadish WR, Cook TD, T. CD. *Experimental and Quasi-Experimental Designs for Generalized Causal Inference*: Wadsworth Publishing; 2001. 656 p.
73. King G, Nielsen R. Why Propensity Scores Should Not Be Used for Matching. *Political Analysis*. 2019;27:1-20.
74. Bolling SF, Li SA, O'Brien SM, Brennan JM, Prager RL, Gammie JS. Predictors of Mitral Valve Repair: Clinical and Surgeon Factors. *Annals of Thoracic Surgery*. 2010;90(6):1904-12.

75. Gammie JS, O'Brien SM, Griffith BP, Ferguson TB, Peterson ED. Influence of hospital procedural volume on care process and mortality for patients undergoing elective surgery for mitral regurgitation. *Circulation*. 2007;115(7):881-7.
76. Ray S. UK Early Mitral Surgery Trial: British Heart Foundation; 2015 [BHF CS/15/2/31331]. Available from: <https://www.bhf.org.uk/research-projects/uk-early-mitral-surgery-trial>.
77. SCTS TSfCSiGBI. Blue Book Online <http://bluebook.scts.org/>: The Society for Cardiothoracic Surgery in Great Britain & Ireland; 2015 [Available from: <http://bluebook.scts.org/>].
78. Suri RM, Clavel M-A, Schaff HV, Michelena HI, Huebner M, Nishimura RA, et al. Effect of Recurrent Mitral Regurgitation Following Degenerative Mitral Valve Repair Long-Term Analysis of Competing Outcomes. *J Am Coll Cardiol*. 2016;67(5):488-98.
79. Rosenhek R, Rader F, Klaat U, Gabriel H, Krejc M, Kalbeck D, et al. Outcome of watchful waiting in asymptomatic severe mitral regurgitation. *Circulation*. 2006;113(18):2238-44.
80. Enriquez-Sarano M, Suri RM, Clavel MA, Mantovani F, Michelena HI, Pislaru S, et al. Is there an outcome penalty linked to guideline-based indications for valvular surgery? Early and long-term analysis of patients with organic mitral regurgitation. *J Thorac Cardiovasc Surg*. 2015;150(1):50-8.
81. Gillam LD, Schwartz A. Primum non nocere: the case for watchful waiting in asymptomatic "severe" degenerative mitral regurgitation. *Circulation*. 2010;121(6):813-21; discussion 21.
82. Enriquez-Sarano M, Sundt TM, 3rd. Early surgery is recommended for mitral regurgitation. *Circulation*. 2010;121(6):804-11; discussion 12.
83. Quintana E, Suri RM, Thalji NM, Daly RC, Dearani JA, Burkhart HM, et al. Left ventricular dysfunction after mitral valve repair-the fallacy of "normal" preoperative myocardial function. *J Thorac Cardiovasc Surg*. 2014;148(6):2752-60.
84. Treibel TA, Lopez B, Gonzalez A, Menacho K, Schofield RS, Ravassa S, et al. Reappraising myocardial fibrosis in severe aortic stenosis: an invasive and non-invasive study in 133 patients. *Eur Heart J*. 2018;39(8):699-709.
85. Weber KT. Cardiac interstitium in health and disease - the fibrillar collagen network. *J Am Coll Cardiol*. 1989;13(7):1637-52.
86. Macchiarelli G, Ohtani O, Nottola SA, Stallone T, Camboni A, Prado IM, et al. A micro-anatomical model of the distribution of myocardial endomysial collagen. *Histology and Histopathology*. 2002;17(3):699-706.
87. Lionetti V, Bianchi G, Recchia FA, Ventura C. Control of autocrine and paracrine myocardial signals: an emerging therapeutic strategy in heart failure. *Heart Failure Reviews*. 2010;15(6):531-42.
88. Weber KT, Janicki JS, Shroff SG, Pick R, Chen RM, Bashey RI. Collagen remodeling of the pressure-overloaded, hypertrophied nonhuman primate myocardium. *Circulation research*. 1988;62(4):757-65.
89. Mewton N, Liu CY, Croisille P, Bluemke D, Lima JAC. Assessment of Myocardial Fibrosis With Cardiovascular Magnetic Resonance. *J Am Coll Cardiol*. 2011;57(8):891-903.
90. Laurent GJ, Sparrow MP, Bates PC, Millward DJ. Turnover of muscle protein in fowl - collagen content and turnover in cardiac and skeletal-muscle of adult fowl and changes during stretch-induced growth. *Biochemical Journal*. 1978;176(2):419-27.

91. Bonnin CM, Sparrow MP, Taylor RR. Collagen-synthesis and content in right ventricular-hypertrophy in the dog. *American Journal of Physiology*. 1981;241(5):H708-H13.
92. Grove D, Zak R, Nair KG, Aschenbr.V. Biochemical correlates of cardiac hypertrophy. Observations on cellular organization of growth during myocardial hypertrophy in rat. *Circulation research*. 1969;25(4):473-&.
93. Kong P, Christia P, Frangogiannis NG. The pathogenesis of cardiac fibrosis. *Cellular and Molecular Life Sciences*. 2014;71(4):549-74.
94. Travers JG, Kamal FA, Robbins J, Yutzey KE, Blaxall BC. Cardiac Fibrosis: The Fibroblast Awakens. *Circulation research*. 2016;118(6):1021-40.
95. Berk BC, Fujiwara K, Lehoux S. ECM remodeling in hypertensive heart disease. *Journal of Clinical Investigation*. 2007;117(3):568-75.
96. Li YY, McTiernan CF, Feldman AM. Interplay of matrix metalloproteinases, tissue inhibitors of metalloproteinases and their regulators in cardiac matrix remodeling. *Cardiovascular research*. 2000;46(2):214-24.
97. Brower GL, Chancey AL, Thanigaraj S, Matsubara BB, Janicki JS. Cause and effect relationship between myocardial mast cell number and matrix metalloproteinase activity. *American journal of physiology Heart and circulatory physiology*. 2002;283(2):H518-25.
98. Brower GL, Janicki JS. Pharmacologic inhibition of mast cell degranulation prevents left ventricular remodeling induced by chronic volume overload in rats. *J Card Fail*. 2005;11(7):548-56.
99. Petrov VV, Fagard RH, Lijnen PJ. Stimulation of collagen production by transforming growth factor-beta1 during differentiation of cardiac fibroblasts to myofibroblasts. *Hypertension*. 2002;39(2):258-63.
100. Watkins SJ, Jonker L, Arthur HM. A direct interaction between TGFbeta activated kinase 1 and the TGFbeta type II receptor: implications for TGFbeta signalling and cardiac hypertrophy. *Cardiovascular research*. 2006;69(2):432-9.
101. Brower GL, Henegar JR, Janicki JS. Temporal evaluation of left ventricular remodeling and function in rats with chronic volume overload. *American Journal of Physiology-Heart and Circulatory Physiology*. 1996;271(5):H2071-H8.
102. Brower GL, Janicki JS. Contribution of ventricular remodeling to pathogenesis of heart failure in rats. *American Journal of Physiology-Heart and Circulatory Physiology*. 2001;280(2):H674-H83.
103. Leroux AA, Moonen ML, Pierard LA, Kolh P, Amory H. Animal Models of Mitral Regurgitation Induced by Mitral Valve Chordae Tendineae Rupture. *J Heart Valve Dis*. 2012;21(4):416-23.
104. Kim KH, Kim YJ, Lee SP, Kim HK, Seo JW, Sohn DW, et al. Survival, Exercise Capacity, and Left Ventricular Remodeling in a Rat Model of Chronic Mitral Regurgitation: Serial Echocardiography and Pressure-Volume Analysis. *Korean Circ J*. 2011;41(10):603-11.
105. Gulch RW, Jacob R. Geometric and muscle physiological determinants of cardiac stroke volume as evaluated on the basis of model-calculations. *Basic Research in Cardiology*. 1988;83(5):476-85.
106. Linzbach AJ. Heart failure from the point of view of quantitative anatomy. *Am J Cardiol*. 1960;5(3):370-82.
107. Gaasch WH, Meyer TE. Left Ventricular Response to Mitral Regurgitation Implications for Management. *Circulation*. 2008;118(22):2298-303.

108. Carabello BA. Mitral valve regurgitation. *Current problems in cardiology*. 1998;23(4):202-41.
109. Gaasch WH, Shah SP, Labib SB, Meyer TE. Impedance to retrograde and forward flow in chronic mitral regurgitation and the physiology of a double outlet ventricle. *Heart*. 2017;103(8):581-5.
110. Schiros CG, Dell'Italia LJ, Gladden JD, Clark D, Aban I, Gupta H, et al. Magnetic Resonance Imaging With 3-Dimensional Analysis of Left Ventricular Remodeling in Isolated Mitral Regurgitation Implications Beyond Dimensions. *Circulation*. 2012;125(19):2334-+.
111. Matsumura T, Ohtaki E, Tanaka K, Misu K, Tobaru T, Asano R, et al. Echo cardiographic prediction of left ventricular dysfunction after mitral valve repair for mitral regurgitation as an indicator to decide the optimal timing of repair. *J Am Coll Cardiol*. 2003;42(3):458-63.
112. Agricola E, Galderisi M, Oppizzi M, Schinkel AFL, Maisano F, De Bonis M, et al. Pulsed tissue Doppler imaging detects early myocardial dysfunction in asymptomatic patients with severe mitral regurgitation. *Heart*. 2004;90(4):406-10.
113. Magne J, Mahjoub H, Pierard LA, O'Connor K, Pirllet C, Pibarot P, et al. Prognostic importance of brain natriuretic peptide and left ventricular longitudinal function in asymptomatic degenerative mitral regurgitation. *Heart*. 2012;98(7):584-91.
114. Cho EJ, Park SJ, Yun HR, Jeong DS, Lee SC, Park SW, et al. Predicting Left Ventricular Dysfunction after Surgery in Patients with Chronic Mitral Regurgitation: Assessment of Myocardial Deformation by 2-Dimensional Multilayer Speckle Tracking Echocardiography. *Korean Circ J*. 2016;46(2):213-21.
115. Le Tourneau T, Messika-Zeitoun D, Russo A, Detaint D, Topilsky Y, Mahoney DW, et al. Impact of Left Atrial Volume on Clinical Outcome in Organic Mitral Regurgitation. *J Am Coll Cardiol*. 2010;56(7):570-8.
116. Le Tourneau T, Deswarte G, Lamblin N, Foucher-Hossein C, Fayad G, Richardson M, et al. Right Ventricular Systolic Function in Organic Mitral Regurgitation Impact of Biventricular Impairment. *Circulation*. 2013;127(15):1597-608.
117. Song Y, Lee S, Kwak YL, Shim CY, Chang BC, Shim JK. Tissue Doppler Imaging Predicts Left Ventricular Reverse Remodeling After Surgery for Mitral Regurgitation. *Annals of Thoracic Surgery*. 2013;96(6):2109-15.
118. Fuster V, Danielson MA, Robb RA, Broadbent JC, Brown AL, Elveback LR. Quantitation of left-ventricular myocardial fiber hypertrophy and interstitial-tissue in human hearts with chronically increased volume and pressure overload. *Circulation*. 1977;55(3):504-8.
119. Kammerlander AA, Marzluf BA, Zotter-Tufaro C, Aschauer S, Duca F, Bachmann A, et al. T1 Mapping by CMR Imaging From Histological Validation to Clinical Implication. *Jacc-Cardiovascular Imaging*. 2016;9(1):14-23.
120. Miller CA, Naish JH, Bishop P, Coutts G, Clark D, Zhao S, et al. Comprehensive Validation of Cardiovascular Magnetic Resonance Techniques for the Assessment of Myocardial Extracellular Volume. *Circ-Cardiovasc Imaging*. 2013;6(3):373-+.
121. Lepojarvi ES, Piira OP, Paakko E, Lammentausta E, Risteli J, Miettinen JA, et al. Serum PINP, PIIINP, galectin-3, and ST2 as surrogates of myocardial fibrosis and echocardiographic left ventricular diastolic filling properties. *Front Physiol*. 2015;6:6.
122. Plaksej R, Kosmala W, Frantz S, Herrmann S, Niemann M, Stork S, et al. Relation of circulating markers of fibrosis and progression of left and right ventricular dysfunction in hypertensive patients with heart failure. *J Hypertens*. 2009;27(12):2483-91.

123. Cicoira M, Rossi A, Bonapace S, Zanolla L, Golia G, Franceschini L, et al. Independent and additional prognostic value of aminoterminal propeptide of type III procollagen circulating levels in patients with chronic heart failure. *J Card Fail.* 2004;10(5):403-11.
124. Moreo A, Ambrosio G, De Chiara B, Pu M, Tran T, Mauri F, et al. Influence of Myocardial Fibrosis on Left Ventricular Diastolic Function Noninvasive Assessment by Cardiac Magnetic Resonance and Echo. *Circ-Cardiovasc Imaging.* 2009;2(6):437-43.
125. Blessberger H, Binder T. Two dimensional speckle tracking echocardiography: basic principles. *Heart.* 2010;96(9):716-22.
126. Lancellotti P, Cosyns B, Zacharakis D, Attenu E, Van Camp G, Gach O, et al. Importance of Left Ventricular Longitudinal Function and Functional Reserve in Patients With Degenerative Mitral Regurgitation: Assessment by Two-Dimensional Speckle Tracking. *J Am Soc Echocardiogr.* 2008;21(12):1331-6.
127. Moody WE, Taylor RJ, Edwards NC, Chue CD, Umar F, Taylor TJ, et al. Comparison of Magnetic Resonance Feature Tracking for Systolic and Diastolic Strain and Strain Rate Calculation With Spatial Modulation of Magnetization Imaging Analysis. *J Magn Reson Imaging.* 2015;41(4):1000-12.
128. Salerno M. Feature Tracking by CMR: A "Double Feature"? *JACC Cardiovascular imaging.* 2017.
129. Circle CI-. Tissue Tracking Plugin 2018 [Available from: <https://www.circlecvi.com/features/product-plugins/plugins-research/tissue-tracking.php>.
130. Holland MR, Wallace KD, Miller JG. Potential relationships among myocardial stiffness, the measured level of myocardial backscatter ("image brightness"), and the magnitude of the systematic variation of backscatter (cyclic variation) over the heart cycle. *J Am Soc Echocardiogr.* 2004;17(11):1131-7.
131. Lythall DA, Bishop J, Greenbaum RA, Ilsley CJD, Mitchell AG, Gibson DG, et al. Relationship between myocardial collagen and echo amplitude in non-fibrotic hearts. *Eur Heart J.* 1993;14(3):344-50.
132. Sheppard MN, Steriotis AK, Sharma S. Letter by Sheppard et al Regarding Article, "Arrhythmic Mitral Valve Prolapse and Sudden Cardiac Death". *Circulation.* 2016;133(13):E458-E.
133. Kellman P, Hansen MS. T1-mapping in the heart: accuracy and precision. *Journal of Cardiovascular Magnetic Resonance.* 2014;16.
134. Moon JC. What is late gadolinium enhancement in hypertrophic cardiomyopathy? *Revista Espanola De Cardiologia.* 2007;60(1):1-4.
135. Pennell DJ, Sechtem UP, Higgins CB, Manning WJ, Pohost GM, Rademakers FE, et al. Clinical indications for cardiovascular magnetic resonance (CMR): Consensus Pane report. *Eur Heart J.* 2004;25(21):1940-65.
136. Hunold P, Schlosser T, Vogt FM, Eggebrecht H, Schmermund A, Bruder O, et al. Myocardial late enhancement in contrast-enhanced cardiac MRI: Distinction between infarction scar and non-infarction-related disease. *American Journal of Roentgenology.* 2005;184(5):1420-6.
137. Wong TC, Piehler KM, Zareba KM, Lin K, Phrampus A, Patel A, et al. Myocardial Damage Detected by Late Gadolinium Enhancement Cardiovascular Magnetic Resonance Is Associated With Subsequent Hospitalization for Heart Failure. *Journal of the American Heart Association.* 2013;2(6).

138. Lee JJ, Liu S, Nacif MS, Ugander M, Han J, Kawel N, et al. Myocardial T1 and Extracellular Volume Fraction Mapping at 3 Tesla. *Journal of Cardiovascular Magnetic Resonance*. 2011;13.
139. Piechnik SK, Ferreira VM, Dall'Armellina E, Cochlin LE, Greiser A, Neubauer S, et al. Shortened Modified Look-Locker Inversion recovery (ShMOLLI) for clinical myocardial T1-mapping at 1.5 and 3 T within a 9 heartbeat breathhold. *Journal of Cardiovascular Magnetic Resonance*. 2010;12.
140. de Ravenstein CdM, Bouzin C, Lazam S, Boulif J, Amzulescu M, Melchior J, et al. Histological Validation of measurement of diffuse interstitial myocardial fibrosis by myocardial extravascular volume fraction from Modified Look-Locker imaging (MOLLI) T1 mapping at 3 T. *Journal of Cardiovascular Magnetic Resonance*. 2015;17.
141. Schelbert EB, Piehler KM, Zareba KM, Moon JC, Ugander M, Messroghli DR, et al. Myocardial Fibrosis Quantified by Extracellular Volume Is Associated With Subsequent Hospitalization for Heart Failure, Death, or Both Across the Spectrum of Ejection Fraction and Heart Failure Stage. *Journal of the American Heart Association*. 2015;4(12).
142. Verhaert D, Thavendiranathan P, Giri S, Mihai G, Rajagopalan S, Simonetti OP, et al. Direct T2 quantification of myocardial edema in acute ischemic injury. *JACC Cardiovascular imaging*. 2011;4(3):269-78.
143. Thavendiranathan P, Walls M, Giri S, Verhaert D, Rajagopalan S, Moore S, et al. Improved detection of myocardial involvement in acute inflammatory cardiomyopathies using T2 mapping. *Circulation Cardiovascular imaging*. 2012;5(1):102-10.
144. Usman AA, Taimen K, Wasielewski M, McDonald J, Shah S, Giri S, et al. Cardiac magnetic resonance T2 mapping in the monitoring and follow-up of acute cardiac transplant rejection: a pilot study. *Circulation Cardiovascular imaging*. 2012;5(6):782-90.
145. Le Tourneau T, Richardson M, Juthier F, Modine T, Fayad G, Polge AS, et al. Echocardiography predictors and prognostic value of pulmonary artery systolic pressure in chronic organic mitral regurgitation. *Heart*. 2010;96(16):1311-7.
146. Roujol S, Weingartner S, Foppa M, Chow K, Kawaji K, Ngo LH, et al. Accuracy, precision, and reproducibility of four T1 mapping sequences: a head-to-head comparison of MOLLI, ShMOLLI, SASHA, and SAPPHERE. *Radiology*. 2014;272(3):683-9.
147. Edwards NC, Moody WE, Yuan MS, Weale P, Neal D, Townend JN, et al. Quantification of Left Ventricular Interstitial Fibrosis in Asymptomatic Chronic Primary Degenerative Mitral Regurgitation. *Circ-Cardiovasc Imaging*. 2014;7(6):946-53.
148. Borg AN, Harrison JL, Argyle RA, Pearce KA, Beynon R, Ray SG. Left ventricular fitting and diastolic myocardial deformation in chronic primary mitral regurgitation. *European Journal of Echocardiography*. 2010;11(6):523-9.
149. Jellis C, Martin J, Narula J, Marwick TH. Assessment of nonischemic myocardial fibrosis. *J Am Coll Cardiol*. 2010;56(2):89-97.
150. Reyhan M, Wang Z, Li M, Kim HJ, Gupta HS, Lloyd SG, et al. Left ventricular twist and shear in patients with primary mitral regurgitation. *J Magn Reson Imaging*. 2015;42(2):400-6.
151. Witkowski TG, Thomas JD, Debonnaire P, Delgado V, Hoke U, Ewe SH, et al. Global longitudinal strain predicts left ventricular dysfunction after mitral valve repair. *Eur Heart J-Cardiovasc Imaging*. 2013;14(1):69-76.
152. Liu B, Edwards NC, Neal DAH, Weston C, Nash G, Nikolaidis N, et al. A prospective study examining the role of myocardial Fibrosis in outcome following mitral

- valve repair IN DEgenerative mitral Regurgitation: rationale and design of the mitral FINDER study. *BMC cardiovascular disorders*. 2017;17(1):282.
153. Crandon S, Elbaz MSM, Westenberg JJM, van der Geest RJ, Plein S, Garg P. Clinical applications of intra-cardiac four-dimensional flow cardiovascular magnetic resonance: A systematic review. *Int J Cardiol*. 2017;249:486-93.
154. Gaasch WH, Meyer TE. Secondary mitral regurgitation (part 1): volumetric quantification and analysis. *Heart*. 2018;104(8):634-8.
155. Goldstein D, Moskowitz AJ, Gelijns AC, Ailawadi G, Parides MK, Perrault LP, et al. Two-Year Outcomes of Surgical Treatment of Severe Ischemic Mitral Regurgitation. *N Engl J Med*. 2016;374(4):344-53.
156. Le V, Jensen GV, Kjoller-Hansen L. Prognostic Usefulness of Cardiopulmonary Exercise Testing for Managing Patients With Severe Aortic Stenosis. *Am J Cardiol*. 2017;120(5):844-9.
157. Taichman DB, McGoon MD, Harhay MO, Archer-Chicko C, Sager JS, Murugappan M, et al. Wide Variation in Clinicians' Assessment of New York Heart Association/World Health Organization Functional Class in Patients With Pulmonary Arterial Hypertension. *Mayo Clinic Proceedings*. 2009;84(7):586-92.
158. Garin O, Herdman M, Vilagut G, Ferrer M, Ribera A, Rajmil L, et al. Assessing health-related quality of life in patients with heart failure: a systematic, standardized comparison of available measures. *Heart Failure Reviews*. 2014;19(3):359-67.
159. Middel B, Bouma J, do Jongste M, van Sonderen E, Niemeijer MG, Crijns H, et al. Psychometric properties of the Minnesota Living with Heart Failure Questionnaire (MLHF-Q). *Clinical Rehabilitation*. 2001;15(5):489-500.
160. Ware JE, Jr., Sherbourne CD. The MOS 36-item short-form health survey (SF-36). I. Conceptual framework and item selection. *Medical care*. 1992;30(6):473-83.
161. Lahoud R, Brennan D, Cho L. Comparing SF-36 score versus biomarkers to predict mortality in primary cardiac prevention patients. *J Am Coll Cardiol*. 2014;63(12):A1383-A.
162. Hansen L, Winkel S, Kuhr J, Bader R, Bleese N, Riess FC. Factors influencing survival and postoperative quality of life after mitral valve reconstruction. *European journal of cardio-thoracic surgery : official journal of the European Association for Cardio-thoracic Surgery*. 2010;37(3):635-44.
163. Wharton G, Steeds R, Allen J, Phillips H, Jones R, Kanagala P, et al. A minimum dataset for a standard adult transthoracic echocardiogram: a guideline protocol from the British Society of Echocardiography. *Echo Res Pract*. 2015;2(1):G9-g24.
164. Wheeler R, Steeds R, Rana B, Wharton G, Smith N, Allen J, et al. A minimum dataset for a standard transoesophageal echocardiogram: a guideline protocol from the British Society of Echocardiography. *Echo Res Pract*. 2015;2(4):G29-G45.
165. Rodevand O, Bjornerheim R, Ljosland M, Maehle J, Smith HJ, Ihlen H. Left atrial volumes assessed by three- and two-dimensional echocardiography compared to MRI estimates. *Int J Card Imaging*. 1999;15(5):397-410.
166. Maceira AM, Prasad SK, Khan M, Pennell DJ. Normalized left ventricular systolic and diastolic function by steady state free precession cardiovascular magnetic resonance. *Journal of Cardiovascular Magnetic Resonance*. 2006;8(3):417-26.
167. Fratz S, Chung T, Greil GF, Samyn MM, Taylor AM, Buechel ERV, et al. Guidelines and protocols for cardiovascular magnetic resonance in children and adults with congenital heart disease: SCMR expert consensus group on congenital heart disease. *Journal of Cardiovascular Magnetic Resonance*. 2013;15.

168. Kellman P, Arai AE. Cardiac imaging techniques for physicians: late enhancement. *Journal of magnetic resonance imaging : JMRI*. 2012;36(3):529-42.
169. Messroghli DR, Radjenovic A, Kozerke S, Higgins DM, Sivananthan MU, Ridgway JP. Modified Look-Locker inversion recovery (MOLLI) for high-resolution T1 mapping of the heart. *Magnetic resonance in medicine*. 2004;52(1):141-6.
170. Moon JC, Messroghli DR, Kellman P, Piechnik SK, Robson MD, Ugander M, et al. Myocardial T1 mapping and extracellular volume quantification: a Society for Cardiovascular Magnetic Resonance (SCMR) and CMR Working Group of the European Society of Cardiology consensus statement. *Journal of cardiovascular magnetic resonance : official journal of the Society for Cardiovascular Magnetic Resonance*. 2013;15:92.
171. Captur G, Gatehouse P, Keenan KE, Heslinga FG, Bruehl R, Prothmann M, et al. A medical device-grade T1 and ECV phantom for global T1 mapping quality assurance—the T-1 Mapping and ECV Standardization in cardiovascular magnetic resonance (TIMES) program. *Journal of Cardiovascular Magnetic Resonance*. 2016;18.
172. Hayer MK, Radhakrishnan A, Price AM, Baig S, Liu B, Ferro CJ, et al. Early effects of kidney transplantation on the heart - A cardiac magnetic resonance multi-parametric study. *International Journal of Cardiology*. 2019.
173. Kehr E, Sono M, Chugh SS, Jerosch-Herold M. Gadolinium-enhanced magnetic resonance imaging for detection and quantification of fibrosis in human myocardium in vitro. *The international journal of cardiovascular imaging*. 2008;24(1):61-8.
174. Vijapurapu R, Hawkins F, Liu BY, Edwards N, Steeds R. A study of the different methodologies used in calculation of extra-cellular volume by CMR imaging. *Heart*. 2018;104:A14-A5.
175. Cerqueira MD, Weissman NJ, Dilsizian V, Jacobs AK, Kaul S, Laskey WK, et al. Standardized myocardial segmentation and nomenclature for tomographic imaging of the heart - A statement for healthcare professionals from the Cardiac Imaging Committee of the Council on Clinical Cardiology of the American Heart Association. *Circulation*. 2002;105(4):539-42.
176. Liu B, Dardeer AM, Moody WE, Hayer MK, Baig S, Price AM, et al. Reference ranges for three-dimensional feature tracking cardiac magnetic resonance: comparison with two-dimensional methodology and relevance of age and gender. *The international journal of cardiovascular imaging*. 2017.
177. Liu B, Dardeer AM, Moody WE, Edwards NC, Hudsmith LE, Steeds RP. Normal values for myocardial deformation within the right heart measured by feature-tracking cardiovascular magnetic resonance imaging. *Int J Cardiol*. 2018;252:220-3.
178. Hamada-Harimura Y, Seo Y, Ishizu T, Nishi I, Machino-Ohtsuka T, Yamamoto M, et al. Incremental Prognostic Value of Right Ventricular Strain in Patients With Acute Decompensated Heart Failure. *Circ-Cardiovasc Imaging*. 2018;11(10).
179. Ross RM. ATS/ACCP statement on cardiopulmonary exercise testing. *American journal of respiratory and critical care medicine*. 2003;167(10):1451; author reply
180. Triantafyllidi H, Kotsas K, Trivilou P, Orfanos SE, Lekakis J, Kremastinos D, et al. The importance of cardiopulmonary exercise testing in the diagnosis, prognosis and monitoring of patients with pulmonary arterial hypertension. *Hellenic journal of cardiology : HJC = Hellenike kardiologike epitheoresi*. 2010;51(3):245-9.
181. Beaver WL, Wasserman K, Whipp BJ. A new method for detecting anaerobic threshold by gas-exchange. *J Appl Physiol*. 1986;60(6):2020-7.



182. MacGowan GA, Janosko K, Cecchetti A, Murali S. Exercise-related ventilatory abnormalities and survival in congestive heart failure. *The American journal of cardiology*. 1997;79(9):1264-6.
183. Sadoul N, Prasad K, Elliott PM, Bannerjee S, Frenneaux MP, McKenna WJ. Prospective prognostic assessment of blood pressure response during exercise in patients with hypertrophic cardiomyopathy. *Circulation*. 1997;96(9):2987-91.
184. Brubaker PH, Kitzman DW. Chronotropic incompetence: causes, consequences, and management. *Circulation*. 2011;123(9):1010-20.
185. Ahmad MN, Yusuf SH, Ullah R, Ahmad MM, Ellis MK, Yousaf H, et al. Multivariate Criteria Most Accurately Distinguish Cardiac from Noncardiac Causes of Dyspnea. *Tex Heart Inst J*. 2015;42(6):514-21.
186. Wasserman K, Hansen JE, Sietsema K, Sue DY, Stringer WW, Sun XG, et al. *Principles of Exercise Testing and Interpretation: Including Pathophysiology and Clinical Applications*. 5th Revised edition. ed: Lippincott Williams and Wilkins; 2011 1 Dec. 2011.
187. Borg GA. Psychophysical bases of perceived exertion. *Medicine and science in sports and exercise*. 1982;14(5):377-81.
188. Liu BY, Edwards NC, Ray S, Steeds RP. Timing surgery in mitral regurgitation: defining risk and optimising intervention using stress echocardiography. *Echo Res Pract*. 2016;3(4):R45-R55.
189. Magne J, Lancellotti P, Pierard LA. Exercise-Induced Changes in Degenerative Mitral Regurgitation. *J Am Coll Cardiol*. 2010;56(4):300-9.
190. Magne J, Lancellotti P, Pierard LA. Exercise Pulmonary Hypertension in Asymptomatic Degenerative Mitral Regurgitation. *Circulation*. 2010;122(1):33-41.
191. Lancellotti P, Magne J. Stress testing for the evaluation of patients with mitral regurgitation. *Curr Opin Cardiol*. 2012;27(5):492-8.
192. Millet GP, Vleck VE, Bentley DJ. Physiological Differences Between Cycling and Running Lessons from Triathletes. *Sports Medicine*. 2009;39(3):179-206.
193. Levey AS, Coresh J, Greene T, Stevens LA, Zhang YL, Hendriksen S, et al. Using standardized serum creatinine values in the modification of diet in renal disease study equation for estimating glomerular filtration rate. *Ann Intern Med*. 2006;145(4):247-54.
194. Sommer C, Straehle C, Kothe U, Hamprecht FA, Ieee. ILASTIK: INTERACTIVE LEARNING AND SEGMENTATION TOOLKIT. 2011 8th Ieee International Symposium on Biomedical Imaging: From Nano to Macro. *IEEE International Symposium on Biomedical Imaging2011*. p. 230-3.
195. Vliegen HW, Vanderlaarse A, Huysman JAN, Wijnvoord EC, Mentar M, Cornelisse CJ, et al. Morphometric quantification of myocyte dimensions validated in normal growing-rat hearts and applied to hypertrophic human hearts. *Cardiovascular research*. 1987;21(5):352-7.
196. Chipeta P, Shim CY, Hong GR, Kim D, Cho IJ, Lee S, et al. Time course of left atrial reverse remodelling after mitral valve surgery and the impact of left ventricular global longitudinal strain in patients with chronic severe mitral regurgitation. *Interact Cardiovasc Thorac Surg*. 2016;23(6):876-82.
197. Shafii AE, Gillinov AM, Mihaljevic T, Stewart W, Batizy LH, Blackstone EH. Changes in left ventricular morphology and function after mitral valve surgery. *The American journal of cardiology*. 2012;110(3):403-8.e3.
198. Mirsky I, Parmley WW. Assessment of passive elastic stiffness for isolated heart muscle and the intact heart. *Circulation research*. 1973;33(2):233-43.

199. Shan K, Bick RJ, Poindexter BJ, Shimoni S, Letsou GV, Reardon MJ, et al. Relation of tissue Doppler derived myocardial velocities to myocardial structure and beta-adrenergic receptor density in humans. *J Am Coll Cardiol*. 2000;36(3):891-6.
200. Kang SJ, Lim HS, Choi BJ, Choi SY, Hwang GS, Yoon MH, et al. Longitudinal strain and torsion assessed by two-dimensional speckle tracking correlate with the serum level of tissue inhibitor of matrix metalloproteinase-1, a marker of myocardial fibrosis, in patients with hypertension. *Journal of the American Society of Echocardiography : official publication of the American Society of Echocardiography*. 2008;21(8):907-11.
201. Fang ZY, Yuda S, Anderson V, Short L, Case C, Marwick TH. Echocardiographic detection of early diabetic myocardial disease. *J Am Coll Cardiol*. 2003;41(4):611-7.
202. Brower RW, Katen HJT, Meester GT. Direct methods for determining regional myocardial shortening after bypass surgery from radiopaque markers in man. *Am J Cardiol*. 1978;41(7):1222-9.
203. Rankin JS, McHale PA, Arentzen CE, Ling D, Greenfield JC, Jr., Anderson RW. The three-dimensional dynamic geometry of the left ventricle in the conscious dog. *Circulation research*. 1976;39(3):304-13.
204. Vo HQ, Marwick TH, Negishi K. MRI-Derived Myocardial Strain Measures in Normal Subjects. *JACC Cardiovascular imaging*. 2017.
205. Kim J, Di Franco A, Seoane T, Srinivasan A, Kampaktsis PN, Geevarghese A, et al. Right Ventricular Dysfunction Impairs Effort Tolerance Independent of Left Ventricular Function Among Patients Undergoing Exercise Stress Myocardial Perfusion Imaging. *Circulation Cardiovascular imaging*. 2016;9(11).
206. de Groote P, Millaire A, Foucher-Hossein C, Nugue O, Marchandise X, Ducloux G, et al. Right ventricular ejection fraction is an independent predictor of survival in patients with moderate heart failure. *J Am Coll Cardiol*. 1998;32(4):948-54.
207. Sun X, Ellis J, Kanda L, Corso PJ. The role of right ventricular function in mitral valve surgery. *The heart surgery forum*. 2013;16(3):E170-6.
208. Lella LK, Sales VL, Goldsmith Y, Chan J, Iskandir M, Gulkarov I, et al. Reduced Right Ventricular Function Predicts Long-Term Cardiac Re-Hospitalization after Cardiac Surgery. *PloS one*. 2015;10(7):e0132808.
209. Lang RM, Badano LP, Mor-Avi V, Afilalo J, Armstrong A, Ernande L, et al. Recommendations for cardiac chamber quantification by echocardiography in adults: an update from the American Society of Echocardiography and the European Association of Cardiovascular Imaging. *Journal of the American Society of Echocardiography : official publication of the American Society of Echocardiography*. 2015;28(1):1-39.e14.
210. Antoni ML, Scherptong RW, Atary JZ, Boersma E, Holman ER, van der Wall EE, et al. Prognostic value of right ventricular function in patients after acute myocardial infarction treated with primary percutaneous coronary intervention. *Circulation Cardiovascular imaging*. 2010;3(3):264-71.
211. Haeck ML, Scherptong RW, Marsan NA, Holman ER, Schalij MJ, Bax JJ, et al. Prognostic value of right ventricular longitudinal peak systolic strain in patients with pulmonary hypertension. *Circulation Cardiovascular imaging*. 2012;5(5):628-36.
212. Morais P, Marchi A, Bogaert JA, Dresselaers T, Heyde B, D'hooge J, et al. Cardiovascular magnetic resonance myocardial feature tracking using a non-rigid, elastic image registration algorithm: assessment of variability in a real-life clinical setting. *Journal of Cardiovascular Magnetic Resonance*. 2017;19(1):24.

213. Koo TK, Li MY. A Guideline of Selecting and Reporting Intraclass Correlation Coefficients for Reliability Research. *Journal of Chiropractic Medicine*. 2016;15(2):155-63.
214. Moody WE, Ferro CJ, Edwards NC, Chue CD, Lin ELS, Taylor RJ, et al. Cardiovascular Effects of Unilateral Nephrectomy in Living Kidney Donors. *Hypertension*. 2016;67(2):368-77.
215. Taylor RJ, Moody WE, Umar F, Edwards NC, Taylor TJ, Stegemann B, et al. Myocardial strain measurement with feature-tracking cardiovascular magnetic resonance: normal values. *Eur Heart J-Cardiovasc Imaging*. 2015;16(8):871-81.
216. Bistoquet A, Oshinski J, Skrinjar O. Left ventricular deformation recovery from Cine MRI using an incompressible model. *Ieee Transactions on Medical Imaging*. 2007;26(9):1136-53.
217. Bistoquet A, Oshinski J, Skrinjar O. Myocardial deformation recovery from cine MRI using a nearly incompressible biventricular model. *Medical Image Analysis*. 2008;12(1):69-85.
218. Liu B, Dardeer AM, Moody WE, Edwards NC, Hudsmith LE, Steeds RP. Normal Values for Myocardial Deformation Within the Right Heart Measured by Feature-Tracking Cardiovascular Magnetic Resonance Imaging. *International Journal of Cardiology*. 2017.
219. Liu B, Dardeer AM, Moody WE, Edwards NC, Hudsmith LE, Steeds RP. Reference ranges and reproducibility studies for right heart myocardial deformation by feature tracking cardiovascular magnetic resonance imaging. *Data in brief*. 2018;16:244-9.
220. Bujang MA, Baharum N. A simplified guide to determination of sample size requirements for estimating the value of intraclass correlation coefficient: a review. *Archives of Orofacial Science*. 2017;12(1):1-11.
221. Hippisley-Cox J, Coupland C, Vinogradova Y, Robson J, Minhas R, Sheikh A, et al. Predicting cardiovascular risk in England and Wales: prospective derivation and validation of QRISK2. *Br Med J*. 2008;336(7659):1475-+.
222. Jasaityte R, Heyde B, D'Hooge J. Current State of Three-Dimensional Myocardial Strain Estimation Using Echocardiography. *J Am Soc Echocardiogr*. 2013;26(1):15-28.
223. Jasaityte R, Heyde B, Ferferieva V, Amundsen B, Barbosa D, Loeckx D, et al. Comparison of a new methodology for the assessment of 3D myocardial strain from volumetric ultrasound with 2D speckle tracking. *Int J Cardiovasc Imaging*. 2012;28(5):1049-60.
224. Nakatani S. Left ventricular rotation and twist: why should we learn? *Journal of cardiovascular ultrasound*. 2011;19(1):1-6.
225. Yingchoncharoen T, Agarwal S, Popovic ZB, Marwick TH. Normal Ranges of Left Ventricular Strain: A Meta-Analysis. *J Am Soc Echocardiogr*. 2013;26(2):185-91.
226. Kleijn SA, Pandian NG, Thomas JD, de Isla LP, Kamp O, Zuber M, et al. Normal reference values of left ventricular strain using three-dimensional speckle tracking echocardiography: results from a multicentre study. *Eur Heart J-Cardiovasc Imaging*. 2015;16(4):410-6.
227. Petersen SE, Aung N, Sanghvi MM, Zemrak F, Fung K, Paiva JM, et al. Reference ranges for cardiac structure and function using cardiovascular magnetic resonance (CMR) in Caucasians from the UK Biobank population cohort. *Journal of Cardiovascular Magnetic Resonance*. 2017;19.
228. Soleimanifard S, Abd-Elmoniem KZ, Sasano T, Agarwal HK, Abraham MR, Abraham TP, et al. Three-dimensional regional strain analysis in porcine myocardial

- infarction: a 3T magnetic resonance tagging study. *Journal of Cardiovascular Magnetic Resonance*. 2012;14:12.
229. Truong VT, Safdar KS, Kalra DK, Gao X, Ambach S, Taylor MD, et al. Cardiac magnetic resonance tissue tracking in right ventricle: Feasibility and normal values. *Magnetic Resonance Imaging*. 2017;38:189-95.
230. Heermann P, Hedderich DM, Paul M, Schülke C, Kroeger JR, Baeßler B, et al. Biventricular myocardial strain analysis in patients with arrhythmogenic right ventricular cardiomyopathy (ARVC) using cardiovascular magnetic resonance feature tracking. *Journal of Cardiovascular Magnetic Resonance*. 2014;16(1):75.
231. Petersen SE, Aung N, Sanghvi MM, Zemrak F, Fung K, Paiva JM, et al. Reference ranges for cardiac structure and function using cardiovascular magnetic resonance (CMR) in Caucasians from the UK Biobank population cohort. *Journal of Cardiovascular Magnetic Resonance*. 2017;19(1):18.
232. Ermacora D BL, Muraru D, Gentian D, Dal Bianco L, Casablanca S, Peluso D, Zoppellaro G, Cucchini U, Iliceto S. Reference values of right ventricular longitudinal strain by speckle tracking echocardiography in 219 healthy volunteers. *European Heart Journal*. 2013;34(Supplement 1):684.
233. Muraru D, Onciul S, Peluso D, Soriani N, Cucchini U, Aruta P, et al. Sex- and Method-Specific Reference Values for Right Ventricular Strain by 2-Dimensional Speckle-Tracking Echocardiography. *Circulation Cardiovascular imaging*. 2016;9(2):e003866.
234. Voigt JU, Pedrizzetti G, Lysyansky P, Marwick TH, Houle H, Baumann R, et al. Definitions for a common standard for 2D speckle tracking echocardiography: consensus document of the EACVI/ASE/Industry Task Force to standardize deformation imaging. *Journal of the American Society of Echocardiography : official publication of the American Society of Echocardiography*. 2015;28(2):183-93.
235. Kuznetsova T, Cauwenberghs N, Knez J, Yang WY, Herbots L, D'Hooge J, et al. Additive Prognostic Value of Left Ventricular Systolic Dysfunction in a Population-Based Cohort. *Circ-Cardiovasc Imaging*. 2016;9(7).
236. Kim HJ, Park SW, Cho BR, Hong SH, Park PW, Hong KP. The role of cardiopulmonary exercise test in mitral and aortic regurgitation: it can predict post-operative results. *The Korean journal of internal medicine*. 2003;18(1):35-9.
237. Holmes C, Briffa N. Patient-Reported Outcome Measures (PROMS) in patients undergoing heart valve surgery: why should we measure them and which instruments should we use? *Open heart*. 2016;3(1):e000315.
238. Lazam S, Vanoverschelde JL, Tribouilloy C, Grigioni F, Suri RM, Avierinos JF, et al. Twenty-Year Outcome After Mitral Repair Versus Replacement for Severe Degenerative Mitral Regurgitation: Analysis of a Large, Prospective, Multicenter, International Registry. *Circulation*. 2017;135(5):410-22.
239. Ludman PF, Moat N, de Belder MA, Blackman DJ, Duncan A, Banya W, et al. Transcatheter aortic valve implantation in the United Kingdom: temporal trends, predictors of outcome, and 6-year follow-up: a report from the UK Transcatheter Aortic Valve Implantation (TAVI) Registry, 2007 to 2012. *Circulation*. 2015;131(13):1181-90.
240. Takagi H, Ando T, Umemoto T. A review of comparative studies of MitraClip versus surgical repair for mitral regurgitation. *Int J Cardiol*. 2017;228:289-94.
241. Goldstone AB, Woo YJ. Is minimally invasive thoracoscopic surgery the new benchmark for treating mitral valve disease? *Ann Cardiothorac Surg*. 2016;5(6):567-72.

242. Kitkungvan D, Nabi F, Kim RJ, Bonow RO, Khan MA, Xu JQ, et al. Myocardial Fibrosis in Patients With Primary Mitral Regurgitation With and Without Prolapse. *J Am Coll Cardiol*. 2018;72(8):823-34.
243. Bui AH, Roujol S, Foppa M, Kissinger KV, Goddu B, Hauser TH, et al. Diffuse myocardial fibrosis in patients with mitral valve prolapse and ventricular arrhythmia. *Heart*. 2017;103(3):204-9.
244. Deigaard LA, Skjolsvik ET, Lie OH, Ribe M, Stokke MK, Hegbom F, et al. The Mitral Annulus Disjunction Arrhythmic Syndrome. *J Am Coll Cardiol*. 2018;72(14):1600-9.
245. Diao KY, Yang ZG, Xu HY, Liu X, Zhang Q, Shi K, et al. Histologic validation of myocardial fibrosis measured by T1 mapping: a systematic review and meta-analysis. *Journal of cardiovascular magnetic resonance : official journal of the Society for Cardiovascular Magnetic Resonance*. 2016;18(1):92.
246. Garbi M, Lancellotti P, Sheppard MN. Mitral valve and left ventricular features in malignant mitral valve prolapse. *Open heart*. 2018;5(2).
247. Corrado D, Basso C, Nava A, Rossi L, Thiene G. Sudden death in young people with apparently isolated mitral valve prolapse. *Giornale italiano di cardiologia*. 1997;27(11):1097-105.
248. Chesler E, King RA, Edwards JE. The myxomatous mitral valve and sudden death. *Circulation*. 1983;67(3):632-9.
249. Kitkungvan D, Yang EY, El Tallawi KC, Nagueh SF, Nabi F, Khan MA, et al. Prognostic Implications of Diffuse Interstitial Fibrosis in Asymptomatic Primary Mitral Regurgitation. *Circulation*. 2019;140(25):2122-4.
250. Gottbrecht M, Kramer CM, Salerno M. Native T1 and Extracellular Volume Measurements by Cardiac MRI in Healthy Adults: A Meta-Analysis. *Radiology*. 2019;290(2):317-26.
251. Enriquez-Sarano M. Mitral Annular Disjunction: The Forgotten Component of Myxomatous Mitral Valve Disease. *JACC Cardiovascular imaging*. 2017;10(12):1434-6.
252. Flett AS, Hayward MP, Ashworth MT, Hansen MS, Taylor AM, Elliott PM, et al. Equilibrium contrast cardiovascular magnetic resonance for the measurement of diffuse myocardial fibrosis: preliminary validation in humans. *Circulation*. 2010;122(2):138-44.
253. Messroghli DR, Walters K, Plein S, Sparrow P, Friedrich MG, Ridgway JP, et al. Myocardial T1 mapping: application to patients with acute and chronic myocardial infarction. *Magnetic resonance in medicine*. 2007;58(1):34-40.
254. Hulten E, Aslam S, Osborne M, Abbasi S, Bittencourt MS, Blankstein R. Cardiac sarcoidosis-state of the art review. *Cardiovascular diagnosis and therapy*. 2016;6(1):50-63.
255. Schwarz F, Mall G, Zebe H, Blickle J, Derks H, Manthey J, et al. Quantitative morphologic findings of the myocardium in idiopathic dilated cardiomyopathy. *The American journal of cardiology*. 1983;51(3):501-6.
256. Guo Y, Song C, Wu X, Zheng X, Lu J, Fang X, et al. Comparison of Outcomes of Mitral Valve Repair for Leaflet Prolapse with Advanced versus Mild/Moderate Myxomatous Degeneration. *International heart journal*. 2018;59(6):1288-95.
257. David TE. Durability of mitral valve repair for mitral regurgitation due to degenerative mitral valve disease. *Ann Cardiothorac Surg*. 2015;4(5):417-21.
258. Bonow RO, Adams DH. The Time Has Come to Define Centers of Excellence in Mitral Valve Repair. *J Am Coll Cardiol*. 2016;67(5):499-501.
259. Bridgewater B, Hooper T, Munsch C, Hunter S, von Oppell U, Livesey S, et al. Mitral repair best practice: proposed standards. *Heart*. 2006;92(7):939-44.

260. Carabello BA. A tragedy of modern cardiology: using ejection fraction to gauge left ventricular function in mitral regurgitation. *Heart*. 2017;103(8):570-1.
261. Ternacle J, Berry M, Alonso E, Kloeckner M, Couetil JP, Rande JLD, et al. Incremental value of global longitudinal strain for predicting early outcome after cardiac surgery. *Eur Heart J-Cardiovasc Imaging*. 2013;14(1):77-84.
262. Kamperidis V, Marsan NA, Delgado V, Bax JJ. Left ventricular systolic function assessment in secondary mitral regurgitation: left ventricular ejection fraction vs. speckle tracking global longitudinal strain. *Eur Heart J*. 2016;37(10):811-6.
263. Walsh SR, Tang TY, Kullar P, Jenkins DP, Dutka DP, Gaunt ME. Ischaemic preconditioning during cardiac surgery: systematic review and meta-analysis of perioperative outcomes in randomised clinical trials. *European journal of cardio-thoracic surgery : official journal of the European Association for Cardio-thoracic Surgery*. 2008;34(5):985-94.
264. Devereaux PJ, Sessler DI. Cardiac Complications in Patients Undergoing Major Noncardiac Surgery. *The New England journal of medicine*. 2015;373(23):2258-69.
265. Guarracino F, Baldassarri R. Cardiovascular complications of cardiac surgery. In: Peter R, Alston. Paul,S,Myles. Marco,Ranucci., editor. *Oxford Textbook of Cardiothoracic Anaesthesia*: Oxford University Press; 2015.
266. Pickering JW, Endre ZH. GFR shot by RIFLE: errors in staging acute kidney injury. *Lancet (London, England)*. 2009;373(9672):1318-9.
267. Bartko PE, Wiedemann D, Schrutka L, Binder C, Santos-Gallego CG, Zuckermann A, et al. Impact of Right Ventricular Performance in Patients Undergoing Extracorporeal Membrane Oxygenation Following Cardiac Surgery. *Journal of the American Heart Association*. 2017;6(8).
268. Chaikriangkrai K, Lopez-Mattei JC, Lawrie G, Ibrahim H, Quinones MA, Zoghbi W, et al. Prognostic Value of Delayed Enhancement Cardiac Magnetic Resonance Imaging in Mitral Valve Repair. *Annals of Thoracic Surgery*. 2014;98(5):1557-63.
269. Quarto C, Dweck MR, Murigu T, Joshi S, Melina G, Angeloni E, et al. Late gadolinium enhancement as a potential marker of increased perioperative risk in aortic valve replacement. *Interact Cardiovasc Thorac Surg*. 2012;15(1):45-50.
270. Grigioni F, Clavel MA, Vanoverschelde JL, Tribouilloy C, Pizarro R, Huebner M, et al. The MIDA Mortality Risk Score: development and external validation of a prognostic model for early and late death in degenerative mitral regurgitation. *Eur Heart J*. 2018;39(15):1281-91.
271. Levett DZH, Jack S, Swart M, Carlisle J, Wilson J, Snowden C, et al. Perioperative cardiopulmonary exercise testing (CPET): consensus clinical guidelines on indications, organization, conduct, and physiological interpretation. *British Journal of Anaesthesia*. 2018;120(3):484-500.
272. Moran J, Wilson F, Guinan E, McCormick P, Hussey J, Moriarty J. The preoperative use of field tests of exercise tolerance to predict postoperative outcome in intra-abdominal surgery: a systematic review. *Journal of clinical anesthesia*. 2016;35:446-55.
273. Chen H, Zeng J, Liu D, Yang Q. Prognostic value of late gadolinium enhancement on CMR in patients with severe aortic valve disease: a systematic review and meta-analysis. *Clin Radiol*. 2018;73(11):983.e7-.e14.
274. Colucci WS, Koliass TJ, Adams KF, Armstrong WF, Ghali JK, Gottlieb SS, et al. Metoprolol reverses left ventricular remodeling in patients with asymptomatic systolic

- dysfunction: the REversal of VEentricular Remodeling with Toprol-XL (REVERT) trial. *Circulation*. 2007;116(1):49-56.
275. Behloul H, Feldman DE, Ducharme A, Frenette M, Giannetti N, Grondin F, et al. Identifying relative cut-off scores with neural networks for interpretation of the Minnesota Living with Heart Failure questionnaire. Conference proceedings : Annual International Conference of the IEEE Engineering in Medicine and Biology Society IEEE Engineering in Medicine and Biology Society Annual Conference. 2009;2009:6242-6.
276. Brokalaki H, Patelarou E, Giakoumidakis K, Kollia Z, Fotos NV, Vivilaki V, et al. Translation and validation of the Greek "Minnesota Living with Heart Failure" questionnaire. *Hellenic journal of cardiology : HJC = Hellenike kardiologike epitheorese*. 2015;56(1):10-9.
277. Lee TC, Qian M, Lip GYH, Di Tullio MR, Graham S, Mann DL, et al. Heart Failure Severity and Quality of Warfarin Anticoagulation Control (From the WARCEF Trial). *Am J Cardiol*. 2018;122(5):821-7.
278. Vaillant-Roussel H, Laporte C, Pereira B, De Rosa M, Eschalier B, Vorilhon C, et al. Impact of patient education on chronic heart failure in primary care (ETIC): a cluster randomised trial. *BMC family practice*. 2016;17:80.
279. Bieleman HJ, Reneman MF, van Ittersum MW, van der Schans CP, Groothoff JW, Oosterveld FG. Self-reported functional status as predictor of observed functional capacity in subjects with early osteoarthritis of the hip and knee: a diagnostic study in the CHECK cohort. *Journal of occupational rehabilitation*. 2009;19(4):345-53.
280. Hsu TW, Chang HC, Huang CH, Chou MC, Yu YT, Lin LY. Identifying cut-off scores for interpretation of the Heart Failure Impact Questionnaire. *Nursing open*. 2018;5(4):575-82.
281. Halliday BP, Wassall R, Lota AS, Khalique Z, Gregson J, Newsome S, et al. Withdrawal of pharmacological treatment for heart failure in patients with recovered dilated cardiomyopathy (TRED-HF): an open-label, pilot, randomised trial. *Lancet (London, England)*. 2019;393(10166):61-73.
282. Lerman BJ, Popat RA, Assimes TL, Heidenreich PA, Wren SM. Association of Left Ventricular Ejection Fraction and Symptoms With Mortality After Elective Noncardiac Surgery Among Patients With Heart Failure. *Jama*. 2019;321(6):572-9.
283. Tribouilloy C, Rusinaru D, Szymanski C, Mezghani S, Fournier A, Levy F, et al. Predicting left ventricular dysfunction after valve repair for mitral regurgitation due to leaflet prolapse: additive value of left ventricular end-systolic dimension to ejection fraction. *European journal of echocardiography : the journal of the Working Group on Echocardiography of the European Society of Cardiology*. 2011;12(9):702-10.
284. Raphael C, Briscoe C, Davies J, Ian Whinnett Z, Manisty C, Sutton R, et al. Limitations of the New York Heart Association functional classification system and self-reported walking distances in chronic heart failure. *Heart*. 2007;93(4):476-82.
285. Musa TA, Treibel TA, Vassiliou VS, Captur G, Singh A, Chin C, et al. Myocardial Scar and Mortality in Severe Aortic Stenosis. *Circulation*. 2018;138(18):1935-47.
286. Everett RJ, Treibel TA, Fukui M, Lee H, Rigolli M, Singh A, et al. Extracellular Myocardial Volume in Patients With Aortic Stenosis. *J Am Coll Cardiol*. 2020;75(3):304-16.
287. Bing R, Everett RJ, Tuck C, Semple S, Lewis S, Harkess R, et al. Rationale and design of the randomized, controlled Early Valve Replacement Guided by Biomarkers of Left Ventricular Decompensation in Asymptomatic Patients with Severe Aortic Stenosis (EVOLVED) trial. *Am Heart J*. 2019;212:91-100.

288. Everett RJ, Tastet L, Clavel MA, Chin CWL, Capoulade R, Vassiliou VS, et al. Progression of Hypertrophy and Myocardial Fibrosis in Aortic Stenosis: A Multicenter Cardiac Magnetic Resonance Study. *Circulation Cardiovascular imaging*. 2018;11(6):e007451.
289. Van de Heyning CM, Magne J, Pierard LA, Bruyere PJ, Davin L, De Maeyer C, et al. Late gadolinium enhancement CMR in primary mitral regurgitation. *Eur J Clin Invest*. 2014;44(9):840-7.
290. Garcia J, Barker AJ, Markl M. The Role of Imaging of Flow Patterns by 4D Flow MRI in Aortic Stenosis. *JACC: Cardiovascular Imaging*. 2019;12(2):252-66.
291. Stoll VM, Hess AT, Rodgers CT, Bissell MM, Dyverfeldt P, Ebberts T, et al. Left Ventricular Flow Analysis. *Circulation Cardiovascular imaging*. 2019;12(5):e008130.
292. Bolger AF, Heiberg E, Karlsson M, Wigstrom L, Engvall J, Sigfridsson A, et al. Transit of blood flow through the human left ventricle mapped by cardiovascular magnetic resonance. *Journal of cardiovascular magnetic resonance : official journal of the Society for Cardiovascular Magnetic Resonance*. 2007;9(5):741-7.
293. Swartz MH, Teichholz LE, Donoso E. Mitral valve prolapse: a review of associated arrhythmias. *The American journal of medicine*. 1977;62(3):377-89.
294. Freed LA, Levy D, Levine RA, Larson MG, Evans JC, Fuller DL, et al. Prevalence and clinical outcome of mitral-valve prolapse. *N Engl J Med*. 1999;341(1):1-7.
295. Stecker EC, Reinier K, Marijon E, Narayanan K, Teodorescu C, Uy-Evanado A, et al. Public Health Burden of Sudden Cardiac Death in the United States. *Circ-Arrhythmia Electrophysiol*. 2014;7(2):212-7.
296. Lewis ME, Lin FC, Nanavati P, Mehta N, Mounsey L, Nwosu A, et al. Estimated incidence and risk factors of sudden unexpected death. *Open heart*. 2016;3(1):e000321.
297. Narayanan K, Uy-Evanado A, Teodorescu C, Reinier K, Nichols GA, Gunson K, et al. Mitral valve prolapse and sudden cardiac arrest in the community. *Heart Rhythm*. 2016;13(2):498-503.
298. Sriram CS, Syed FF, Ferguson ME, Johnson JN, Enriquez-Sarano M, Cetta F, et al. Malignant Bileaflet Mitral Valve Prolapse Syndrome in Patients With Otherwise Idiopathic Out-of-Hospital Cardiac Arrest. *J Am Coll Cardiol*. 2013;62(3):222-30.
299. Anders S, Said S, Schulz F, Puschel K. Mitral valve prolapse syndrome as cause of sudden death in young adults. *Forensic Science International*. 2007;171(2-3):127-30.
300. La Vecchia L, Ometto R, Centofante P, Varotto L, Bonanno C, Bozzola L, et al. Arrhythmic profile, ventricular function, and histomorphometric findings in patients with idiopathic ventricular tachycardia and mitral valve prolapse: Clinical and prognostic evaluation. *Clinical Cardiology*. 1998;21(10):731-5.
301. Akcay M, Yuce M, Pala S, Akcakoyun M, Ergelen M, Kargin R, et al. Anterior Mitral Valve Length is Associated with Ventricular Tachycardia in Patients with Classical Mitral Valve Prolapse. *Pace-Pacing and Clinical Electrophysiology*. 2010;33(10):1224-30.
302. Lown B, Wolf M. Approaches to sudden death from coronary heart disease. *Circulation*. 1971;44(1):130-42.
303. Heart rate variability: standards of measurement, physiological interpretation and clinical use. Task Force of the European Society of Cardiology and the North American Society of Pacing and Electrophysiology. *Circulation*. 1996;93(5):1043-65.
304. Zheutlin TA, Roth H, Chua W, Steinman R, Summers C, Lesch M, et al. Programmed electrical stimulation to determine the need for antiarrhythmic therapy in patients with complex ventricular ectopic activity. *Am Heart J*. 1986;111(5):860-7.



305. Gomes JA, Cain ME, Buxton AE, Josephson ME, Lee KL, Hafley GE. Prediction of long-term outcomes by signal-averaged electrocardiography in patients with unsustained ventricular tachycardia, coronary artery disease, and left ventricular dysfunction. *Circulation*. 2001;104(4):436-41.
306. Mancini DM, Wong KL, Simson MB. Prognostic value of an abnormal signal-averaged electrocardiogram in patients with nonischemic congestive cardiomyopathy. *Circulation*. 1993;87(4):1083-92.
307. Breithardt G, Cain ME, Elsherif N, Flowers NC, Hombach V, Janse M, et al. Standards for analysis of ventricular late potentials using high-resolution or signal-averaged electrocardiography - A statement by a Task-Force committee for the European-Society-of-Cardiology, the American-Heart-Association, and the American-College-of-Cardiology. *J Am Coll Cardiol*. 1991;17(5):999-1006.
308. Cain ME, Mason JW, Anderson JL, Sheinman MM, Arnsdorf MF, Waldo AL. Signal-averaged electrocardiography. *J Am Coll Cardiol*. 1996;27(1):238-49.
309. Frolkis JP, Pothier CE, Blackstone EH, Lauer MS. Frequent ventricular ectopy after exercise as a predictor of death. *The New England journal of medicine*. 2003;348(9):781-90.
310. Jouven X, Zureik M, Desnos M, Courbon D, Ducimetiere P. Long-term outcome in asymptomatic men with exercise-induced premature ventricular depolarizations. *The New England journal of medicine*. 2000;343(12):826-33.

## APPENDIX I:

### PILOT STUDY ON FIBROSIS AND ARRHYTHMIC RISK

#### 10.1 Background

It remains unclear why some patients develop LGE, whilst others do not. An interest in LGE is not unfounded as its presence in aortic stenosis has recently been reported to be independently associated with a two-fold increase in mortality regardless of valve intervention (285). In Chapter 5, we reported LGE to be present in one-third of our study cohort; patients with LGE possessed more severe MR than those without. However, LGE has also been reported to be present in approximately 30% of patient cohorts containing mild or moderate MR, suggesting that more severe MR is not the pathophysiology behind LGE development (32, 289). It has been proposed that the mechanism for the development of LGE in MR is the systolic mechanical stretch of LV and papillary myocardium adjacent to the valve (41).

The prognostic implications of LGE in MR is not well understood. The Mitral FINDER study did not find LGE to affect postoperative outcomes, although an association between fibrosis, MVP, ventricular arrhythmia and sudden cardiac death have been highlighted since the 1970s (293). In one study, 30 patients with MVP (with >5mm leaflet thickening) and complex ventricular arrhythmias were compared against 14 patients with MVP but only minor ventricular arrhythmia (41). It was noted that 93% of patients with complex ventricular arrhythmias possessed LGE in the papillary muscles and infero-basal left ventricular wall, compared to only 14% in those without complex ventricular arrhythmias. The areas of LGE corresponded well to the areas of histological fibrosis on post-mortem analyses of SCD victims with MVP due to myxomatous valve disease, suggesting that myocardial fibrosis may represent the pro-arrhythmic substrate in MVP patients (41).

The difficulty arises however when taking into account the prevalence of MVP across the general population. For example, one group reported a 1.3% incidence of “classic MVP”, defined as possessing a maximal valve leaflet thickness of >5mm amongst 3491 participants of the Framingham Heart Study. Meanwhile, 1.1% had “non-classic MVP” with maximal leaflet thickness of <5mm (294). Given the high prevalence of MVP across the general population, we would expect to observe far greater numbers of MVP related arrhythmic events across cardiology clinics. In reality, SCD which itself is a rare phenomenon at 30-60 cases per 100000 person-years amongst the general population (295, 296), is only associated with isolated MVP in 1-2% of all SCD cases (132, 297). This has

raised doubts over a causal link between MVP, myocardial fibrosis and cardiac arrhythmia.

Part of the challenge is the overlapping terminologies used within this field and being able to diagnose the exact cause for MVP or MR. For the MVP characterisation cohort of the Framingham Heart Study (294), it is unclear how many of the classic MVP cases represented BD, and whether the non-classic MVP cases represented FED or FED+ phenotypes. It is also not well established whether the subtypes of primary degenerative MR are associated with different arrhythmic and SCD risks. One report from the Mayo Clinic identified 10 out of 24 patients with idiopathic out-of-hospital cardiac arrest to possess bileaflet MVP (298), which is more suggestive of underlying BD. An association between BD and SCD has been similarly established by a case series featuring 6 young female adults who had histologically confirmed BD with mucopolysaccharide infiltration of the valve (299). However, the MVP subtype has been less well characterised by many other studies within this field (300, 301), and there is an increasing drive to suggest that the culprit pathophysiology is unrelated to MR subtype, but rather the presence of MAD (244). Further work is required in this field to elucidate the relationship between MR subtype, leaflet prolapse, MAD and the development, as well as electrophysiological consequences of LGE.

#### 10.1.1 Aims and hypotheses

We hypothesise that LGE occurs in MR due to traction from the prolapsing leaflet, and is more prominent in BD due to bileaflet involvement and MAD. The development of LGE is associated with increased arrhythmic risk and ventricular ectopy burden.

The aims of this study include:

- 1) Assessing the relationship between MR subtype, mechanism and prevalence of LGE
- 2) Quantifying the arrhythmia burden and arrhythmia risk in MR patients
- 3) Assess the relationship between LGE, MR subtype, and markers of arrhythmia burden and arrhythmia risk

## 10.2 Methods

The diagnoses of BD vs FED within the Mitral FINDER cohort were established based on consensus between two experienced imaging cardiologists, following the independent review of the leaflet morphology, leaflet thickness, chords, annulus, timing of MR, scallop involvement, and presence or absence of MAD on echocardiography and CMR, taking into account, when available, the surgeon's report of MV morphology on direct intra-operative visualisation. Where a consensus could not be reached, a label of "indeterminate" was employed and the patient was excluded from analyses.

For arrhythmia quantification, sinus rhythm patients underwent 3-channel 24-hour Holter ECG recordings using Lifecard CF monitors (Spacelabs Healthcare, Snoqualmie, U.S.A.). Holter data were analysed as part of routine clinical care with commercially available Pathfinder SL software (Spacelabs Healthcare, Snoqualmie, U.S.A.). Holter recordings were analysed for VE burden as per Lown-Wolf grading (**Table 10.1**) (302), as well as automated time-domain analyses of heart rate variability (HRV) and interpreted as per European guidelines (303). Complex ventricular ectopy was defined as Lown-Wolf grade

$\geq 3$  (304). Particular attention was placed towards HRV standard deviation of the beat-to-beat (or N to N) interval (SDNN), and triangular index (calculated by the integral of the density distribution of NN intervals divided by the maximum of the density distribution). HRV were categorised according to established European SDNN and triangular index cut-off points (303). Data surrounding the prognostic implications of depressed HRV is most prevalent in ischaemic heart disease where an SDNN of  $<50\text{ms}$  has been linked to worst, and  $>100\text{ms}$  to best long-term survival. Similarly, an HRV triangular index of  $\leq 15$  predicts lower post myocardial infarction survival compared to patients with a triangular index of  $>20$ .

Recognising that the absolute risk of malignant arrhythmias is likely low in the general MR cohort, we also assessed patients for the presence of ventricular late potentials (VLP) using signal-averaged ECG (SA-ECG) recordings in patients with sinus rhythm and without evidence of bundle branch block. The presence of VLP on SA-ECG has been demonstrated to predict arrhythmic deaths in a range of ischaemic (305) and non-ischaemic cardiomyopathies (306), therefore was felt to be a suitable surrogate marker of future arrhythmic risk. SA-ECGs were completed as per established methodology by averaging 250 heartbeats using a MAC<sup>®</sup> 5500 system (GE Healthcare, Illinois, U.S.A.) at a filter setting of 40-250Hz, aiming for a noise level of  $<0.3\mu\text{V}$  (305, 307). The presence of late potential was defined by the presence of 1) a filtered QRS complex  $>114\text{ms}$  duration; 2) a signal  $<20\mu\text{V}$  in the last 40ms of the filtered QRS complex; and 3) voltage  $<40\mu\text{V}$  in the terminal QRS complex for  $>38\text{ms}$  (308).

As frequent premature VE during exercise (N=6101) and on post-exercise recovery (N=29244) have both been linked with increased risk of cardiovascular death during long-term follow-up of large observational cohort (309, 310), we quantified their prevalence in our sinus rhythm patients. However, as there are no standardised definitions of what constituted “frequent” VEs, we extracted exercise-induced VE burden from CPET and ESE ECGs and categorised patients according to Lown-Wolf grading (302). Meanwhile, frequent premature VE on post-exercise recovery ECGs were defined according to established definitions (presence of seven or more ventricular premature beats per minute, ventricular bigeminy or trigeminy, ventricular couplets or triplets, ventricular tachycardia, ventricular flutter, torsade de pointes, or ventricular fibrillation (309)).

**Table 10.1** Lown-Wolf classification of ventricular ectopy

<b>Grade</b>	<b>Definition</b>
0	No ventricular premature beat
1	<30 ventricular premature beats/hour
2	$\geq 30$ ventricular premature beats/hour or $> 1$ /minute
3	Multiform ventricular extra systoles
4a	Couplets
4b	Salvos
5	R on T (RV/QT less than 1)

### 10.3 Results

Baseline demographics of the Mitral FINDER cohort have been described in Chapter 4.

No significant relationship between the prevalence of LGE and MR subtype was present (**Table 10.2**).

81 sinus rhythm patients underwent SA-ECG for the detection of VLP, 59 completed three-channel 24-hour Holter ECG recordings for VE burden according to the Lown-Wolf classification, meanwhile, exercise and recovery ECGs from treadmill stress testing were available for 89 patients. None possessed symptomatic or asymptomatic atrial or ventricular arrhythmias during the preoperative monitoring period. The overall ventricular ectopy burden across the cohort was low (ventricular ectopic beats accounting for  $0.0001 \pm 0.0003\%$  of all heartbeats on Holter recording). However, a significant proportion of patients did possess complex ventricular ectopy (**Table 10.3**).

No significant association were detected between LGE or MR subtype parameters and electrophysiological parameters (**Table 10.3**). There were no statistically significant correlations between ECV or CVF and electrophysiological parameters (all P values  $>0.05$ ).



**Table 10.2** Relationship between LGE presence and MR subtype

	<b>LGE absent</b>	<b>LGE present</b>	<b>P</b>
Fibroelastic deficiency	39 (37%)	25 (24%)	0.444
Barlow's disease	28 (27%)	13 (12%)	
Anterior leaflet involvement	9 (9%)	3 (3%)	0.661
Posterior leaflet involvement	38 (36%)	24 (23%)	
Bileaflet involvement	20 (19%)	11 (10%)	
MAD absent	50 (48%)	27 (26%)	0.691
MAD present	17 (16%)	11 (10%)	

*Data are reported as N (%), with p-values from chi<sup>2</sup>-tests.*

**Table 10.3** Electrocardiographic characteristics of surgical and non-surgical cohorts

	LGE			MR subtype			MAD		
	+ve	-ve	P	BD	FED	P	+ve	-ve	P
<b>Lown-Wolf classification on Holter</b>									
○ Complex ventricular ectopy absent	9	16	0.620	16	6	0.095	5	17	0.357
○ Complex ventricular ectopy present	14	19		16	16		11	21	
<b>Ventricular ectopy on exercise ECG</b>									
○ Complex ventricular ectopy absent	12	29	0.116	23	12	0.520	10	25	0.856
○ Complex ventricular ectopy present	21	25		27	19		14	32	
<b>Frequent VE on recovery</b>									
○ Absent	24	41	0.851	36	25	0.535	19	42	0.825
○ Present	9	14		14	7		6	15	
<b>Ventricular late potentials on SA-ECG</b>									
○ Absent	27	26	0.191	35	22	0.413	19	38	0.875
○ Present	4	12		8	8		5	11	
<b>HRV SDNN (N)</b>									
○ <50ms	0	1	0.636	0	1	0.470	0	1	0.730
○ 50-100ms	6	7		7	5		3	9	
○ >100ms	17	27		25	16		13	28	
<b>HRV triangular index (N)</b>									
○ ≤15	1	2	0.799	1	2	0.363	1	2	0.903
○ 15-19	0	0		0	0		0	0	
○ ≥20	22	32		30	20		15	35	

Data are reported as N (%), with p-values from chi<sup>2</sup>-tests.

## 10.4 Discussion

This study demonstrates that the burden of ventricular arrhythmia is low, and indices of HRV are favourable within a general population of severe MR patients. Due to the absence of any significant ventricular arrhythmia within our cohort, markers of arrhythmic risk, including ventricular ectopy burden, VLP, and HRV, were employed as surrogate markers.

Our study findings appear to contradict previous reports on a causal link between MVP and arrhythmic death (41, 299-301), although significant differences in the underlying study population can explain the observed differences. In the report by Basso et al., victims of SCD possessed a mean fibrosis area of 30.5-33.1% (41); this contrasts with our surgical cohort where a much lower  $CVF_{\text{mean}}$  of 14.6% [IQR 7.4-20.3] was present (Chapter 5).

MVP patients with complex ventricular arrhythmias in the Basso et al. study also possessed significantly higher LGE burdens than MVP patients without ventricular arrhythmia (median LGE coverage of across the myocardium: 1.2% vs 0%,  $P < 0.001$ ) (41). In this respect, the Mitral FINDER cohort is similar to the control group within the Basso et al. study. Therefore, it would appear that the typical MR patient with MVP does not possess sufficient degrees of myocardial fibrosis to generate ventricular arrhythmias. Similar reasons may explain why we were unable to identify any relationship between markers of ventricular ectopy and LGE or MR subtype.

If a large fibrosis burden is needed before the fibrosis can function as a pro-arrhythmic substrate, then the underlying mechanism for fibrosis development, particularly LGE, remains of interest. Previous groups have proposed mechanical stretch from the prolapsing

valves as the causative factor in the development of LGE within the LV and papillary muscles (39, 41). Within this current study, we were unable to identify a significant relationship between LGE and MR mechanism or subtype.

More recently, Dejgaard et al. proposed that it was not MVP or LGE, but rather MAD which is the true underlying arrhythmogenic entity. MAD defined as the abnormal atrial displacement of the MV hinge point away from the LV, is commonly found in MVP patients – but the two can also occur independently (244). In a study of 116 patients with MAD, 34% possessed ventricular arrhythmia, 14 of whom experienced sustained ventricular tachycardia or aborted cardiac arrest. Such a high incidence of ventricular arrhythmias is again unusual for the general MR population. Dejgaard et al. reported 78% of their MAD patients to possess MVP. Given the high prevalence of MVP (294), the low incidence of ventricular arrhythmias present in our general MR cohort, and the close association between MAD and MVP, selection bias is likely to be present within the study by Dejgaard et al. This may explain why we did not observe a similar relationship between MAD and markers of ventricular arrhythmia risk within our current study.

In summary, contrary to previous studies on high-risk patient populations, ventricular arrhythmia risk is low in a general population cohort of severe MR patients. We find no association between BD or MAD and markers of ventricular arrhythmia risk and were unable to identify a causal relationship between prolapsing of a leaflet and development of LGE. Further studies are required on elucidating why approximately one-third of MR patients develop LGE.

## APPENDIX II:

### LIST OF PUBLICATIONS ARISING DIRECTLY FROM THIS WORK

- **Liu B**, Edwards NC, Ray S, Steeds RP. Timing surgery in mitral regurgitation: defining risk and optimising intervention using stress echocardiography. *Echo Res Pract.* 2016;3(4):R45-R55.
- **Liu B**, Edwards NC, Neal DAH, Weston C, Nash G, Nikolaidis N, et al. A prospective study examining the role of myocardial Fibrosis in outcome following mitral valve repair IN DEgenerative mitral Regurgitation: rationale and design of the mitral FINDER study. *BMC cardiovascular disorders.* 2017;17(1):282.
- **Liu B**, Dardeer AM, Moody WE, Hayer MK, Baig S, Price AM, et al. Reference ranges for three-dimensional feature tracking cardiac magnetic resonance: comparison with two-dimensional methodology and relevance of age and gender. *The international journal of cardiovascular imaging.* 2017.
- **Liu B**, Dardeer AM, Moody WE, Edwards NC, Hudsmith LE, Steeds RP. Normal Values for Myocardial Deformation Within the Right Heart Measured by Feature-Tracking Cardiovascular Magnetic Resonance Imaging. *International Journal of Cardiology.* 2017.
- **Liu B**, Dardeer AM, Moody WE, Edwards NC, Hudsmith LE, Steeds RP. Reference ranges and reproducibility studies for right heart myocardial deformation by feature tracking cardiovascular magnetic resonance imaging. *Data in brief.* 2018;16:244-9.
- **Liu B**, Edwards NC, Pennell D, Steeds RP. The evolving role of cardiac magnetic resonance in primary mitral regurgitation: ready for prime time? *European heart journal cardiovascular Imaging.* 2019;20(2):123-30.

## APPENDIX III:

### LIST OF ABSTRACTS ARISING DIRECTLY FROM THIS WORK

- **Liu B**, Neil D, Premchand M, Bhabra M, Patel R, Barker T, et al. Definitive histological evidence of myocardial fibrosis in primary degenerative mitral regurgitation: causation of symptoms? *Heart*. 2019;105 (Suppl 6):A102-A. Winner of the British Cardiology Society 'Best of the Best' abstract in the field of Valve disease/pericardial disease/cardiomyopathy.
- **Liu B**, Neil D, Bhabra M, Hayer M, Baig S, Price A, et al. Sex differences in left ventricular remodelling in volume overload due to primary degenerative mitral regurgitation. *European Heart Journal Supplements*. 2018;39 (Suppl 1).
- Vijapurapu R, Hawkins F, **Liu B**, Edwards N, Steeds R. A study of the different methodologies used in calculation of extra-cellular volume by CMR imaging. *Heart*. 2018;104 (Suppl 5):A14-A5.
- **Liu B**, Edwards N, Steeds R, Bhabra M, Barker T, Patel R. Myocardial deformation on cardiac magnetic resonance imaging as an early marker of ventricular dysfunction in asymptomatic moderate-severe primary mitral regurgitation. *AATS Mitral Conclave*; 2017.
- **Liu B**, Edwards N, Bhabra M, Barker T, Patel R, Steeds R. Late gadolinium enhancement in primary degenerative mitral regurgitation predicts adverse right ventricular remodelling and exercise induced pulmonary hypertension. *Heart*. 2017;103 (Suppl 5):A81-A2. Winner of the British Cardiology Society 'Best of the Best' abstract in the field of Imaging.
- **Liu B**, Sinha A, Moody W, Leyva F, Edwards N, Steeds R. New normal ranges and superior reproducibility of 3d myocardial strain on cardiovascular magnetic resonance-feature tracking. *Heart*. 2017;103 (Suppl 5):A82-A3.
- **Liu B**, Hayer M, Baig S, Shah T, Rooney S, Edwards N, et al. The Role of Cardiac Magnetic Resonance Imaging in Patients with Carcinoid Heart Disease. *Heart*. 2016;102 (Suppl 6):A89-A.
- **Liu B**, Baig S, Hayer M, Edwards N, Steeds R. Characterising cardiomyopathy in mitral regurgitation due to barlow disease: role of CMR. *European Heart Journal Supplements*; 2016. p. ii228.

- **Liu B, Baig S, Hayer M, Edwards N, Steeds R.** Echocardiographic characterisation of Barlow's disease versus fibroelastic deficiency. *European Heart Journal Supplements*; 2016. p. ii262.